

Estudio de la segregación cromosómica en *Saccharomyces cerevisiae* bajo la presencia de uniones persistentes entre las moléculas de ADN de las cromátidas hermanas.



Jonay García Luis

December 18th, 2015

A study of chromosome segregation where
persistent DNA junctions are present
between sister chromatids carried out in
Saccharomyces cerevisiae.



Jonay García Luis

December 18th, 2015

**D. Félix M. Machín Concepción, director de la tesis
doctoral presentada por el licenciado Jonay García Luis**

Certifica que:

La memoria presentada por el Licenciado en Biología Jonay García Luis titulada “Estudio de la segregación cromosómica en *Saccharomyces cerevisiae* bajo la presencia de uniones persistentes entre las moléculas de ADN de las cromátidas hermanas” ha sido realizada bajo su dirección en la Unidad de Investigación del Hospital Universitario Nuestra Señora de Candelaria, y considerando que reúne las condiciones de calidad y rigor científico, se autoriza para que pueda ser presentada y defendida ante la comisión nombrada al efecto para optar al grado de Doctor con Mención Internacional por la Universidad de La Laguna.



La Laguna, Octubre de 2015

Fdo: **Dr. D. Félix M. Machín Concepción**

A mis padres

A Elisa

Abstract

The fidelity of chromosome inheritance is of utmost importance to all living organisms. During every cell division precisely one copy of the parental genome must be segregated into each of the two daughter cells in order to allow the stable existence of progeny. This is achieved initially by the complete and faithful duplication of the chromosomes during DNA replication. Following replication each chromosome is comprised of two identical sister chromatids. Next, sister chromatids are fully resolved from each other, ensuring that no physical connection exists between them. Finally, the sisters are segregated to opposite ends of the dividing cell, guaranteeing that when cell division is completed, both daughter cells have a full complement of genetic information.

After replication sister chromatids are held together by three defined kind of linkages: 1) proteinaceous linkages, mediated by the cohesin complex: a ring shaped structure that embraces both sister chromatids. 2) Topological linkages, mostly intertwines between double helixes. 3) DNA-DNA linkages formed by regions of the chromosome that have not been fully replicated, or by intermediates of the homologous recombination (HR) DNA repair process, i.e. recombination intermediates.

Complete replication of the chromosomes, cleavage of cohesin and removal of catenations are essential to segregate chromosomes correctly. If the cell leaves these linkages unresolved, they lead to the formation of DNA filaments connecting the nuclei of both daughter cells, known as chromosome bridges. If the chromosome bridges are not resolved they can be severed during cytokinesis leading to double strand breaks of the DNA molecule and genome instability. Formation of chromosome bridges is a key characteristic of tumorous cells and it is considered as one the first events in the transformation from a somatic to a cancerous cell, since it favours gross chromosomal rearrangements, amplification of oncogenes and elimination of tumour suppressor genes.

However, it is unknown if recombination intermediates can lead to the formation of chromosome bridges. Recombination intermediates appear as a consequence of the DNA repair processes that uses homologous recombination pathway. In this pathway the undamaged sister chromatid provides a template which facilitates the restoration of the original sequence of a broken DNA molecule.

I have used the budding yeast *Saccharomyces cerevisiae* as a model organism to study the sources of chromosome bridges. I have used a haploid *cdc15-2* mutant as a reference strain. This mutant can be blocked in telophase with the genome correctly segregated between the two daughter cells. Using this strain I have studied whether persistent recombination intermediates, more specifically those that depend on structure specific endonucleases (SSEs) for their resolution, can lead to chromosome bridges. To this purpose, I modified the steady-state levels of these joint molecules (JMs) by deleting different combinations of the yeast SSEs genes together with exogenously

forcing the cells to bypass replication stress by utilising HR. I found that both Mus81-Mms4 and Yen1, but not Slx4-related SSEs, are essential and compensate each other in preventing and resolving a specific type of chromosome bridge, which mostly comprises noncanonical (discontinuous) forms of the Holliday Junction (HJ) molecule.

In addition I found that the SSE Yen1 is targeted to the nucleus by the mitotic master phosphatase Cdc14, acting as a 'last resort' endonuclease to deal with any remaining HJs that might compromise chromosome segregation. This result highlights the essential role of early-activated Cdc14; through the FEAR network, Cdc14 effects the removal of all kinds of non-proteinaceous linkage that preclude faithful sister chromatid segregation in anaphase.

Table of contents

ACKNOWLEDGMENTS	9
ABSTRACT	15
TABLE OF CONTENTS	19
LIST OF FIGURES	23
LIST OF TABLES	25
LIST OF ABBREVIATIONS.....	27
1 INTRODUCTION	29
1.1 SACCHAROMYCES CEREVISIAE AS A MODEL ORGANISM	31
1.2 MITOTIC CHROMOSOME SEGREGATION IN BUDDING YEAST.....	32
1.2.1 Nature of the physical linkages between DNA molecules after replication.....	32
1.2.2 Molecular mechanisms regulating the elimination of the physical linkages between DNA molecules after replication	33
1.3 DNA DAMAGE AND REPAIR PATHWAYS	35
1.3.1 Single stranded DNA damage repair	37
1.3.1.1 Direct reversal pathway.....	37
1.3.1.2 Mismatch repair pathway.....	37
1.3.1.3 Nucleotide excision repair pathway	37
1.3.1.4 Base excision repair pathway	37
1.3.2 Double strand DNA damage repair	38
1.3.2.1 Homologous recombination repair.....	38
1.3.2.1.1 Phases of homologous recombination	39
Pre-synapsis	39
Synapsis	39
Post-Synapsis	39
1.3.2.1.2 Homologous recombination repair pathways	40
Break Induced Replication	40
dHJ pathway.....	41
Synthesis-dependent strand annealing.....	42
1.3.3 Pathways of replication fork restart.....	42
1.4 PROCESSING OF JOINT MOLECULE INTERMEDIATES DURING HOMOLOGOUS RECOMBINATION.....	45
1.4.1 Dissolution of Holliday Junctions	45
1.4.2 Resolution of Holliday Junctions	46
1.4.2.1 Mus81-Mms4.....	46
1.4.2.2 Yen1.....	49
1.4.2.3 Slx1-Slx4.....	50
1.5 SPECIAL SEGREGATION REQUIREMENTS OF THE rDNA IN S. CEREVISIAE	52
1.6 CHROMOSOME SEGREGATION FAILURE AS AN ORIGIN OF CHROMOSOME BRIDGES AND CANCEROUS CELLS	53
2 AIMS.....	57
3 MATERIALS AND METHODS.....	59
3.1 CULTURE CONDITIONS FOR S. CEREVISIAE.....	61

3.1.1	<i>Asynchronous to telophase arrest</i>	61
3.1.2	<i>G1 to telophase arrest</i>	61
3.1.3	<i>G2 to telophase to G1</i>	63
3.1.4	<i>Transformant cells</i>	64
3.2	TRANSFORMATION OF <i>S. CEREVISIAE</i>	64
3.2.1	<i>Preparation of competent cells</i>	64
3.2.2	<i>Transformation</i>	64
3.3	POLYMERASE CHAIN REACTION	65
3.4	PRIMERS	66
3.5	DNA PREPARATIONS	67
3.5.1	<i>High molecular weight-DNA preparation</i>	67
3.5.2	<i>Genomic DNA preparation from <i>S. cerevisiae</i></i>	67
3.6	DNA ELECTROPHORESIS	68
3.6.1	<i>Agarose electrophoresis</i>	68
3.6.2	<i>Pulsed-Field Gel Electrophoresis</i>	68
3.6.3	<i>Two-dimensional neutral-neutral DNA electrophoresis (NN-2D)</i>	69
3.6.4	<i>Three-dimensional neutral-neutral-alkaline DNA electrophoresis (NNA-3D)</i>	69
3.6.5	<i>DNA modifying enzymes used on agarose plugs</i>	70
3.6.5.1	RuvC	70
3.6.5.2	T4 DNA ligase	70
3.7	SOUTHERN-BLOT ANALYSIS	70
3.7.1	<i>Probe synthesis</i>	70
3.7.2	<i>DNA transfer from the gel to the membrane</i>	71
3.7.3	<i>Probe hybridization and detection</i>	71
3.7.4	<i>Stripping</i>	71
3.7.5	<i>Signal quantification</i>	72
3.8	WESTERN BLOT ANALYSIS	72
3.8.1	<i>Protein extraction</i>	72
3.8.2	<i>SDS-PAGE</i>	72
3.8.3	<i>Protein transfer and detection</i>	72
3.9	MICROSCOPY	73
3.10	FLOW CYTOMETRY	74
4	RESULTS	75
4.1	ARTICLE 1: NONDISJUNCTION OF A SINGLE CHROMOSOME LEADS TO BREAKAGE AND ACTIVATION OF DNA DAMAGE CHECKPOINT IN G2	77
4.2	ARTICLE 2: MUS81-MMS4 AND YEN1 RESOLVE A NOVEL ANAPHASE BRIDGE FORMED BY NONCANONICAL HOLLIDAY JUNCTIONS	105
4.3	ARTICLE 3: CDC14 TARGETS THE HOLLIDAY JUNCTION RESOLVASE YEN1 TO THE NUCLEUS IN EARLY ANAPHASE	127
5	DISCUSSION	137
5.1	THE <i>CDC15-2</i> BLOCK AS A MODEL TO STUDY MISSEGREGATION AND ANAPHASE BRIDGES FORMATION	139
5.2	THE <i>MMS4Δ YEN1Δ</i> DOUBLE MUTANT ACCUMULATES RECOMBINATION INTERMEDIATES THAT LEAD TO CHROMATIN ANAPHASE BRIDGES AND ULTRAFINE ANAPHASE BRIDGES	140
5.3	MMS4 AND YEN1 ARE ABLE TO RESOLVE HOMOLOGOUS RECOMBINATION INTERMEDIATES COMPRISED BY NONCANONICAL HOLLIDAY JUNCTIONS	143
5.4	CDC14 TARGETS YEN1 TO THE NUCLEUS IN EARLY ANAPHASE	145

5.5	YEN1 ACTS AS A LAST RESOURCE BACKUP OF MUS81-MMS4 RESOLVING JOINT MOLECULES	146
6	CONCLUSIONS	149
7	LITERATURE CITED	151
8	APPENDIX: MEDIA, SOLUTIONS & SUPPLIERS	171

List of figures

Figure 1.1.: Life cycle of yeast.....	31
Figure 1.2: Schematic of the role of the FEAR network in completing chromosome segregation during early anaphase.	35
Figure 1.3: DNA-repair pathways.	36
Figure 1.4: Schematic of the first two steps during HR repair after a DSB.....	40
Figure 1.5: Schematic of the HR repair pathways.....	41
Figure 1.6: Pathways of replication fork restart depending on the kind of DNA damage and which strand is affected.....	43
Figure 1.7: Substrate specificity of eukaryotic structure-specific endonucleases.	47
Figure 1.8: Spatiotemporal regulation of HJ processing enzymes in <i>S. cerevisiae</i> and humans.	49
Figure 1.9: Regulation of the Slx4-Dpb11 complex during the cell cycle.....	51
Figure 1.10: Structure of rDNA repeats in <i>S. cerevisiae</i>	53
Figure 3.1: Schematic of the experiment of telophase block	61
Figure 3.2: Schematic of the experiment of G1 to telophase arrest	61
Figure 3.3: Schematic of the experiment of G1 to telophase arrest with induction of Yen1 or Mms4 in the telophase arrest	62
Figure 3.4: Schematic of the experiment of G1 to telophase arrest with induction of Yen1 in the G1 arrest	62
Figure 3.5: Schematic of the experiment of G1 to telophase arrest with DNA damage induction.....	63
Figure 3.6: Schematic of the experiment of G2-to-telophase-to-G1 with induction of Yen1 in the G2 arrest	63
Figure 3.7: Schematic overview of the PCR program used to amplify DNA to transform yeast.	65

Figure 3.8: Schematic overview of the PCR program used to amplify DNA to check transformant clones. 65

Figure 5.1: Schematic representing the potential substrates of Mms4 or Yen1 upon overexpression in telophase in a *mms4Δ yen1Δ* background. 141

List of tables

Table 3.1: List of primers used in this thesis	66
Table 3.2: : List of filter cubes used during this thesis.	73
Table 3.3: List of microscope settings used for capturing images for each tagged protein and DAPI used in this thesis.....	74
Table 4: List of suppliers	176

List of abbreviations

- APC- anaphase promoting complex.
- ARS- autonomously replicating sequence.
- AU- absorbance unit.
- BIR- break-induced replication.
- bp- base pair.
- cXII.- chromosome XII
- cXIIr - right arm of chromosome XII
- CDK- cyclin-dependent kinase.
- cm- centimetre.
- CPT.- camptothecin.
- dHJ- double Holliday junction.
- iHJ- intact Holliday Junction.
- nHJ- nick Holliday Junction .
- D-loop- displacement loop.
- DNA- deoxyribonucleic acid.
- dNTP- deoxynucleotide tri-phosphate.
- DSB- double-strand break.
- DSBR- double-strand break repair.
- dsDNA.- double-stranded DNA.
- FACS- fluorescence-activated cell sorting.
- FEAR- Cdc14 early anaphase release.
- GCR- gross chromosomal rearrangement.
- GFP- green fluorescent protein.
- h- hour.
- HJ- Holliday junction.
- HR- homologous recombination.
- HU.- hydroxyurea.
- Kb- kilobases.
- LOH- loss of heterozygosity.
- M- molar.
- MEN- mitotic exit network.
- min- minute.
- ml- millilitre.
- mM- millimolar.
- MMS- methyl methanesulfonate.

- ng- nanogram.
- NHEJ- non-homologous end joining.
- nm- nanometre.
- °- degree.
- °C- degree Celsius.
- OD 600 - optical density measured at 600 nanometres-wavelength.
- PCR- polymerase chain reaction.
- PFGE- pulsed-field gel electrophoresis.
- rDNA- ribosomal DNA array.
- RF- Replication fork.
- RFB- replication fork barrier.
- RNA- ribonucleic acid.
- ROS- reactive oxygen species.
- RPA- replication protein A.
- rpm- revolutions per minute.
- rRNA- ribosomal ribonucleic acid.
- RT- room temperature.
- s- second.
- SC- synthetic complete.
- SDSA- synthesis-dependent strand annealing.
- SPB- spindle pole body.
- SSA- single-strand annealing.
- ssDNA- single-stranded DNA.
- SSE.- structure specific endonuclease.
- STR complex- Sgs1-Top3-Rmi complex.
- UFB- ultrafine bridge
- UV- ultraviolet.
- V- volts.
- v/v- volume/volume.
- w/v- weight/volume.
- WT- wild type
- YFP- yellow fluorescent protein.
- α F- α -factor.
- μ g- microgram.
- μ l- microliter.
- μ m- micrometre.
- μ M- micromolar.

1 Introduction

1.1 *Saccharomyces cerevisiae* as a model organism

Saccharomyces cerevisiae (baker's or budding yeast) is one of the most intensively studied eukaryotic microorganisms. It has been used as a model organism because many fundamental processes such as cell cycle control, DNA replication, chromosome segregation regulation, and DNA repair are highly conserved from yeast to humans.

Several properties make yeast particularly suitable for genetic, biochemical and cell biology studies. Yeast have a rapid growth (generation time is less than 2 hours under optimal conditions) and can be cultured in an economic manner. Genetic engineering is highly efficient: It occurs via homologous recombination (HR) mediated through short fragments of homologous linear DNA (Knop et al. 1999; Janke et al. 2004). *S. cerevisiae* can stably exist as either a haploid or a diploid. Both haploid and diploid yeast cells are able to reproduce by mitosis. Haploid cells can be divided in two mating types, **a** cells and **α** cells. Haploid cells of different mating types are able to mate with each other to produce a diploid cell. When diploid cells face stressful conditions such as nutrient deprivation they can undergo meiosis to produce four haploid spores: two **a** spores and two **α** spores (**Fig 1.1**). Working with the haploid form has a great advantage in terms of genetic manipulation, as just one copy of each gene is present to be manipulated (Hartwell 1974).

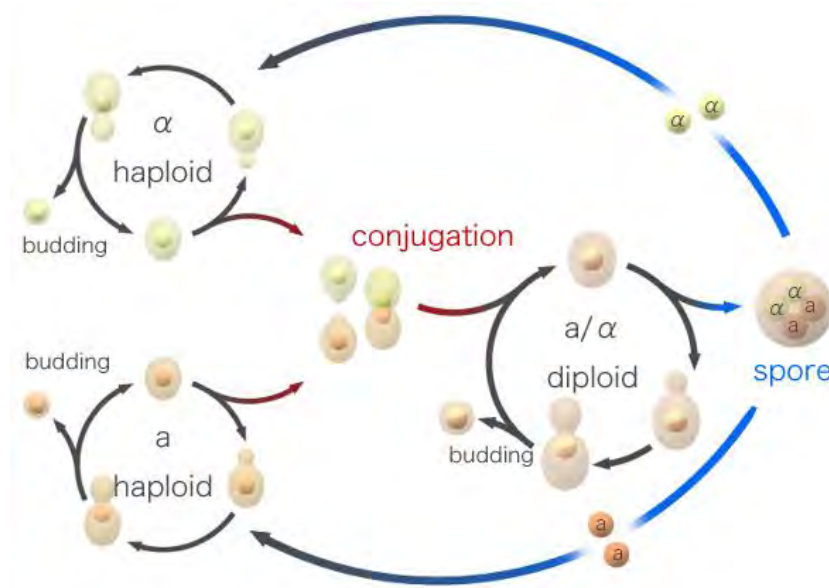


Figure 1.1.: Life cycle of yeast. Yeast grow vegetatively as either haploid or diploid cells. The transition from haploid to diploid occur via mating between two cells of different mating type. The transition from diploid to haploid occurs via meiosis.(Taken from http://wiki.yeastgenome.org/images/e/ea/Yeast_life_cycle.png)

Additionally the *S. cerevisiae* genome has been sequenced and is publicly available since 1996. The genome has a size of 12.1 million base-pairs (bp) with about 6000 genes distributed in 16 chromosomes. Several comprehensive genome-wide gene deletion and protein fusion libraries have been created that are now available for the scientific community (Winzeler et al. 1999; Cherry et al. 2012). These libraries are an excellent resource and have had a great impact on the yeast research community and on genomics in general.

1.2 Mitotic chromosome segregation in budding yeast

The mitotic cell cycle can be divided in four phases: Two gap phases, G1 and G2, an S phase, where synthesis of the DNA occurs and the genetic material is duplicated, and an M phase, also called mitosis, in which the genetic material is divided equally and the cell divides. After the S phase, duplicated chromosomes consists of two sister chromatids that are maintained together by physical linkages. During mitosis it is of paramount importance to eliminate any linkages between different DNA molecules in order to segregate chromosomes correctly between the two daughter cells.

1.2.1 Nature of the physical linkages between DNA molecules after replication

After S phase, sister chromatids are associated by three types of linkages: a) proteinaceous linkages, represented by the cohesin complex, b) topological linkages and c) DNA-DNA linkages represented by recombination intermediates.

- a) Cohesin has been referred to as the molecular glue that maintain sister chromatids together. This function is essential to identify each sister chromatid and ensure that one and only one chromatid of each chromosome is delivered into each daughter cell. The cohesin complex has a ring shape structure composed of Smc1, Smc3, Scc1 and Scc3. It is thought that this structure embraces both sister chromatids after DNA replication and this interaction is stably maintained until the cells reach anaphase (Michaelis et al. 1997; Guacci et al. 1997; Haering et al. 2002; Gruber et al. 2003; Ivanov & Nasmyth 2005).
- b) DNA molecules are also topologically linked. During DNA replication termination, overwinding superhelical tension is generated ahead of the fork by the activity of replication helicases. This tension can be diffused into the region behind of the fork by rotation of the whole fork relative to the unreplicated DNA. As a consequence of the fork rotation, the topological stress ahead of the fork is relaxed at the expense of generation of DNA catenations behind the fork (Champoux & Been 1980; Peter et al. 1998;

Baxter 2015). The eukaryotic type-II topoisomerase (Topo II in mammals, Top2 in yeast) is essential to remove these catenations before cells enter anaphase (Nitiss 2009).

- c) Additionally DNA recombination intermediates maintain sister chromatid physical association (Torres-Rosell et al. 2005; Ho et al. 2010; Sarbajna et al. 2014; García-Luis & Machín 2014). Recombination between two sister chromatids provides an error-free pathway to repair DNA damage. Nevertheless this DNA repair pathway leaves as a by-product, DNA molecules physically linked by recombination intermediates (See sections 1.3.2.1 and 1.3.3). These links are eliminated mainly by the Sgs1-Top3-Rmi1 complex (STR) also called dissolvasome (Mankouri et al. 2011; Bizard & Hickson 2014). As well as this mechanism to eliminate recombination intermediates, the cell has SSEs that are able to recognize and resolve different structures that arise during the recombination process (See section 1.4).

Faithful chromosome segregation also requires of condensin. Condensin is highly conserved and is essential in all eukaryotes. In budding yeast, condensin is a multiprotein complex comprised of 5 subunits; Smc2, Smc4, Ycs4, Ycg1 and Brn1 (Strunnikov et al. 1995; Freeman et al. 2000; Ouspenski et al. 2000; Bhalla 2002; Lavoie et al. 2000; Hirano 2005). The segregation defects observed in condensin mutants are very similar to those observed in topoisomerase II mutants. This observation suggest that condensin may be governing the function of topoisomerase II in its decatenation activity (Freeman et al. 2000; Hirano 2000; Bhalla 2002; Lavoie et al. 2004; Machín et al. 2005; Morgan 2007)

1.2.2 Molecular mechanisms regulating the elimination of the physical linkages between DNA molecules after replication

The mitotic phase of the cell cycle can be further subdivided into prophase, metaphase, anaphase, telophase and cytokinesis. In prophase the chromosomes condense to form a compact structure that is able to then align to the division plane in metaphase. At this point the chromosomes are connected to the spindle pole bodies (SPB, centrosome in animal cells) the machinery that is going to pull from the chromosomes to each daughter cell. In anaphase each sister chromatid is pulled to a different daughter by the forces exerted by the SPB. Finally in telophase the nuclei are totally separated and in cytokinesis the cytoplasm is physically divided into the two daughter cells.

By the time the cell reaches anaphase all the physical linkages that maintained sister chromatids together must be eliminated to ensure that each chromatid is segregated correctly, one to each daughter cell. Two main mechanisms govern the elimination of the physical linkages between the sister chromatids and progression through anaphase: activation of the anaphase promoting complex (APC) and dephosphorylation of many targets of the cyclin dependent kinase Cdc28. (Stegmeier & Amon 2004; Pines 2011).

The APC is only activated when replicated chromosomes are aligned to the metaphase plane and have established bivalent spindle attachment. If the chromosomes are not aligned or any DNA damage is detected, the cell will activate checkpoint signalling cascades that will maintain the APC inactive. These will halt the cell cycle progression in order to give enough time to attach spindles correctly or to repair the DNA damage (Hartwell & Weinert 1989; Paulovich et al. 1997).

Anaphase onset is triggered when the APC binds to the specificity factor Cdc20 (APC^{Cdc20}) causing its activation. The APC is a tightly regulated ubiquitin ligase. Ubiquitinated targets will be destroyed by the 26S proteasome (Pines 2011). One of the key targets of the APC^{Cdc20} is the securin Pds1, an inhibitor of the protease Esp1, also known as separase. Thus APC activation leads to degradation of Pds1 and thereby activation of Esp1 (Cohen-Fix et al. 1996; Yamamoto et al. 1996). Esp1 then cleaves Scc1, one of the components of the ring-shaped structure cohesin that entrap sister chromatids. The cleavage of Scc1 releases sister chromatids to allow chromosome segregation (Uhlmann et al. 1999).

In addition to its proteolytic function, Esp1 has a second non-proteolytic activity that leads to the activation of Cdc14. Cdc14 is the cell cycle master phosphatase in budding yeast that ensures the elimination of any remaining physical linkage between DNA molecules and exit from mitosis. This phosphatase is tightly regulated throughout the cell cycle in a stepwise fashion (**Fig.1.2**) (Visintin et al. 1998; Stegmeier et al. 2002; Stegmeier & Amon 2004). Before anaphase, Cdc14 is found in the nucleolus in an inactive form bound to Net1 as part of the rDNA-binding RENT complex (Shou et al. 1999; Visintin et al. 1999; Traverso et al. 2001). Esp1, as well as cleaving Scc1, downregulates the phosphatase PP2A. This allows Net1 to be phosphorylated by Cdc5, and prevents its dephosphorylation by PP2A, thereby allowing Cdc14 to be released from Net1. Thus Cdc14 is released from the nucleolus into the nucleoplasm in what is known as Cdc14 early anaphase release pathway (FEAR). (Uhlmann et al. 1999; Sullivan & Uhlmann 2003; Azzam et al. 2004; Queralt et al. 2006; Rahal & Amon 2008). In this way Cdc14 reaches and dephosphorylates its nuclear targets.

Cdc14 activation ensures correct chromosome segregation in several ways: 1) It associates with the SPB and the mitotic spindle and dephosphorylates Pds1 leading to an increased affinity of APC^{Cdc20} for Pds1. This produces a positive feedback that

allows an increased smoothness in chromosome segregation (Holt et al. 2008). 2) It ensures efficient segregation of the rDNA and repetitive sequences by switching off transcription. This allows loading of condensin and Top2 to eliminate catenations (see section 1.5) (Clemente-Blanco et al. 2009; Clemente-Blanco et al. 2011). 3) Cdc14 activation allows spindle stabilization and activation of motor proteins needed for spindle elongation (Higuchi & Uhlmann 2005; Roccuzzo et al. 2015) 4) Furthermore Cdc14 is required for the activation of the Mitosis Exit Network (MEN) (D'Amours & Amon 2004). The MEN pathway produces a second wave of Cdc14 activation, giving access to its nuclear and cytoplasmic targets and thereby promoting exit from mitosis and cytokinesis (Visintin et al. 1999; Shou et al. 1999; Kuilman et al. 2015)

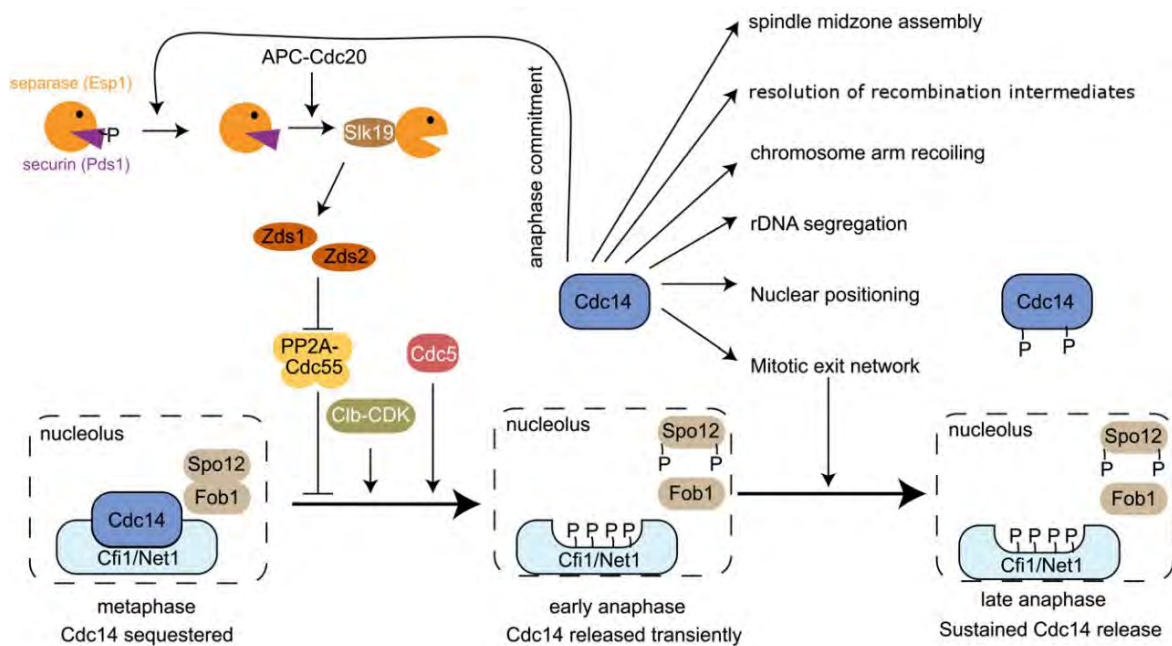


Figure 1.2: Schematic of the role of the FEAR network in completing chromosome segregation during early anaphase. See text for explanation. Modified from Marston 2014

1.3 DNA damage and repair pathways

Most of the modifications that alter the structure or the nucleotide sequence of the DNA molecule are considered to be DNA damage. DNA damage sources can be subdivided into two main types: endogenous and exogenous damage. Endogenous damage is caused by errors introduced during replication, recombination, DNA repair or from the attack of reactive oxygen species (ROS) that have been produced as a normal metabolic by-product. Exogenous damage is caused by external physical or chemical agents. Examples of physical agents are the ultraviolet (UV) light radiation, X-rays radiation or gamma rays. On the other hand examples of mutagenic chemical agents include DNA intercalating agents, alkylating agents, oxidizing agents or DNA crosslinking agents. Many anticancer drugs exert their effect via the production of

deleterious DNA damage, and these include DNA topoisomerases inhibitors and the DNA alkylating agents (Vilenchik & Knudson 2003).

Types of DNA damage can be initially classified as single-stranded or double-stranded. Single stranded DNA damage repair, includes Direct Reversal, Base Excision Repair (BER) Nucleotide excision repair (NER) and Mismatch Repair (MMR). In the latter three processes one or more nucleotides at the lesion are eliminated forming a gap, then filled and religated. Double strand damage is repaired using Double Strand Break Repair (DSBR) mechanisms, namely Non-Homologous End Joining (NHEJ) and HR based systems. The latter can be further divided into the double Holliday junction (dHJ) pathway, Synthesis-Dependant Strand Annealing (SDSA), Break Induced Replication (BIR) and Single Strand Annealing (SSA) (Fig. 1.3).

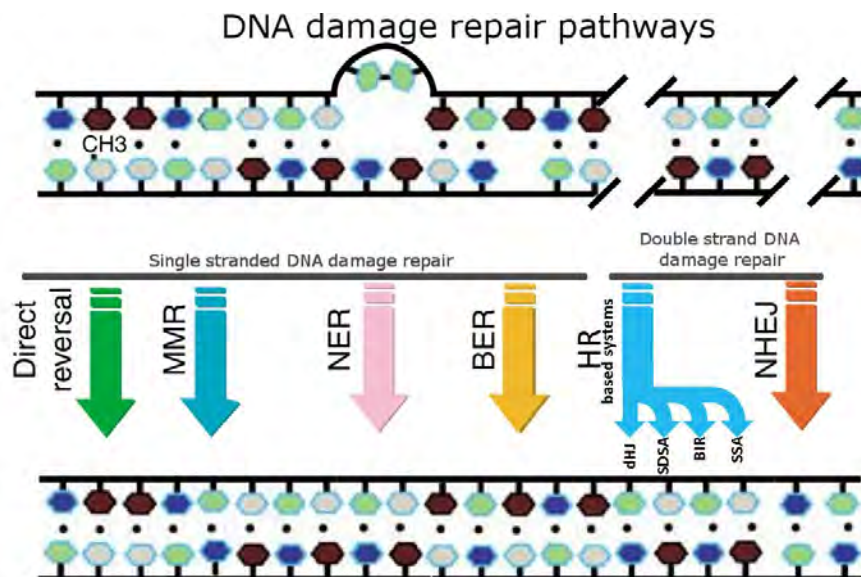


Figure 1.3: DNA-repair pathways. Classification of the different DNA repair pathways. Direct reversal pathway, the mismatch repair pathway (MMR), the Nucleotide Excision Repair pathway (NER), the Base Excision Repair pathway (BER), the Homologous Recombination based pathways that include: double Holliday junction pathway (dHJ), Synthesis-Dependant Strand Annealing (SDSA), Break Induced Replication (BIR) and Single Strand Annealing (SSA) and Non-Homologous end Joining (NHEJ). Modified from (Hakem 2008)

1.3.1 Single stranded DNA damage repair

1.3.1.1 Direct reversal pathway

Direct reversal repair allows cells to remove damage to bases by chemically reversing it. This requires one specific enzyme for each type of base damage. For instance, when cells are exposed to UV light dimers of pyrimidines can be formed. The cells are able to remove pyrimidine dimers by the direct action of photolyases that split the covalent bonds generated by the UV light (Britt 2004). Also alkylating agents can produce methylation of DNA. A particularly important type of methylation is the O⁶ position of guanine, because the product, O⁶-methylguanine, forms complementary base pairs with thymine instead of cytosine. This damage can be repaired directly by a single enzyme, the O⁶-methylguanine-DNA methyltransferase (MGMT) that transfer the methyl group to its active site in a suicide reaction that leads to inactivation of the enzyme (Gerson 2004; Mishina et al. 2006).

1.3.1.2 Mismatch repair pathway

Despite the high accuracy of the replication machinery some nucleotides are mis-incorporated. The main task of MMR is to remove base mismatches and small insertion/deletion loops introduced during replication. In eukaryotes two kinds of protein Msh (Msh2, Msh3 and Msh6) and Mlh (Mlh1, Mlh2, Mlh3 and Pms1) repair this kind of damage. They scan the genome for mismatches and when one is found this proteins act cooperatively to nick and degrade the newly synthesized strand, removing the mismatch and allowing DNA synthesis in the single-stranded DNA (ssDNA) gap to finally ligate the nick, this gives rise to a DNA molecule as it was in the parental strands (Strand et al. 1993; Kolodner 1996).

1.3.1.3 Nucleotide excision repair pathway

DNA bases as it has been mention before can be modified by UV light and other bulky lesions. This kind of lesion can be repaired by the NER pathway in two ways, global genome repair (GGR) that recognise and repair the damage along all the genome or transcription coupled repair (TCR), which specifically repairs the transcribed strand of active genes. Each sub-pathway requires different factors that recognise and unwind the DNA around the bulky lesion to finally produce an incision in 3' and 5' from the damaged base. In this way the damage is released in a 24-32 nucleotide long oligonucleotide to allow new DNA synthesis and ligation (Reardon & Sancar 2005).

1.3.1.4 Base excision repair pathway

Not all the lesions produced on the DNA bases are bulky. Among the non-bulky lesions we can find those produced by alkylation, oxidation or base deamination. To

deal with this damage the cells have developed the BER pathway. This pathway is mainly based in the existence of DNA glycosylases that are able to recognize a broad substrate spectrum of modified bases (Hegde et al. 2010). These glycosylases break the N-glycosylic bond releasing the nitrogen base and generating an apurinic/apyrimidinic (AP site). Then the AP site can be removed in two ways: 1) The AP site is cleaved by an AP endonuclease in the sugar-phosphate backbone 3' to the AP. The resulting fragmented sugar residue is removed by a phosphodiesterase activity, contributed by either an AP endonuclease or by DNA polymerase β . The one-nucleotide gap is filled by Pol β and ligated 2) an AP endonuclease cuts 5' to the AP site, providing a primer for DNA polymerase β . Pol β incorporates a nucleotide and its deoxyribophosphodiesterase activity removes the 5' moiety. The remaining nick is sealed by ligation (Krokan & Bjørås 2013).

1.3.2 Double strand DNA damage repair

Double strand break (DSB) damage represents one of the most toxic forms of DNA damage, which, if left unrepaired, leads to chromosome aberrations, genomic instability, or cell death (Jackson 2002; Sonoda et al. 2006). In eukaryotic cells the efficient repair of a DSB is essential to ensure cell survival. Two main pathways have evolved to deal with these kinds of lesions: HR and NHEJ.

The utilization of either NHEJ or HR depends on the nature of the DSB, the cell type and the cell cycle stage. In *S. cerevisiae* NHEJ is efficient in repairing DSB with cohesive overhangs but not blunt ends or ends with non-cohesive overhangs, which must be left to HR. Regarding cell type, NHEJ and HR are both active in haploid cells, whereas in diploid cells NHEJ is suppressed. Despite HR and NHEJ being active in haploid cells, NHEJ is especially important in G1 stage, when the 5' to 3' resection of the DSB ends, is blocked. (Lieber 1999; Lee et al. 1999; Frank-Vaillant & Marcand 2001; Ira et al. 2004; Rothkamm et al. 2003; Lieber 2008). Since DNA damage repair by HR is a major source of physical linkages between DNA molecules in this thesis I will focus on homologous recombination repair based systems

1.3.2.1 Homologous recombination repair

HR mediated DSB repair can be divided in three phases: pre-synapsis, in which recognition and resection of the DSB ends is carried out, synapsis, where a joint molecule between the damaged DNA and its homologous template is formed and post-synapsis where the joint molecule is further processed and resolved in two repaired homologous DNA molecules.

Different homologous repair systems start from different phases of the HR pathway. After the DNA resection in the pre-synaptic phase the cell can repair the DSB

by SSA if the DSB is flanked by direct repeats. During the post-synaptic phase several pathways can then occur ensuing in completion of repair: dHJ pathway, SDSA and BIR.

1.3.2.1.1. Phases of homologous recombination

Pre-synapsis

Shortly after the DSB is formed, nucleolytic degradation of the 5' DNA ends at the break occur. It is carried out by the complex Mre11-Rad50-Xrs2 coupled with the Sae2 endonuclease yielding 3' ssDNA overhangs of about 100 nts (**Fig 1.4**). Subsequently, extensive resection is catalysed by the 5'-3' exonuclease Exo1, or by the combined action of Sgs1 helicase and Dna2 endonuclease (Mimitou & Symington 2008; Gravel et al. 2008; Zhu et al. 2008; Shim et al. 2010). Exo1 removes mononucleotides from the DNA ends and Sgs1-Top3-Rmi1 unwinds DNA that is then degraded by the endonuclease Dna2 (Mimitou & Symington 2008; Huertas et al. 2008; Zhu et al. 2008). While resection happens the heterotrimeric complex replication protein A (RPA) binds and protects the ssDNA. Rad51 recombinase then replaces RPA, forming a filament along the ssDNA. To achieve this critical step several proteins known as recombination mediators load Rad51 on ssDNA. The recombination mediators are Rad52, Rad51 paralog proteins Rad55- Rad57 and Shu1-Shu2-Csm2-Psy3 complex (called SHU complex). Rad52 is the most important recombination mediator. When it is deleted HR is totally abolished, revealing its essential role in HR

Synapsis

During synapsis, the ssDNA coated with Rad51 interrogate the genome looking for homologous double-strand DNA. When a donor duplex is found, DNA-strand invasion occurs, producing a displacement loop (D-loop). While Rad51 can perform synapsis by itself, it is greatly stimulated by the double-stranded DNA (dsDNA) motor protein Rad54 (Sung 1994; Van Komen et al. 2000; Tan et al. 2003; Heyer et al. 2006; Qi et al. 2015). Following strand invasion the invading 3' end is extended using either DNA polymerase Pol δ or DNA polymerase Pol ϵ together with the help of their processivity factor PCNA, and Dpb11. This step is critical to restore the information lost during DSB resection. (Wang et al. 2004; Li et al. 2009; Germann et al. 2011; Hicks et al. 2011; Symington et al. 2014).

Post-Synapsis

After this step of DNA synthesis, HR pathway can proceed following four alternative pathways: BIR, SDSA or dHJ pathway.

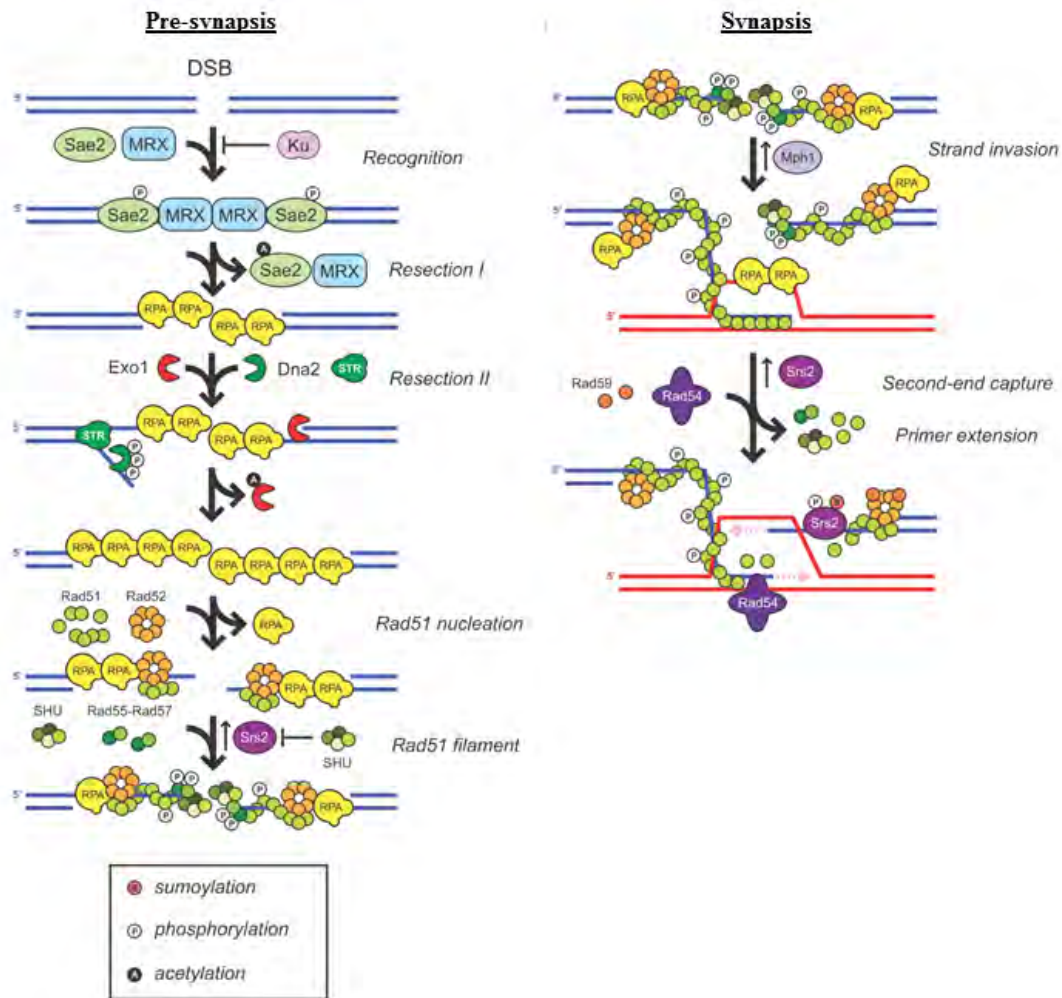


Figure 1.4: Schematic of the first two steps during HR repair after a DSB: synapsis, where DSB recognition, DNA resection and formation of the Rad51 filament happen and post-synapsis where homologous pairing and strand invasion happen. Modified from Mathiasen & Lisby 2014

1.3.2.1.2. Homologous recombination repair pathways

Break Induced Replication

This pathway has been implicated in the restart of collapsed replication forks (RF), alternative lengthening of the telomeres in telomerase impaired cells and repairing of one-ended DSB after the severing of chromosomes during cytokinesis (Teng et al. 2000; Michel et al. 2001; Lydeard et al. 2007; Iraqui et al. 2012). According to existing models, after creation of a D-loop intermediate BIR proceeds with extension of the invading strand in the D-loop, which can be continued as far as the end of the donor chromosome (Davis & Symington 2004; McEachern & Haber 2006). Repair by this pathway can be dangerous for the cell because extensive loss of heterozygosity (LOH) occurs if the donor molecule is a homologous chromosome (**Fig. 1.5**). Furthermore, BIR

can be initiated at ectopic chromosome location, and with several rounds of strand invasion, DNA synthesis and dissociation, this leads to chromosome rearrangements. BIR initiation is a slow process. It can take as long as 5 hours for the replication machinery to be assembled. This means that SDSA usually outcompetes BIR in DSB repair (Bosco & Haber 1998; Malkova et al. 2005; Smith et al. 2007; Jain et al. 2009).

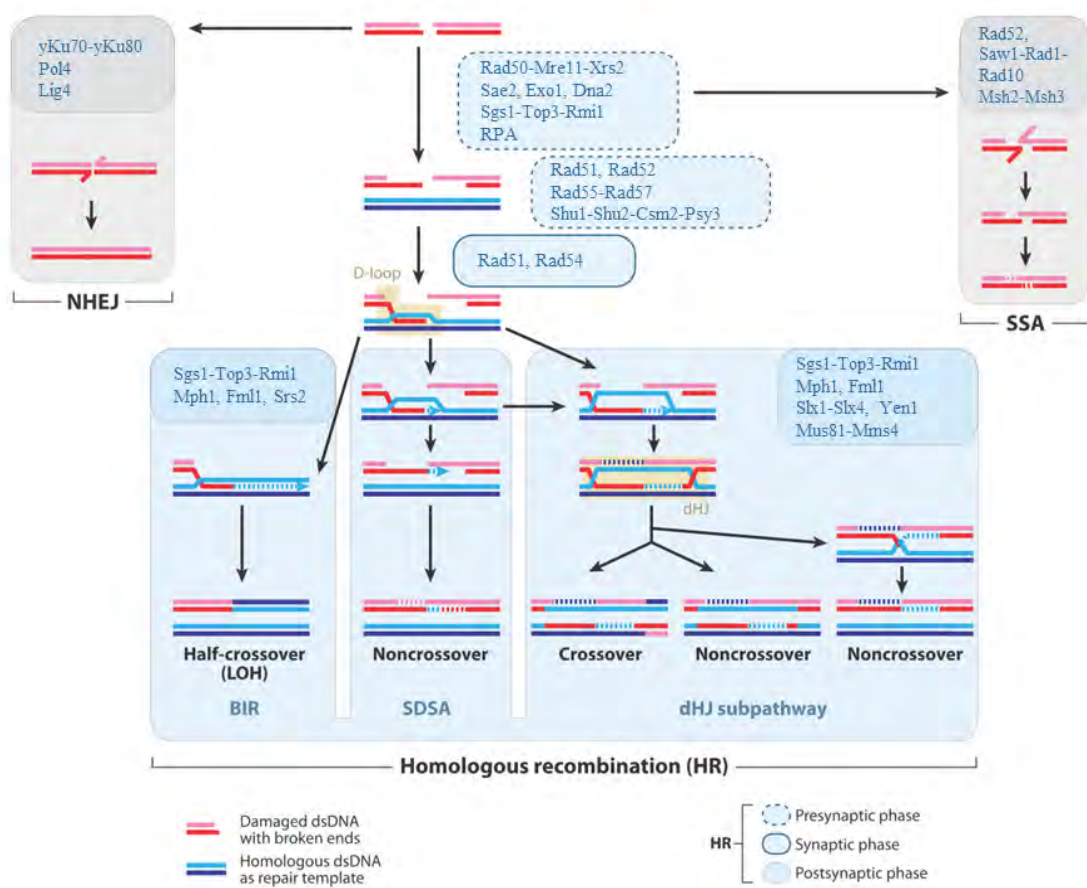


Figure 1.5: Schematic of the HR repair pathways. Modified from Heyer et al. 2010

dHJ pathway

The dHJ pathway model was first suggested by Resnick (Resnick 1976) and later by Szostak (Szostak et al. 1983) based on the earlier conceptions of Holliday (Holliday 1964). After formation of the D-loop structure, the invading strand can be extended by DNA polymerases, mainly Pol δ and Pol ϵ (Hicks et al. 2010; Sebesta et al. 2011). The ssDNA at the other end of the DSB can anneal with the displaced ssDNA from the donor molecule, a process known as second end capture. This process leads to the formation of two Holliday junctions (HJ) (Pâques & Haber 1999; Bzymek et al. 2010; Mehta & Haber 2014). Then this HJ can be processed by the dissolvasome, composed by Sgs1-Top3-Rmi1, or can be resolved by different SSEs (See section 1.4). All dHJs that are processed by the STR complex will lead to noncrossovers (NCO), while those processed by SSEs (depending on which pair of strands they cut) will lead

to noncrossovers or crossovers (CO) (Symington et al. 2014). COs implicate exchange of genetic material between the two homologous chromosomes while in a NCO there is only unidirectional transfer of genetic material from a “donor” sequence to a highly homologous “acceptor” (leading to gene conversion when synthesis changes the content of an open reading frame). The cell preferentially repairs the damage through the dissolvasome activity since it only leads to NCOs. COs are a pernicious product of the homologous recombination repair pathway because they cause loss of heterozygosity, a phenomenon linked to appearance of cancerous cells (**Fig 1.5**).

Synthesis-dependent strand annealing

The dHJ model explains many properties of the meiotic recombination, but mitotic recombination shows lower levels of CO products than expected if the cell only could use the dHJ pathway (Bzymek et al. 2010). This situation led to the elaboration of another model called SDSA. Similarly to the dHJ subpathway the D-loop structure is formed, and the 3' end of the invading strand is extended using the donor molecule as a template. The newly synthesized strand is then displaced from the donor molecule and returned to the broken molecule pairing with the resected 3' ssDNA at the other end of the DSB (Ferguson & Holloman 1996; Haber et al. 2004). Alternatively both ssDNA 3' ends can invade the donor molecule, and after limited DNA synthesis this structure is dismantled with the help of DNA helicases, and the nascent complementary strands anneal (Nassif et al. 1994). After this, DNA synthesis to fill-in the gaps and ligation is carried out to restore the broken molecule. What differentiates SDSA from the dHJ pathway is that SDSA exclusively produces NCO outcomes, and that the DNA synthesis is conservative, and all the newly synthesized DNA is in the recipient molecule. How the nascent DNA strand is unwound from the template in the SDSA pathway is not known in detail but helicases Mph1, Srs2 and the Sgs1-Top3-Rmi1 complex play a crucial role (**Fig 1.5**).

1.3.3 Pathways of replication fork restart

Inhibition of replication fork progression presents a challenge to the maintenance of genome stability. Paused RFs lose activity as a function of time, and the ssDNA generated is the substrate for DNA strand exchange proteins. The normal progression of the RFs during S phase can be interrupted in different ways. Stalling of the replication fork can be generated by DNA sequences that give rise to secondary structures, like those encoding transfer RNA (tRNA), or those with trinucleotide repeats (León-Ortiz et al. 2014). In addition, progression of replisomes is inhibited by topological constraints (Baxter & Diffley 2008a). Proteins that bind strongly to the DNA also cause the RFs to slow down or to stop replication. Regarding this last situation, the most studied case is the replication of ribosomal DNA in budding yeast, where the fork is forced to go mainly in one direction because of the presence of the replication fork block sequence, which binds tightly to Fob1. Fob1 wraps the replication fork block

sequence around itself and arrests forks moving in the 3' to 5' direction, avoiding collisions of replication and transcription (Kobayashi 2003; Takeuchi et al. 2003). However the most dangerous barriers are chemical modifications of the DNA like those produced by UV light (thymine dimers) or methylation of DNA nitrogenous bases by methylating agents like methyl methanesulfonate (MMS). How the stalled replication fork is recued depends on the kind of blockage and where it is localized: in the lagging or in the leading strand (**Fig. 1.6**).

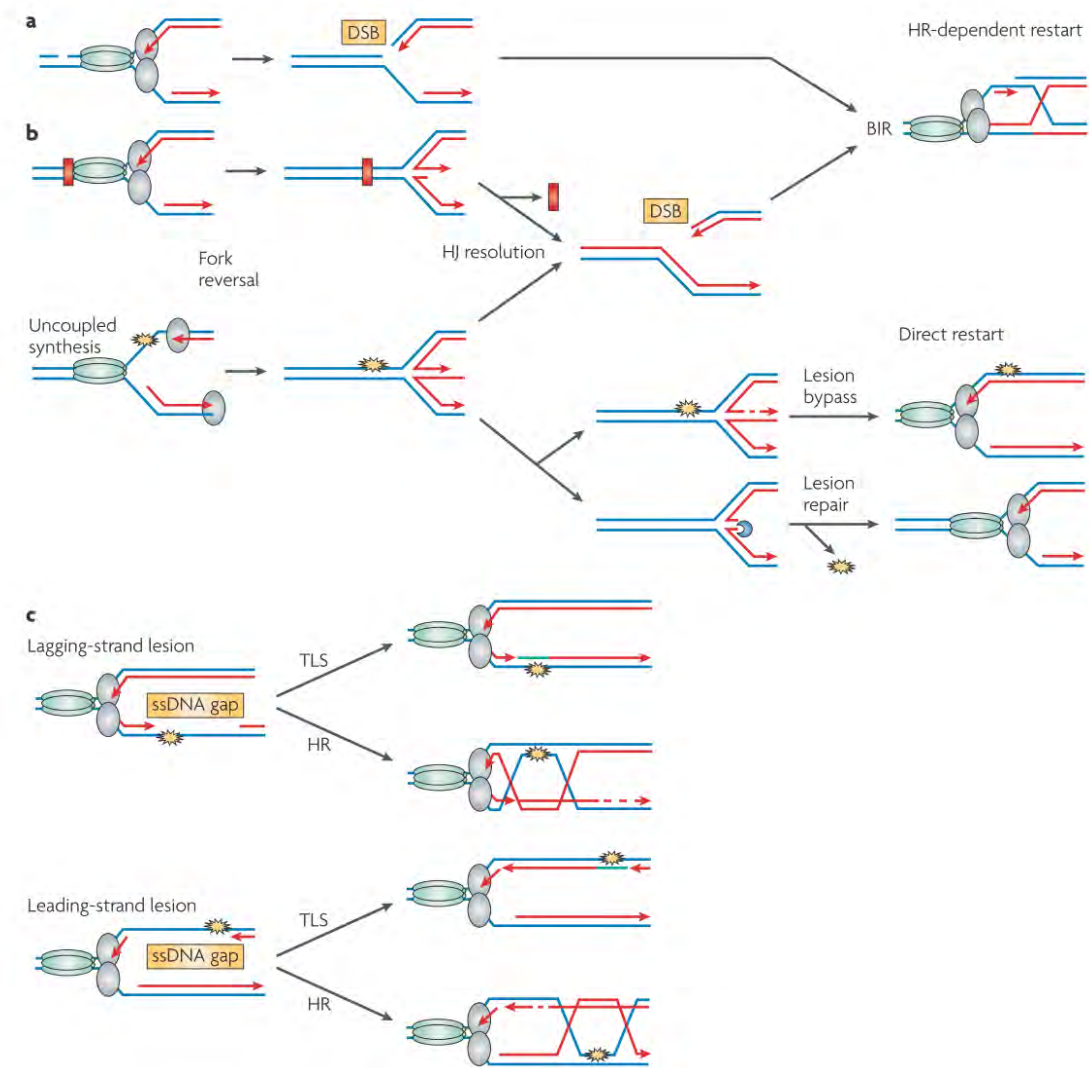


Figure 1.6: Pathways of replication fork restart depending on the kind of DNA damage and which strand is affected. See text for explanation. Taken from Aguilera & Gómez-González 2008.

- a) If the replication fork encounters a discontinuity, it will produce the breakdown of the replication fork and release of one of the sister duplexes with a dsDNA end (McGlynn & Lloyd 2002; Aguilera & Gómez-González 2008). This is a substrate of recombination proteins that will lead to the

formation of a D-loop (**Fig 1.6a**). If a converging fork arrives by the time a D-loop is formed, the two merge to form a HJ, which is cleaved by Mus81 or Yen1. Alternatively the D-loop can be cleaved by Mms4-Mus81 to form a stable fork structure (Mehta & Haber 2014; Mayle et al. 2015).

- b) Blockage of the replication fork progression call upon RF processing enzymes in order to continue replication. Multiple SSEs are able to recognize structures resembling RFs. The heterodimers Mus81-Mms4, and Slx4-Slx1 have been implicated in recombination repair of stalled RFs (Osman & Whitby 2007; Schwartz & Heyer 2011; Muñoz-galván et al. 2012; Rass 2013). RF cleavage may also occur after conversion of the three-way junction into a four-way HJ intermediate by reannealing of the parental DNA strands, a process known as RF reversal or RF regression. The cleavage of these by SSEs release a one ended dsDNA that recombine back to the sister duplex producing a D-loop substrate for replisome reloading (Atkinson & McGlynn 2009; Neelsen & Lopes 2015). Alternatively, when the replication fork encounters genotoxic stress the synthesis of the leading and the lagging strand is uncoupled resulting in accumulation of ssDNA. The reannealing of this ssDNA can lead to the formation of a reversed fork. Several helicases/ translocases have been implicated in fork regression in vitro such as Sgs1, Mph1, Rad5 or Rad54 (Karow et al. 2000; Gari et al. 2008; Zheng et al. 2011; Bugreev et al. 2011). If the damage is present in the leading strand, the regressed fork will allow extension of the blocked leading strand using the nascent lagging strand as a template. Reversal of fork regression or exonucleolytic degradation of the regressed arm by Dna2 and Sgs1 allow the bypass of the original lesion and reloading of the replisome at the fork thus facilitating the access to the repair machinery to remove the damage (**Fig 1.6b**) (Thangavel et al. 2015; Neelsen & Lopes 2015).
- c) Genotoxic lesions that block the synthesis of the lagging strand do not produce fork stalling but create a ssDNA gap between two flanking Okazaki fragments. If the genotoxic damage is in the leading strand, it can be bypassed by a replication fork that restarts downstream of the lesion, leaving a gap of ssDNA behind the fork. These tracts of ssDNA can be repaired by low fidelity polymerases of the translesion synthesis (TLS) pathway. Alternatively, the presence of ssDNA itself can promote HR repair using the sister chromatid as a template (Berdichevsky et al. 2002; Lopes et al. 2006; Heller & Marians 2006; Ortiz-Bazán et al. 2014) .

1.4 Processing of joint molecule intermediates during homologous recombination.

In eukaryotic cells HR is a key pathway that repairs DSBs or stalled RFs. Despite being the most reliable pathway to repair DNA damage, it generates recombination intermediates that link the DNA molecules that are to be segregated to different daughter cells during chromosome segregation. The cells have to eliminate these linkages before the end of anaphase. A failure to eliminate recombination intermediates by anaphase could lead to chromosome missegregation, chromosome bridges, aneuploidy and gross chromosome rearrangements (GCR), or so it was thought before we carried out this study. Cells have evolved a sequential and tightly regulated system to ensure the complete elimination of all types of chromosomal interactions in preparation for efficient chromosome segregation.

1.4.1 Dissolution of Holliday Junctions

HR is crucial during DNA repair. dHJs appear as an intermediate in the HR repairing process (see section 1.3.2.1) (Bzymek et al. 2010). dHJs can be eliminated by the STR complex or by SSEs. If the dHJ is cleaved by SSEs it can give rise to COs or NCOs depending on whether the cleavage is carried out asymmetrically or symmetrically. In the case of the dHJ being formed between homologous chromosomes and cut by SSEs, COs and LOH can potentially be generated. If the dHJ is present between two homeologous sequences and is cut by SSEs, GCRs can occur. Thus, during mitosis the cell uses an alternative mechanism to process dHJs without producing COs. Such a mechanism is termed dHJ dissolution and is carried out by the STR complex (Szostak et al. 1983; Wu & Hickson 2003; Bellaoui et al. 2003).

During dHJ dissolution the two HJs migrate towards one another until they form a hemicatenane which is then eliminated by the activity of Top3. This reaction regenerates the original DNA molecules present before starting HR. In somatic cells, this pathway is essential to avoid sister chromatid exchange and loss of heterozygosity (Nasmyth 1982; Wang et al. 1990; Wu & Hickson 2003).

The STR complex plays a primary role in dHJ processing, dissolving them into NCO products. How the STR complex is regulated during the cell cycle is not well understood, but the JM dissolution by the STR complex is likely to happen from early S-phase until G2/M when Mms4-Mus81 is activated (Matos et al. 2011; Wechsler et al. 2011). Combinations of mutations in any of the subunits of the STR complex with resolvases Mms4-Mus81, Slx1-Slx4, cause synthetic lethality. On the contrary, combined mutations of Yen1 and any of the components of the STR complex behave as the STR single mutant (Ashton et al. 2011)

1.4.2 Resolution of Holliday Junctions

Alternatively to the dHJ dissolution pathway, the cell can process the HJs by HJ resolution reactions mediated by SSEs. Depending on the cleavage axis, either a CO or NCO are generated. Studies from various organisms indicate that there are at least three HJs resolvases. In budding yeast these involve the Mus81-Mms4, Slx1-Slx4 and Yen1 endonucleases (Kaliraman et al. 2001; Fricke & Brill 2003; Ip et al. 2008). HJ resolvases can be classified as canonical or noncanonical depending on their similarity to RuvC bacterial HJ resolvase. Canonical resolvases act as homodimers that introduce two symmetrically opposed nicks across the helical junction. This reaction yields a two nicked DNA duplexes that can be repaired by direct nick ligation. Noncanonical resolvases act as heterodimers and cleave the junction with asymmetric nicks. In this case the reaction yields a gapped and a flapped DNA duplex that cannot be directly ligated. In addition to cleaving HJs, some of these SSEs have activity towards a variety of complex DNA lesions and other joint molecules *in vitro* (Wyatt & West 2014). The *in vitro* and *in vivo* activities and regulation along the cell cycle of each SSE in *S. cerevisiae* are discussed below.

1.4.2.1 Mus81-Mms4

Mus81 forms a dimer with its regulatory subunit Mms4 (EME1 in humans and Eme1 in fission yeast) (Mullen et al. 2001; Kaliraman et al. 2001). That Mus81-Mms4 forms as a heterodimer is supported by the findings that yeast *mms4Δ mus81Δ* double mutants have identical phenotypes (Boddy et al. 2001; de los Santos et al. 2001; Kaliraman et al. 2001).

Mus81-Mms4 is a noncanonical HJ resolvase. *In vitro* studies with partially purified MUS81-EME1 from human cells as well as Mus81-Eme1 from fission yeast have demonstrated that their activity on intact iHJs of this heterodimer is magnesium dependent. During the enzymatic reaction Mus81-Mms4/EME1 introduce two asymmetric nicks yielding one gapped and one flapped DNA duplex that cannot be ligated *in vitro* (Boddy et al. 2001; Chen et al. 2001; Constantinou et al. 2002). However purified Mus81-Mms4/EME1 cleaves iHJs with very low efficiency compared to recombination intermediates, such as D-loops or nHJs. Furthermore replication intermediates such as RF or 3'-flaps are preferred substrates for Mus81-Mms4/EME1 (**Fig 1.7**) (Gaillard et al. 2003; Osman et al. 2003; Ciccina et al. 2003; Ciccina et al. 2008; Wyatt & West 2014). The available structural information on MUS81-EME1 protein suggests that nicked substrates are the preferred substrate because the arms of nicked junctions are flexible to position the incision point into the catalytic site (Chang et al. 2008).

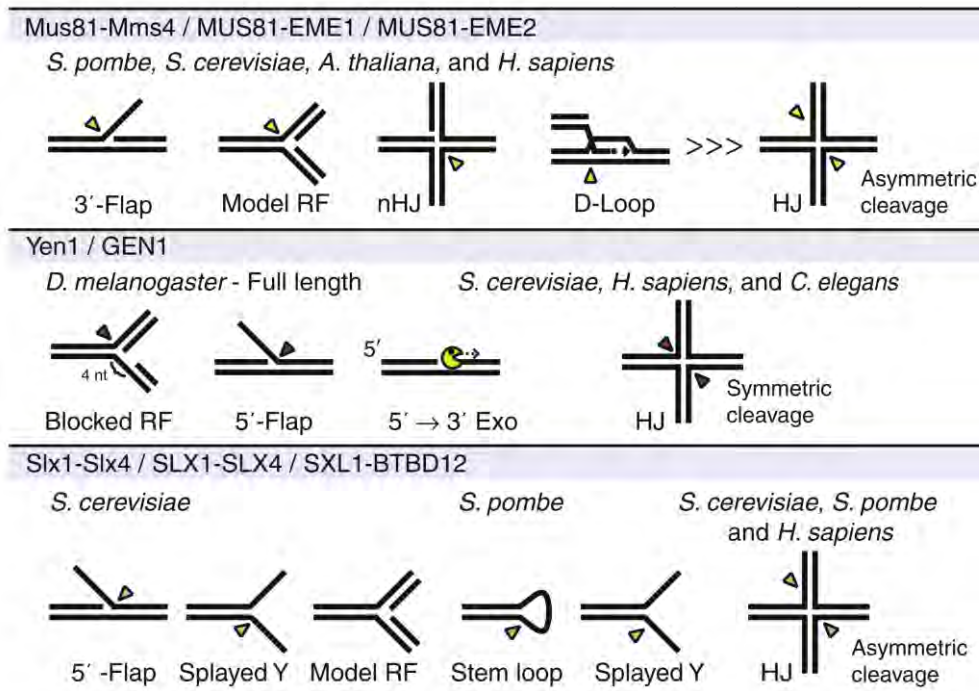


Figure 1.7: Substrate specificity of eukaryotic structure-specific endonucleases. The arrowheads show the incision sites of the SSE on the substrate. Taken from Schwartz & Heyer 2011

In vivo studies with *mms4Δ* or *mus81Δ* mutants show that under unperturbed conditions they display elevated levels of spontaneous GCR and increased accumulation of HJs in the rDNA probably due to stalling of the RF at the Replication Fork Barrier (RFB). These phenotypes show that this heterodimer is required for normal growth and viability of unperturbed cycling cells (Boddy et al. 2000; Abraham et al. 2003; Smith et al. 2004; Noguchi et al. 2004; Dendouga et al. 2005; Zhang et al. 2006). Additionally *mms4Δ* or *mus81Δ* mutants are hypersensitive to UV light, MMS, camptothecin (CPT) and hydroxyurea (HU) (Interthal & Heyer 2000; Boddy et al. 2001; Doe et al. 2002; Abraham et al. 2003; Fu & Xiao 2003). The Mus81-Mms4 complex is required to process problems that arise when RFs are blocked by such lesions. This idea is supported by the observation in human cells where MUS81 localizes to regions of UV-induced damage during S-phase and is further supported by the fact that in *S. pombe* ectopic expression of RusA (HJ resolvase from bacteriophage) partially recues sensitivity to genotoxic agents and meiotic defects (Gao 2003; Ashton et al. 2011). Importantly combinations of mutations in any of the subunits of the STR complex with Mms4 or Mus81 produce synthetic lethality and aberrant recombination intermediates in meiosis. The synthetic lethality of *mus81Δ sgs1Δ* cells is suppressed when HR is eliminated by deletion of key RAD52 epistasis group genes such as RAD51 or RAD52 (Fabre et al. 2002; Ashton et al. 2011). In addition it has been shown that Mus81-Mms4 has a role in BIR. Extension of the D-loop via the BIR pathway is limited to within a few kilobases from the break. This is due to two factors: the Mus81-Mms4 complex

can cleave the D-loop and help to re-establish a stable fork structure, or alternatively a converging fork can transform the migrating D-loop to a HJ structure, later resolved by Mus81-Mmms4 or Yen1. Both processes help avoid the use of the rearrangement-prone repair mechanism BIR (Mayle et al. 2015).

Combining *mus81Δ* or *mms4Δ* mutants with the canonical HJ resolvase *yen1Δ* leads to a greater sensitivity to genotoxic agents compared to the single mutants. Under unperturbed conditions *mus81Δ yen1Δ* mutants show growth defect, Rad53 phosphorylation indicative of checkpoint activation, decreased spore viability compared to the single mutants and chromosomal loss. The higher rate of chromosomal loss is associated with a failure in the elimination of recombination intermediates between sister chromatids, causing chromosome nondisjunction and chromosome loss. These defects are greatly reduced by the deletion of RAD51 or RAD52 (Blanco et al. 2010; Ho et al. 2010; Tay & Wu 2010; Agmon et al. 2011; García-Luis & Machín 2014). Also overexpression of Yen1 in an *mms4Δ* background recues the sensitivity of this single mutant to MMS. All these results are consistent with Mus81-Mmms4 acting in a parallel overlapping pathway with Sgs1 and Yen1 targeting D-loops, (regressed) forks or by processing recombination intermediates (Boddy et al. 2001; Doe et al. 2002; Osman & Whitby 2007; Blanco et al. 2010; García-Luis & Machín 2014).

The Mms4 subunit of the Mms4-Mus81 complex has been found to undergo cell cycle dependent phosphorylation. It is phosphorylated following S-phase, when the bulk of DNA replication has taken place and before chromosome segregation. This phosphorylation was found to be dependent on Cdc28 and Cdc5. These two kinases phosphorylate the N-terminal region of Mms4 enhancing the nuclease activity of its partner Mus81. This late activation of Mms4-Mus81 in the cell cycle supports the idea that the dissolution pathway mediated by the STR complex is the primary pathway for the cells to eliminate intermediates that originate during replication associated DSB repair or fork stalling (**Fig 1.8**) (Matos et al. 2011; Gallo-Fernández et al. 2012; Matos et al. 2013; Szakal & Branzei 2013; Blanco & Matos 2015).

In *S. pombe* the regulation of Emel1 (*S. pombe* Mms4 homolog) is slightly different to *S. cerevisiae*. It is also phosphorylated in a cell cycle dependent manner by Cdc2/Cdk1 but independent of Plo1 (*S. pombe* Cdc5 homolog). However in *S. pombe* Emel1 is further phosphorylated in response to DNA damage, enhancing the nuclease activity. This regulation strategy contrasts with that of *S. cerevisiae* and humans (see below), where the detection of DNA damage inactivates Cdc5 and blocks cell cycle progression precluding the activation of Mms4-Mus81 (Saugar et al. 2013; Matos et al. 2013; Dehé et al. 2013; Matos & West 2014).

In humans, the MUS81-EME1 complex interacts with the SLX1-SLX4 complex increasing its nuclease activity. This interaction is triggered in a cell cycle dependent manner by CDK1 phosphorylation of EME1. PLK1 (Homolog of Cdc5 in *S. cerevisiae*)

form part of the complex MUS81-EME1 and potentially phosphorylates SLX4, but its activity appears to be dispensable for the bulk of SLX-MUS complex formation at the G2/M transition (Svendsen et al. 2009; Wyatt et al. 2013; West et al. 2015). Additionally, in response to DNA damage MUS81-EME1 is phosphorylated by WEE1 inhibiting its activity and protecting stalled forks from being recognised by this complex (Domínguez-Kelly et al. 2011)

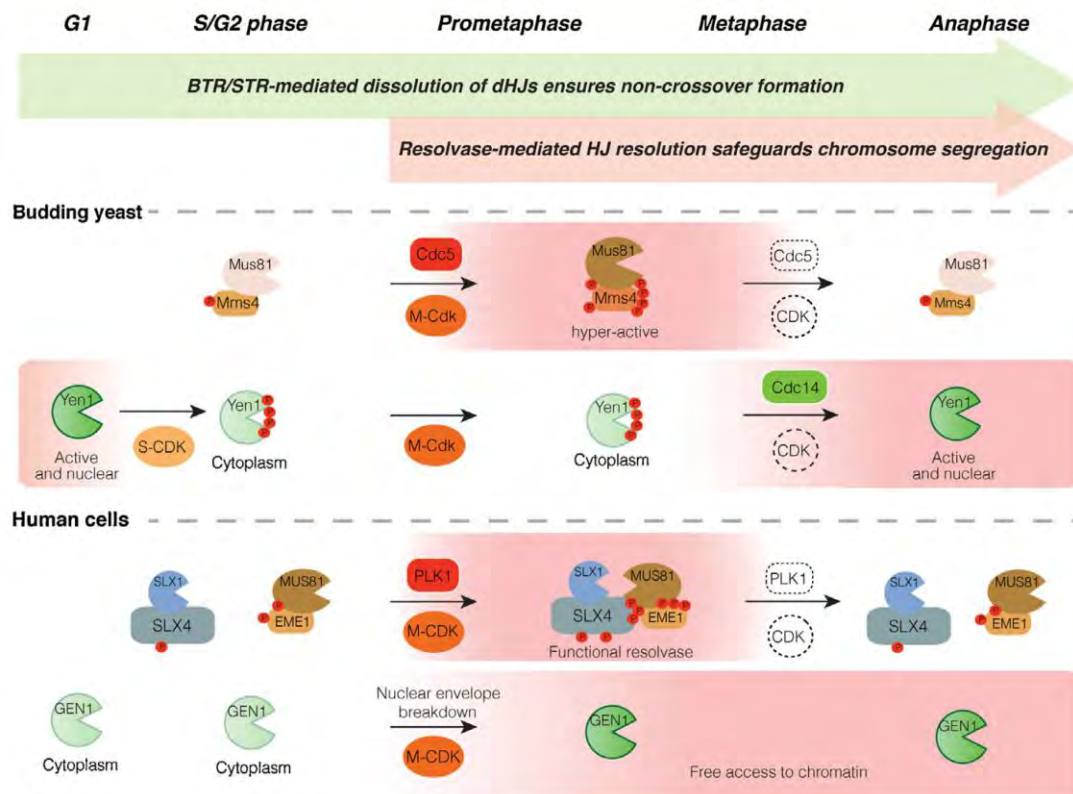


Figure 1.8: Spatiotemporal regulation of HJ processing enzymes in *S. cerevisiae* and humans. See text for explanation. Taken from Matos & West 2014

1.4.2.2 Yen1

The first gene product identified as a canonical HJ resolvase in mammals was GEN1 (Elborough & West 1990; Ip et al. 2008). Homologs of GEN1 have been identified in other eukaryotes including budding yeast (Yen1) but strikingly it is absent in *S. pombe* (Ip et al. 2008). GEN1 and Yen1 promote HJ resolution by a symmetrical cleavage mechanism analogous to that shown by RuvC.

In vitro studies on the amino-terminal fragment of human GEN1 (hGEN1¹⁻⁵²⁷) and Yen1 purified from *S.cerevisiae* have shown that hGEN1 and Yen1 are able to cut 5'-flaps, RFs and nicked or intact HJs (Ip et al. 2008; Rass et al. 2010; Blanco et al. 2014). Unlike other resolvases Yen1/Gen1 is monomeric in solution and it dimerizes

when it binds to its substrate before introducing two symmetrically opposed nicks in a coordinated way (Rass et al. 2010).

The *S. cerevisiae yen1Δ* mutant does not seem to have any detectable phenotype. It shows normal cell growth, viability, resistance to genotoxic agents, recombination rate and meiotic CO formation (Blanco et al. 2010; Tay & Wu 2010; Agmon et al. 2011; Ho et al. 2010; García-Luis & Machín 2014). Similarly, depletion of Yen1 homologs in other organisms such as *C. elegans* or human cells does not cause any detectable phenotype. However the ability of GEN1 and Yen1 to cut HJs *in vivo* is supported by several genetic experiments. As afore mentioned, the double mutant *mms4Δ yen1Δ* in *S. cerevisiae* accumulates recombination intermediates. Similarly, *S. cerevisiae sgs1Δ* or *top3Δ* mutants accumulate recombination intermediates that are eliminated by ectopically expressing hGEN1¹⁻⁵²⁷ (Mankouri et al. 2011). Furthermore *C. elegans mus-81 xpf-1* mutants are synthetic lethal: They accumulate recombination intermediates between pairs of homolog chromosomes. Injection of hGEN1¹⁻⁵²⁷ eliminates the recombination intermediates and suppresses DNA bridges formation between homolog chromosomes (O'Neil et al. 2013). Despite the fact that Yen1 and its homologs in other organisms were identified as the canonical resolvases in eukaryotes, it seems that their role is obscured by the redundant activity of other SSEs, suggesting that Yen1 provides a backup activity of other resolvases. In the case of *S. cerevisiae* Yen1 backs up the activity of the Mus81-Mms4 heterodimer and in humans the MUS-SLX complex (Ho et al. 2010; García-Luis & Machín 2014; Sarbajna et al. 2014).

1.4.2.3 Slx1-Slx4

Slx1 belong to the YIG family of endonucleases and its sequence is relatively evolutionary conserved. By contrast, Slx4 is evolutionarily diverse, although in *S. cerevisiae*, *S. pombe*, *C. elegans* and humans SLX4 contained a conserved SAP domain localized to the C-terminal region that is thought to mediate DNA binding and substrate specificity (Schwartz & Heyer 2011).

In vitro experiments with Slx1-Slx4 have shown that it is a noncanonical HJ resolvase. It has a broad substrate specificity with a preference to cut 5'-flaps, Y-splayed arms, model RFs, as well as mobile and fixed HJs (Fricke & Brill 2003; Wyatt et al. 2013; Gaur et al. 2015). Mechanistic studies with human Slx1-Slx4 have shown that it cuts HJs in an uncoordinated manner. It makes first a nick near the junction and then dissociates from the substrate before a second nick can occur (Wyatt et al. 2013)

In vivo studies on Slx1-Slx4 in yeast show that single *slx1Δ* or *slx4Δ* mutant have wild-type (WT) growth rate and sporulation efficiency (Mullen et al. 2001). However both subunits are required for suppression of GCR and for resistance to DNA damage induced by MMS (Fricke & Brill 2003; Zhang et al. 2006). The *in vivo* function of this complex has been better characterized from its genetic and physical interaction

with other genes and proteins. In the same screening where *slx1Δ* and *slx4Δ* were identified as synthetic lethal with deletion of *sgs1*, *MUS81* and *MMS4* were also identified (Mullen et al. 2001). The lethality of *mus81Δ* or *mms4Δ* with *sgs1Δ* was suppressed by a HR defect caused by deletion of *RAD51*, *RAD52* or *RAD54* (Fabre et al. 2002). This observation strongly suggests that HR generates recombination intermediates that have to be processed by the STR complex or Mus81-Mms4 resolvase. Surprisingly mutations of the genes implicated in the initial steps of the HR did not suppress the lethality of *slx1Δ* or *slx4Δ* with *sgs1Δ* (Fricke & Brill 2003). This data together with the information from studies on *in vitro* preference of cleavage of replication structures, lead to the hypothesis that this complex is implicated in maintaining the structural integrity of stalled RFs. This hypothesis is further supported by the fact that the double mutants *sgs1-34* (temperature sensitive allele) *slx4Δ* has replication defect at the rDNA (Kaliraman & Brill 2002). How Slx1-Slx4 is regulated, is not well understood. However, it is known that Slx1 forms a stable homodimer in which the active site is blocked. Conversion of the Slx1 homodimer to the Slx1-Slx4 heterodimer exposes the active site and activates Slx1 (Gaur et al. 2015). In addition in the recent years it has become clear that the Slx4 subunit of the Slx1-Slx4 nuclease acts as a scaffold that coordinates the actions of a number of proteins involved in DNA processing during cell cycle progression. Slx4 binds to Rad1 in a mutually exclusive way with respect to Slx1 and stimulates the 5' flap endonuclease activity of Rad1-Rad10 during SSA DNA repair pathway (Toh et al. 2010). In yeast Slx4 also forms a complex with at least two other scaffold proteins, Dpb11 and Rtt107 (Fig 1.9) (Ohouo et al. 2010; Gritenaite et al. 2014).

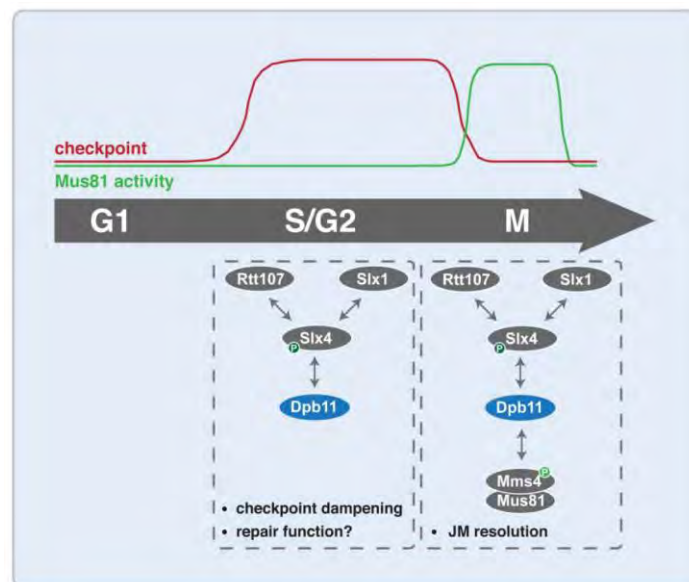


Figure 1.9: Regulation of the Slx4-Dpb11 complex during the cell cycle. See text for explanation. Taken from Princz et al. 2015.

The formation of this complex is heavily regulated by posttranslational modifications, integrating two cellular signals: cell cycle stage through Cdc28 dependent phosphorylation and DNA damage checkpoint activation through Mec1 dependent phosphorylation (Gritenaite et al. 2014; Princz et al. 2015).

In S phase, upon Cdk1 phosphorylation of Slx4, an interaction between Slx4 and Dpb11 is established. Slx4 also binds to Rtt107 and Slx1. In G2/M phosphorylation of Mms4 by Cdc5 promotes the additional association of Mus81-Mms4 with the complex, promoting joint molecules resolution. In the case of DNA damage detection, the DNA damage checkpoint is activated and counteracts Mus81-Mms4 binding to the Dpb11-Slx4 complex (Gritenaite et al. 2014; Princz et al. 2015). In higher eukaryotes Slx4 also forms part of the SLX-MUS complex. (See Mus81-Mms4 section) (Cybulski & Howlett 2011)

1.5 Special segregation requirements of the rDNA in *S. cerevisiae*

In all eukaryotes the RNA that forms part of the ribosomes (rRNAs) is transcribed from multicopy genes that are spread over the entire genome or clustered to certain regions. In *S. cerevisiae*, the rRNA genes are located in a single genomic location. 450 kb left from the centromere and 610 kb from the right end of chromosome XII (cXII) . It consists of 150-200 tandemly repeated copies of 9.1 kb rDNA units, representing almost 10% of the yeast genome and making cXII the longest *S. cerevisiae* chromosome (Petes 1979). Each 9.1 kb unit contains two transcribed regions, the 35S precursor rRNA and 5S rRNA, and two non-transcribed regions, NTS1 and NTS2. The DNA encoding the 35S rRNA and 5S rRNA is transcribed by RNA polymerase I (Pol I) and III (Pol III) respectively. Each rDNA unit has a RFB localized in the NTS1 and an autonomous replicating sequence localized in the NTS2 (**Fig 1.10**) (Brewer & Fangman 1988; Linskens & Huberman 1988).

Apart from the highly repetitive nature of the locus, the rDNA has other characteristics that differentiates it from the rest of the genome. It is replicated unidirectionally in the direction of 35S rRNA transcription due to the presence of the RFB (Brewer & Fangman 1988; Linskens & Huberman 1988). Importantly, the rDNA is highly transcribed. In an exponential growing culture 60% of the total transcription is devoted to ribosomal RNA (Warner 1999). Due to this high level of transcription and the presence of the RFB that stalls the RFs coming from the opposite direction, the rDNA is a hot spot for recombination (Gottlieb & Esposito 1989; Takeuchi et al. 2003). Transcription in the rDNA is regulated by the histone deacetylase Sir2. Sir2 along with Net1 and the Cdc14 phosphatase comprises the nucleolar complex called RENT (REGulator of Nucleolar silencing and Telophase exit). The RENT complex interacts with the rDNA through Fob1 and RNA polymerase I (Straight et al. 1999; Shou et al.

1999; Huang & Moazed 2003). It is thought that the high levels of transcription are responsible for the increased catenation accumulation at the rDNA locus (Baxter & Aragón 2010).

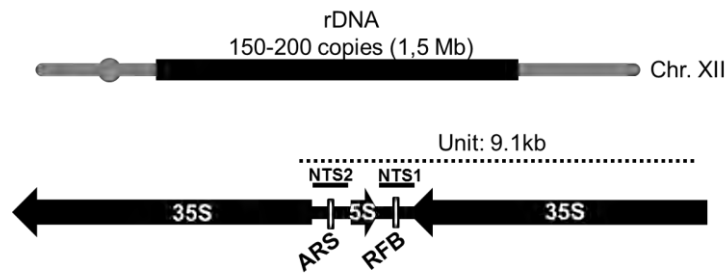


Figure 1.10: Structure of rDNA repeats in *S. cerevisiae*. The rDNA repeats, present in 150-200 copies on chromosome XII, are indicated. Each repeat contains the coding sequence for 35S rRNA and 5S rRNA, transcribed in the direction of the arrows, and NTS1 and NTS2 regions that are not transcribed. NTS1 and NTS2 contain the RFB and ARS, respectively.

Due to its special characteristics, the rDNA requires additional mechanisms to be segregated correctly. It has been demonstrated that the rDNA locus is the last region of the genome to be segregated during mitosis. Its segregation not only needs the pulling forces of the spindle but also its Cdc14-dependent condensation (Freeman et al. 2000; D'Amours et al. 2004; Sullivan et al. 2004; Torres-Rosell et al. 2004; Machín et al. 2005). At the time of anaphase Cdc14 dephosphorylates the RNA polymerase I subunit Rpa135, causing inhibition of the RNA polymerase I transcription. Switching off the rDNA transcription is necessary to allow condensin loading onto the rDNA, which then condense the locus short enough to avoid lagging DNA at the cytokinetic plane (Freeman et al. 2000; Lavoie et al. 2004; Machín et al. 2006; Clemente-Blanco et al. 2009). Furthermore condensin loading onto the DNA is essential to recruit Top2 to chromatin allowing removal of catenations from the DNA and correct segregation of chromosomes (Bhalla 2002).

1.6 Chromosome segregation failure as an origin of chromosome bridges and cancerous cells

If the cells fail to segregate chromosomes or repair DNA damage, there is a risk of daughter cells obtaining an incorrect or aberrant chromosomal endowment. If this happens chromosomal instability can occur. Chromosomal instability is a condition defined by frequent changes in chromosome structure and number.

Chromosomal instability is a key characteristic of tumorous cells and it is considered as one the first events in the transformation from a somatic to a cancerous cell (Colnaghi et al. 2011; Bakhoun & Compton 2012; Heng et al. 2013). The failure in

sister chromatids resolution has been proposed as an important trigger of chromosome instability, along with many other mechanisms that can seed genome instability. Once the cell has entered anaphase, if two sister chromatids remain attached, even partially, the mitotic division has three possible outcomes: aneuploidy of the non-resolved chromosome, formation of an anaphase bridge followed by breakage during cytokinesis, or cytokinesis abortion.

Chromosome bridges were first described by Barbara McClintock in maize cells (McClintock 1941). She observed that after exposing the cells to DNA damage, broken chromosomes appear. These chromosomes fused to one another giving rise to dicentric chromosomes. In the next cell division these chromosomes attached to both spindle poles which led to chromosome bridges. These bridges were broken during the cytokinesis and were formed again in the next interphase, thus starting a cycle of breakage-fusion-bridge. This process can cause the amplification of oncogenes or elimination of tumour suppressor genes.

The connection between tumorous cells, GCR and anaphase bridges warrants further research. There is a strong link between anaphase bridges and human tumour cells (Gisselsson 2003; Hoffelder et al. 2004; Payne et al. 2011) and it has been suggested as a clinical diagnostic tool to identify neoplastic tissues (Montgomery et al. 2003)

The mechanisms by which chromosome bridges are formed has attracted much attention from the scientific community in the last decade. This has led to the characterization of different kinds of anaphase bridges and the mechanisms that give rise to them.

From a cytological point of view, the anaphase bridges can be classified in two main classes. The first class comprises the chromatin anaphase bridges which are stained by conventional DNA dyes (e.g. DAPI). Chromatin bridges contain nucleosomes and other chromatin components. They are easily noticeable under the microscope and since the late 30's have been described as a potential origin of chromosome rearrangements (McClintock 1932; McClintock 1941). The second class of anaphase bridges are not stained with conventional dyes. They were first described in mammalian cells in 2007 and named as ultrafine anaphase bridges (UFBs). The UFBs do not contain histones and can only be revealed specifically by immunostaining of BLM (the human ortholog *S. cerevisiae* Sgs1), PICH (the human ortholog *S. cerevisiae* Rad26) or TopBP1 (the human ortholog *S. cerevisiae* Dpb11) or by BrdU incorporation followed by immunofluorescence staining. (Chan et al. 2007; Germann et al. 2014).

Thus far, at least three potential origins of UFBs are known to exist in higher eukaryotes. (1) Those that come from unreplicated regions of the genome. They are formed between a pair of FANC2/I foci that already exist on their sister chromatids in

late S-phase/G2 and are induced upon replication stress conditions. They localize mainly to templates that are difficult to replicate, known as fragile sites (Chan et al. 2009; Germann et al. 2014). (2) Those thought to come from unresolved catenanes and that do not contain the FANCD2/FANCI protein complex. They are predominantly found at centromeres and are induced by catalytic inhibitors of topoisomerase II. (Chan et al. 2007; Baumann et al. 2007; Chan & Hickson 2009; Germann et al. 2014). (3) In yeast, recombination intermediates have been demonstrated to lead to chromatin bridges and UFBs. Cells depleted for the SSEs Yen1 and Mms4 formed not only chromatin anaphase bridges detected by DAPI but also UFBs (García-Luis & Machín 2014) (see also Discussion).

2 Aims

The aims of this thesis are:

1. To elaborate a model strain to study the sources of chromosome bridges.
2. To determine if recombination intermediates are a source of anaphase bridges, at least those intermediates that can be enriched by deleting the structure-specific endonucleases (SSEs) involved in their final resolution.
3. To study the effect that these deletions have on cell cycle progression and chromosome segregation
4. To characterize the physical nature of the joint molecules that maintain sister chromatids together in the absence of SSEs
5. To determine how is regulated the resolution of joint molecules during the cell cycle.

3 Materials and Methods

3.1 Culture conditions for *S. cerevisiae*.

All the strains were stored in YPD/20% glycerol at -80°C in Eppendorf tubes. I first took the strain I wanted to work with and struck it on YPD plates. Then I normally incubated the plate in a 25°C incubator since I regularly worked with temperature sensitive strains (*cdc14-1* or *cdc15-2*). After three days I used a 1µl inoculating loop to inoculate a liquid culture. Then I grew the culture overnight in an air incubator at 200 rpm and 25°C. The following day the culture had an OD₆₀₀ of 0.8-1. Then, I diluted the culture to an OD₆₀₀ of 0.3 and grew it further for 3 hours. Then I diluted the cells to an OD₆₀₀ of 0.5 to start the experiment.

3.1.1 Asynchronous to telophase arrest

To block the cells in telophase in a *cdc14-1* or *cdc15-2* background I incubated the asynchronous culture at 37°C for 3 hours.

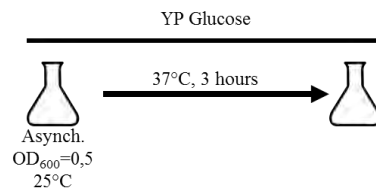


Figure 3.1: Schematic of the experiment of telophase block

3.1.2 G1 to telophase arrest

As a standard procedure for the G1-to-telophase experiments I synchronized the cells in G1 by adding the pheromone α -factor to a final concentration of 50 ng/ml to the asynchronous culture for 3 hours at 25°C, since the sexual type of all yeasts used in this case were MAT α and strains harboured the mutation *bar1 Δ* . Then I released the cells from G1 by washing the cells twice with YPD, and resuspended them in fresh YPD media containing 0.1mg/ml of pronase E. Finally I incubated the cultures at 37°C for 4 hours to inactivate *Cdc14-1* or *Cdc15-2* and induce a telophase arrest.

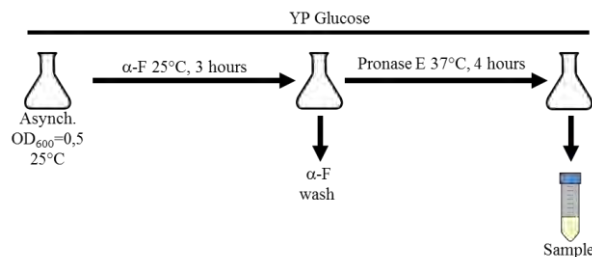


Figure 3.2: Schematic of the experiment of G1 to telophase arrest

For the G1-to-telophase experiments, where I induced the expression of Yen1 or Mms4 in telophase I followed the standard procedure for the G1-to-telophase experiments except that I grew the cells with raffinose as a carbon source all through the G1-to-telophase synchronous cell cycle, and I added galactose at 2% (w/v) at the time of the *cdc15-2* telophase block to induce the expression of Yen1 or Mms4 while keeping the yeast culture at 37°C.

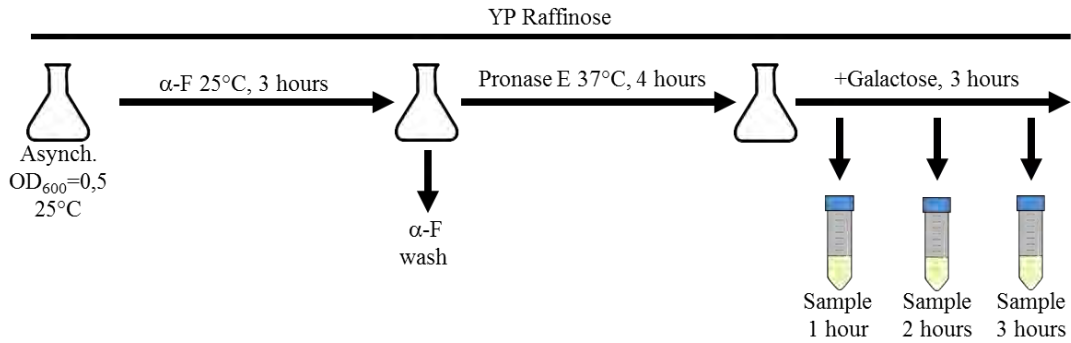


Figure 3.3: Schematic of the experiment of G1 to telophase arrest with induction of Yen1 or Mms4 in the telophase arrest

For the G1-to-telophase experiments where I induced the expression of Yen1-GFP in G1, I followed the standard procedure for the G1-to-telophase experiments except that I grew the cells with raffinose as a carbon source and supplemented the media with adenine 0.08 mg/ml. I supplemented the media with adenine to decrease the autofluorescence due to accumulation of metabolic intermediates of the adenine synthesis pathway, since these strains were *ade2*. Then I induced Yen1-GFP for 2 hours by adding galactose at 2% (w/v). I monitored the induction by fluorescence microscopy. Then I switched off the expression of Yen1 by adding glucose 2% (w/v). I continued all through the telophase arrest using a combination of raffinose 2% (w/v) + galactose 2% (w/v) + glucose 2% (w/v) as a carbon source. Throughout the G1-to-telophase cell cycle, I took samples at different timepoints for further analysis.

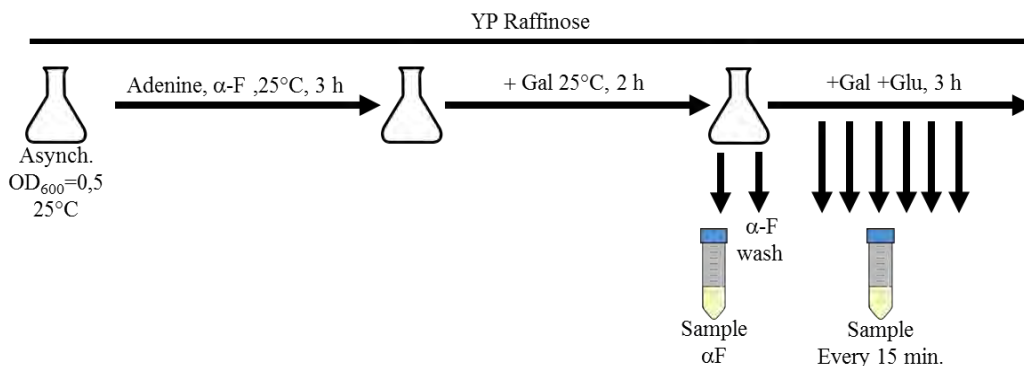


Figure 3.4: Schematic of the experiment of G1 to telophase arrest with induction of Yen1 in the G1 arrest

When I needed to induce DNA damage in the G1-to-telophase experiments I added MMS to the flask at the time of the G1 release. In the dose-response experiments, I split the cell cultures into ten flasks at the time of the G1 release. To 9 of the flasks I added 1:3 serial dilutions of MMS. The MMS final concentrations ranged from 0.1 to 0.000015% (v/v). I left a tenth culture without MMS as a control.

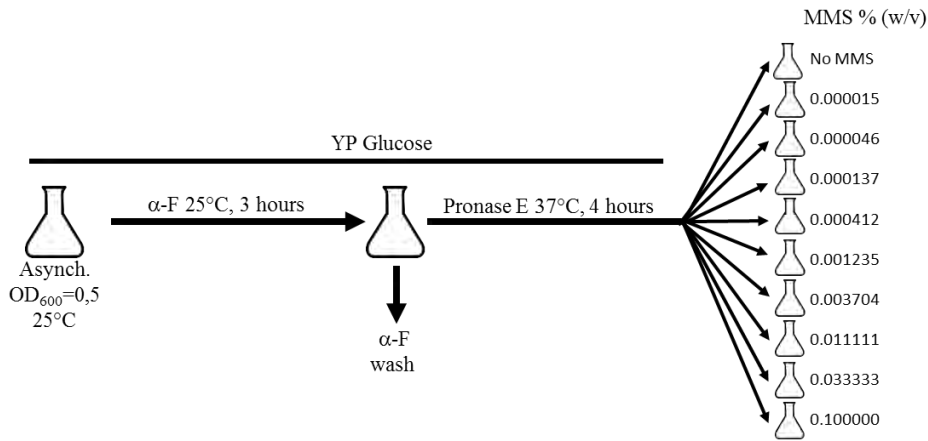


Figure 3.5: Schematic of the experiment of G1 to telophase arrest with DNA damage induction

3.1.3 G2 to telophase to G1

For the G2-to-telophase experiments where I induced Yen1-GFP in G2 block cells I grew the cells with raffinose as a carbon source all through the G2 arrest. I synchronized the cells in G2 by adding nocodazole (Nz) to a final concentration of 15 $\mu\text{g/ml}$ to the asynchronous culture for 3 hours at 25°C. Then I added galactose for 1.5 hours to induce the expression of Yen1-GFP. I shut off the expression by adding 2% (w/v) of glucose. Then I released the cells from the G2 arrest by washing out the Nz with fresh YP with a mix of raffinose 2% (w/v) + galactose 2% (w/v) + glucose 2% (w/v) as a carbon source and shifting the temperature to 37°C. For the telophase-to-G1 release, I shifted the temperature to 25°C and added 50 ng/ml of αF .

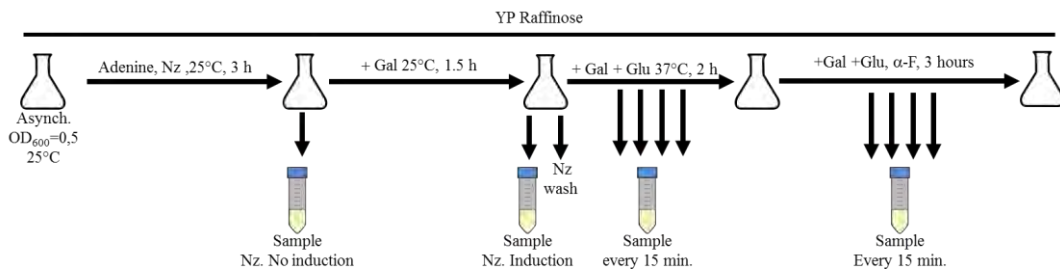


Figure 3.6: Schematic of the experiment of G2-to-telophase-to-G1 with induction of Yen1 in the G2 arrest

3.1.4 Transformant cells

After transformation, I plated the cells on solid media with the appropriate selective medium according to the marker used for selection. When I used auxotrophic markers for selection, I plated the cells on SC medium without the amino acid or nucleotide used for selection. To prepare this media I first mixed both Yeast Nitrogen Base and a commercial dropout lacking adenine, histidine, leucine, tryptophan and uracil at the recommended concentration according to supplier's instruction. Next, I added glucose (working concentration 2%) and required additional nutrients (working concentrations: 10 µg/ml adenine, 50 µg/ml histidine, 100 µg/ml leucine, 100 µg/ml tryptophan, 10 µg/ml uracil). When I used antibiotics for selection I grew cells in liquid YPD without antibiotics for 3 h after heat shock and before plating on selective medium containing the appropriate antibiotic (working concentrations used: 300 µg/ml G-418 sulphate, 300 µg/ml hygromycin B, 100 µg/ml nourseothricin and phleomycin 7.5 µg/ml).

3.2 Transformation of *S. cerevisiae*.

To generate new strains of *S. cerevisiae* I used the lithium acetate protocol adapted for frozen competent cells (Knop et al. 1999; Janke et al. 2004) with slight modifications.

3.2.1 Preparation of competent cells

I inoculated 50 ml of YPD and grew the culture at 25°C until cells reached an OD₆₀₀ of 1. Then, I harvested cells and discarded supernatant. I washed pellet once with 30 ml of sterile milliQ water and once with 10 ml of SORB solution. Finally, I resuspended cells in 350 µl of SORB solution and mixed it with 50 µl of carrier DNA (sonicated and denatured salmon or herring sperm DNA). I stored competent cells at -80°C until use.

3.2.2 Transformation

I put 50 µl of competent cells suspension and 8 µl of DNA (directly from either a PCR reaction or a digestion) into an Eppendorf tube. I added 348 µl of PEG solution to the cells/ DNA suspension and incubated it for 30 min at room temperature. I put the tube into a water bath pre-heated at 42°C and incubated it at 42°C for 15 min. After heat-shock, I harvested cells by centrifuging them at 2000 rpm for 3 min. I discarded the supernatant and, if selection was done using auxotrophic markers, I resuspended cells in 150 µl of water and plated them onto selective medium. If selection was done using antibiotics, I resuspended cells in 1 ml of YPD medium and I incubated them for 3 h at 25 °C before plating on selective medium.

3.3 Polymerase chain reaction

I performed PCRs to amplify DNA for transformation and to check clones after a yeast transformation. To amplify DNA, I used the T100™ Thermal Cycle (Bio-Rad). To amplify DNA for transformation, I used the commercial kit Expand™ Long Range (Roche Applied Science), following instructions as recommended by the supplier. For each PCR reaction, I used the following working concentrations: 2.5 mM of Mg²⁺, 0.5 mM of each dNTP, 0.2 μM of each primer, 3.3% (v/v) DMSO and 0.07 U/μl of enzyme with the provided reaction buffer. In general, I used the following program:

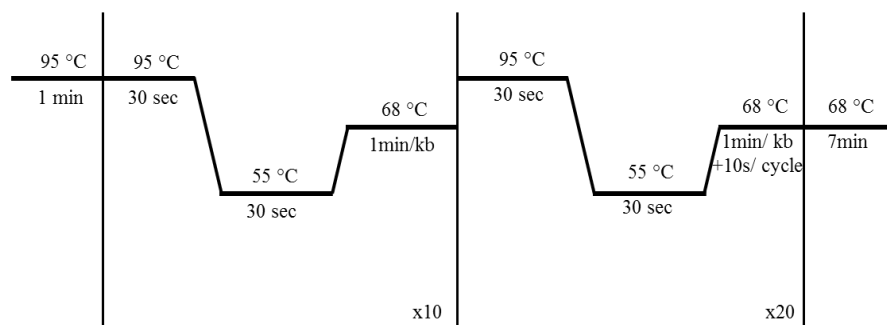


Figure 3.7: Schematic overview of the PCR program used to amplify DNA to transform yeast.

To check yeast transformation, I routinely made a genomic DNA preparation. For the PCR, I used the GoTaq enzyme (Promega), to a final concentration of 0.025 U/μl. I also used the provided reaction buffer and the working concentration of the rest of the reaction components was as follows: 2 mM of Mg²⁺, 0.2 mM of each dNTP, 3.3% (v/v) DMSO and 0.4 μM of each primer. I used the following program:

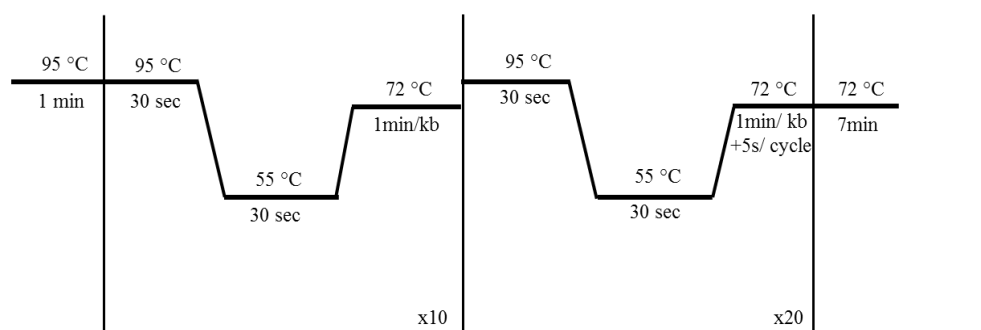


Figure 3.8: Schematic overview of the PCR program used to amplify DNA to check transformant clones.

3.4 Primers

Table 3.1: List of primers used in this thesis

Name	Sequence	Description
Yen1 (-493)-F	GGTAAAAATTTGGTATATGACCGC	To check <i>yen1</i> deletion
Yen1 (-401)-F	ACCTCTGACCACAATCCTGAGCA	To amplify <i>yen1</i> Δ for transformation.
Yen1 (+3680)-R	TCCGCAAAATCTGTGTCACCACCA	To check <i>yen1</i> deletion. To amplify <i>yen1</i> Δ for transformation. To check <i>YEN1</i> C- terminal tag
Yen1-F-pUG6	CATTTTACCTACTTGTATATTCTGGATACTG CACAAGAAACAGCTGAAGCTTCGTACGC	To delete <i>YEN1</i>
Yen1-R-pUG6	CAACTGTGGTGGCGGATTTTTGACGCTGT GCCCCGTTAACGCATAGGCCACTAGTGGAT CTG	To delete <i>YEN1</i>
YEN1 (+578)-R	CCCTCCCCACATGCGATTAC	To check Gal promotor insertion in <i>YEN1</i>
YEN1-S1	AGTTCTATTGCATTTTACCTACTTGTATATT CTGGATACTGCACAAGAAAATGCGTACGC TGCAGGTCGAC	To introduce Gal promotor in <i>YEN1</i>
YEN1-S4	CTGGAATCTTGCAGATATGGCTTCAAAAAT TCCCATATTTGTGAGACACCCATCGATGAA TTCTCTGTGC	To introduce Gal promotor in <i>YEN1</i>
YEN1-S2	GCGCGATCAACTGTGGTGGCGGATTTTTTG ACGCTGTGCCGTTAACTCAATCGATGAAT TCGAGCTCG	To tag <i>YEN1</i> in its C- terminal end
YEN1-S3	CAGTCGACCGGTTTGTAGCCTGTGACAGT GATAGCAGTAGCACTATTGAACGTACGCT GCAGGTCGAC	To tag <i>YEN1</i> in its C- terminal end
Mms4 (-398)-F	CAGTGACGTTTTTATTCTACACA	To check <i>mms4</i> deletion
Mms4 (-253)-F	ACACCTTTGCTGGTTGCTTGTGA	To delete <i>MMS4</i>
Mms4 (+3346)-R	ATCGAGCCTCTAAAGGACAGACTT	To check <i>mms4</i> deletion. To amplify <i>mms4</i> Δ for transformation.
MMS4 (+725)-R	TTGCCATGGATGTCCCATCTTC	To check Gal promotor insertion in <i>MMS4</i>
MMS4-S1	GTATGGATTATGGTATAGAATAATAGTAGTC ACATATTGCAGCTAGTTAAATGCGTACGCT GCAGGTCGAC	To introduce Gal promotor in <i>MMS4</i>
MMS4-S4	CTGGCATCGTTTCTTGAATCTTGTCTCAA CAAAATCAACGATCTGGCTCATCGATGAAT TCTCTGTGC	To introduce Gal promotor in <i>MMS4</i>
Rad52-F(-150)	TAAGAAAAGACGAAAAATATAG	To amplify <i>rad52</i> Δ for transformation.
Rad52-R(+150)	AAGTAAATATTAATACGACAC	To amplify <i>rad52</i> Δ for transformation. To check <i>rad52</i> deletion
Rad52(-332)F	GTCTTGACACACGTCGCTAAA	To check <i>rad52</i> deletion.
5' CDC14 (-275)	AGCTATGAGCCTGATAACGTGAGTC	To amplify <i>cdc14-1</i> allele
3' CDC14 (+2000)	CGATTTTAAAGATTGGCATATCGAG	To amplify <i>cdc14-1</i> allele
3' Cdc15 (+3179)	TTTAACAAAAAGCCACCTTCTAGAGTC	To amplify <i>cdc14-2</i> allele
5' Cdc15 (+818)	ACTCTACCGAAAATGTGAAGGTCGAC	To amplify <i>cdc14-2</i> allele
SPC42-S2	AGAACGCTTTAAGAATGCGCCATACTCCTT AACTGCTTTTTAAATCATCAATCGATGAATT CGAGCTCG	To tag <i>SPC42</i> in its C- terminal end
SPC42-S3	CTGAAAATAATATGTCAGAAACATTCGCAA CTCCCACTCCCAATAATCGACGTACGCTG CAGGTCGAC	To tag <i>SPC42</i> in its C- terminal end
spe42(+770)-F	AGCTGAAGCGTGTGCAAGAA	To amplify <i>SPC42</i> tagged in its C- terminal end. To check <i>SPC42</i> C- terminal tag
spe42(+1402)-R	TGACACTAACCATCCACCATTT	To amplify <i>SPC42</i> tagged in its C- terminal end
spe42(+1530)-R	ACTTAGATGAAAGTTGTTGGT	To check <i>SPC42</i> C- terminal tag
Slx4 5' (-500)	TTTAGCGAAAGATTTTTATTCA	To amplify <i>slx4</i> Δ for transformation.
Slx4 3' (+500)	ATCGTGCAAGAATTCAGGACGAA	To amplify <i>slx4</i> Δ for transformation. To check <i>slx4</i> deletion
5-SLX4 (-600)	TTGTACCTTTAGCTATGATCTTAGC	To check <i>slx4</i> deletion
yITS1-F	GTGAACCTGCGGAAGGATC	To make ITS fluorescein-labelled probe
yITS2-R	CCTACCTGATTTGAGGTCAAAC	To make ITS fluorescein-labelled probe

3.5 DNA preparations

3.5.1 High molecular weight-DNA preparation

As large DNA molecules are extremely fragile and break down into pieces in standard manipulations of molecular biology, they should be prepared in a solid support such as agarose plugs. Thus, for the preparation of yeast chromosome sized-DNA I embedded cells in low melting point agarose plugs prior to extract DNA. For this purpose, I collected 4ml of culture at OD₆₀₀ of 1. I harvested cells and washed the pellet twice with 50 mM EDTA (pre-chilled to 4°C). I resuspended cells in 10 µl of pre-chilled 50 mM EDTA. Then, I mixed this cell suspension with 20 µl of solution SB1 and 60 µl of LMPA solution pre-heated at 50°C. When suspension was perfectly homogeneous, I dispensed it onto plug moulds. After solidified, I put plugs into tubes filled with solution SB2. I incubated tubes overnight at 37°C. Next, I replaced solution SB2 for solution SB3 and I incubated tubes overnight at 37°C. Finally, I retired completely solution SB3 and I added plug storage solution. Plugs were stored at -20°C until used.

3.5.2 Genomic DNA preparation from *S. cerevisiae*

To perform a genomic DNA (gDNA) extraction to check clones by PCR, I performed a standard phenol-chloroform genomic DNA extraction. For this purpose, I inoculated a single colony in 1 ml of selective medium and I grew culture until stationary phase. Then, I harvested cells and I washed the pellet with milliQ water. I resuspended the pellet in 200 µl of breaking buffer, 200ul of phenol: chloroform: isoamyl alcohol (25:24:1, v/v) and added 200 µl of 710-1,180 µm-acid glass beads (Sigma-Aldrich). I vortexed suspension for 2 min to mechanically break the cells. After breakage, I added 200 µl of TE 1X. Then I transferred the lysate to a new tube and centrifuged it for 5 minutes at 13,000 rpm. After centrifugation I took the upper aqueous phase and transferred it to a new tube. To this tube I added 1 ml of ethanol 100% and centrifuged it 5 min at 13000 rpm. After centrifugation I removed all the ethanol and let the DNA pellet to dry at RT. Then I resuspended the DNA in 50 µl of sterile milliQ water and added 1µg/ml of RNase A. I incubated for 15 min and stored suspension at -20°C until use.

3.6 DNA electrophoresis

3.6.1 Agarose electrophoresis

I used this type of electrophoresis to routinely check PCR products and when required gDNA extractions. I usually loaded 1-5 μ l of sample and I used Loading Dye (Promega) as loading buffer. I adjusted the final concentration of agarose (ranging from 0.7 to 2%, w/v, in 1X TAE) depending on the expected DNA size, using 1X TAE as running buffer.

Gels were stained in a solution of 50 μ g/ml of ethidium bromide in milliQ water to visualize DNA bands under UV light by using the *Gel Doc* system (Bio-Rad).

3.6.2 Pulsed-Field Gel Electrophoresis

I used this technique to assess the integrity of *S. cerevisiae* chromosomes. There are several types of PFGE, varying in the electric field applied. During this thesis, the system I used was CHEF (Chu et al. 1986), and, specifically, the system CHEF-DRIII (Bio-Rad).

All PFGE performed during this thesis were done on an 0.8% (w/v) agarose gel in 0.5X TBE, and using 0.5X TBE at 12°C as running buffer. To visualize all chromosomes, I used the following settings:

- voltage.- 6 V/cm.
- switching time.- 80 s (initial) to 150 s (final).
- angle.- 120°.
- running time.- 20/40 h.

To assess the size of the cXII, I used the following settings

- voltage.- 3 V/cm.
- switching time.- 300 s (initial) to 900 s (final).
- angle.- 120°.
- running time.- 68 h.

Gels were stained in a solution of 50 µg/ml of ethidium bromide in milliQ water for 45 min and de-stained for 20 min in milliQ water, prior to visualize DNA bands under UV light by using the *Gel Doc* system (Bio-Rad).

3.6.3 Two-dimensional neutral-neutral DNA electrophoresis (NN-2D)

I used DNA extracted from yeast embed in low melting point agarose plugs (see section 3.5.1). I washed the agarose plugs with 1mg/ml of Pefabloc SC (Roche Applied Science) for 1 hour to inhibit the remaining of proteinase K used during the DNA extraction process. Then I wash the plugs for 1 h twice with TE 1X to remove the Pefabloc. Next I digested the plug overnight with 1500 U/ml of the restriction enzyme BglIII (New England Biolabs).

After this I cut one-half of the plug and loaded it onto a 0.35% (w/v) agarose gel prepared with TBE 1X (Brewer & Fangman 1988). I ran the first dimension at 0.8 V/cm for 24 h. Next, I sliced the lane and trimmed it to take 1 cm under the weight of the restriction fragment and 2 cm over the double of the weight of the restriction fragment. I re-oriented it 90 ° anticlockwise and ran the second dimension. For the second dimension I prepared 1% (w/v) agarose with TBE 1X, cooled it down to 60 ° C and poured it in the tray with the slice from the first dimension. I ran the gel at 6 V/cm for 9 h under the presence of 0.3 µg/ml of ethidium bromide in both the gel and the running buffer. Importantly, I left the buffer recirculating through a cooling system to keep constant the running temperature at 16 °C. Then the gel was transferred to a positively charged membrane (Roche) for Southern blot analysis.

3.6.4 Three-dimensional neutral-neutral-alkaline DNA electrophoresis (NNA-3D)

In the case of NNA-3D electrophoresis (Lucas & Hyrien 2000), the agarose gel that I obtained after the NN-2D electrophoresis was first soaked in 0.04N NaOH plus 2 mM EDTA five times for 1 h each, to allow alkaline equilibration. Then, I trimmed the gel to cut only the region where the DNA was expected to run according to the running time, temperature and gel percentage. Next I ran a third electrophoresis in the same orientation as the first one was. I ran this third dimension at 0.8V/cm for 38 h at 16 °C using alkaline buffer with the same composition than the one used for the alkaline equilibration . Finally, this 3D gel was used for Southern blot analysis

3.6.5 DNA modifying enzymes used on agarose plugs

3.6.5.1 RuvC

To treat the agarose plugs with RuvC enzyme (Abcam) I used a procedure similar to one used elsewhere (Wehrkamp-Richter et al. 2012). I first wash twice (for 30 min each) the plug in 300 µl of RuvC buffer. The first wash was done at RT and the second at 4 °C. Then I digest the plugs by adding 150 µl of RuvC buffer with 3 µg of RuvC. I incubated it for 4 h at 4 °C and then 1 h at 55 °C. As a control I did the same procedures in parallel with another plug but without enzymes. Then, I loaded this plug onto an agarose gel to start a NN-2D electrophoresis.

3.6.5.2 T4 DNA ligase

To treat the agarose plugs with T4 DNA ligase enzyme (Roche) I employed an adaptation of the RuvC protocol for this enzyme, taking also into account general protocols for the T4 ligase. I wash twice (for 30 min each) the plug in 300 µl of T4 ligase buffer. The first wash was done at RT and the second at 4 °C. Then the plugs were incubated in 150 µl of buffer with 3,500 cohesive end units of T4 DNA ligase either at 19 °C or 37 °C. As a control I did the same procedures in parallel with another plug but without enzymes. Then I load this plug onto an agarose gel to start a NN-2D electrophoresis.

3.7 Southern-blot analysis

After visualization of the PFGE or NN-2D gels stained with ethidium bromide, DNA was transferred from the gel to a membrane, in order to detect specific regions by using non-radioactive labelled probes.

3.7.1 Probe synthesis

Probes were labelled with fluorescein using the commercial kit Fluorecein-High Prime kit (Roche Applied Science). As a starting point I used a heat denaturalized PCR product from which I wanted to generate a probe. With this method, the complementary DNA strand of denatured DNA, (in my case a PCR product) is synthesized by Klenow polymerase using the 3'-OH termini of the random oligonucleotides as primers. The Klenow polymerase introduces Fluorescein-12-dUTP in the new DNA synthesized molecules. I did the labelling reaction according to supplier's instructions. After the labelling reaction I cleaned the probe with QIAquick PCR Purification Kit (Qiagen), to eliminate small labelled molecules that can increase background during the detection process.

3.7.2 DNA transfer from the gel to the membrane

Before the transfer I washed the gel with milliQ water for 5 min. Then I deproteinized it with 0.4% HCl for 10 min. Next, I washed it again with milliQ water for 5 min and soaked it in denaturing solution for 30 min. After a brief washing with water, I equilibrated gels with neutralization solution for an additional 30 min. Finally I did an overnight upward capillary transfer onto a positively charged membrane (Roche) using 20X SSC as transfer buffer. After the transfer the DNA was crosslinked to the membrane using a Stratalinker UV crosslinker set up at 1200 J/cm². I stored the membranes between Whatman papers until used.

In the case of PFGE I carried out a saline downwards transference onto positively charged membrane. This procedure improved the transference of the wells to the nylon membrane.

3.7.3 Probe hybridization and detection

First, I washed briefly the membranes with 2X SSC. Then after introducing the membrane in the hybridization tube I added 50 ml of blocking solution and incubated it at 65°C for 2 h. Next I added the probe, previously denatured, to the blocking solution and incubated it overnight.

Prior to detection I washed the membranes twice at 65°C with primary washing solution for 10 min. I did two extra washes with secondary washing buffer at 65°C for 5 min each. Then I rinsed the membrane in AB buffer for 5 min at RT. For the detection I block the membranes in AB buffer with 1% of milk (w/v) for 2 h. Next I washed it with 50 ml of AB buffer for 5 min and proceed to incubate it with 250 ml of AB buffer with anti-fluorescein antibody conjugated to alkaline phosphatase (1/250,000 dilution) for 1 h. After this, I wash the membrane three times for 10 min each adding 300 ml of AB buffer with 0.2% Tween.

Finally I added CDP-Star Chemiluminescent Substrate (Sigma) to the membrane and after eliminating the excess of CDP-Star. Next in the case of being a PFGE I exposed the membrane to a Lumi-Film Chemiluminescent Detection film (Roche Applied Science) to then developed the film in a Konica SRX-201 machine. In the case of NN-2D and NNA-3D I exposed the membrane in a ChemiDoc MP apparatus (BioRad)

3.7.4 Stripping

For the stripping with fluorescein labelled probes I used a harsh treatment based in pouring boiling 0.1 % SDS onto the blot and allowing it to cool to room temperature. I did this treatment twice to ensure elimination of the probe used previously. Finally, I

washed the membranes with 2X SSC solution, prior to block and hybridize with a new probe.

3.7.5 Signal quantification

For quantifications I used the software ImageLab (BioRad). I picked a time exposure in all cases (360 s) where the signal of the X-shaped molecules was visible but not saturated. I then picked another time exposure for all linear 1N DNA signals where they were not saturated either (1 s). The 1N signals include the monomer spot and the smear that appeared during the first dimension. Finally, I calculated the quotient [background-subtracted intensity of the Xs/ background-subtracted intensity of the 1N]. To calculate the relative amount of discontinuous HJs over the whole of X-shaped molecules, I directly quantified the ssDNAs resolved from the X-shaped structure after the NNA-3Ds according to the following formulae: [background-subtracted intensity of the full-length ssDNA line/background-subtracted intensity of the arc for smaller ssDNAs].

3.8 Western blot analysis

3.8.1 Protein extraction

I used an equivalent of 5 OD₆₀₀ of culture to extract total proteins by using an alkaline procedure. I harvested yeast cells and discarded the supernatant. I washed cells with milliQ water, resuspended the pellet in 100 µl of SDS 2% and added 100 µl of 180 µm-acid glass beads (Sigma-Aldrich). Then I vortexed the sample for 2 min and added 100 µl of 2X Laemmli buffer. Next, I boiled the samples for 1 min and briefly centrifuged them. Finally I loaded 20 µl of the sample.

3.8.2 SDS-PAGE

I performed protein acrylamide electrophoresis in one dimension under denaturing conditions (SDS-PAGE). Proteins were separated by using an 8 % acrylamide gel (acrylamide/bisacrylamide 29:1 proportion). The electrophoresis system I used was Mini-Protean (Bio-Rad), using the running buffer and conditions recommended by the supplier (60 mA/gel).

3.8.3 Protein transfer and detection

After electrophoresis, I transferred proteins from gel to an Immobilon-P PVDF membrane (Millipore) by using the humid transfer system Mini Trans-Blot (Bio-Rad). First, I removed the stacking gel and then I washed the separating gel with transfer

buffer before the transfer. Next, I did an overnight transfer at 30 V and 4 °C by using conditions recommended by Bio-Rad. Then, I blocked the membranes with milk 5% (w/v) in TBST for 1 h at RT. After the blocking I incubated the membrane with the primary antibody anti- GFP from rabbit at 1:8,000 (Abcam) in 5% milk. I did 3 washes with TBST (10 min each) and incubated the membrane with the secondary antibody anti-rabbit-AP (1:50,000) (Promega) in 5% milk/TBST for 1 h. Finally, I did 3 additional washes with TBST (10 min each) and spread 500 µl of Amersham ECL Prime Western Blotting Detection Reagent (GE Healthcare) over the membrane. As a last step I exposed the membranes to a Lumi-Film Chemiluminescent Detection film (Roche Applied Science) and develop them in a Konica SRX-201 machine.

3.9 Microscopy

For the visualization and imaging of cells, I used the Leica DMI6000B epifluorescence microscope (Leica), using a 63X/1.30 immersion objective, immersion oil with a refractive index of 1.515-1.517, the appropriate filter cube for each tag (table 2) and an ultrasensitive DFC350 digital camera. Before imaging, I froze the cells pellet at -20 °C for 48 h. This was done to store the cells and to increase the permeability of the DAPI staining afterwards. Then I defrost the cells and stained them using DAPI at 0.05 µg/ml and Triton X-100 0.01 % (v/v) as final concentration. When I needed to do *in vivo* fluorescence microscopy I did it in freshly harvested cells without any staining.

Table 3.2: : List of filter cubes used during this thesis.

Filter Cube	Fluorochrome	Excitation range	Excitation filter	Dichromatic mirror	Supression filter
A	DAPI	UV	BP 360/40	400	BP 470/40
CFP	CFP	violet / blue	BP 436/20	455	BP 480/40
RFP	RedStar	green	BP 546/12	560	BP 605/75
YFP	YFP, GFP	blue	BP 500/20	515	BP 535/30

For each image, I first captured series of 20 z-focal plane images (0.3 µm depth between each consecutive image) to detect chromosomes tagged with the *tetO/tetR* system or 10 z-focal plane images (0.6 µm depth between each consecutive image) to monitor live cells. Then, I processed them using the ImageJ software (Abràmoff et al. 2004). When measurements where required I did them using 2D maximum intensity projections. Intensity, gain and exposure settings for each single fluorescent protein can be found on table 3.

Table 3.3: List of microscope settings used for capturing images for each tagged protein and DAPI used in this thesis.

Protein/ compound	Exposure (s)	Gain	Intensity
DAPI	0.02	1.5	1
TetR-YFP	1	2.5	4
LacI-CFP	1	7	4
Yen1-GFP	1	7	5
Spc42-RFP	2	7	4

*Gain can vary from 1 to 10. Intensity can vary from 1 to 5

3.10 Flow cytometry

To determine DNA content of cells, I pelleted 1 ml of culture of each time point and resuspended it in 500 μ l of 75 % ethanol (v/v). Then I centrifuged suspension at 13,000 rpm for 1 min and I discarded supernatant. Then I centrifuged again for 10 seconds and removed the excess of ethanol. Next, I resuspended the pellet in 250 μ l of 1X SSC with 10 μ g/ml RNase A and I incubated it overnight at 37°C. The day after, I added 50 μ l of 1X SSC with proteinase K (working concentration: 1 mg/ml) and I incubated it at 50°C for 1 h. Finally, I added 3 μ g/ml of propidium iodide in 1X SSC and I incubated it at room temperature for 1 h. I stored the samples at 4 °C until use.

Prior to analysis, I sonicated samples for 5 s in a water bath sonicator (Branson). I analysed around 200,000 events, by using CellQuest Pro software (BD Biosciences)

4 Results

4.1 Article 1: Nondisjunction of a Single chromosome leads to breakage and activation of DNA damage checkpoint in G2.

In the first article included in this thesis, the cellular response after the resumption of the cell cycle from a *cdc14-1* block was studied. I specifically characterized the chromosome bridges that appear in a *cdc14-1* block. I measured the segregation status of chromosome V, XII and XIV telomeres. I determined that telomeres of chromosomes other than the one on the right arm of cXII (cXIIr) barely missegregated after a *cdc14-1* release. This characteristic makes the *cdc14-1* mutant an outstanding model to study the cellular response to the presence of anaphase bridges comprised of just one chromosome during mitosis.

As a parallel control for this experiments I used a *cdc15-2* strain where I measured the segregation status for the same loci than for the *cdc14-1* mutant. I determined that in a *cdc15-2* block all the chromosome telomeres are segregated correctly. I used the cXIIr tagged *cdc15-2* strain as a reference strain for the following study of this thesis.

Nondisjunction of a Single Chromosome Leads to Breakage and Activation of DNA Damage Checkpoint in G2

Oliver Quevedo¹, Jonay García-Luis¹, Emiliano Matos-Perdomo¹, Luis Aragón², Félix Machín^{1*}

¹ Unidad de Investigación, Hospital Universitario Nuestra Señora de Candelaria, Santa Cruz de Tenerife, Spain, ² Cell Cycle Group, MRC Clinical Sciences Centre, Imperial College London, London, United Kingdom

Abstract

The resolution of chromosomes during anaphase is a key step in mitosis. Failure to disjoin chromatids compromises the fidelity of chromosome inheritance and generates aneuploidy and chromosome rearrangements, conditions linked to cancer development. Inactivation of topoisomerase II, condensin, or separase leads to gross chromosome nondisjunction. However, the fate of cells when one or a few chromosomes fail to separate has not been determined. Here, we describe a genetic system to induce mitotic progression in the presence of nondisjunction in yeast chromosome XII right arm (cXIIr), which allows the characterisation of the cellular fate of the progeny. Surprisingly, we find that the execution of karyokinesis and cytokinesis is timely and produces severing of cXIIr on or near the repetitive ribosomal gene array. Consequently, one end of the broken chromatid finishes up in each of the new daughter cells, generating a novel type of one-ended double-strand break. Importantly, both daughter cells enter a new cycle and the damage is not detected until the next G2, when cells arrest in a Rad9-dependent manner. Cytologically, we observed the accumulation of damage foci containing RPA/Rad52 proteins but failed to detect Mre11, indicating that cells attempt to repair both chromosome arms through a MRX-independent recombinational pathway. Finally, we analysed several surviving colonies arising after just one cell cycle with cXIIr nondisjunction. We found that aberrant forms of the chromosome were recovered, especially when *RAD52* was deleted. Our results demonstrate that, in yeast cells, the Rad9-DNA damage checkpoint plays an important role responding to compromised genome integrity caused by mitotic nondisjunction.

Citation: Quevedo O, García-Luis J, Matos-Perdomo E, Aragón L, Machín F (2012) Nondisjunction of a Single Chromosome Leads to Breakage and Activation of DNA Damage Checkpoint in G2. *PLoS Genet* 8(2): e1002509. doi:10.1371/journal.pgen.1002509

Editor: Soni Lacey, Indiana University, United States of America

Received: September 28, 2011; **Accepted:** December 8, 2011; **Published:** February 16, 2012

Copyright: © 2012 Quevedo et al. This is an open-access article distributed under the terms of the Creative Commons Attribution License, which permits unrestricted use, distribution, and reproduction in any medium, provided the original author and source are credited.

Funding: This work was supported by Spanish Ministry of Science and Innovation through the “Ramón y Cajal” program (2005/1354 to FM); Instituto de Salud Carlos III (06/1211, 09/00106); Fundación Canaria de Investigación y Salud (06/21, 08/42 to JG-L); Spanish Ministry of Education (AP2009-2511 to JG-L); and Agencia Canaria de Investigación, Innovación y Sociedad de la Información (BOC-A-2010-023-596 to OQ). All financial support co-financed by the EU-FEDER. LA laboratory is supported by the Medical Research Council (MRC) of the UK. The funders had no role in study design, data collection and analysis, decision to publish, or preparation of the manuscript.

Competing Interests: The authors have declared that no competing interests exist.

* E-mail: fmacconw@gmail.com

Introduction

Chromosomes lagging or bridging during anaphase are believed to be one of the main sporadic causes of cytokinesis failure, which leads to tetraploid cells with multicentrosomes, a hallmark of early tumorigenesis [1,2]. Conversely, if these anaphase bridges break apart, chromosomes could enter the so-called breakage-fusion-bridge cycle [3–5], which has been related to oncogene amplification and intratumour heterogeneity [6–8]. Carcinogens such as cigarette smoke, dysfunction of key cancer genes, bacterial toxins, and, paradoxically, many antitumour chemotherapeutic treatments (e.g. topoisomerase inhibitors) are known to cause anaphase bridges [9–12].

Chromosomes bridge in anaphase because they have either more than one centromere or problems in resolving the sister chromatids. Most of our knowledge on the biology of sister chromatid resolution comes from studies in yeast. In *Saccharomyces cerevisiae*, as in the rest of eukaryotes, sister chromatids are kept together after replication by both the cohesin complex and DNA-DNA topological entanglement arising from DNA metabolism

(i.e., catenations) [13]. During anaphase onset, cohesion is lost through the regulated cleavage of cohesin by separase [14], and catenations are removed by the combined actions of condensin [15] and type 2 topoisomerase (Top2) [16]. Yeast mutants for any of these players show knotted nuclear masses in anaphase with trailing distal chromosome regions which cannot be resolved in otherwise bipolarly attached centromeres [15–20]. Despite these anaphase problems, all these mutants often perform cytokinesis, leading to a “cut” phenotype characterized by aneuploid daughter cells carrying broken chromosomes [14,17,21]. Not surprisingly, many daughter cells are not able to enter a new cell cycle after cytokinesis [14–16]. This has precluded use of those mutants as tools to follow up the short-term consequences in the progeny of anaphase bridges formed by unresolved sister chromatids.

The last genomic region to get resolved in yeast is the ribosomal DNA array (rDNA) [19,22–24]. Importantly, resolution at this locus depends on a third player, besides condensin and Top2: the late mitotic phosphatase Cdc14 [22–27]. This is because Cdc14 inactivates transcription by RNA polymerase I in late anaphase, which allows the loading of condensin to the rDNA, its

Author Summary

When cells divide they must segregate copies of their chromosomes to each of their daughters. A particular harmful situation arises when those copies are glued to each other (i.e., nondisjunction) at the moment of division. Previously, it has been possible to genetically favour this scenario, yet it has been difficult to limit the extent of nondisjunction to a single chromosome. We have developed and studied a yeast model where we control nondisjunction of one of its sixteen chromosomes. We show that dividing cells manage to complete nuclear and cell fission and therefore break that chromosome. We further show that new daughter cells then trigger a DNA damage response, yet only after they initiate a new round of replication. Remarkably, an uncommon repair strategy seems to be used to deal with this damage, which involves part of the homologous recombination machinery (i.e., RPA complex and Rad52) but lacks its primary sensor Mre11. Importantly though, both daughter cells arrest their cell cycle in G2 to prevent further damage from occurring. After a while, the cell that still carries an entire copy of the chromosome often survives, leading to aberrant forms of the chromosome in the progeny.

condensation and further resolution with the help of Top2 [22,23,27–31]. Other findings also suggest that these Cdc14 actions could serve to finish up replication within this locus [32,33]. When Cdc14 is inactivated by means of thermosensitive conditional alleles such as *cdc14-1*, the anaphase segregation problem is much milder than that observed for the other aforementioned mutants. Indeed, *cdc14-1* cells get arrested in telophase with the bulk of the nuclear masses segregated yet the rDNA bridging between mother and daughter cells [23,24].

In a previous report we demonstrated that re-activation of the thermosensitive protein Cdc14-1 restores its cell cycle functions and is enough to exit mitosis [28]. Nevertheless, a portion of cells do this in spite of failing, in the end, to segregate the rDNA. Because little is known about the behaviour and fate of cells that commit to a new cell cycle once they have failed to resolve sister chromatids, we decided to address these questions taking advantage of this *cdc14-1* re-activation phenotype. Herein, we show that *cdc14-1* release leads to severing of the rDNA anaphase bridge and a new Rad9-dependent G2/M arrest. We followed the DNA damage response (DDR) in these cells and observed that they elicit a Rad52 long-lasting response that is independent of Mre11. We further discuss how our system provides a model for the study of DNA double strand breaks (DSB) where the ends finish up in different compartments (i.e., “one-ended”).

Results

Release from a *cdc14-1* telophase block leads to a pre-anaphase arrest in the following cell cycle

Since the pioneering works by Hartwell and collaborators on yeast cell cycle control, it is known that conditional mutants for two essential genes, *CDC14* and *CDC15*, give a telophase block with mostly binucleated dumbbell cells [34]. Nevertheless, we also now know that at least some *cdc14* mutants have problems in the resolution and segregation of chromosomes during anaphase [22–24,33]. As for the rDNA-bearing chromosome XII right arm (cXIIr), the telophase block elicited by the *cdc14-1* allele prevents sister chromatid resolution, and therefore segregation, of regions that extend from somewhere within the large rDNA locus to the

end of that chromosome arm [23]. Consequently, cXIIr forms an anaphase bridge between the connected daughter nuclei (Figure 1 for a scheme, “a” phenotype). In a previous work, we surprisingly found that, after reactivating the thermosensitive Cdc14-1 protein, cells were able to resume the cell cycle in spite of often failing to complete the resolution and segregation of such distal regions [28]. In general, around 50% of the cells coming out of a *cdc14-1* block do not change their missegregation pattern, whereas the other 50% fully complete segregation of cXIIr (Figure 1, “a” & “b” phenotypes respectively).

We began our study by closely monitoring the cell cycle that follows *cdc14-1* release in a strain where the cXIIr telomere is labelled (*tetO:1061*). We further included a side-by-side isogenic *cdc15-2* strain as a control, after confirming that the cXIIr is fully segregated in its telophase block (Figure S1). In the same experiment we monitored: (i) the budding pattern after the release (Figure 2A); (ii) the morphological changes of the nuclei and the overall resolution and segregation of the cXIIr telomere (Figure 2B and 2C); (iii) the changes in DNA content by flow cytometry (i.e., bulk replication) (Figure 2D); and (iv) chromosome behaviour in a pulsed-field gel electrophoresis (PFGE) (i.e., individual chromosome replication and integrity) (Figure 2E). For the first two, we

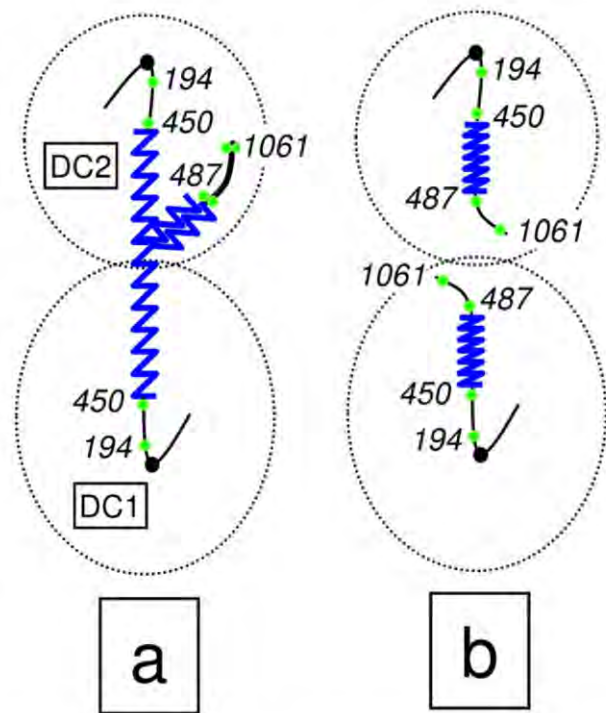


Figure 1. Scheme of the chromosome XII anaphase bridge (cXIIr) in a *cdc14-1* telophase block. According to our previous findings [23,28], two major phenotypes are found at either the telophase block or after the release (see main text for details): (a) non-disjunction goes from within the rDNA to the telomere of the chromosome XII right arm (cXIIr); and (b) the chromosome is fully segregated. Chromosome positions of *tetOs* used to determine the extent of non-disjunction are numbered and shown as green dots; rDNA is depicted as a serrated blue line; and thicker lines indicate non-resolved sister chromatids. “DC1” depicts the daughter-to-be cell which carries just one copy of the resolved part of chromosome XII (from left telomere to somewhere within the rDNA); whereas “DC2” carries one entire sister chromatid plus the unresolved part of the other one (from somewhere within the rDNA to the right telomere). doi:10.1371/journal.pgen.1002509.g001

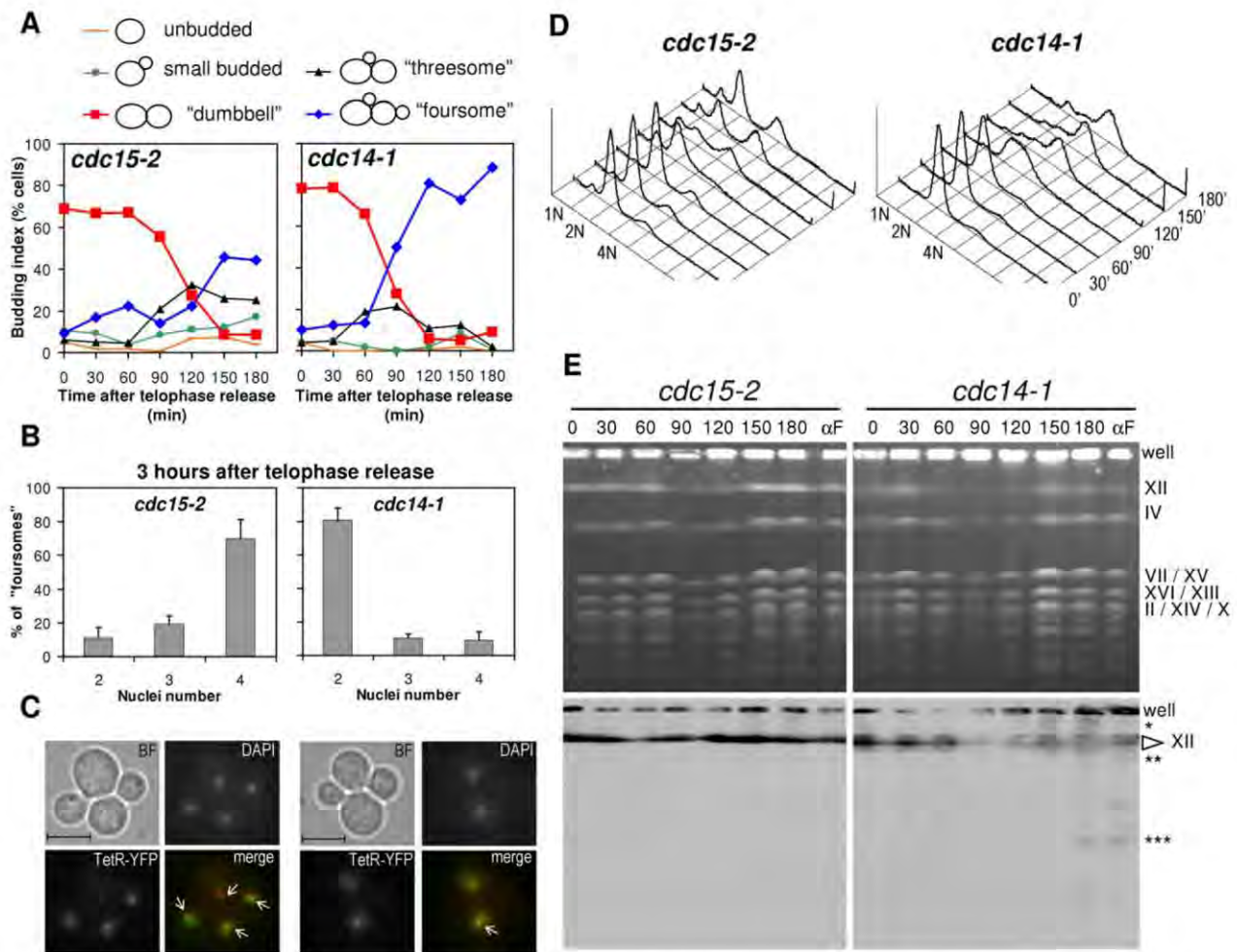


Figure 2. Cells arrest in G2 after a *cdc14-1* release with chromosome XII integrity compromised. Strains FM588 (*cdc15-2 tetO:1061 TetR-YFP*) and FM322 (*cdc14-1 tetO:1061 TetR-YFP*) were arrested in telophase by incubation at 37°C for 3 hours (time=0 minutes) and then released from the arrest by dropping the temperature to 25°C. Samples were taken every 30 minutes for 3 hours and analysed by microscopy (A, B & C), flow cytometry (D) and PFGE (E). (A) Time course of cell morphology after the release. Note the transition from the telophase arrest (dumbbell cells) to the main foursome category. (B) Number of nuclei in foursomes 3 h after the release. Note how *cdc15-2* has entered a new anaphase (four nuclei) while *cdc14-1* is still stuck in a pre-anaphase stage (2 nuclei). The charts represent mean \pm SEM, $n=3$ (one of which is the particular experiment used for the rest of the figure). (C) Micrographs of the main foursome types observed for *cdc15-2* and *cdc14-1* at that time point. We used the *tetOs:1061* to assess cXIIr segregation (main text for details). White arrows point to *tetOs*. Bar, 5 μ m. (D) Flow cytometry analyses of the releases. Peaks of DNA content (1 N, 2 N & 4 N) are indicated. Telophase arrest gives a 2 N peak. 4 N peak appears in foursomes provided each daughter replicates its DNA. Note how the 4 N peak is reached after the *cdc14-1* release. (E) Pulsed-field gel electrophoresis of the same releases. Note that: (i) most chromosomes were replicated after the *cdc14-1* release (chromosome bands faded away at 90' and reappeared by 150'); (ii) chromosome XII band specifically faded away from time 30' in *cdc14-1* and never reappeared fully; and (iii) lower (single-asterisk) and faster (double- and triple-asterisks) migrating forms of chromosome XII appeared after the *cdc14-1* release. Lanes for samples taken from a release into a new G1 block (αF) are also included. Correspondence between main bands and chromosomes is indicated on the right. doi:10.1371/journal.pgen.1002509.g002

looked under the microscope and counted individual cells. The telophase release led to rebudding of the initial dumbbell mitotic cell for both mutants (Figure 2A). Virtually all cells were able to resume the cell cycle in a synchronous way as indicated by the drop of the dumbbell category (in red) to values below 10%. Around 120 minutes after the release, most cells had rebudded again. Since most daughter cells remain together for a while after the release, this rebudding gave "threesomes" (i.e., single-rebudded or three cell bodies) and "foursomes" (i.e., double-rebudded or four cell bodies). Foursomes (in blue) remained the most abundant category from 120 minutes onwards ($\sim 90\%$ in the *cdc14-1* release, and $\sim 50\%$ in the *cdc15-2* release). The lesser

amount of foursomes in the *cdc15-2* release occurred because daughter cells from this mutant were eventually able to separate from each other, whereas daughters for *cdc14-1* remained tightly together even long after becoming foursomes (see below). When we followed the release for longer periods we noticed that the budding pattern of the *cdc15-2* release became complex and tended to be oscillatory. By contrast, *cdc14-1* was much simpler and many cells stalled as the foursome category throughout (data not shown and Figure S2). A critical difference between the observed threesomes and foursomes for *cdc15-2* and *cdc14-1* became evident when we looked at the nuclei by DAPI. Thus, *cdc15-2* foursomes had 4 nuclei (i.e., both daughters have entered

and completed another nuclear division round) in ~70% of the cases at minute 180. By contrast, the *cdc14-1* release had less than 10% of the foursomes in this situation at that time (Figure 2B and Figure S2). When we looked at the segregation pattern of the cXIIr telomere (*tetO:1061*) in these strains, we found that *cdc15-2* always segregated it faithfully in the two cell division that took place ($94.0 \pm 0.1\%$ [mean \pm SEM, $n = 3$] of foursomes with four nuclei had one *tetO* in each nucleus) (Figure 2C for a representative micrograph). In the case of *cdc14-1*, $63.6 \pm 1.7\%$ (mean \pm SEM, $n = 3$) of foursomes with 2 nuclei had already missegregated cXIIr as expected [28], and no more cell divisions proceeded in that period (Figure 2C).

We repeated this block-and-release experiment in different yeast strains and backgrounds and found that the main conclusion was conserved (i.e., long-lasting arrest of many *cdc14-1* cells as foursomes in a pre-anaphase stage). However, we observed slight differences in terms of synchrony after the release, time of rebudding, and number of daughter cells able to separate from each other. For instance, in the W303 background, *cdc15-2* cells got released earlier and the synchrony was much better throughout (Figure S2).

We further explored the spindle apparatus (spindle itself using Tub1-GFP and spindle pole bodies with Tub4-CFP) in the *cdc14-1* foursomes and observed that each of the two nuclei contained duplicated spindle pole bodies and a metaphase-like spindle (Figure S3). This shows that the single nucleus observed for each daughter cell in the *cdc14-1* foursome represents a genuine pre-anaphase arrest and not a highly tangled anaphase.

Daughter cells complete DNA replication after a *cdc14-1* release

The fact that *cdc14-1* cells stalled as binucleated foursomes after the telophase release indicated that cells got arrested somewhere between S phase (whose beginning coincides with the rebudding event) and anaphase. We next narrowed the window of this arrest to G2/M by demonstrating that cells completed DNA replication after the *cdc14-1* release. This was possible because, at the time we took samples for microscopy in the above-mentioned experiment, we also took samples for following DNA replication in the cell population by flow cytometry and PFGE (Figure 2D and 2E).

When we performed flow cytometry analysis, we observed a duplication of the DNA amount in cells coming from a *cdc14-1* release (Figure 2D). Since these cells ended up as foursomes, replication could be clearly assessed by simply observing how cells transitioned from a 2N to a 4N peak. In the case of *cdc15-2*, the assessment was a little more difficult since the release gave rise to a complex mixture of single cells (both unbudded and budded) and rebudded cells still connected through the cell wall (threesomes and foursomes). However, the three major peaks for DNA content visible during this release accounted well for the observed amounts of each cell type (Figure 2D, left panel), and indicate that these cells also replicated their DNA. An important conclusion we reached from these data is that replication started and finished at the same time for both mutants, at least for the bulk of their DNA.

When we performed PFGE for those samples, we further confirmed that chromosome replication is mostly completed for all chromosomes after the *cdc14-1* release. We ascertained this using the fact that yeast chromosomes cannot enter a PFGE while being replicated [35]. Thus, we observed that a new replication round for all chromosomes started at around minute 90 in both mutants and that most chromosomes re-entered the gel ~60 minutes later (Figure 2E, upper panel; and S4). This individual chromosome replication behaviour fits well with the bulk replication seen by flow cytometry in Figure 2D.

Chromosome XII integrity is compromised after a *cdc14-1* release

Although chromosome XII also started replication after the *cdc14-1* release, the recovery of the whole band was incomplete. In fact, we observed just by ethidium bromide staining that chromosome XII became fainter than any other chromosome after the *cdc14-1* release (Figure 2E, upper panels; and S4). This did not happen during the *cdc15-2* release. Importantly, when we performed a southern blot with a probe against the rDNA we could see that other shorter bands appeared (Figure 2E, lower panels, double- and triple-asterisks). These new bands were visible after the new round of replication was completed, but they were also visible if we prevented replication after the *cdc14-1* release by blocking daughter cells in G1. Again, this G1 block also led to a 50% drop of chromosome XII band intensity in the ethidium bromide staining; and this drop was specific to the *cdc14-1* release (Figure S4). Besides, a smear above the band for the entire chromosome was also seen during the *cdc14-1* release, especially after chromosome replication (Figure 2E, lower panels, single-asterisk). Although we do not know what this smear might be, we speculate that it could account for chromosome XII with replication or recombination intermediates. Interestingly, the cell population in this *cdc14-1* strain may have up to three rDNA sizes (Figure 2E, lower panel, cXII arrow); which would indicate that the rDNA array is more unstable in this mutant.

The new arrest is long-lasting for those cells that were unable to resolve and segregate the chromosome XII right arm

Because the *tetO:1061* can still be segregated in ~50% of the cells coming from a *cdc14-1* release [28], we next decided to specifically assess whether these cells eventually bypass the arrest as foursomes. For that purpose we filmed any re-budding beyond that point and compared it to the previous cXIIr segregation outcome. We followed up 22 dumbbell *cdc14-1* cells as they transitioned out of the telophase arrest on minimal medium agarose patches. Twelve out of these 22 cells ended up missegregating the *tetO* (54.5%). As expected, all daughter cells rebudded again, although it took around an hour longer than when we performed the release in liquid cultures (half-life of the dumbbell phenotype was ~135 minutes for agarose patches versus ~75 minutes for cells in culture). Importantly, no foursomes that originally missegregated the cXIIr had rebudded a third time by 6 hours after the telophase release ($n = 12$); whereas 80% of foursomes had done so when cXIIr segregation had been correct ($n = 10$). This difference is statistically very significant ($p < 0.001$, Fisher's exact test on the 2×2 contingency table).

Cells complete karyokinesis and cytokinesis after the *cdc14-1* release, even in those cells that missegregated the chromosome XII right arm

At the telophase block, *cdc14-1* strains have daughter-to-be cells still connected through the bud neck as cytokinesis has not yet been completed [36]. A key question to understand the observed G2/M block is to address the fate of the cXIIr anaphase bridge after the release; importantly, whether or not *cdc14-1* cells complete cytokinesis and hence sever the bridge. We addressed this question two ways.

First we looked at karyokinesis microscopically (i.e., nuclear fission) in a strain where the distal part of the rDNA is tagged (*tetO:487*) and the nuclear TetR-YFP is overexpressed. In this strain we can see both the cXIIr bridge and the nucleoplasm. When Z stacks of microscope pictures were taken at the *cdc14-1*

block, the *tetO:487* was seldom segregated and a clear nucleoplasm bridge was visible across the bud neck (Figure 3A, 0' picture; Figure S5, hollow pointers). The nucleoplasm bridge (soluble TetR-YFP, do not mistake nucleoplasm bridge for anaphase bridge) was also observed for all cells blocked with the *cdc15-2* allele. This suggests that karyokinesis has not yet taken place in both telophase blocks. Noticeably, the nucleoplasm bridge had

bulges in the *cdc14-1* block (Figure S5, filled pointers), yet was a thin and straight line in the *cdc15-2* block. We tested whether this bulge accommodates the unresolved rDNA and distal regions of the cXIIr by using another yeast strain that also carries the nucleolar marker Net1 fused to CFP. We found that the nucleolus colocalized with the bulge in more than 95% of the cells (Figure S5B). After the *cdc14-1* telophase release, the nucleoplasm bridge

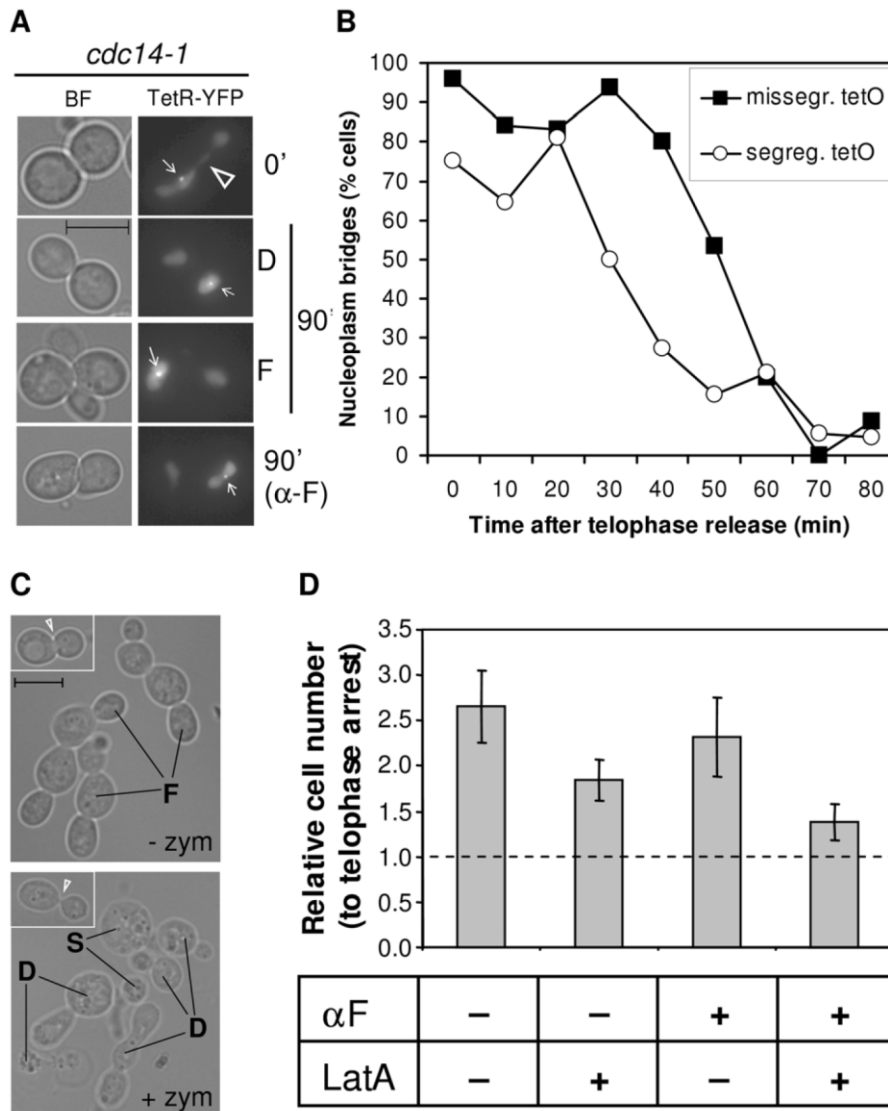


Figure 3. Cells complete karyo- and cytokinesis after a *cdc14-1* release, irrespective of the cXIIr segregation status. (A) Strain FM518 (*cdc14-1 tetO:487 TetR-YFP*) was first arrested at 37°C for 3 hours and micrographed in the conditions described to see the tetR-YFP nucleoplasm bridge (0', see also Figure S5). Then it was released at 25°C. Part of the yeast culture was released into fresh medium containing alpha-factor to arrest the daughter cells in G1. At 90 minutes after the release, more photos were taken and representative cells are shown. The two main cell morphologies at that time for a normal release, dumbbells [D] and foursomes [F], are depicted. The hollow triangle points to the nucleoplasm bridge. White pointers indicate the missegregated *tetO*. Note that cells have no nucleoplasm bridge. (B) Time course of nucleoplasm bridge disappearance for the same strain relative to the cXIIr segregation status. (C) Strain FM515 (*cdc14-1 RAD52-YFP*) was arrested in telophase by incubation at 37°C for 3 hours. Then the cell culture was shifted back to 25°C to enter a new cell cycle. At the time of the telophase block and 2 hours after the release, samples were taken and fixed with formaldehyde. Contrasted bright field micrographs of representative cells before and after zymolyase treatment are shown. Left corner photos show cells at the telophase block. The white triangle highlights the difference in bud neck thickness after zymolyase treatment. Main photos depict cells 2 hours after the telophase release. "F" points to foursomes, "D" to dumbbells and "S" to single cells. No foursomes (<3%) were seen after zymolyase treatment. (D) Strain FM515 (*cdc14-1 RAD52-YFP*) was treated to inhibit cytokinesis (+LatA) and/or cell cycle progression beyond G1 (+αF). The number of cells was counted in a haemocytometer after the zymolyase treatment. The chart represents cell number two hours after the release relative to their telophase block (mean ± SEM, n=3). doi:10.1371/journal.pgen.1002509.g003

eventually disappeared in dumbbell cells and was never visible in daughter cells that had already rebudded (Figure 3A, dumbbells [D] and foursomes [F] at minute 90). A similar behaviour was seen for *cdc15-2* release (data not shown). Importantly, no *cdc14-1* foursomes had a nucleoplasm bridge, even if they had previously missegregated cXIIr. A conclusive proof that karyokinesis took place before the daughter cells became foursomes was obtained when cells were arrested in G1 right after the *cdc14-1* release. Thus, the nucleoplasm bridge was never visible after the release in cells treated with alpha-factor, irrespective of the cXIIr segregation status (Figure 3A, photo α -F at minute 90).

Although rDNA-missegregating cells ended up performing karyokinesis, it was somehow striking we did not observe a delay in the cell cycle during the *cdc14-1* release. Such delay is expected since a checkpoint has been described to sense the presence of anaphase bridges in yeast (i.e., NoCut checkpoint) [37,38]. We took advantage of having the aforementioned strain to look at the nucleoplasm and the cXIIr bridges simultaneously and check whether the maintenance of the cXIIr bridge after the release correlated with a delay in the karyokinesis (Figure 3B). We performed a time course of the *cdc14-1* release and followed daughter cells (as dumbbells) throughout the new G1. We observed that the nucleoplasm bridge (again do not mistake for the cXIIr bridge) took around 20 minutes longer to be severed in those cells that finally failed to segregate the cXIIr (Figure 3B, half-life for the nucleoplasm bridge was ~30 minutes for cells with segregated cXIIr versus ~50 minutes for missegregated cXIIr). We believe that this 20 minute delay in karyokinesis may account for the NoCut checkpoint. In any case, the time of disappearance of the nucleoplasm bridge (i.e., karyokinesis) was short and the NoCut checkpoint did not preclude cells with the cXIIr bridge from finally completing karyokinesis.

In order to confirm that the fate of the cXIIr bridge is to be severed after the *cdc14-1* release, we also looked at cytokinesis indirectly. We employed an assay based on the fact that formaldehyde-fixed cells that have not completed cytokinesis are resistant to separation by cell wall digesting enzymes (i.e., zymolyase) [39]. At the *cdc14-1* block, when most cells were dumbbells, zymolyase treatment was not able to separate the daughters, although the bud neck that connects them became very thin (Figure 3C, left-corner photos). By contrast, foursomes seen two hours after the release could be split in two (Figure 3C, main lower photo). The drop of foursomes after zymolyase treatment was high (from ~70% to ~3%). In another set of experiments, we also counted cell number after zymolyase treatment under different chemical conditions to inhibit either cytokinesis or S-phase. To inhibit cytokinesis, we added the F-actin inhibitor Latrunculin A (LatA) [40]. Since its action against cytokinesis is optimal if cells are incubated before they reach telophase but after they have budded, we employed an initial arrest in G2/M [40]. Then we let them transit from the G2/M arrest to the telophase arrest. To inhibit the new S-phase, we blocked cells in G1 with alpha-factor, added at the telophase release. As expected, overall cell number doubled two hours after the release relative to the telophase arrest in a culture without LatA (Figure 3D). Importantly, this separation could be partially prevented by incubating the *cdc14-1* cells with LatA (*cdc14-1* release with versus without LatA gave a $p = 0.036$, Student's T test). Moreover, we also demonstrated that cytokinesis occurred before the daughters entered the new S-phase. Thus, alpha-factor prevented dumbbells from becoming foursomes after the release, but it did not circumvent cell separation after zymolyase treatment (Figure 3D). Again, this separation was prevented when LatA was added during the G2/M to telophase transition

(*cdc14-1* release to alpha-factor with versus without LatA gave a $p = 0.028$, Student's T test).

On the whole, we can conclude from this set of experiments about chromosome XII integrity (Figure 2E) and karyo/cytokinesis (Figure 3) that cells physically separate from each other irrespective of the presence of the cXIIr bridge. The logical consequence of this should be the generation of at least a DSB near or within the rDNA.

The new G2/M arrest that follows the *cdc14-1* release is dependent on Rad9

The observed karyokinesis, cytokinesis and cXIIr breakage, followed by the arrest in G2/M in the new cell cycle, likely implies that a DSB-mediated DNA damage checkpoint is activated after the *cdc14-1* release. A critical component of this checkpoint is Rad9. Mutants for this protein allow cells with DSBs to enter a new segregation round [41]. Hence, we decided to check whether our observed pre-anaphase arrest could be overcome by deleting *RAD9*. We did this in our *cdc14-1 TUB1-GFP* strain to follow spindle morphology as well as nuclear division after the release (Figure 4A). In contrast to the single mutant *cdc14-1 TUB1-GFP*, the double mutant *cdc14-1 rad9 Δ TUB1-GFP* could enter anaphase by 3 hours after the release, becoming foursomes with more than two nuclei masses (i.e., at least one of the daughter cells entered a new anaphase) (Figure 4A, upper panels). Accordingly, when we looked at spindle morphology using Tub1-GFP, we observed a transition from metaphase-like spindles to other patterns in the *cdc14-1 rad9 Δ* double mutant (mainly G1-like Tub1 dot signals) (Figure 4A, lower panels).

Besides this, we tested the responsiveness of foursomes to the G1-specific pheromone alpha-factor. We reasoned that if cells were able to progress beyond the G2/M arrest, they would become responsive to the pheromone and change their morphology accordingly (i.e., acquire the shmoo phenotype). Thus, we treated *cdc14-1* cells with the pheromone, not at the time of the release as in other experiments above, but after they became foursomes (2 hours after the release). Then, we left them in alpha-factor for another 3 hours. We first noticed that some *rad9 Δ* backgrounds, like the one that carries the *TUB1-GFP*, were able to split the foursomes after this 5 hours incubation time. Therefore, we used one of the W303 backgrounds that kept the foursome category in these conditions. Importantly, all cells in most *cdc14-1 rad9 Δ* foursomes were responsive to the pheromone (Figure 4B). Also, these foursomes had four segregated nuclei (Figure 4C). Interestingly, cells in the *cdc14-1 RAD9* foursome distributed in three peaks: one with no responsive cells, one with all four cells responsive, and a third subgroup with just two cells responding to the pheromone (Figure 4B). Within this subgroup, the two responsive cells were always a partner and each has a nucleus (Figure 4C). In order to determine where these two cells come from, we repeated this assay with the *cdc14-1* strain that carries the labelled cXIIr telomere. We found that in 92% of foursomes ($n = 39$) both responsive cells had a *telO*, whereas there was no *telO* in either of the two non-responsive cells. This means that: (i) this subgroup came from *cdc14-1* cells where missegregation occurred in the first place, and (ii) the cell that retained the intact chromosome XII plus the broken cXIIr was able to eventually pass the G2/M arrest.

Therefore, we concluded that cells coming from a *cdc14-1* release activated the Rad9 checkpoint to prevent daughter cells from entering anaphase, and that this G2/M arrest persists for a long time in the daughter cell that lost an intact copy of chromosome XII (i.e., DC1).

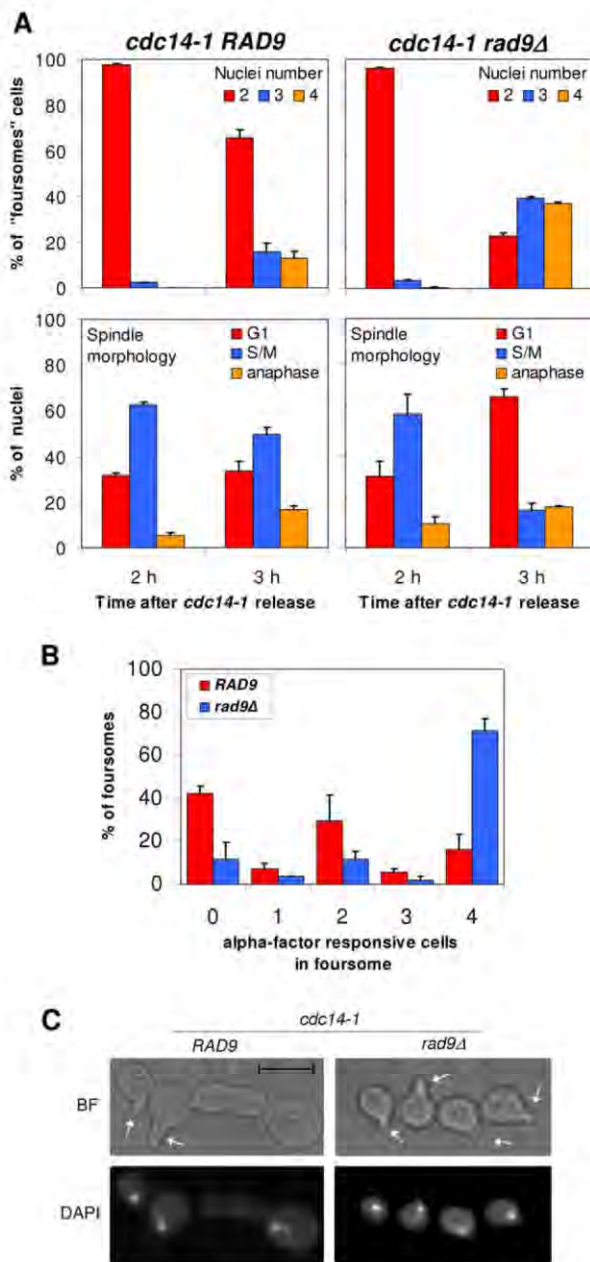


Figure 4. The G2/M arrest that follows a *cdc14-1* release is dependent on Rad9. (A) Strains FM459 (*cdc14-1 TUB1-GFP*) and FM576 (*cdc14-1 rad9Δ TUB1-GFP*) were arrested at 37°C for 3 h and then released. Samples were taken and micrographed 2 and 3 hours after the release. Upper panels show nuclei number after DAPI staining for the major foursome category. Lower panels indicate spindle morphologies for each nucleus in the foursomes (mean \pm SEM, $n=3$). (B) Strains FM515 (*cdc14-1 RAD52-YFP*) and FM883 (*cdc14-1 rad9Δ RAD52-YFP*) were arrested and released as in A. Two hours after the release, alpha-factor was added and cells were then incubated for 3 more hours before samples were taken and micrographed. Chart represents how many cells in each foursome responded to alpha-factor. Note how *cdc14-1 RAD9* was distributed in three major categories peaking at 0, 2 and 4 responsive cells; whereas most *cdc14-1 rad9Δ* foursomes had all cells responding to alpha-factor (i.e., all progeny passed the G2/M arrest) (mean \pm SEM, $n=2$). (C) Representative cells of a *cdc14-1 RAD9* foursome with two cells responding to alpha-factor and a *cdc14-1 rad9Δ* foursome with all its 4 cells responding (white arrows point to the shmoo). Note how there are 3 nuclei in the former (two of them in

each of the responding cells) and 4 nuclei in the latter (see main text for more details).
doi:10.1371/journal.pgen.1002509.g004

Missegregation of chromosome XII right arm leads to accumulation of Rad52 foci after a *cdc14-1* release

The Rad9-dependent cell cycle arrest means that daughter cells sense the DSB(s). Therefore, they must accordingly trigger a DNA damage response (DDR). At this point, we started looking at proteins that cytologically mark this DDR by appearance in nuclear foci. Rad52 is a key mediator in the DDR that comprises the preferred homologous recombination (HR) pathway for repair [42]. This pathway is central in the DDRs that occur throughout S-phase and well into mitosis [43]. We reasoned that, because daughter cells reached and completed S-phase on schedule after a *cdc14-1* release (Figure 2) and then get arrested in G2/M in a Rad9-dependent manner (Figure 2 and Figure 4), Rad52 should be involved in the DDR. Importantly, Rad52-YFP forms widely studied nuclear foci after induced DNA damage [43]. Thus, we looked at Rad52 foci in our telophase block-and-release experiments. We indeed observed foci after a *cdc14-1* release for a subset of cells (Figure 5). Rad52 foci number and intensity were clearly superior in the *cdc14-1* release relative to a side-by-side experiment with the *cdc15-2* strain (Figure 5A). Importantly, there was no difference between the strains when growing asynchronously at 25°C (only ~5% of budded cells had foci). Foci were observed at the telophase block for neither *cdc14-1* nor *cdc15-2*, further indicating that DNA damage has not yet taken place at this stage. Foci started around 90 minutes after the release and always after rebudding (Figure 5B for a typical time-lapse movie). Furthermore, Rad52 foci were rather dynamic at the beginning of the new S-phase and, within the subgroup that, at some point, had Rad52-YFP foci, tended to end up as either just one major focus in the foursomes (in one of its two nuclei) or 2 foci, one located in each nucleus (Figure 5A and 5B).

Remarkably, the percentage of foursomes acquiring at least one long-lasting single Rad52-YFP focus during the release was ~50% (Figure 5A). We noticed that this percentage of cells was equivalent to that of rDNA/cXIIr missegregation [28]. We therefore hypothesised that cells with Rad52 foci may represent those that had failed in rDNA segregation. We addressed this important question in two ways. First we made use of a second mutation that worsens rDNA segregation after a *cdc14-1* release (i.e., deletion of *FOB1* gene) [28] (Figure S6). Second, we double labelled two *cdc14-1* strains (one in the S288C background and the other one in W303) with a tag for the rDNA and a tag for the Rad52 protein. For the S288C background, we employed our strain with the *tetO:487* and added a RAD52-RedStar2 allele (Figure S7). As for W303, we employed a previously described strain that bears both Rad52-YFP and a tag inserted within the rDNA (*tetOs/TetR-mRFP* system) [44] and that we made *cdc14-1* (Figure 5C). By using the *cdc14-1 job1Δ* double mutant, we could correlate worsening of the rDNA segregation with a higher frequency of foursomes carrying at least one bright Rad52 focus (Figure S6; $p<0.0001$, Pearson's chi-square test). On the other hand, double labelling of Rad52 and the rDNA further and strongly confirmed that Rad52 foci are more frequent in cells that missegregated the rDNA (Figure 5C and Figure S7; $p<0.0001$, Pearson's chi-square test). Moreover, these strains allowed us to determine that the first and strongest Rad52 focus appeared in the daughter cell that does not carry the *tetOs* (i.e., cell DC1). Thus, 75% of these foci were located in that cell versus only 8% of Rad52 single foci seen in the daughter cell that carries the *tetOs* (the remaining 17% of foursomes had one Rad52 focus in each daughter cell). We

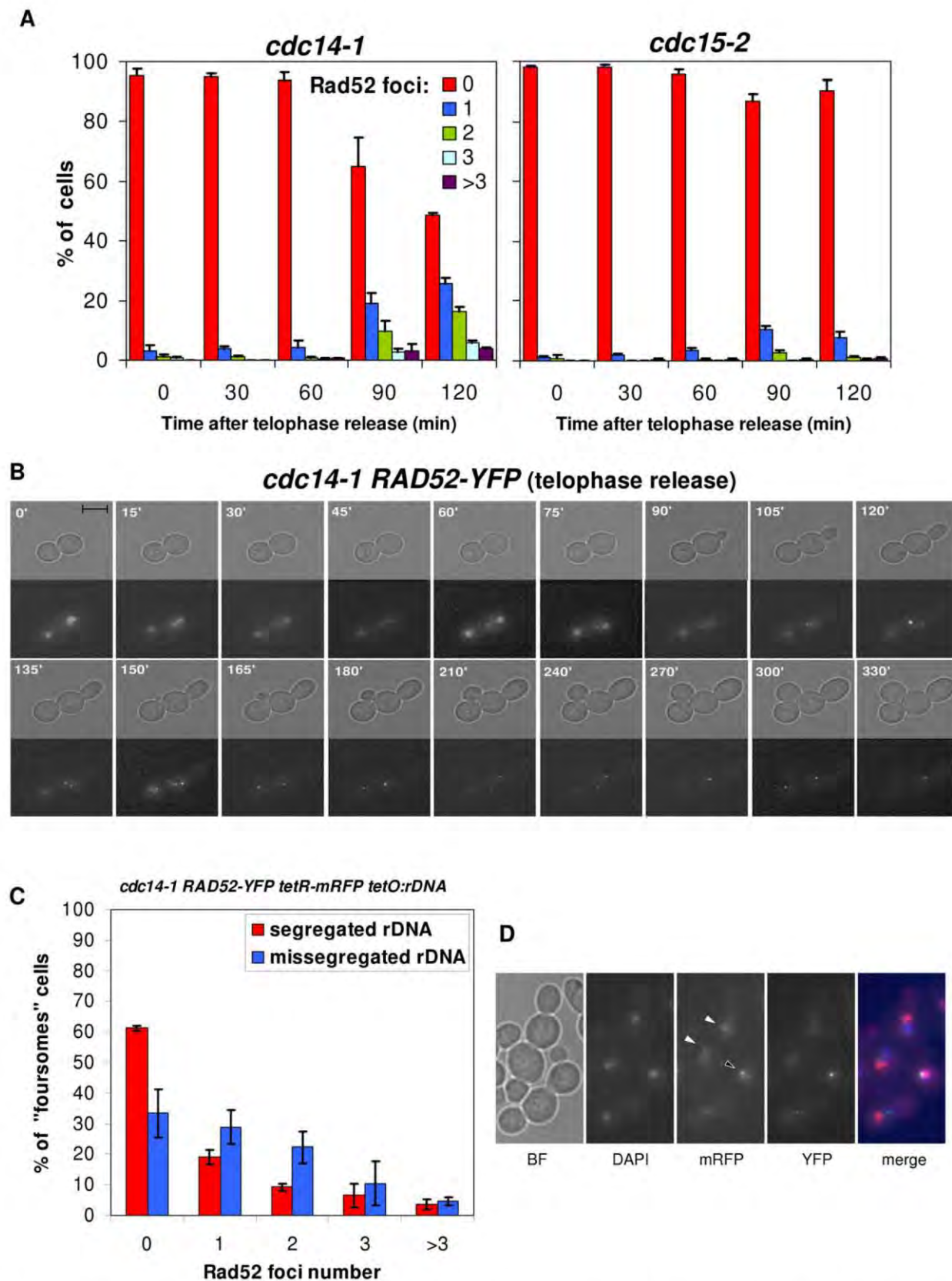


Figure 5. Cells coming from a *cdc14-1* release frequently form Rad52 repair factories, which accumulate when rDNA missegregation had previously occurred. (A) Strains FM531 (*cdc15-2 RAD52-YFP*) and FM515 (*cdc14-1 RAD52-YFP*) were treated as in Figure 2. Cells from samples taken every 30' were scored (>200 cells each) for number of Rad52-YFP foci (mean \pm SEM, $n=3$). (B) Time-lapse fluorescence microscopy (every 15–

30' for 6 h) of a FM515 (*cdc14-1 RAD52-YFP*) cell starting at the time of the telophase release. (C) Strain FM551 (*cdc14-1 RAD52-YFP tetO:rDNA tetR-mRFP*) was first arrested in the *cdc14-1* block and then released into a new cell cycle. After 2 hours, Rad52 foci were scored for those foursomes that have either segregated or missegregated the rDNA (mean \pm SEM, $n=3$). (D) A representative micrograph of two foursomes, one showing segregated *tetOs* (white triangles) and the other one with unresolved *tetOs* (the black triangle). Note the Rad52 focus near the unresolved *tetOs*. In the merged micrograph, mRFP is pseudocoloured in blue and DAPI in red.
doi:10.1371/journal.pgen.1002509.g005

believe that this is an important result since the genetic material that each daughter carries in the anaphase bridge is different as stated above (Figure 1, “a” phenotype). Hence, “DC1” cell (the one without the *tetOs*) bears just one broken copy of the resolved part of chromosome XII (from left telomere to somewhere within the rDNA), whereas “DC2” cell carries one entire sister chromatid plus the unresolved part of the other one (from somewhere within the rDNA to the right telomere). The fact that Rad52 foci are stronger and long-lasting in DC1 might indicate that this cell struggles to repair the DSB, while DC2 might end up repairing its broken end. This is in agreement with what we observed when deleted *RAD9* (Figure 4B). Finally, it is worth mentioning that, for those Rad52 foci visible in the *tetO*-carrying nuclei, the fluorescent dots were almost always in close proximity (Figure 5D). However, these Rad52 foci did not localize within the nucleolus when we used a nucleolar marker (Figure S8). This is not surprising though as broken rDNA sequences are transported out of the nucleolus towards nuclear Rad52 factories [44].

Overall, these observations fit well with the prediction of a DDR occurring preferentially in those daughter cells that failed in rDNA segregation during the preceding division.

Release from the *cdc14-1* block also leads to Rfa1 foci, yet only after cells reach the new S-phase

We expected the DSB to occur shortly after the release into G1, when karyo- and cytokinesis took place (Figure 3) and chromosome XII appeared partly broken (Figure 2E). We were intrigued by the fact that cells did not, however, delay G1 (Figure 2). A possible explanation for this anomaly would be that the DSB is clean (i.e., with little associated single-stranded DNA [ssDNA] at the edges). This is the type of DSB generated by inducible endonucleases like HO as opposed to DSBs obtained after ionizing irradiation, which are rich in ssDNA (i.e., ragged ends) [45,46]. It has been shown that clean ends are poorly resected in G1, forming little ssDNA, whereas ragged DSBs can already bind ssDNA-binding proteins such as the RPA complex. The formation of ssDNA and the binding of the RPA complex to it are key steps in checkpoint activation [47,48]. Because of this, we also included the RPA complex as a reporter to study the DDR that follows the *cdc14-1* release. YFP-tagged Rfa1 (one of the complex subunits) also forms foci under the presence of DSBs [49]. Crucially, Rfa1 can form foci in G1 provided that the DSB takes place at this stage and, as just mentioned, the break is ragged [46,49,50]. Thus, we observed Rfa1 foci for a subset of cells coming from a *cdc14-1* release (Figure 6A and 6B). Rfa1 foci were as dynamic as those of Rad52 and also tended to end up as a major focus, one per nucleus in the foursome at the most (Figure 6C). Moreover, it was noticeable that Rfa1-YFP eventually gave very intense foci (Figure 6B). Nevertheless, all foci began to appear around 60'–90' after the release (Figure 6A), and always after rebudding (Figure 6C). Accordingly, foci were not observed in *cdc14-1* cells transiting from telophase to a G1 arrest with alpha-factor (Figure 6B). This likely means that the new type of DSB generated by the severing of the cXIIr bridge has little associated ssDNA (i.e., the DSB is clean) and therefore it is not recognized by the RPA complex in G1.

The Rad52 response to the severing of the chromosome XII right arm anaphase bridge is independent of Mre11

In the canonical model for DSB recognition and repair by HR, RPA and Rad52 are downstream players to the MRX complex (Mre11-Rad50-Xrs2) [49]. This complex is supposed to recognize each DSB end, bring them together and help in the first stages of end processing to allow template searching for HR. The expected “one-ended” nature of the DSB, a consequence of the anaphase bridge severing (i.e., the two ends cannot be brought together), prompted us to further study this important component in the DSB signalling and repair. We made use of Mre11-YFP as a reporter of the DSB-specific MRX complex. Unlike Rad52 and Rfa1, Mre11 foci have been observed in all cell cycle stages (including G1) and for all types of “two-ended” DSBs generated [46,49]. We were not able to observe Mre11 foci for *cdc14-1* throughout the release (less than 1% of cells at any one time point in 10 minutes intervals, data not shown). Nevertheless, Mre11 was fully functional in *cdc14-1* cells growing at the permissive temperature since it forms foci when DSBs were chemically generated (Figure S9). We further ruled out any role of the MRX complex in the observed Rad52-dependent response after the release by looking at Rad52 foci in a *cdc14-1 mre11Δ* double mutant. Indeed, we saw Rad52 foci at a number and intensity comparable to that of a *cdc14-1 MRE11* strain in foursomes taken 2 and 4 hours after the telophase release (Figure 7A and 7B). Because *mre11Δ* gave some background of Rad52 foci at the *cdc14-1* arrest (Figure 7A, time 0'), we filmed cells during the release and observed that about 75% of cells with Rad52 foci at the arrest never entered a new cell cycle (data not shown). Therefore, almost all foci measured in the foursomes likely came from cells without foci at the previous arrest. We thus concluded that Rad52 foci in *cdc14-1* foursomes were independent of Mre11.

The *cdc14-1* anaphase bridge comprises few chromosome arms aside from the chromosome XII right arm

Although the cXIIr is a hotspot for missegregation in *cdc14* mutants, it seems not to be the only genomic region affected. Thus, at least one telomere of a chromosome other than XII appeared missegregated at the telophase block in previous works that made use of another thermosensitive allele (i.e., *cdc14-3*) [22,33]. Therefore, we decided to address whether telomeres other than cXIIr were also missegregated during the *cdc14-1* release. We looked at four different telomeres located in two chromosomes (V & XIV) [51]. Chromosome V has the right telomere labelled with the *lacO/LacI-CFP* system, whereas its left telomere (V-L) is labelled with the *tetO/TetR-YFP* system. On the other hand, chromosome XIV has the right telomere (XIV-R) labelled with the *tetO/TetR-YFP* system and its left telomere labelled with the *lacO/LacI-CFP* system. It is important to note that telomere V-L was the one used in the above-mentioned *cdc14-3* studies. When we carried out the *cdc14-1* telophase block at 37°C we often failed to detect the CFP signal, so we focused on missegregation after the release (CFP signal recovered after the temperature drop). Since the *cdc15-2* release gave only few binucleated foursomes (Figure 2 and Figure S2), and in order to avoid a possible bias, we compared

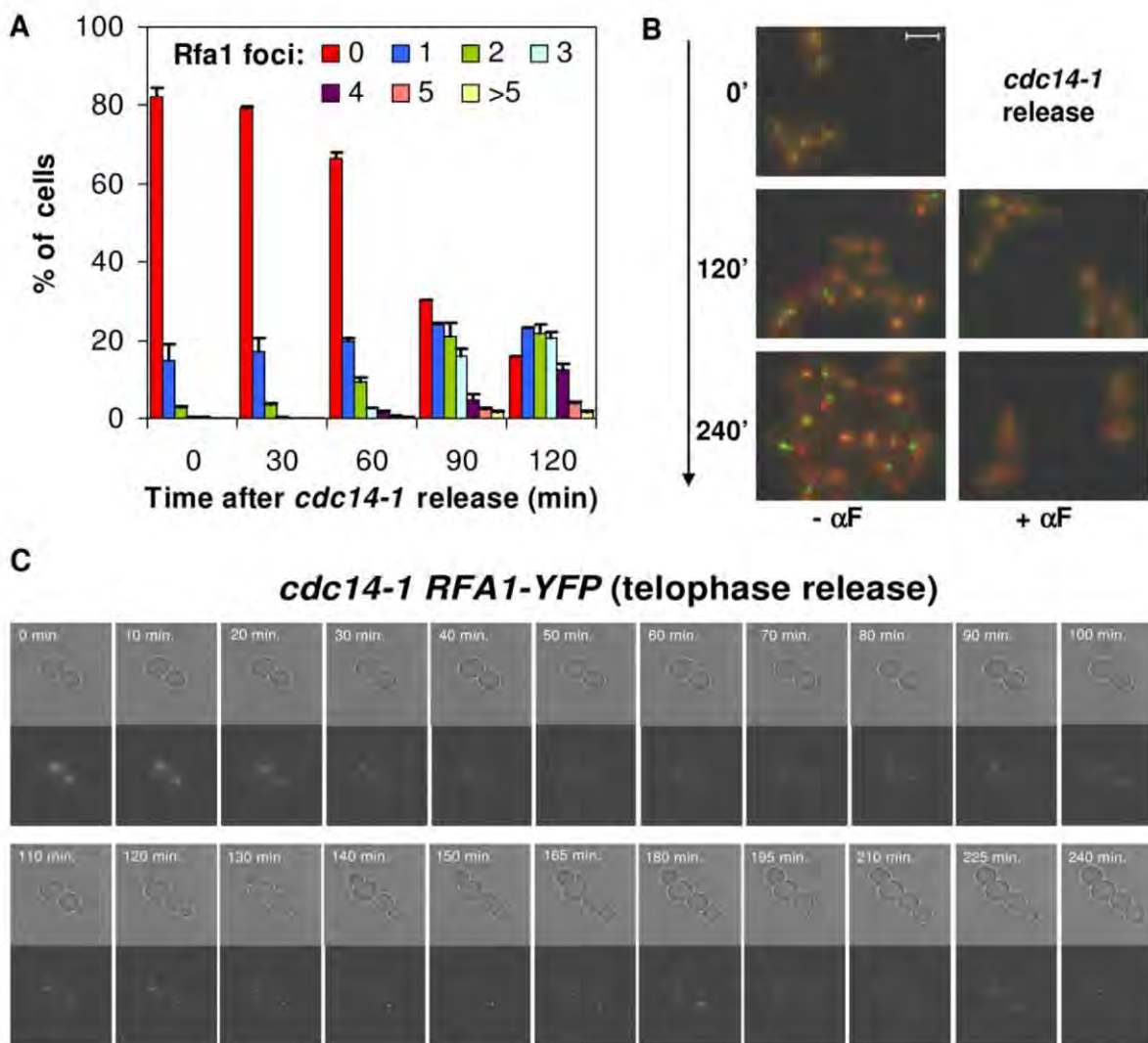


Figure 6. Cells coming from a *cdc14-1* release form Rfa1 factories only after reaching S-phase. (A) Strain FM513 (*cdc14-1 RFA1-YFP*) was treated as in Figure 2. Samples were taken every 30' after the release and Rfa1-YFP foci quantified per cell (mean \pm SEM, $n=3$). (B) Representative micrographs of FM513 cells at the telophase arrest (0'), 2 hours (120') and 4 hours (240') after the release into fresh medium with or without α -factor. Bright field photos are superimposed over the two fluorescent channels (red for DAPI and green for Rfa1-YFP). (C) Time-lapse fluorescence microscopy (every \sim 10–15' for 4 hours) of one FM513 cell starting at the time of the telophase release. doi:10.1371/journal.pgen.1002509.g006

the *cdc14-1* release to the *cdc15-2* telophase block. To preserve the CFP signal, we arrested *cdc15-2* cells at 34°C (at least for the YFP-labelled telomeres there was no difference between 34°C and 37°C in terms of segregation, data not shown). We observed that missegregation in *cdc14-1* binucleated foursomes was low for all four telomeres and comparable to that observed at the *cdc15-2* block (Table 1). From these data, and from the pattern of chromosome integrity shown in Figure S4, we can conclude that in a *cdc14-1* release many chromosomes are expected to be fully segregated. Thus, the anaphase bridge severed after the *cdc14-1* release must be relatively enriched with cXIIr fragments.

Aberrant forms of chromosome XII can be recovered from daughter cells that survived the *cdc14-1* release

In a previous paper, we demonstrated that less than 1% of daughter cells can survive passage through multiple mitoses (>25) without Cdc14 (regulated overexpression of the cyclin-dependent

kinase inhibitor Sic1 through *GAL-SIC1* was employed to overcome Cdc14 roles in the Mitotic Exit Network) [28]. In that work, we found that all survivors had dramatically shortened the rDNA locus (although other chromosome rearrangements were not obvious from the PFGE analysis). We also showed that the small survival capability depended on Rad52 (i.e., HR is needed to repair the DNA damage and survive). This prompted us to study whether our *cdc14-1* block-and-release approach, where only one cell cycle is compromised, leads to similar results. Because Rad52 also seems to play an important role after the transient Cdc14 inactivation (Figure 5, Figures S6 and S7), we also tested whether *RAD52* was essential in this system by including a double mutant *cdc14-1 rad52 Δ* . Thus, we performed the block-and-release experiment for both *cdc14-1* and *cdc14-1 rad52 Δ* and plated the foursomes to obtain isolated colonies after 3–5 days (Figure 8A). We also plated cells right before the block-and-release experiment, while growing asynchronously at 25°C. At the time of plating, we

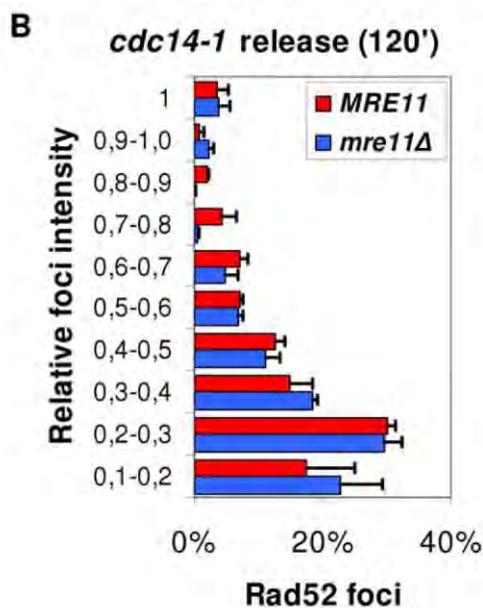
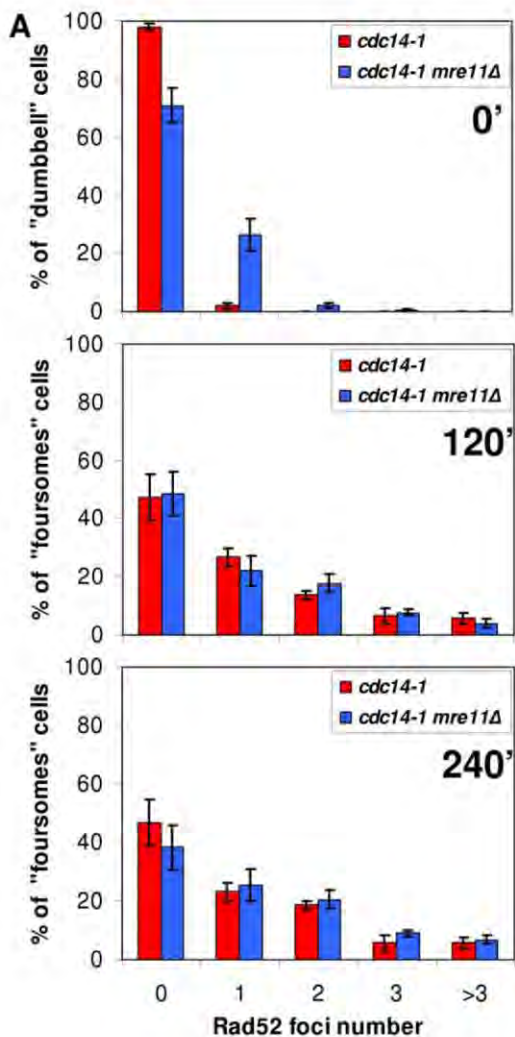


Figure 7. Accumulation of Rad52 foci after the *cdc14-1* release is independent on Mre11. (A) Strains FM515 (*cdc14-1 RAD52-YFP*) and FM572 (*cdc14-1 RAD52-YFP mre11Δ*) were arrested at 37°C for 3 hours and then released at 25°C. Rad52 foci were counted in dumbbells at the telophase block (0') and in foursomes 2 and 4 hours after the release (mean \pm SEM, n=3). (B) Intensity quantification of Rad52 foci in *MRE11* and *mre11Δ* strains 2 hours after the release (see methods for details). doi:10.1371/journal.pgen.1002509.g007

counted cells with a haemocytometer to determine overall viability. Surprisingly, we did not see a great loss of viability after the transient Cdc14 inactivation (Figure 8A and table underneath). As for the single *cdc14-1* mutant, this loss was around 25% at the most, whereas double mutant *cdc14-1 rad52Δ* showed no drop in viability at all. This demonstrates that at least one of the daughter cells of the foursome often survives and gives raise to a colony. Taking into account that 50% of foursomes missegregated the cXIIr (equivalent values of missegregation were seen during a *cdc14-1 rad52Δ* release: 48%), the observed percentage of viable cells might indicate that 50% and 100% of the daughter cells that carry an intact cXII (i.e., DC2) must survive in *cdc14-1* and *cdc14-1 rad52Δ* respectively. Other results we showed above already pointed towards this possibility. For instance, DC2 was often able to pass the G2/M block after a while (Figure 4B). Besides, Rad52 foci seem to eventually disappear in that cell. All these data indicate that DC2 might sometimes repair the damage and carry on dividing until it forms a colony. Importantly, we did notice that around one third of those colonies grew much more slowly in *cdc14-1* (Figure 8A, "s" colonies). These slow-growing colonies were also observed when *cdc14-1* cells were plated while normally growing at the permissive temperature. However, there was a three-fold increase in their number when plated after the transient Cdc14 inactivation (Figure 8A and table underneath). Strikingly, deletion of *RAD52* prevented these very slow-growing colonies from appearing, although most colonies grew \sim 30% more slowly after the *cdc14-1* release (Figure 8A and table underneath).

The different effects of both the block-and-release experiment and the presence of Rad52 on the colony size of survivors prompted us to analyse the state of chromosome XII in the different outcomes (Figure 8B). Thus, we grew several colonies at

Table 1. Telomeres of chromosome arms other than cXIIr barely missegregated after a *cdc14-1* release.

	% missegregation (mean \pm SD, n=3)		p values ^c
	<i>cdc14-1</i> release ^a	<i>cdc15-2</i> block ^b	
tel V-L	8.23 \pm 1.35	5.82 \pm 3.93	0.372
tel V-R	10.59 \pm 4.85	5.39 \pm 2.78	0.1824
tel XIV-L	4.51 \pm 1.48	3.02 \pm 1.49	0.2865
tel XIV-R	4.15 \pm 2.63	3.22 \pm 1.65	0.6313

^aStrains FM565 (*cdc14-1 tel V-L::tetO tel V-R::lacO tetR-YFP LacI-CFP*) and FM573 (*cdc14-1 tel XIV-L::lacO tel XIV-R::tetO tetR-YFP LacI-CFP*) were arrested in telophase (37°C) for 3 h and then released to 25°C. Samples were then taken, micrographed after DAPI staining and scored for telomere missegregation (binucleated foursomes only).

^bStrains FM567 (*cdc15-2 tel V-L::tetO tel V-R::lacO tetR-YFP LacI-CFP*) and FM574 (*cdc15-2 tel XIV-L::lacO tel XIV-R::tetO tetR-YFP LacI-CFP*) were arrested in telophase (34°C) for 3 h. Samples were then taken, micrographed after DAPI staining and scored for telomere missegregation (binucleated dumbbells only).

^cStatistical significance of cross-comparison between *cdc14-1* release (2 h) and *cdc15-2* block. Student's T test.

doi:10.1371/journal.pgen.1002509.t001

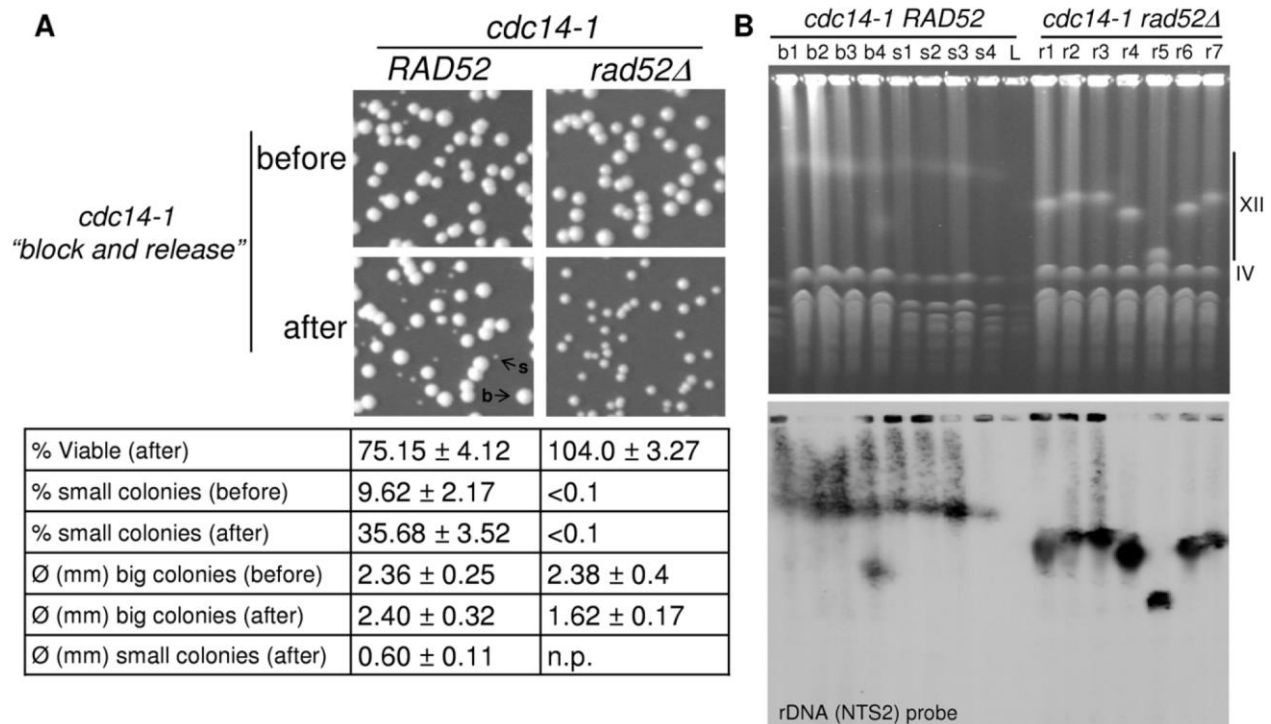


Figure 8. One of the two daughter cells often survives the chromosome XII missegregation event, even in the absence of Rad52. Strains FM518 (*cdc14-1 tetO:487 TetR-YFP*) and FM539 (*cdc14-1 rad52Δ tetO:487 TetR-YFP*) were arrested at 37°C for 3 hours and then released at 25°C for 2 hours. Before and after this block-and-release treatment, samples were taken and cells counted in a haemocytometer. Then, cell concentration was adjusted accordingly and serial dilution were prepared and plated on YPD. (A) Representative photos of colonies growing on YPD plates for the different strains and conditions. Examples of colonies of different sizes are indicated ("b" and "s" point to big and small colonies respectively). Underneath, a table sums up the main features of the growing colonies, including: an estimate of viable cells (actual colony number divided by cells counted before plating, mean ± SEM, n = 3), percentage of slow-growing colonies (mean ± SEM, n = 3) and colony diameter of each type (mean ± SD, n > 30). Note: (i) the loss of 25% of viability after the block-and-release treatment just for *cdc14-1 RAD52* (one-way student's t test, p < 0.05); (ii) the three-fold increase in very small colonies for that strain after the treatment (Student's t test, p < 0.01); (iii) the clear difference of size between big and small colonies for the *cdc14-1 RAD52* strain (Student's t test, p < 0.01); and (iv) the 30% decrease in colony size for *cdc14-1 rad52Δ* after the block-and-release treatment (Student's t test, p < 0.01). (B) PFGE of several survivors isolated after the block-and-release treatment in both *cdc14-1 RAD52* and *cdc14-1 rad52Δ* strains. Survivors from *cdc14-1 RAD52* that formed a big colony have the prefix "b", those where colonies were small have "s" as the prefix, and "r" was used for the *cdc14-1 rad52Δ* strain. Note how the size of chromosome XII changed in most *cdc14-1 rad52Δ* and that survivor b4 has two chromosome XIs.
doi:10.1371/journal.pgen.1002509.g008

the permissive temperature and carried out PFGE. We found that chromosome XII was shorter in the *cdc14-1 rad52Δ* strain we used (Figure 8B) than in its parental *cdc14-1 RAD52* strain. Interestingly, chromosome XII was highly unstable in the *cdc14-1 rad52Δ* survivors, whereas it remained more constant in *cdc14-1 RAD52*, even in the slow-growing survivors (Figure 8B). One of the *cdc14-1 RAD52* survivors (#b4) could have duplicated chromosome XII as suggested by the presence of two rDNA-containing bands.

From this set of experiments we conclude that many foursomes where cXIIr missegregation occurred can still carry on dividing for many generations (DC2 likely seeds these survivors). In addition to this, chromosome XII rearrangements and a reduced fitness are frequent outcomes of transient inactivation of Cdc14 for one cell cycle.

Discussion

The *cdc14-1* release experiment as a model to study severing of anaphase bridges comprising unresolved sister chromatids

The major manifestation of entering anaphase without completing sister chromatid resolution is the appearance of

anaphase bridges. Herein, we have introduced a new model to study the short-term consequences of these bridges based on the primary phenotype observed for the *cdc14-1* mutant of *Saccharomyces cerevisiae* [23,24,28]. From a technical point of view this model presents several key advantages that facilitate cell biology studies on anaphase bridges: (i) non-resolution specificity for few genomic regions (e.g., cXIIr, see below); (ii) cell mixtures of segregated and missegregated cXIIr in the same population and experiment [28] (Figure 2); (iii) synchrony of the cells exiting mitosis (Figure 2); (iv) capability to monitor and cross-compare both daughter cells as they remain together after a *cdc14-1* release (Figure 2 and Figure 3); and (v) availability of a proper parallel control that mostly behaves like *cdc14-1* but does segregate the cXIIr (i.e., *cdc15-2* conditional allele) [22] (Figure 2, Figures S1 and S4).

The *cdc14-1* anaphase bridge and its fate in comparison to what is observed in separate, condensin, and *top2* mutants

Because Cdc14 controls condensin and Top2 in anaphase and directs their activities to the rDNA [22,27,28,30,31], the overall

expectation of our system is that the *cdc14-1* anaphase bridge is like those of condensin and *top2* mutants, however mainly restricted to a single chromosome arm (i.e., cXIIr). Therefore, it is interesting to compare our results to those previously reported for condensin and *top2* mutants. We also include here mutants for cohesin removal due to their similarities. All these mutants form anaphase bridges comprised of trailing and distally unresolved sister chromatids as we depict in Figure 1 and Figure 9 (just for chromosome XII in those figures [i.e., *cdc14-1*], more chromosome arms are like cXIIr for these other mutants). This pattern of non-resolution likely arises from the spindle forces being able to slide cohesin and catenations away from bipolarly attached centromeres. Importantly, these mutants differ in the extent of non-resolution along the chromosome arms and the number of affected chromosomes, cohesin-removal mutants having the strongest phenotype and *cdc14-1* the mildest [14,19,20,23]. Accordingly, a common outcome in cells where cohesin or catenation removal have been impaired is the appearance of an anaphase where the nuclear mass cannot be split in two. For instance, condensin or *top2* conditional mutants show rod-like nuclei in anaphase [15,16]. The same outcome is seen in mutants where cohesin cleavage is inhibited in anaphase (e.g., separase mutants or non-cleavable forms of cohesin) [14]. Importantly, this unresolved nucleus does not abort cytokinesis, which eventually takes place leading to a “cut” phenotype in all cases. This

phenotype is characterized by aneuploid daughter cells carrying broken chromosomes [14,16,32]. Another common feature of those daughter cells is that many are unable to resume the cell cycle, likely because of the massive chromosome breakage observed. The results we present in this work indicate that the anaphase bridge in *cdc14-1* and its fate is somewhat different. First, the *cdc14-1* block does not lead to a rod-like nucleus in anaphase, rather it is able to split the two DNA masses, which end up in each daughter cell [23–25,34]. Likely, this is the consequence of most chromosome arms being able to segregate at the block. It is important to point out that we have assessed four telomeres of two other chromosomes (V and XIV) and found little missegregation in *cdc14-1* foursomes relative to a *cdc15-2* block (Table 1). Moreover, the drop of band intensity in the PFGE was only seen for chromosome XII in the *cdc14-1* release (Figure 2E and Figure S4). Taking into account that, even in *top2* and condensin mutants, small and medium-sized chromosomes segregate despite the rod-like nuclear phenotype [19,21], we believe that the anaphase bridge in *cdc14-1* mutants must comprise few chromosome arms; and that those severed by cytokinesis after the *cdc14-1* release are fewer than for the other mutants. This in turn would explain why both daughter cells reach G2/M (Figure 2 and Figure S2). If more than four chromosome arms were severed, we would expect a G1 delay [45], which we did not observe.

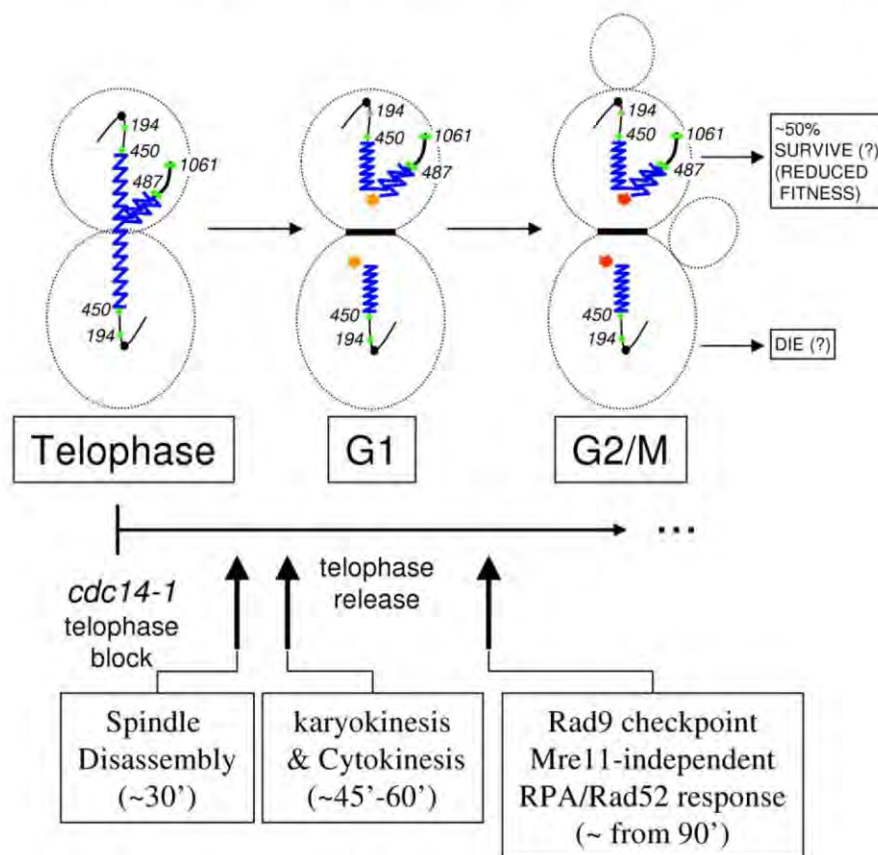


Figure 9. Model of how the cell cycle progresses after the presence of the cXIIr bridge. Location of *tetOs* is shown as green dots; rDNA is depicted as a serrated blue line; and thicker lines indicate non-resolved sister chromatids. Stars indicate the expected “one-ended” double strand break (orange star means that the break does not elicit a strong DNA damage response; whereas red star means it does). Main cell cycle events described in this article are indicated in a time line underneath. The likely long-term fate of each daughter cell (as deduced from Figure 8) is also indicated.

doi:10.1371/journal.pgen.1002509.g009

On the other hand, in all mutants but *cdc14-1*, cytokinesis is followed by cell separation. This makes difficult to follow up and cross-compare both daughter cells, a key advantage we show for *cdc14-1*. It is unclear why *cdc14-1* daughter cells are unable to separate from each other. However, this phenotype can be also seen when overcoming the *cdc14-1* block by overexpressing Sic1 [28,52]; and it was then shown that cytokinesis was completed [52]. Our data also suggest that cytokinesis is completed after *cdc14-1* re-activation (Figure 3). Thus, a possible role of Cdc14 in cell septation could be responsible for this phenotype (Figure 2). A role that could actually be extended to the mitotic exit network as *cdc15-2* also has a partial defect in cell separation.

Finally, the anaphase bridges formed in cohesin and some *top2* mutants have been employed to define a checkpoint that delays cytokinesis (i.e., NoCut checkpoint) [37]. The actual length of such delay has been difficult to measure. In our case, the *cdc14-1* anaphase bridge gave a short delay of about 20 minutes when comparing karyokinesis relative to the maintenance of the cXIIr bridge after the release (Figure 3B), and likely accounts for the NoCut checkpoint. Nevertheless, this delay was difficult to see by other means. For instance, it was observed neither relative to *cdc15-2* (at least in the S288C background) nor as a biphasic drop of dumbbell cells in *cdc14-1* (i.e., cells able to segregate the cXIIr versus those with the cXIIr bridge) (Figure 2A and Figure S2). Besides, the dynamics of the spindle disassembly after the release were quick for dumbbell cells (within the first hour, Figure S3A, left panel). It may be possible that a greater number of chromosomes in the anaphase bridge obtained by other mutants may trigger a stronger checkpoint signal.

The *cdc14-1* anaphase bridge and its fate in comparison to bridges of a different physical nature

As stated above, the *cdc14-1* anaphase bridge is supposed to be similar to condensin and *top2* mutants, yet restricted to cXIIr. Notably, there are other situations where we can predict anaphase bridges of a different nature. For instance, anaphase bridges formed by partly replicated chromatids which nevertheless enter anaphase. For instance, *sic1* and *smc5/6* mutants behave this way [53,54]. As with the difference between *top2* and *cdc14-1*, *sic1* and *smc5/6* also differ in the actual number of chromosomes in the bridge, cXIIr being enriched in mutants for the Smc5/6 complex [44,53,54]. Despite the cytological similarities of the anaphase bridges between *top2* and *sic1*, and between *cdc14-1* and *smc5/6*, the bridge appeared broken in anaphase before completing cytokinesis in *sic1* and *smc5/6* mutants and a DDR can be also observed in that cell cycle stage [53,54]. These findings highlight a key difference between the anaphase bridges formed by tangled sister chromatids and those where replication is incomplete: breakage before cytokinesis occurs in the latter, perhaps due to more fragile DNA in the unreplicated material. Finally, it is interesting to point out that other *cdc14* mutants might enter anaphase with unreplicated DNA as well [33]. However, the behaviour of our *cdc14-1* bridge is much closer to *top2* and condensin than to what is observed in *sic1* and *smc5/6*. This is, the chromosome can enter a PFGE in the *cdc14-1* block (Figure 2E) and no DDR is observed at the block (Figure 5A and Figure 6A).

Another distinct anaphase bridge is that accomplished by the use of conditional dicentric chromosomes [55–57]. Like our *cdc14-1* model, this approach has multiple technical advantages such as: (i) an anaphase bridge formed by a single chromosome; and (ii) cells with and without the bridge in the same population and experiment (~50% chance of having two centromeres

within a single sister chromatid attached to opposing SPBs). Nevertheless, the physical nature of the bridge is rather different. In the dicentric model, the bridge is formed by the sister chromatids being in an anti-parallel conformation. Moreover, sisters are supposed to be completely resolved from each other. In *cdc14-1*, the bridge is often formed by just one sister, the other one being out of the cytokinetic plane (Figure 1 and Figure 9) [23]. Thus, the expected DSBs and the broken genetic material in daughter cells are different when a dicentric chromosome is used. In relation to this system, it is interesting to note that the conditional dicentric chromosome triggers a Rad9-dependent mid-anaphase checkpoint (characterized by short spindles) that we did not see (data not shown) [24,56]. Regardless, this and other dicentric models, like *top2/condensin/cdc14-1* mutants, do not seem to break the anaphase bridge until cytokinesis takes place [57,58].

On the DNA damage generated after severing the *cdc14-1* chromosome XII right arm anaphase bridge

A key conclusion of this work is that at least one DSB near or within the rDNA is produced after the release from the *cdc14-1* block (Figure 2, Figure 3, Figure 4). Unlike DSBs generated by endonucleases, radiation or any other means within a single nucleus [49], DSBs generated during anaphase bridge severing cause the ends of the broken DNA molecule(s) to migrate to opposing compartments which cannot be brought together anymore (i.e., nuclei of daughter cells). In the first scenario, the two ends of the DSB can be physically tied again and repaired by either non-homologous end joining (NHEJ) or HR. However, in the second case, the severing of the DNA molecule during nuclear division leads to a DSB where only one end can be found in each daughter nucleus (i.e., a “one-ended” DSB). Importantly, the state of each daughter cell is actually different with regard to chromosome XII dose (see Figure 1 and Figure 9 for schemes). While one cell (i.e., “DC2”) would have an entire chromosome XII plus the broken distal region of the right arm of the same chromosome (from the DSB to the telomere), the other one (i.e., “DC1”) would retain a fragment of a single chromosome XII (from the left telomere to the DSB, including its centromere). It is difficult to envisage how each DSB end might be repaired. For instance, break-induced replication, *de novo* telomere addition, chromosome translocation and/or elimination of the broken sisters might well be possible. Confounding matters, if the DSB takes place within the rDNA, which may happen often according to our data, cells can find a template for HR in another copy of the array. This latter situation can lead to an uncertain outcome (e.g., extrachromosomal circles?). Whichever way daughter cells face the problem, our results provide several interesting observations: i) the DSB(s) does not trigger a strong DDR in the new G1 (Figure 2 and Figure 6); ii) the MRX complex (i.e., Mre11) has no role in DSB(s) processing (Figure 7 and Figure S9); iii) the Rad9 checkpoint protein, the RPA complex and Rad52 are part of the mechanism to deal with these DSBs as soon as both daughter cells reach S-phase (Figure 4, Figure 5, Figure 6, Figure S6, and Figure S7); iv) the activity of these key proteins is long lasting and cumulative, especially in the daughter cell that only carries a fragmented cXIIr copy (i.e., DC1) (Figure 4, Figure 5, Figure 6); and v) DC2 often survives and might get rid of the broken distal fragment of cXIIr in order to do so (without using it as a template for HR, see below and Figure 8).

In relation to the absence of both a G1 arrest and Rfa1 foci in the new G1, our results indicate that the DSB generated after *cdc14-1* release is similar to that generated by endonucleases (i.e., a “clean” DSB) as opposed to those generated by ionizing radiation

contingency table could be built (e.g., segregation vs. missegregation). For other categorical variables with more than two possible outcomes (e.g., number of Rad52 foci), the Pearson's chi-square test was employed. Individual comparisons between means of independent experiments were performed by the Student's T test. All tests were two-tailed.

Supporting Information

Figure S1 Cells faithfully segregate chromosome XII in a *cdc15-2* telophase block. Strains FM304 (*cdc14-1 tetO:194 TetR-YFP*), FM307 (*cdc14-1 tetO:450 TetR-YFP*), FM518 (*cdc14-1 tetO:487 TetR-YFP*), FM322 (*cdc14-1 tetO:1061 TetR-YFP*), FM593 (*cdc15-2 tetO:194 TetR-YFP*), FM582 (*cdc15-2 tetO:450 TetR-YFP*), FM584 (*cdc15-2 tetO:487 TetR-YFP*) and FM588 (*cdc15-2 tetO:1061 TetR-YFP*) were arrested at 37°C for 3 hours and resolution and segregation status of *tetOs* (mean \pm SEM, $n=3$) were scored for dumbbell binucleated cells (>200 cells each). (TIF)

Figure S2 Cells do not enter anaphase after a *cdc14-1* release in the W303 background. Strains DOM0114 (*cdc15-2*) and MGY146a (*cdc14-1*) were arrested in telophase by incubation at 37°C for 3 hours (time = 0') and then released from the arrest by dropping the temperature to 25°C. Samples were taken every 15–30 minutes for 4 hours, stained with DAPI and analysed by microscopy for budding pattern (upper panels) and nuclear morphology (lower panels). For the nuclear morphology analysis only daughter cells that have rebudded are included and each daughter is counted individually for simplicity. Note how *cdc15-2* gave an oscillatory behaviour indicative of cells cycling; whereas *cdc14-1* got stuck as foursomes with just two nuclear masses (one mass per daughter cell). (TIF)

Figure S3 A *cdc14-1* release leads to daughter cells stuck with metaphase spindles. (A) Strain FM459 (*cdc14-1 TUB1-GFP*) was treated as in Figure S2 and cells were scored for spindle morphology in either unbudded dumbbells (left panel) or rebudded daughter cells (right panel) (mean \pm SEM, $n=3$). Each rebudded daughter was counted as an individual new cell. (B) Strain FM458 (*cdc14-1 TUB4-CFP*) was arrested in telophase by incubation at 37°C for 3 hours (time = 0') and then released from the arrest by dropping the temperature to 25°C. Samples taken 2 hours after the shift (120') were stained with DAPI and analysed by microscopy. Note: Around 80% of nuclear masses have two CFP foci. Bar, 5 μ m. (TIF)

Figure S4 Chromosome band quantification of *cdc15-2* and *cdc14-1* telophase releases. The pulsed-field gel depicted in the upper panels of Figure 3B and two more independent experiments were scanned to quantify each chromosome band and normalized to that at the telophase block (mean \pm SEM, $n=3$). In the graphs we show the results for the two largest chromosomes (XII and IV) and for other bands containing medium size chromosomes. Note how all chromosomes entered a successful replication round (i.e., bands faded away and came back later) for both mutants; whereas chromosome XII dropped shortly after the *cdc14-1* release (minute 60) and never came back in full. Also note how this drop was observed when replication was prevented by releasing into α -factor (G1 column). (TIF)

Figure S5 The nucleoplasm bridge of soluble TetR-YFP as seen in the *cdc15-2* and *cdc14-1* telophase blocks. (A) Strains

FM584 (*cdc15-2 tetO:487 TetR-YFP*) and FM518 (*cdc14-1 tetO:487 TetR-YFP*) were arrested at 37°C for 3 h and micrographed. (B) Strain FM304 (*cdc14-1 tetO:194 TetR-YFP NET1-CFP*) was arrested as in A. Each photo represents different Z-stacks in 0.3 μ m intervals. Hollow triangles point to the nucleoplasm bridge. Filled triangles point to the bulge in the bridge observed at the *cdc14-1* block. Bar, 5 μ m. Note how the nucleoplasm bridge is seen in all cells at both telophase blocks, the bulge is seen only in *cdc14-1*, and that the bulge contains the bulk of the rDNA (Net1-CFP).

(TIF)

Figure S6 Worsening of chromosome XII segregation through deletion of *FOB1* increases the number of Rad52 repair factories. Strains FM515 (*cdc14-1 RAD52-YFP*) and FM547 (*cdc14-1 fob1 Δ RAD52-YFP*) were first arrested in the *cdc14-1* block and then released into a new cell cycle. After 2 hours, foursomes were scored for number of Rad52 foci (mean \pm SEM, $n=3$). Note how foursomes with no Rad52 foci dropped from ~50% to ~20% when the *fob1 Δ* mutation was present (rDNA missegregation increased from ~50% to ~95% relative to *FOB1*).

(TIF)

Figure S7 Presence of Rad52 repair factories correlates to previous failure in rDNA segregation after a *cdc14-1* release. Strain FM753 (*cdc14-1 RAD52-RedStar2 tetO:487 tetR-YFP*) was first arrested in the *cdc14-1* block and then released into a new cell cycle. After 2 hours, Rad52 foci were scored for those foursomes that have either segregated or missegregated the *tetO* (mean \pm SEM, $n=3$).

(TIF)

Figure S8 Rad52 repair factories localize out of the nucleolus after a *cdc14-1* release. Strain FM460 (*cdc14-1 RAD52-YFP NOP1-DsRed*) was first arrested and micrographed in the telophase block (0') and then two hours after the release (120'). Representative micrographs of the major cell types are shown. In the channel composite, DAPI is pseudocoloured in red and Nop1 in blue. Note how Rad52 foci in foursomes (at 120') do not colocalize with the nucleolar marker Nop1.

(TIF)

Figure S9 Mre11 is functional under the *cdc14-1* background and concentrates in nuclear factories after chemically-generated DNA double strand breaks. Strain FM514 (*cdc14-1 MRE11-YFP*) was grown at 25°C until log phase and directly treated with either 25 μ g/ml phleomycin or 0.03% v/v MMS. Then, samples were taken every 10 minutes and micrographed under the microscope. Mre11-YFP started concentrating in foci after just 20 minutes. Example micrographs taken after 2 hours of treatments are shown. White filled triangles point to Mre11-YFP foci.

(TIF)

Acknowledgments

We thank M. Lisby, R. Rothstein, and S. Gasser for strains. We gratefully thank S. Colman for her support in revising the manuscript.

Author Contributions

Conceived and designed the experiments: OQ JG-L EM-P LA FM. Performed the experiments: OQ JG-L EM-P FM. Analyzed the data: OQ JG-L EM-P LA FM. Contributed reagents/materials/analysis tools: OQ JG-L EM-P LA FM. Wrote the paper: FM.

Table 2. Strains used in this work.

Strain name	Relevant genotype	Origin
AS499	(S288C) <i>bar1Δ</i>	A. Strunnikov
GA2199	(W303) <i>BAR1 Telomere V-L:TetO TetR-YFP Telomere V-R:lacO CFP-lacI</i>	S. Gasser
GA2468	(S288C) <i>BAR1 Telomere XIV-L:lacO Telomere XIV-R:tetO CFP-lacI TetR-YFP</i>	S. Gasser
W3749-14c	(W303) <i>bar1Δ RAD5 RAD52-YFP</i>	D. Rothstein
W3775-12c	(W303) <i>bar1Δ RAD5 RFA1-YFP</i>	D. Rothstein
W3483-10a	(W303) <i>bar1Δ RAD5 MRE11-YFP</i>	D. Rothstein
ML118-1D	(W303) <i>BAR1 RAD5 tetOx224:rDNA TetR-mRFP RAD52-YFP</i>	M. Lisby
DOM0114	(W303) <i>bar1Δ cdc15-2</i>	D. Morgan
MGY146a	(W303) <i>bar1Δ cdc14-1</i>	C. Nombela
FM304 (CCG1605)	AS499 <i>tetOx224:chrmXII(194 Kb) TetR-YFP cdc14-1 NET1-CFP</i>	L. Aragon
FM307 (CCG1607)	AS499 <i>tetOx224:chrmXII(450 Kb) TetR-YFP cdc14-1 NET1-CFP</i>	L. Aragon
FMS18 (CCG1679)	AS499 <i>tetOx224:chrmXII(487 Kb) TetR-YFP cdc14-1</i>	L. Aragon
FM322 (CCG1609)	AS499 <i>tetOx224:chrmXII(1061 Kb) TetR-YFP cdc14-1 NET1-CFP</i>	L. Aragon
FMS93	AS499 <i>tetOx224:chrmXII(194 Kb) TetR-YFP cdc15-2</i>	This work
FMS82	AS499 <i>tetOx224:chrmXII(450 Kb) TetR-YFP cdc15-2</i>	This work
FMS84	AS499 <i>tetOx224:chrmXII(487 Kb) TetR-YFP cdc15-2</i>	This work
FMS88	AS499 <i>tetOx224:chrmXII(1061 Kb) TetR-YFP cdc15-2</i>	This work
FM459	MGY146a <i>GFP-TUB1 cdc14-1</i>	This work
FM576	MGY146a <i>GFP-TUB1 cdc14-1 rad9Δ</i>	This work
FM458	MGY146a <i>TUB4-CFP cdc14-1</i>	This work
FM565	GA2199 <i>Tel V-L:TetO TetR-YFP Tel V-R:lacO CFP-lacI cdc14-1</i>	This work
FM573	GA2468 <i>Tel XIV-L:lacO Tel XIV-R:tetO CFP-lacI TetR-YFP cdc14-1</i>	This work
FM567	GA2199 <i>Tel V-L:TetO TetR-YFP Tel V-R:lacO CFP-lacI cdc15-2</i>	This work
FM574	GA2468 <i>Tel XIV-L:lacO Tel XIV-R:tetO CFP-lacI TetR-YFP cdc15-2</i>	This work
FM515	W3749-14c <i>RAD52-YFP cdc14-1</i>	This work
FM531	W3749-14c <i>RAD52-YFP cdc15-2</i>	This work
FM547	W3749-14c <i>RAD52-YFP cdc14-1 fob1Δ</i>	This work
FM883	W3749-14c <i>RAD52-YFP cdc14-1 rad9Δ</i>	This work
FM460	W3749-14c <i>RAD52-YFP cdc14-1 NOP1-DsRed</i>	This work
FM551	ML118-1D <i>tetOx224:rDNA TetR-mRFP RAD52-YFP cdc14-1</i>	This work
FM753	AS499 <i>tetOx224:chrmXII(487 Kb) TetR-YFP cdc14-1 RAD52-RedStar2</i>	This work
FM513	W3775-12c <i>RFA1-YFP cdc14-1</i>	This work
FM514	W3483-10a <i>MRE11-YFP cdc14-1</i>	This work
FMS72	W3749-14c <i>RAD52-YFP cdc14-1 mre11Δ</i>	This work
FMS39	AS499 <i>tetOx224:chrmXII(487 Kb) TetR-YFP cdc14-1 rad52Δ</i>	This work

doi:10.1371/journal.pgen.1002509.t002

the growth media by the addition of formaldehyde to 5% final concentration. After incubation at 25°C for 1 h with gentle rocking, fixed cells were washed twice with PBS and then once with 1 M sorbitol in 50 mM KPO₄, pH 7.5. Cells were incubated with 0.2 mg/ml zymolyase 20T (Zymo Research) in the above sorbitol buffer containing 2 mM DTT for 20 minutes at 37°C. After zymolyase treatment, cell numbers were counted on a haemocytometer.

Special chemical treatments in these assays (i.e., nocodazole, alpha-factor and latrunculin A) were performed as follows: The arrest in G2/M was carried with 15 μg/ml of nocodazole at 25°C for 2.5 hours. Latrunculin A (100 μM) was added right at the G2/M release and alpha-factor (50 ng/ml) was added right at the telophase release. Release from the G2/M arrest was accomplished by washing away the nocodazole. Incubation for

1.5 hours at 37°C was used to block cells in telophase after a G2/M release. For the telophase release, cultures were shifted back to 25°C. Samples for this cytokinesis assay were taken at the telophase block and two hours after the telophase release. We used a *cdc14-1* strain of the W303 background in these assays because it gave better synchrony, especially during the double block-and-release experiments (first at G2/M and then at telophase).

Statistics

Error bars in graphs represent the standard error of the mean (SEM) unless stated otherwise. The number of experiments is indicated in the corresponding figure legend or table. Statistic inference for cross-comparison of categorical variables distributions were performed by the Fisher's exact test when a 2×2

(i.e., “ragged” DSBs) [45,46,49]. Also, it indicates that the number of DSBs should be below four or five (i.e., few chromosome arms are part of the anaphase bridge) [45]. Besides this, it is interesting that the processing of these DSBs is independent of Mre11 (Figure 7). Perhaps the MRX complex is not needed because the one-ended nature of each DSB means that there is no need to join both broken ends. Perhaps other molecular players are required in this context. In any case, others have previously reported that cells deficient in Mre11 and other MRX components can still generate a strong DDR and repair DSB through HR [59]. An alternative explanation for the Rfa1/Rad52 foci would be related to a sort of *de novo* damage generated as a consequence of DNA replication through an unrepaired or faultily-repaired chromosome XII. Future works are also needed in this direction.

As for the long-term consequences of this type of one-ended DSB, it is interesting that we observed that the DC2 cell can eventually recover in many cases (Figure 4 and Figure 8). Most surprising was the fact that viability got better when *RAD52* was deleted. We interpret this as indicating that checkpoint adaptation followed by loss of the acentric fragment might be the main pathway that allows DC2 to progress. Accordingly, surviving *cdc14-1 rad52Δ* foursomes grew ~30% more slowly (they actually took around one extra day to be visible on plates) relative to the same cells plated before the block-and-release experiment (Figure 8A). Indeed, the presence of Rad52 might compromise the chances of *cdc14-1* DC2 cells surviving with a good fitness (Figure 8A). Contrary to expectations, though, PFGE of survivors showed that chromosome XII was more unstable in *cdc14-1 rad52Δ*. Also, the slow-growing colonies of *cdc14-1 RAD52* did not show visible abnormal chromosome patterns. Despite our having checked only a few surviving colonies, it is interesting that none show evidence of chromosome XII rearrangements that involve translocations, although one might have duplicated the chromosome. Thus, we concluded that the DC2 cell very often survives and that it might repair the broken cXIIr in two ways; one which is dependent on Rad52 (e.g., through break induced replication, a likely event at least in the survivor with two chromosome XIIs), and a second Rad52-independent manner that somehow makes more likely changes in chromosome XII size.

As far as we know, this is the first time that an analysis of the DNA damage generated by cytokinetic severing of a single chromosome is conducted in yeast. A recent paper has just described the DDR after cytokinesis severs lagging chromosomes in human cells [60]. Many conclusions from that paper agree with those we observed in our work, although the system is clearly distinct (i.e., more than one chromosome is affected, both sister chromatids are severed, etc). In these human cells, DSBs arise after cytokinesis and are often repaired by NHEJ in G1, leading to aberrant chromosomes. The difference in the mechanism of repair in our yeast system is nevertheless expected, since yeast basically rely on HR acting through S and G2 rather than NHEJ in G1 [42]. Another key difference between both systems is the ploidy of the dividing cells. Human cells are diploids and may repair broken sisters using homologous chromosomes as templates. Our yeast strains were all haploids. It would be interesting to study whether *cdc14-1* diploids also missegregate cXIIr and whether the DDR is different from what we describe here for haploids. Future work will be carried out to this aim.

Conclusion

In this study we have assessed the fate of cells that have an anaphase bridge formed by the right arm of chromosome XII (Figure 9 for a model and summary). We show how cells can go

through a new G1, although they sever the bridge as they complete cytokinesis, and reach G2/M where they get arrested in a Rad9-dependent manner. We also show that the expected DNA damage response comprised RPA and Rad52, but is independent of Mre11. All these data shed light on how one-ended DSBs generated by a “cut” phenotype may be processed in eukaryotic cells. This work provides the first systematic study of the cell responses to a previous failure in sister chromatid resolution.

Materials and Methods

Yeast strains, growth, and experimental conditions

All yeast strains used in this work are listed in Table 2. Strains with the *tetOs* along chromosome XII right arm and those with tags for chromosome XIV telomeres were S288C background. Those with Rad52-YFP, Rfa1-YFP, Mre11-YFP, GFP-Tub1 and Tub4-CFP tags, and those with tags for chromosome V telomeres were W303. C-terminal tagging with GFP variants, gene deletions and allele replacements were performed using PCR methods [61,62]. All strains were grown overnight at 25°C in YPD media. For telophase block-and-release experiments, asynchronous cultures were first adjusted to OD₆₆₀/ml = 0.2, incubated at 37°C for 3 h in air orbital incubators and then shifted back to 25°C. To arrest cells in G1 in the cell cycle that follows the telophase release, cells were treated with alpha-factor (50 ng/ml) for 2 hours after the 25°C shift (all tested strains were *bar1Δ*). Flow cytometry analysis was carried out as described [54] in a BD FACScalibur machine, adjusting the peaks for 1 N and 2 N with an asynchronous culture at 25°C before reading the samples. PFGE to see all yeast chromosomes was performed using a CHEF DR-III system (Bio-Rad) in a 0.8% agarose gel in 0.5× TBE buffer and run at 12°C for 20 h at 6 V/cm with an initial switching time of 80 seconds, a final of 150 seconds, and an angle of 120°. PFGE to assess the size of chromosome XII was performed at 3 V/cm for 68 h with 300 and 900 seconds of initial and final switching time respectively. Ethidium bromide was used to visualize the chromosome bands in the gel. Band quantifications were performed with ImageJ software (NIH). Chromosome XII band(s) was identified by Southern blot using a Digoxigenin-labelled probe (Roche) against the NTS2 region within the rDNA.

Fluorescence microscopy

Fluorescent proteins and chromosome tags were analysed by wide-field fluorescence microscopy. Series of z-focal plane images (10–20 planes, 0.15–0.3 μm depth) were collected on a Leica DMI6000, using a 63×/1.30 immersion objective and an ultrasensitive DFC 350 digital camera, and processed with the AF6000 software (Leica). Scale bars in micrographs depict 5 μm. For nuclear morphology studies, DNA was stained using DAPI at 4 μg/ml final concentration after short cell treatment with 1% Triton X-100. Time-lapse movies were filmed without Triton/DAPI treatment on minimal medium agarose patches. Imaging was done at room temperature. Nucleoplasm pictures using nuclear-tagged TetR-YFP was also done without Triton/DAPI treatment. Rad52 foci recognition was performed either manually or using the CellProfiler software [63]. For the latter, whole images were normalized following the procedure: most intense focus in the first photo taken was set to 1, least intense pixel of the background was set to 0. A lower threshold of 0.1 was set for foci recognition.

Cytokinesis assays

Cytokinesis was monitored as previously described [39] with minor modifications. Briefly, aliquots of cells were fixed directly in

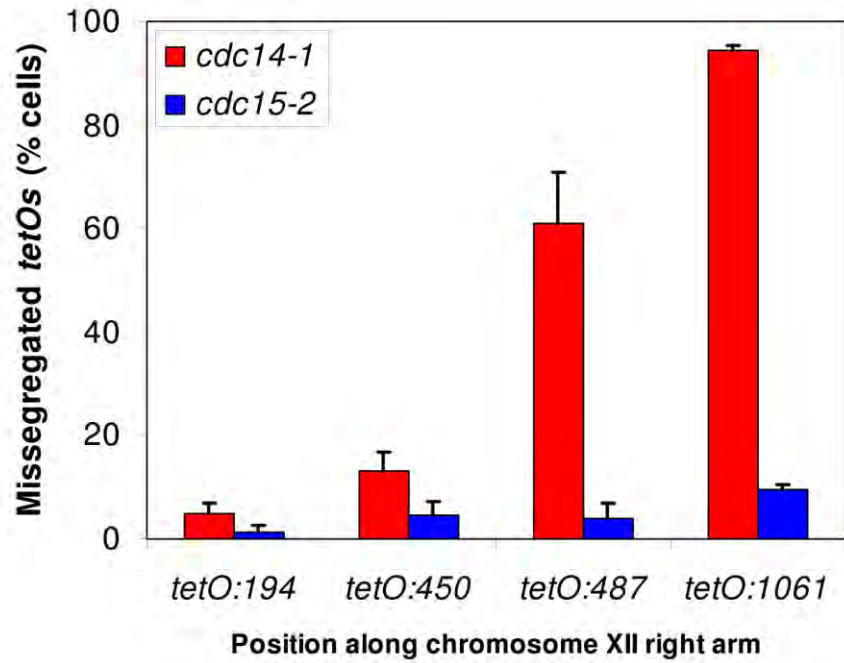
References

- Fujiwara T, Bandi M, Nitta M, Ivanova EV, Bronson RT, et al. (2005) Cytokinesis failure generating tetraploids promotes tumorigenesis in p53-null cells. *Nature* 437: 1043–7.
- Shi Q, King RW (2005) Chromosome nondisjunction yields tetraploid rather than aneuploid cells in human cell lines. *Nature* 437: 1038–42.
- Bajer A (1964) Cine-Micrographic Studies On Dicentric Chromosomes. *Chromosoma* 15: 630–51.
- McClintock B (1939) The Behavior in Successive Nuclear Divisions of a Chromosome Broken at Meiosis. *Proc Natl Acad Sci USA* 25: 405–16.
- McClintock B (1941) The Stability of Broken Ends of Chromosomes in *Zea Mays*. *Genetics* 26: 234–82.
- Gisselsson D, Pettersson L, Höglund M, Heidenblad M, Gorunova L, et al. (2000) Chromosomal breakage-fusion-bridge events cause genetic intratumor heterogeneity. *Proc Natl Acad Sci USA* 97: 5357–62.
- Shimizu N, Shingaki K, Kaneko-Sasaguri Y, Hashizume T, Kanda T (2005) When, where and how the bridge breaks: anaphase bridge breakage plays a crucial role in gene amplification and HSR generation. *Exp Cell Res* 302: 233–43.
- Vukovic B, Beheshti B, Park P, Lim G, Bayani J, et al. (2007) Correlating breakage-fusion-bridge events with the overall chromosomal instability and in vitro karyotype evolution in prostate cancer. *Cytogenet Genome Res* 116: 1–11.
- French JD, Dunn J, Smart CE, Manning N, Brown MA (2006) Disruption of BRCA1 function results in telomere lengthening and increased anaphase bridge formation in immortalized cell lines. *Genes Chromosomes Cancer* 45: 277–89.
- Cuevas-Ramos G, Petit CR, Marcq I, Boury M, Oswald E, et al. (2010) *Escherichia coli* induces DNA damage in vivo and triggers genomic instability in mammalian cells. *Proc Natl Acad Sci USA* 107: 11537–42.
- Giménez-Abián JF, Clarke DJ, Giménez-Martin G, Weingartner M, Giménez-Abián MI, et al. (2002) DNA catenations that link sister chromatids until the onset of anaphase are maintained by a checkpoint mechanism. *Eur J Cell Biol* 81: 9–16.
- Luo LZ, Werner KM, Gollin SM, Saunders WS (2004) Cigarette smoke induces anaphase bridges and genomic imbalances in normal cells. *Mutat Res* 554: 375–85.
- Díaz-Martínez La, Giménez-Abián JF, Clarke DJ (2008) Chromosome cohesion - rings, knots, orcs and fellowships. *J Cell Sci* 121: 2107–14.
- Uhlmann F, Lottspeich F, Nasmyth K (1999) Sister-chromatid separation at anaphase onset is promoted by cleavage of the cohesin subunit Scc1. *Nature* 400: 37–42.
- Strunnikov AV, Hogan E, Koshland D (1995) SMC2, a *Saccharomyces cerevisiae* gene essential for chromosome segregation and condensation, defines a subgroup within the SMC family. *Genes Dev* 9: 587–599.
- Holm C, Goto T, Wang JC, Botstein D (1985) DNA topoisomerase II is required at the time of mitosis in yeast. *Cell* 41: 553–63.
- Holm C, Stearns T, Botstein D (1989) DNA topoisomerase II must act at mitosis to prevent nondisjunction and chromosome breakage. *Mol Cell Biol* 9: 159–68.
- DiNardo S, Voelkel K, Sternglanz R (1984) DNA topoisomerase II mutant of *Saccharomyces cerevisiae*: topoisomerase II is required for segregation of daughter molecules at the termination of DNA replication. *Proc Natl Acad Sci USA* 81: 2616–20.
- Freeman L, Aragon-Alcaide L, Strunnikov A (2000) The condensin complex governs chromosome condensation and mitotic transmission of rDNA. *J Cell Biol* 149: 811–24.
- Bhalla N, Biggins S, Murray AW (2002) Mutation of YCS4, a budding yeast condensin subunit, affects mitotic and nonmitotic chromosome behavior. *Mol Biol Cell* 13: 632–45.
- Spell RM, Holm C (1994) Nature and distribution of chromosomal intertwinnings in *Saccharomyces cerevisiae*. *Mol Cell Biol* 14: 1465–76.
- D'Amours D, Stegmeier F, Amon A (2004) Cdc14 and condensin control the dissolution of cohesin-independent chromosome linkages at repeated DNA. *Cell* 117: 455–69.
- Machin F, Torres-Rosell J, Jarmuz A, Aragón L (2005) Spindle-independent condensation-mediated segregation of yeast ribosomal DNA in late anaphase. *J Cell Biol* 168: 209–19.
- Torres-Rosell J, Machin F, Jarmuz A, Aragón L (2004) Nucleolar segregation lags behind the rest of the genome and requires Cdc14p activation by the FEAR network. *Cell cycle* 3: 496–502.
- Granot D, Snyder M (1991) Segregation of the nucleolus during mitosis in budding and fission yeast. *Cell Motil Cytoskeleton* 20: 47–54.
- Stegmeier F, Amon A (2004) Closing mitosis: the functions of the Cdc14 phosphatase and its regulation. *Annu Rev Genet* 38: 203–32.
- Sullivan M, Higuchi T, Katis VL, Uhlmann F (2004) Cdc14 phosphatase induces rDNA condensation and resolves cohesin-independent cohesion during budding yeast anaphase. *Cell* 117: 471–82.
- Machin F, Torres-Rosell J, Piccoli GDe, Carballo JA, Cha RS, et al. (2006) Transcription of ribosomal genes can cause nondisjunction. *J Cell Biol* 173: 893–903.
- Guacci V, Hogan E, Koshland D (1994) Chromosome condensation and sister chromatid pairing in budding yeast. *J Cell Biol* 125: 517–30.
- Clemente-Blanco A, Mayán-Santos M, Schneider DA, Machin F, Jarmuz A, et al. (2009) Cdc14 inhibits transcription by RNA polymerase I during anaphase. *Nature* 458: 219–22.
- Wang B-D, Yong-Gonzalez V, Strunnikov AV (2004) Cdc14p/FEAR pathway controls segregation of nucleolus in *S. cerevisiae* by facilitating condensin targeting to rDNA chromatin in anaphase. *Cell cycle* 3: 960–7.
- Baxter J, Diffley JFX (2008) Topoisomerase II inactivation prevents the completion of DNA replication in budding yeast. *Mol Cell* 30: 790–802.
- Dulev S, Renty Cde, Mehta R, Minkov I, Schwob E, et al. (2009) Essential global role of CDC14 in DNA synthesis revealed by chromosome under-replication unrecognized by checkpoints in cdc14 mutants. *Proc Natl Acad Sci USA* 106: 14466–71.
- Culotti J, Hartwell LH (1971) Genetic control of the cell division cycle in yeast. 3. Seven genes controlling nuclear division. *Exp Cell Res* 67: 389–401.
- Hennessy KM, Lee A, Chen E, Botstein D (1991) A group of interacting yeast DNA replication genes. *Genes Dev* 5: 958–969.
- Burke DJ, Church D (1991) Protein synthesis requirements for nuclear division, cytokinesis, and cell separation in *Saccharomyces cerevisiae*. *Mol Cell Biol* 11: 3691–8.
- Mendoza M, Norden C, Durrer K, Rauter H, Uhlmann F, et al. (2009) A mechanism for chromosome segregation sensing by the NoCut checkpoint. *Nat Cell Biol* 11: 477–83.
- Norden C, Mendoza M, Dobbelaere J, Kotwaliwale CV, Biggins S, et al. (2006) The NoCut pathway links completion of cytokinesis to spindle midzone function to prevent chromosome breakage. *Cell* 125: 85–98.
- Hartwell LH (1971) Genetic control of the cell division cycle in yeast. IV. Genes controlling bud emergence and cytokinesis. *Exp Cell Res* 69: 265–76.
- Tolliday N, VerPlank L, Li R (2002) Rho1 directs formin-mediated actin ring assembly during budding yeast cytokinesis. *Curr Biol* 12: 1864–70.
- Weinert TA, Hartwell LH (1988) The RAD9 gene controls the cell cycle response to DNA damage in *Saccharomyces cerevisiae*. *Science* 241: 317–22.
- Pâques F, Haber JE (1999) Multiple pathways of recombination induced by double-strand breaks in *Saccharomyces cerevisiae*. *Microbiol Mol Biol Rev* 63: 349–404.
- Lisby M, Rothstein R, Mortensen UH (2001) Rad52 forms DNA repair and recombination centers during S phase. *Proc Natl Acad Sci USA* 98: 8276.
- Torres-Rosell J, Sunjevaric I, Piccoli GDe, Sacher M, Eckert-Boulet N, et al. (2007) The Smc5-Smc6 complex and SUMO modification of Rad52 regulates recombinational repair at the ribosomal gene locus. *Nat Cell Biol* 9: 923–31. doi:10.1038/ncb1619.
- Zierhut C, Diffley JFX (2008) Break dosage, cell cycle stage and DNA replication influence DNA double strand break response. *EMBO J* 27: 1875–85.
- Barlow JH, Lisby M, Rothstein R (2008) Differential regulation of the cellular response to DNA double-strand breaks in G1. *Mol Cell* 30: 73–85.
- Garvik B, Carson M, Hartwell L (1995) Single-stranded DNA arising at telomeres in cdc13 mutants may constitute a specific signal for the RAD9 checkpoint. *Mol Cell Biol* 15: 6128–38.
- Zou L, Elledge SJ (2003) Sensing DNA damage through ATRIP recognition of RPA-ssDNA complexes. *Science* 300: 1542–8.
- Lisby M, Barlow JH, Burgess RC, Rothstein R (2004) Choreography of the DNA damage response: spatiotemporal relationships among checkpoint and repair proteins. *Cell* 118: 699–713.
- Gerald JNF, Benjamin JM, Kron SJ (2002) Robust G1 checkpoint arrest in budding yeast: dependence on DNA damage signaling and repair. *J Cell Sci* 115: 1749–57.
- Bystricky K, Laroche T, Houwe Gvan, Blaszczyk M, Gasser SM (2005) Chromosome looping in yeast: telomere pairing and coordinated movement reflect anchoring efficiency and territorial organization. *J Cell Biol* 168: 375–87.
- Fitzpatrick PJ, Toyn JH, Millar JB, Johnston LH (1998) DNA replication is completed in *Saccharomyces cerevisiae* cells that lack functional Cdc14, a dual-specificity protein phosphatase. *Mol Gen Genet* 258: 437–41.
- Lengronne A, Schwob E (2002) The yeast CDK inhibitor Sic1 prevents genomic instability by promoting replication origin licensing in late G(1). *Mol Cell* 9: 1067–78.
- Torres-Rosell J, Machin F, Farmer S, Jarmuz A, Eydmann T, et al. (2005) SMC5 and SMC6 genes are required for the segregation of repetitive chromosome regions. *Nat Cell Biol* 7: 412–9.
- Hill A, Bloom K (1989) Acquisition and processing of a conditional dicentric chromosome in *Saccharomyces cerevisiae*. *Mol Cell Biol* 9: 1368–70.
- Yang SS, Yeh E, Salmon ED, Bloom K (1997) Identification of a mid-anaphase checkpoint in budding yeast. *J Cell Biol* 136: 345–54.
- Thrower DA, Bloom K (2001) Dicentric chromosome stretching during anaphase reveals roles of Sir2/Ku in chromatin compaction in budding yeast. *Mol Biol Cell* 12: 2800–12.
- Haber JE, Thorburn PC (1984) Healing of broken linear dicentric chromosomes in yeast. *Genetics* 106: 207–26.
- Haber JE (1998) The many interfaces of Mre11. *Cell* 95: 583–6.
- Janssen A, van der Burg M, Szuhai K, Kops GJ, Medema RH (2011) Chromosome Segregation Errors as a Cause of DNA Damage and Structural Chromosome Aberrations. *Science* 333: 1895–1898.
- Knop M, Siegers K, Pereira G, Zachariae W, Winsor B, et al. (1999) Epitope tagging of yeast genes using a PCR-based strategy: more tags and improved practical routines. *Yeast* 15: 963–72.

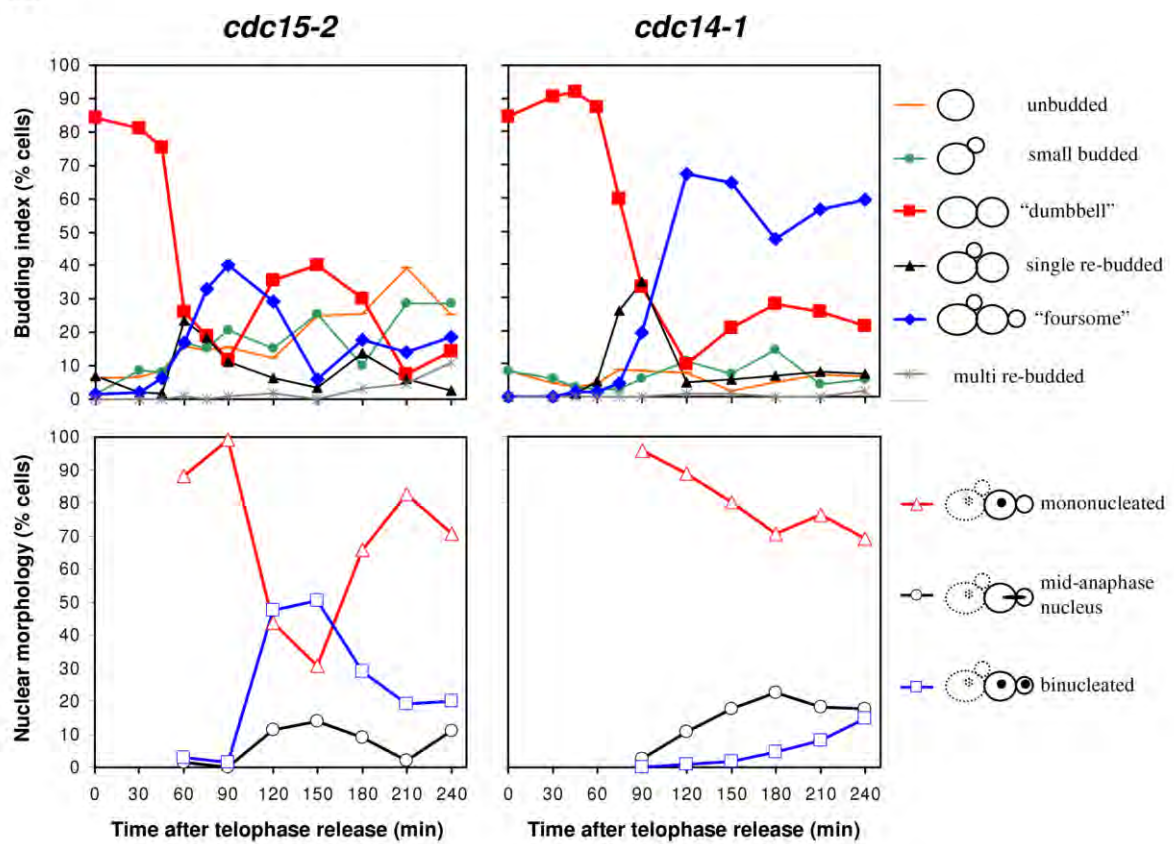
62. Janke C, Magiera MM, Rathfelder N, Taxis C, Reber S, et al. (2004) A versatile toolbox for PCR-based tagging of yeast genes: new fluorescent proteins, more markers and promoter substitution cassettes. *Yeast* 21: 947–62.
63. Carpenter AE, Jones TR, Lamprecht MR, Clarke C, Kang IH, et al. (2006) CellProfiler: image analysis software for identifying and quantifying cell phenotypes. *Genome Biol* 7: R100. Available: <http://genomebiology.com/content/7/10/R100>.



S1

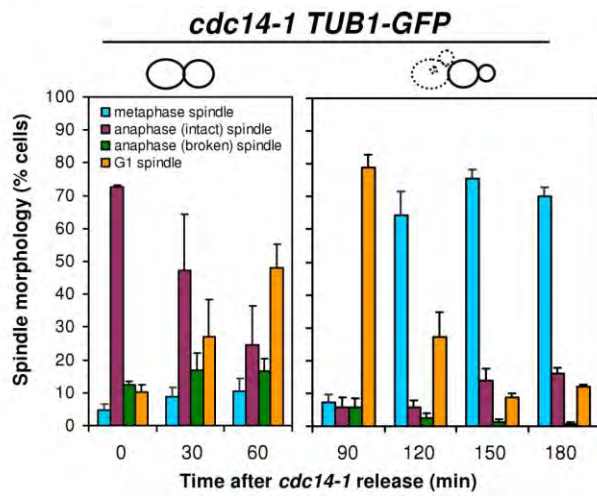


S2

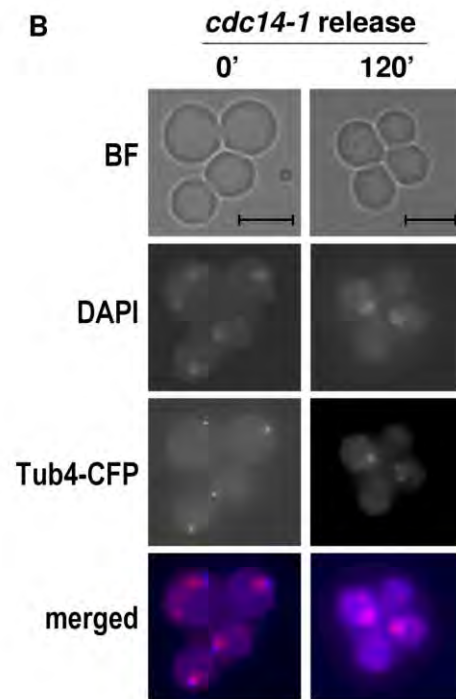


S3

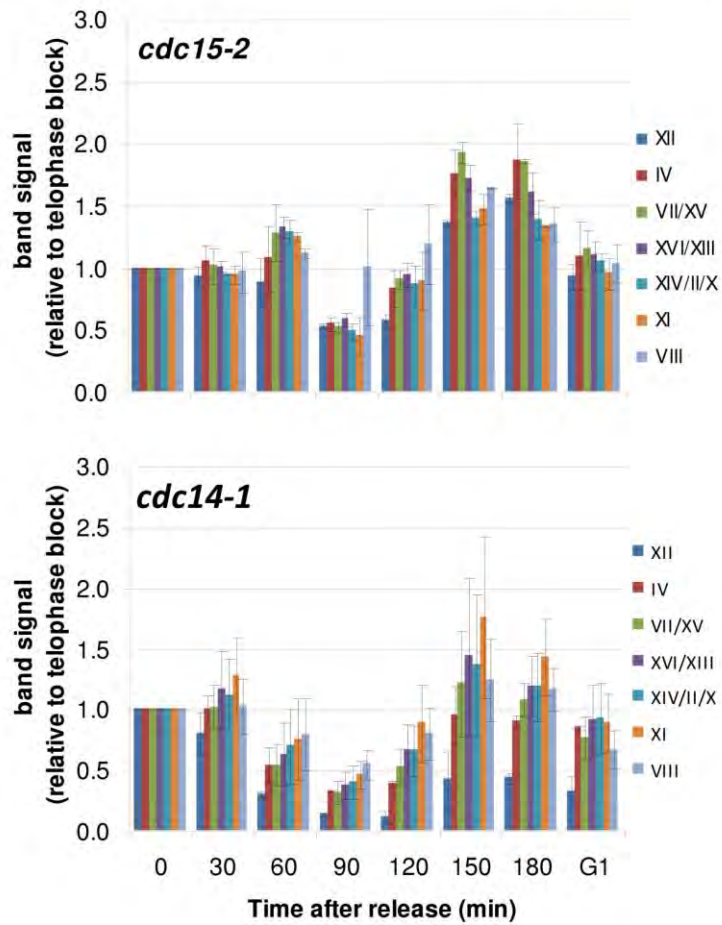
A

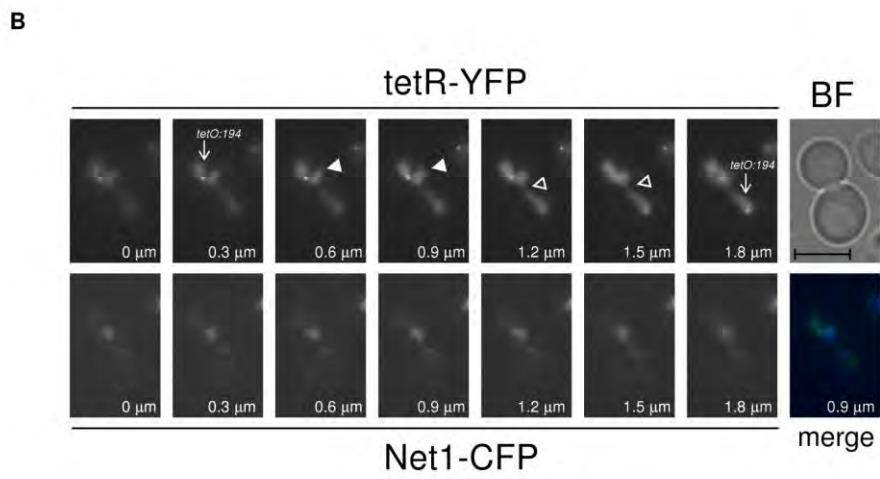
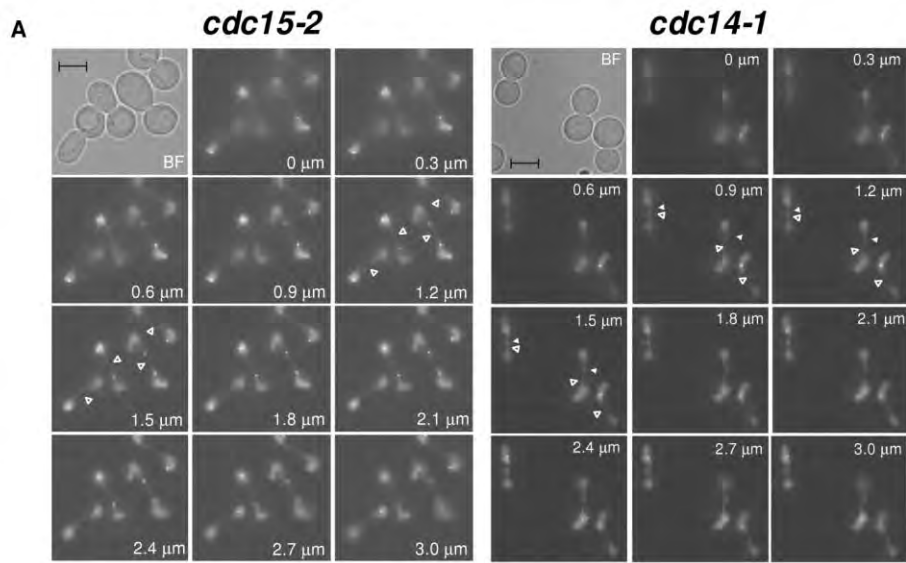


B

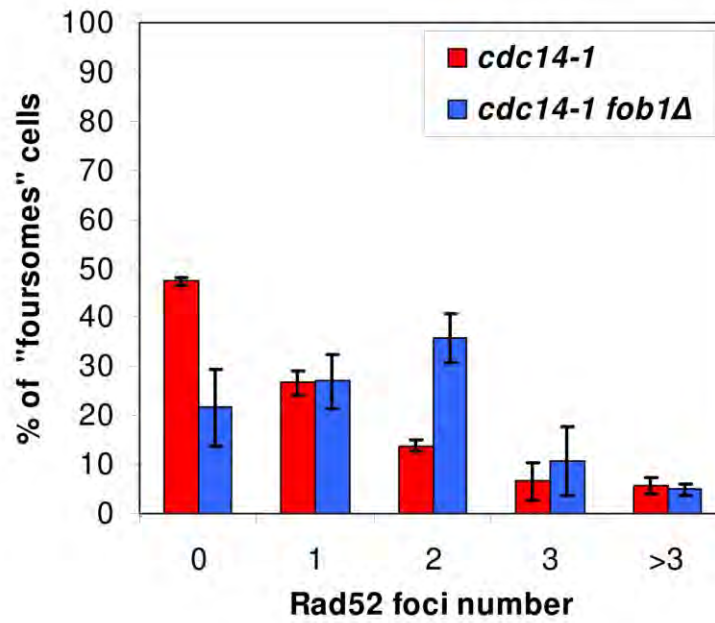


S4

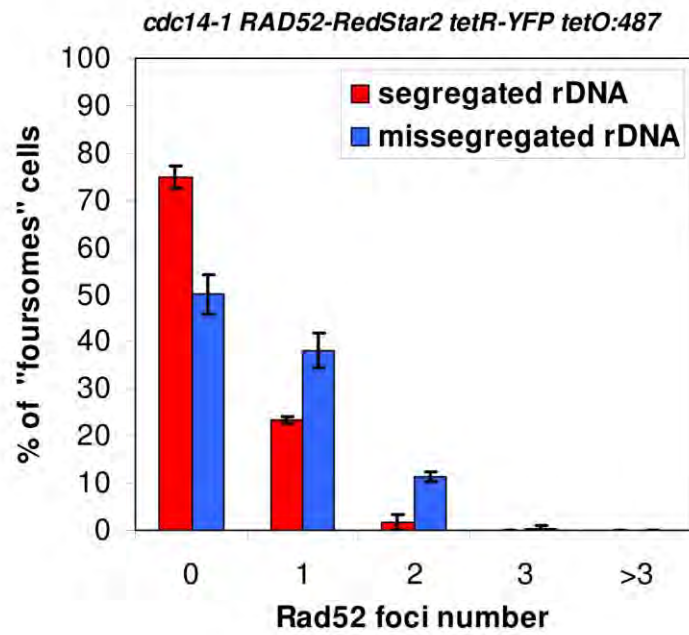




S6

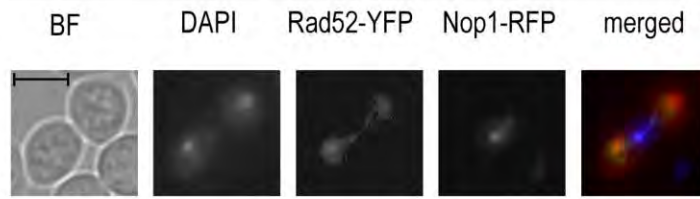


S7

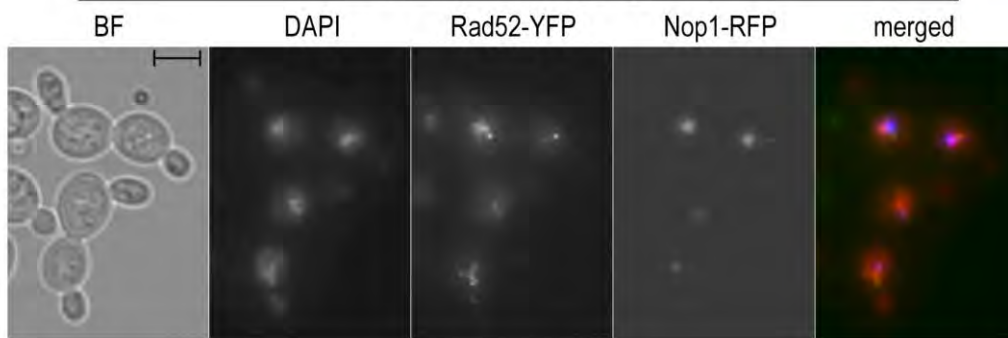


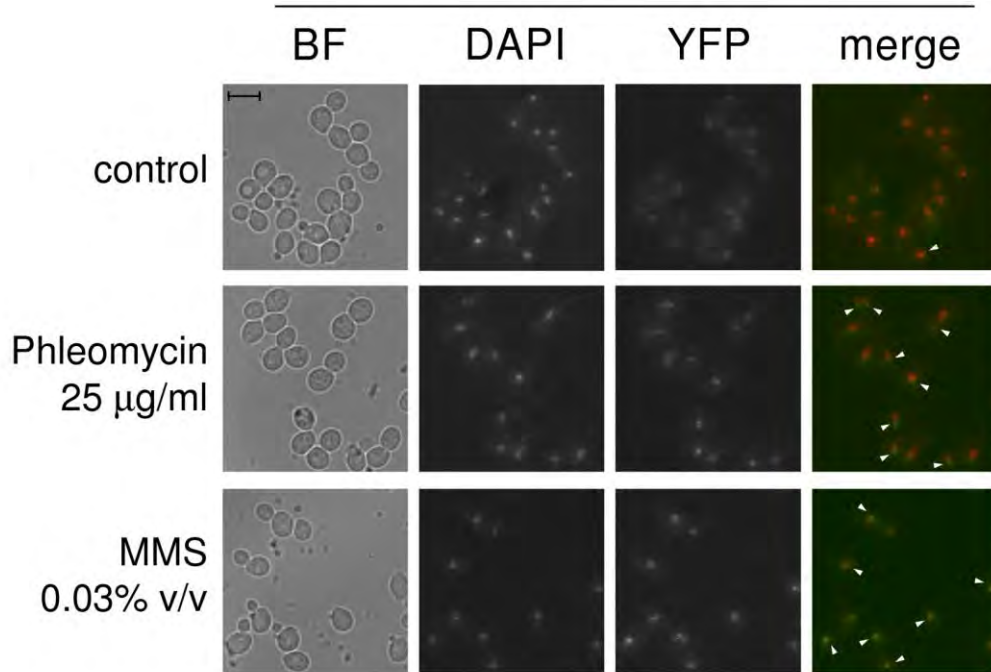
S8

***cdc14-1* release (0')**



***cdc14-1* release (120')**



cdc14-1 MRE11-YFP

4.2 Article 2: Mus81-Mms4 and Yen1 resolve a novel anaphase bridge formed by noncanonical Holliday junctions

In this second paper I used a *cdc15-2* strain tagged in the subtelomeric region of cXII with the system *tetO/TetR* to study how accumulation of recombination intermediates affect chromosome segregation. I chose to measure the segregation of this specific locus because it is thought to be the worst-case scenario in terms of segregation. cXII is the longest chromosome in yeast and it contains the rDNA locus. The rDNA is highly transcribed and replicated unidirectionally, and these in turn produce accumulation of catenations and high rates of recombination.

In this work, I aimed to determine whether the persistence of joint molecules dependant on SSEs for their resolution cause the formation of anaphase bridges. In order to test this I increased the steady-state levels of joint molecules by deleting different combinations of SSEs genes and exposing the cells to genotoxic agents that boost the usage of homologous recombination. I found that both Mus81-Mms4 and Yen1, but not Slx4-Slx1, are essential and compensate each other in preventing and resolving not only chromatin bridges but also ultrafine bridges that mostly comprise noncanonical HJs.

ARTICLE

Received 21 Mar 2014 | Accepted 24 Oct 2014 | Published 3 Dec 2014

DOI: 10.1038/ncomms6652

Mus81-Mms4 and Yen1 resolve a novel anaphase bridge formed by noncanonical Holliday junctions

Jonay García-Luis^{1,†} & Félix Machín¹

Downregulation of separase, condensin, Smc5/6, topoisomerase II and Cdc14 in *Saccharomyces cerevisiae* yields anaphase bridges formed by unresolved sister chromatids (SCBs). Here we report that the overlapping actions of the structure-selective endonucleases (SSEs) Mus81-Mms4/EME1 and Yen1/GEN1, but not Slx1-Slx4, are also essential to prevent the formation of spontaneous SCBs that depend on the homologous recombination pathway. We further show that the frequency of SCBs is boosted after mild replication stress and that they contain joint molecules enriched in non-canonical forms of the Holliday junction (HJ), including nicked-HJ (nHJ). We show that SCBs are mostly reversible upon activation of either Mus81-Mms4 or Yen1 in late anaphase, which is concomitant with the disappearance of non-canonical HJs and restoration of viable progeny. On the basis of these findings, we propose a model where unresolved recombination intermediates are a source of mitotic SCBs, and Mus81-Mms4 and Yen1 play a central role in their resolution *in vivo*.

¹Unidad de Investigación, Hospital Universitario Nuestra Señora de Candelaria, Carretera del Rosario, 145, 38010 Santa Cruz de Tenerife, Spain. † Present address: Cell Cycle Group, MRC Clinical Sciences Centre, Imperial College London, Du Cane Road, London W12 0NN, UK. Correspondence and requests for materials should be addressed to F.M. (email: fmacconw@gmail.com).

Failure to remove proteinaceous cohesion, topological catenations, or to complete DNA replication by mitosis in the budding yeast *S. cerevisiae* causes sister chromatid nondisjunction and the formation of anaphase bridges^{1–5}. Importantly, anaphase bridges have been shown as a source of genetic instability linked to cancer onset and intratumour heterogeneity in humans^{6–8}. Failure to timely process recombination intermediates in which sister chromatids are linked again through pairing of complementary strands, that is, forming joint molecules (JMs), is also expected to cause deleterious consequences in anaphase^{8,9}.

During the mitotic division, inter-sister recombination intermediates arise when the homologous recombination pathway (HR) is called on to repair several DNA insults such as double-strand breaks (DSBs), interstrand crosslinks, stalled replication forks (SRFs) and post-replicative gaps. In budding yeast, as well as in humans, the processing of JMs involves several helicases and at least three structure-selective endonucleases (SSEs): Slx1-Slx4, Mus81-Mms4 (EME1 in the fission yeast and humans) and Yen1 (GEN1 in humans)^{9–11}. Among the helicases, the helicase-topoisomerase complex formed by the budding yeast helicase Sgs1 (Bloom's syndrome BLM in humans), the type I topoisomerase Top3 (TOPOIII α) and the cofactor Rmi1 (RMI1-RMI2) is by far the most studied in JM resolution^{9–12}. This complex (hereafter refer to as STR) appears active throughout the cell cycle and removes JMs mainly through a process known as double Holliday junction (dHJ) dissolution¹². The dHJ is the archetypical JM that arises when HR repairs a two-ended DSB by the so-called DSB repair pathway^{13–15}. HR can also lead to other types of JMs as a consequence of DSBs being one-ended, DSBs being repaired by other pathways, or HR being called on to bypass SRFs, fill post-replicative gaps and so on^{9,13,16}. In many of these cases, dHJs are not generated but, instead, other JMs, such as D-loops, and single intact or nicked Holliday junctions (iHJ and nHJ, respectively) are the intermediates that physically link the sister chromatids^{9–11,13,16}. Several lines of evidence support that single iHJ and nHJ are mainly processed by SSEs, and that SSEs also backup STR in the processing of dHJs and other helicases in the processing of D-loops^{9–11,16}. Thus, null mutants for *SLX4*, *MMS4* and *MUS81* are synthetically lethal with the genes that encode the STR complex¹⁷. Besides, double-mutant combinations for different SSEs, or the SSEs and the STR, greatly increase the *in vivo* steady-state levels of JMs, not only in yeast but also in humans and flies^{18–25}. Last, several *in vitro* studies have shown that SSEs can efficiently process prototypical JMs such as D-loops, iHJs and nHJs. For instance, Mus81-Mms4 (EME1) from *S. cerevisiae*, and also from other eukaryotes, efficiently processes D-loops and nHJs^{25–27}; Yen1/GEN1 is thought to be the analogous of prokaryotic RuvC HJ resolvase and mainly processes iHJs²⁸, whereas Slx1-Slx4 is a more promiscuous SSE whose function appears more related to overcome problems arising during DNA replication^{18,29}. In addition, *in vivo* studies have also placed the regulatory subunit Slx4 as a component of other Slx1-independent SSE activities. Thus, very recently, mammalian SLX4 has been suggested to regulate the activity and specificity of the MUS81-EME1 and XPF-ERCC1 (refs 30–33), whereas yeast Slx4 appears to associate with the Rad1-Rad10 flap endonuclease³⁴.

In this work, we aim to determine whether persistent JMs, more specifically those that depend on SSEs for their resolution, cause anaphase bridges in anaphase. To this purpose, we modify the steady-state levels of these JMs by deleting different combinations of the yeast SSE genes together with exogenously forcing the cells to bypass replication stress by calling on HR. We find that both Mus81-Mms4 and Yen1, but not Slx4-related SSEs, are essential and compensate each other in preventing and

resolving a new type of sister chromatid anaphase bridge, which mostly comprises noncanonical (discontinuous) forms of the HJ molecule.

Results

Mus81-Mms4 and Yen1 co-work to prevent missegregation. With the objective of determining whether persistent JMs were a source of anaphase bridges, we began this work by testing whether an increase in the SRF and JM steady-state levels caused anaphase problems in *Saccharomyces cerevisiae*. As a reference, we used a *cdc15-2* strain in which the chromosome XII right arm (cXIIr) telomere was labelled with a green fluorescent dot^{5,35,36}. We reasoned that this strain would allow us to microscopically visualize a plethora of aberrant anaphase phenotypes that might arise once we modify the basal levels of SRFs and JMs. First, the *cdc15-2* temperature-sensitive allele blocks the cell cycle in telophase when the temperature is shifted to 37 °C. As mother and daughter cells remain together at the block, the segregation outcome of all mitoses can be easily followed. Of note, this block also helps in stabilizing any anaphase bridge present as cytokinesis is also prevented³⁶. Second, cXIIr is the longest and most segregation-challenging chromosome arm in the yeast genome as it carries the highly transcribed ribosomal DNA locus (rDNA)^{5,35–37}. Accordingly, it forms the most frequent single segregation defect in yeast, often invisible by DAPI staining, although clearly evident when labelling distal regions in the arm^{4,5,35–40}. Aside from being rich in catenations, the rDNA is a natural place for SRFs and a hot-spot for spontaneous JMs^{41–43}. Hence, we hypothesized that if persistent SRFs and/or JMs posed a problem for sister chromatid segregation, cXIIr would be the best single chromosome arm to look at. To increase the SRF and JM steady-state levels we used the alkylating agent MMS and made single, double and triple mutants for the three SSEs expected to resolve JMs in eukaryotes^{9–11,44}.

We first observed that the cell cycle profile in response to MMS was not very different between the reference *cdc15-2* strain and the SSE mutant combinations (Supplementary Figs 1–3 and left-most panel in Fig. 1a). Thus, in a dose-response experiment carried out on a synchronous G1-to-telophase cell cycle (Supplementary Fig. 1), MMS concentrations higher than 0.03% (v/v) caused cells to stay in G1 in all cases, whereas most cells got arrested in G2/M at 0.01%, and only concentrations below this value (that is, 0.004% or lower) allowed cells to enter anaphase. In addition, a G1-to-telophase time-course showed that the S-phase window (from minutes 30 to 90) and the anaphase onset (at ~90 min) were equivalent for the reference and all SSE mutant strains in the absence of MMS (Supplementary Figs 2 and 3). The presence of 0.004% MMS did not basically change the timing of these cell cycle events. Only in the *slx4Δ combinations there was a slight delay (~15–30 min) and a minor decrease in cells able to reach anaphase (~25%), which were not enhanced when the other SSEs were also deleted (Supplementary Figs 2 and 3, and Fig. 1a). This behaviour in the *slx4Δ-carrying strains is likely due to the additional Slx4 role as an anti-checkpoint protein⁴⁵. The overall conclusion from the cell cycle profiles is that at least the *mms4Δ and *yen1Δ mutant combinations do not abolish the G1/S and G2/M DNA damage checkpoints triggered on MMS treatment, nor do they lead to their hyperactivation.****

Remarkably, we did observe frequent anaphase abnormalities for several SSE mutants, especially when they were treated with MMS (Fig. 1a, two central panels, and Fig. 1b). These anaphase problems were mostly observed in the form of cXIIr missegregation and less frequently as DAPI-stained bridges. Thus, the *mms4Δ mutant missegregated cXIIr in up to 20% of the anaphases on low MMS exposure, and this situation was*

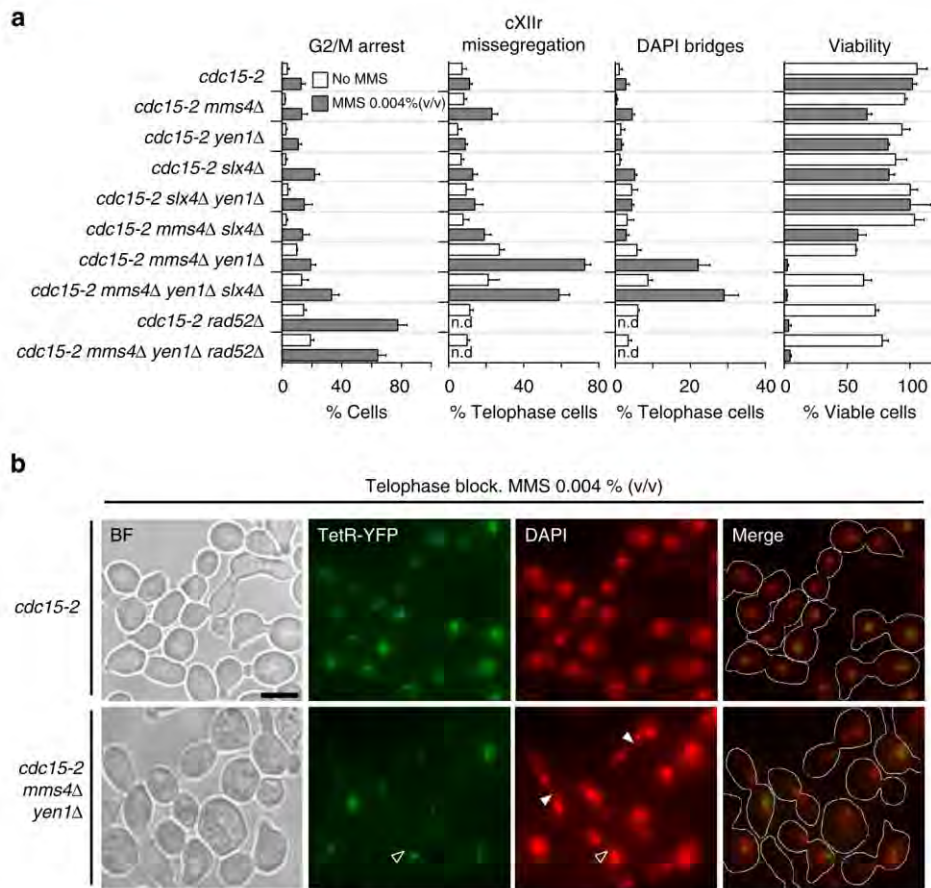


Figure 1 | Combined deletion of *MMS4* and *YEN1* causes *Rad52*-dependent spontaneous and MMS-induced anaphase bridges. Overnight cultures of the strain FM588 (*cdc15-2 Tel-cXIIr:tetO tetR-YFP*), knocked out single-mutant derivatives of FM588 for *RAD52*, *SLX4*, *MMS4* and *YEN1*, double mutants combinations for the endonucleases and the triple mutants *slx4Δ mms4Δ yen1Δ* and *mms4Δ yen1Δ rad52Δ* were first arrested in G1 at 25 °C. They were then split into two media, one of them containing MMS 0.004% (v/v), and finally released into a synchronous cell cycle at 37 °C for 4 h. **(a)** Percentage of cells that did not pass G2/M (left-most panel), chromosome XII missegregation (left-middle panel), DAPI-stained anaphase bridges (right-middle panel) and viable progeny after the telophase release (right-most panel) (mean ± s.e.m., *N* = 3). DAPI-stained anaphase bridges and chromosome XII (cXII) missegregation are relative to cells able to reach telophase, that is, cells that passed G2/M. Open bars plot results obtained without exogenously induced DNA damage, whereas filled bars plot results upon 0.004% (v/v) MMS treatment. Strains carrying *rad52Δ* did not pass G2/M in MMS and therefore cXII missegregation and DAPI-stained bridges could not be determined (n.d.). **(b)** Representative micrographs of z-stack maximum projections from the telophase block of the *cdc15-2* and the *cdc15-2 mms4Δ yen1Δ* strains in MMS 0.004% (v/v). White full triangles point to DAPI-stained anaphase bridges and white open triangles point to DAPI-invisible anaphase bridges comprising cXIIr (see text for details and Fig. 3 for further support). Scale bar in bright field (BF) micrograph represents 5 μm.

exacerbated in the double mutant *mms4Δ yen1Δ*. In this mutant, cXIIr missegregation was around 25% in the absence of MMS and 70% in its presence. In addition, 30% of the cells with missegregated cXIIr in MMS also contained DAPI-stained bridges (Fig. 1b). Interestingly, the missegregation of cXIIr appeared as an end point outcome in all cases; that is, no transient higher peaks of missegregation were seen throughout the time-course (Supplementary Fig. 3). In agreement with these anaphase abnormalities, the viability of the progeny after a telophase release (right-most panel in Fig. 1a) or on continuous growth in 0.004% MMS (Supplementary Fig. 4a) was greatly reduced in the *mms4Δ yen1Δ* combinations. Interestingly, the progeny for the *mms4Δ yen1Δ* double mutant developed into microcolonies ranging from four to more than fifty cells before becoming unviable in MMS (Supplementary Fig. 4b). Strikingly, deletion of *SLX4* did not enhance the observed anaphase abnormalities in any case. This latter result differs from very recent findings in humans showing that *SLX4* and *GEN1* play the major role in preventing DAPI-stained anaphase bridges^{30,31}.

Noteworthy, human *SLX4* interacts with *MUS81-EME1* (refs 30–32), a feature not reported at first in yeast⁴⁶. Although we reasoned that by deleting *SLX4* we were covering all known yeast *Slx4*-related SSE activities (that is, *Slx1-Slx4* and *Rad1-Rad10-Slx4*)³⁴, the cell cycle delay of the *slx4Δ* combinations prompted us to further use *slx1Δ* to confirm that the *Slx1-Slx4* complex had no role in preventing the missegregation of cXIIr and the DAPI-stained bridges. Indeed, the different *slx1Δ* combinations did not differ from their *SLX1* counterparts (Supplementary Fig. 5). Altogether, we concluded from these experiments that *Mus81-Mms4* and *Yen1*, but not *Slx1-Slx4*, jointly contribute to the faithful segregation of chromosomes in anaphase. Correspondingly, we also propose that loss of viability in *mms4Δ yen1Δ* mutants likely occurs through mitotic catastrophe (see also below) and that previous observations of a G2/M arrest in the double mutant after prolonged MMS exposure likely accounts for DNA damage sensed in daughter cells that have suffered from such catastrophe^{36,47}. Besides, our cytological results point out that at least part of the genetic instability

previously associated with the *mus81Δ yen1Δ* double mutant may be caused after passing through aberrant mitoses rather than mistakenly resolving JMs, also in agreement with previous observations²¹.

The *mms4Δ yen1Δ* mutant carries anaphase-persistent JMs. We next addressed whether the anaphase problems observed in the *mms4Δ yen1Δ* double mutant were due to the presence of persistent SRFs or JMs. To discern between SRFs and JMs, we looked at whether the anaphase problems genetically depended on HR. As HR is called on to bypass SRFs at the expense of producing JMs behind the restored RFs, HR-defective strains are expected to increase their SRF steady-state levels (or DSBs after SRF collapse) and decrease the JM levels⁴³. We thus deleted *RAD52*, a central gene in HR, in the *mms4Δ yen1Δ* combinations. This deletion happened to yield a G2/M arrest and a substantial loss of viability in the presence of even very low MMS concentrations (Supplementary Figs 1–3 and Fig. 1). Hence, we only determined whether *rad52Δ mms4Δ yen1Δ* rescued the cXIIr missegregation phenotype of *mms4Δ yen1Δ* in an MMS-free media, which was the case (Fig. 1a, lowest two bars). We concluded that an increase of spontaneous JMs in *mms4Δ yen1Δ*, and not persistent SRFs, was the cause of the observed 25% cXIIr missegregation (see below for further support).

Next, we employed pulse-field gel electrophoresis (PFGE) to achieve several goals based on the fact that branched DNA structures preclude chromosomes from running in a PFGE^{21,48}. This approach has been used before to show that the *mus81Δ yen1Δ* double mutant bears persistent MMS-dependent JMs in G2-blocked cells²¹. First, we wondered whether chromosome XII (cXII), and other chromosomes, still had JMs in anaphase, or rather, cXIIr missegregation was an indirect consequence of a transient increase in JMs during S/G2. Second, we intended to determine which chromosomes were more prone to have persistent JMs. Last, we wanted to check whether cXII broke down when cells entered anaphase. Thus, we observed that the intensity of cXII able to enter the gel greatly faded away for the *mms4Δ yen1Δ* strain in MMS (Fig. 2a). Relative intensity among chromosomes also showed that cXII was more severely affected than any other and that cIV, the second largest chromosome, was somewhat affected as well (Fig. 2b). Finally, we could not see evidence of chromosome breakage for cXII using a probe against the rDNA, rather cXII remained trapped in the well in the *mms4Δ yen1Δ* strain upon MMS treatment (Fig. 2a). As mentioned above, entrapment within the well is indicative of branched DNA structures.

Re-activation of either *Mms4* or *Yen1* resolves JMs and SCBs.

Next, we addressed whether the cXIIr missegregation phenotype was reversible on addition of either SSE in telophase-blocked cells (Fig. 3). This is an important issue as the actual cause of the observed cXIIr missegregation could be due to either cXIIr breakage or unresolved cXIIr sister chromatids. The fact that we did not see a fragmented cXII in a PFGE supports the latter. Nevertheless, it was puzzling that we did not see transient cXIIr missegregation in the time-courses (Supplementary Fig. 3), nor did we observe DAPI-stained bridges for a significant proportion of anaphases with missegregated cXIIr (Fig. 1). It is worth mentioning though that an anaphase bridge formed by just the cXIIr is poorly stained by DAPI³⁶. Furthermore, a novel type of DAPI-invisible anaphase bridge has been described in higher eukaryotes^{8,49}. It may well happen that cXIIr was forming one of these DAPI-invisible anaphase bridges. We reasoned that if cXIIr sister chromatids were part of an anaphase bridge, there was a chance of reversing cXIIr missegregation on JM resolution,

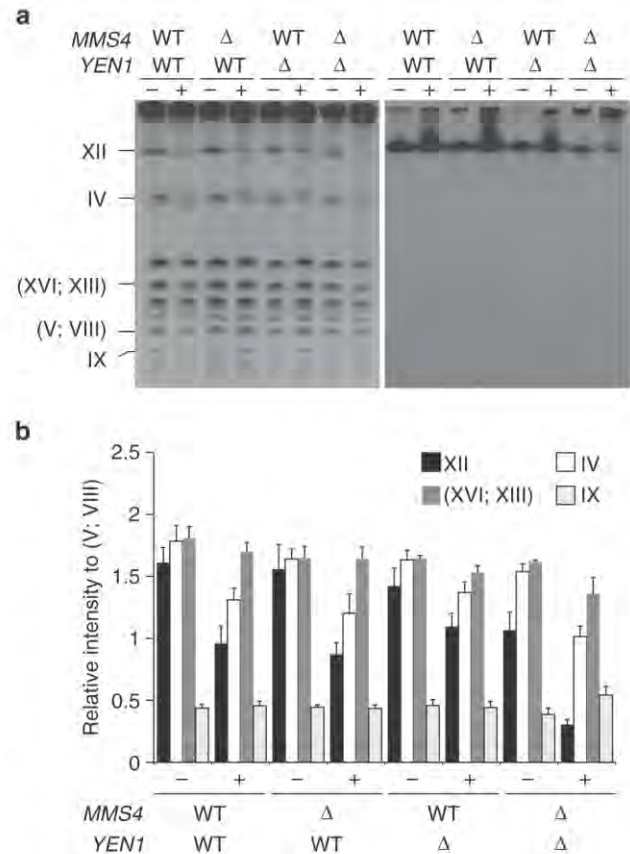


Figure 2 | *Mms4* and *Yen1* compensate one another in resolving chromosomes XII and IV sister chromatids DNA-DNA linkages on ongoing DNA damage. Strains FM588 (*cdc15-2 Tel-cXIIr::tetO tetR-YFP*) and its derivatives carrying either *mms4Δ* or *yen1Δ*, plus the double mutant *mms4Δ yen1Δ*, were treated as in Fig. 1. (a) Pulsed-field gel electrophoresis (PFGE) of all yeast chromosomes at the *cdc15-2* telophase block. Left picture: gel after ethidium bromide staining. Right picture: Southern blot of that gel against an rDNA probe, that is, cXII. (b) Quantitation of chromosome bands for XII, IV, XVI + XIII and IX relative to the V + VIII chromosome band intensity. The plot is from the gel shown plus two more independent experiments (mean \pm s.e.m., $N = 3$). The minus and plus signs represent the absence of MMS or the presence of 0.004% (v/v) MMS in the cultures, respectively.

as we have shown previously in the case of topological entanglements^{35,36}. On the contrary, a broken cXIIr would make missegregation necessarily irreversible. Thus, we carried out the G1-to-telophase experiment with and without MMS in two strains that respectively bore *mms4Δ GAL-YEN1* and *GAL-MMS4 yen1Δ*. In raffinose both strains are like the *mms4Δ yen1Δ* double mutant because they do not express the corresponding gene under the GAL promoter. Once they reached telophase, galactose was added to express the GAL-controlled gene. Strikingly, the cXIIr missegregation phenotype was reverted in both strains, as was the presence of DAPI-stained bridges in MMS (Fig. 3a). This was not the case in the *mms4Δ yen1Δ* strain, ruling out any side effect due to the sugar switch. Noteworthy, the resolution and segregation of cXIIr correlated with the ability of cXII to re-enter a PFGE (Fig. 3b,c) and to a better offspring viability (Fig. 3d). From this experiment we concluded that the observed cXIIr missegregation is due to an anaphase bridge formed by the sister chromatids of that chromosome arm that remain partly unresolved in telophase, that is, cXIIr forms a sister chromatid

either *MMS4* or *YEN1* was not toxic; rather, it conferred resistance to MMS (Supplementary Fig. 6), a result that does not fit well with Mus81-Mms4 or Yen1 being deregulated to cut RFs when overproduced.

JMs at the rDNA in *mms4Δ yen1Δ* comprise non-canonical HJs. A key mechanistic insight into how JMs might get resolved by these SSEs could also be derived from the above experiment. As Mus81-Mms4 and Yen1 can largely suppress the aberrant phenotypes of the double mutant in late anaphase, they must process similar or dynamically interchangeable anaphase-stable JMs. This is a critical issue as many reports have highlighted that Mus81-Mms4/EME1 and Yen1/GEN1 process different JMs *in vitro*^{26–28,46,50,51}. Hence, we now focused our efforts on the physical nature of JMs in the *mms4Δ yen1Δ* telophase block and after induction of either SSE. To this aim, we studied the branched DNA structures present within the rDNA sequence. As mentioned, we expected the rDNA to be the most important JM hot-spot^{42,43}, and so suggest the microscopy and PFGE results (Figs 1 and 2). Neutral, neutral two-dimensional DNA electrophoresis (NN-2D) is the reference technique to assess the physical nature of branched DNA structures. NN-2D has been recently used to show that the *mus81Δ yen1Δ* double mutant bears higher levels of DSB-dependent X-shaped JMs in G2-blocked cells^{23,25}. When we performed NN-2D for all telophase blocks, we observed a clear correlation between the severity of cXIIr missegregation and the spike that corresponds to X-shaped molecules (Fig. 4a,b).

Noteworthy, the spike disappeared almost completely upon induction of either *MMS4* or *YEN1* in telophase (Fig. 4c,d).

As mentioned before, a key difference between Mus81-Mms4 and Yen1 is the *in vitro* preference they show for the HJ substrate^{27,28,46}. Thus, Mus81-Mms4 preferentially cleaves a HJ with a nick very close to the junction (nHJ), whereas Yen1 cleaves the intact HJ (iHJ). Having shown that either SSE resolves most of the X-shaped spike *in vivo*, we wondered whether they were both acting on the same substrates and whether iHJs and nHJs actually coexisted in the 2D spike. To address this, we run a third alkaline dimension to our NN-2Ds (NNA-3D)⁵². DNA denaturation would cause an iHJ to split into four identical single-stranded DNA molecules (ssDNA), whereas nHJs would split into three identical ssDNAs plus one (symmetrical nHJ) or two (asymmetrical nHJ) smaller ssDNAs (Supplementary Fig. 7 for a schematic). Strikingly, we observed in the *mms4Δ yen1Δ* X-shaped spike the NNA-3D pattern expected for nHJs with the nick located just at the junction (Fig. 5a,b and Supplementary Fig. 7). When we measured the normalized intensities between the full-length ssDNAs and the sum of the smaller ssDNAs, we obtained a ratio of 2.86 ± 0.17 (mean \pm s.e.m., $N = 11$). This value is strikingly very close to the 3:1 ratio expected if all X-shaped molecules were nHJs (Supplementary Fig. 7). To shed more light on this structure we further subjected the samples to the action of the purified bacterial HJ resolvase RuvC and the T4 DNA ligase (Fig. 5c). With these assays we intended to address two issues: first, to corroborate that the X-shaped spike was actually a HJ and

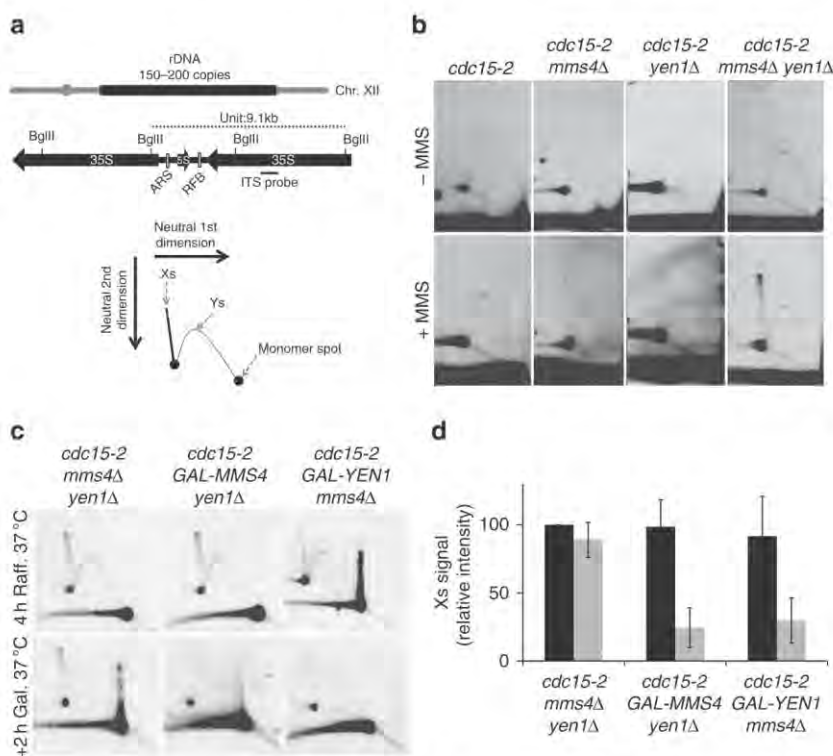


Figure 4 | X-shaped molecules are the main source of the DNA-DNA linkages observed in telophase-blocked cells deficient for both Mus81-Mms4 and Yen1. (a) A schematic of the chromosome XII rDNA array and the BglIII rDNA fragment chosen for the NN-2Ds. The branched DNA molecules detectable with a probe against the selected BglIII fragment is depicted underneath (Xs, HJs, hemicatenanes and so on; Ys, replication forks, single-end invasions and so on). (b) The strain FM588 (*cdc15-2 Tel-cXIIr:tetO tetR-YFP*) and its derivatives carrying either *mms4Δ* or *yen1Δ*, plus the double mutant *mms4Δ yen1Δ*, were treated as in Fig. 1. Samples taken at the telophase block were processed for NN-2D to assess the physical nature of the branched DNA molecules. (c) The strain FM1185 (*cdc15-2 Tel-cXIIr:tetO tetR-YFP mms4Δ yen1Δ*) and derivatives carrying either *GAL-MMS4 yen1Δ* or *mms4Δ GAL-YEN1* were treated as in Fig. 3. Samples taken at the telophase block in raffinose and 2 h after galactose addition were processed for NN-2D as in (b). (d) Quantitation of the normalized amounts of the X-shaped molecules relative to the *mms4Δ yen1Δ* strain before the GAL induction (mean \pm s.e.m., $N = 3$). Dark and light grey bars depict relative signals before and after the GAL induction, respectively.

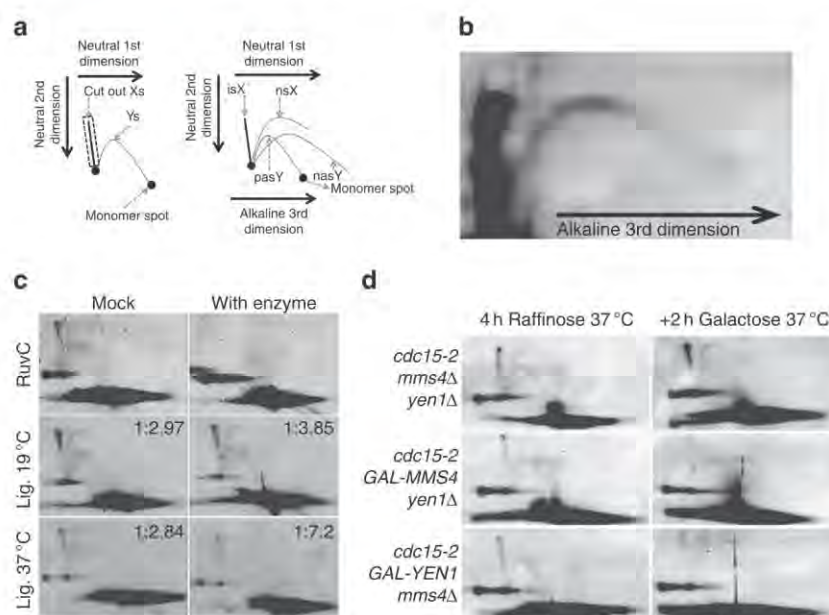


Figure 5 | The X-shaped DNA found in the *mms4Δ yen1Δ* telophase-blocked cells comprises the Holliday molecule with a discontinuity at the junction. (a) Schematic of the two strategies used to analyse by alkaline electrophoresis the physical nature of the NN-2D X-shaped spike. On the left, run a NN-2D and then run an alkaline electrophoresis for just the spike cut out of the gel. On the right, turn the NN-2D gel 90° and run a third alkaline dimension (NNA-3D). The expected ssDNA species in the NNA-3D are depicted: isX, intact full-length strands coming from the Xs; nsX, strands of a smaller size due to a nick (or a small gap) in the Xs; pasY, parental strands in the Y-shaped molecules; nasY, nascent strands in the Y-shaped molecules. (b) Several parallel two NN-2D as the one shown in Fig. 4b were run for the *mms4Δ yen1Δ* double mutant in 0.004% (v/v) MMS and, using the Southern blot of one of them as a reference, the expected location of the X-shaped molecule was cut out of the second gel and run under alkali conditions to analyse the four strands in the Xs (see also text and Supplementary Fig. 7). A representative result is shown. (c) NNA-3Ds for the telophase-blocked *mms4Δ yen1Δ* double mutant after *in vitro* treatment of the agarose embedded DNA with the DNA processing enzymes RuvC and T4 DNA ligase. Mock denotes parallel treatments in which the enzymes were omitted. The nsX versus isX ratio of the ligase treatments is indicated at the upper-right corner of the corresponding pictures. (d) NNA-3Ds for an endonuclease induction experiment as the one shown in Fig. 4c.

not a hemicatenane and, second, to biochemically test whether the discontinuity in one of the strands was actually a nick or, rather, it may correspond to a small gap (impossible to differentiate from the NNA-3D profile). Hemicatenanes, which are recombination intermediate that might also link two sister chromatids, comigrate with HJs in the NN-2D spike and are expected to comigrate with the full-length ssDNAs in the NNA-3D. Although the 3:1 ratio in the NNA-3D strongly suggests the absence of hemicatenanes, as well as iHJs, we decided to treat our samples with RuvC, which has been traditionally used to distinguish between HJs and hemicatenanes^{43,53}. Importantly, RuvC cuts both iHJs and nHJs⁵⁴. Hence, we wondered whether any of the X-shaped molecules observed in the *mms4Δ yen1Δ* mutant were resistant to RuvC, but found that all X-shaped DNA disappeared on RuvC treatment (Fig. 5c), supporting the idea that the observed X-shaped molecules are HJs. To distinguish between nHJs and any HJ whose discontinuous strand actually carries a small gap, we tested whether previous treatment with T4 DNA ligase abolished the splitting of the X-shaped spike in the NNA-3D. Although we could not achieve complete absence of the smaller ssDNAs in the NNA-3D (Fig. 5c), the full/partial-length ssDNA ratio rose to 7:1, suggesting that at least half of the discontinuous nHJs are ligatable nHJs. The other half might be unligatable nHJs, HJs with small gaps and/or due to an incomplete reaction of the ligase. Finally, we wondered whether these X-shaped JMs were resolved on expression of either SSE in telophase, and thus correlated with the previous observation of unlinkage and segregation of cXII (Fig. 3). Indeed, we found that these JMs largely disappeared on induction of either *GAL-MMS4* or *GAL-YEN1* in telophase (Fig. 5d).

Discussion

The persistence of linkages between sister chromatids in anaphase is broadly believed to lead to a catastrophic mitosis. Previously, many reports using the model organism *S. cerevisiae* have shown that anaphase bridges form when these linkages comprise topological catenations, unresolved cohesion or unfinished replication^{1–5}. Now, we show that this phenotype can be extended to the persistence of unresolved recombination intermediates (inter-sister JMs). We critically demonstrate this by controlling the activity of two of the SSEs that deal with these JMs (Mus81-Mms4 and Yen1) and then measuring chromosome segregation at the distal regions of the chromosome arm that carries the hot-spot locus for spontaneous JMs (the rDNA locus at cXIIr) (Figs 1–5). Importantly, we provide several additional evidences that support the statement that unresolved inter-sister JMs cause anaphase bridges. First, the cXIIr missegregation observed in the absence of both Mus81-Mms4 and Yen1 depends on a functional HR pathway. Second, the cXIIr missegregation is reverted upon activation of either SSE in telophase. Third, increasing the steady-state levels of JMs by low doses of MMS boosts the presence of anaphase bridges (for example, visible by DAPI staining), which can nevertheless be still reverted in telophase by either SSE. Fourth, we directly visualize the presence of JMs at the rDNA and correlate their levels with the observed degree of cXIIr missegregation (both in the absence of the SSEs and after their reactivation in telophase). It is worth mentioning that it was not until very recently that several reports have been able to visualize DAPI-stained anaphase bridges when knocking down several SSEs in human-derived cell lines^{30,31}. However, it was not clear

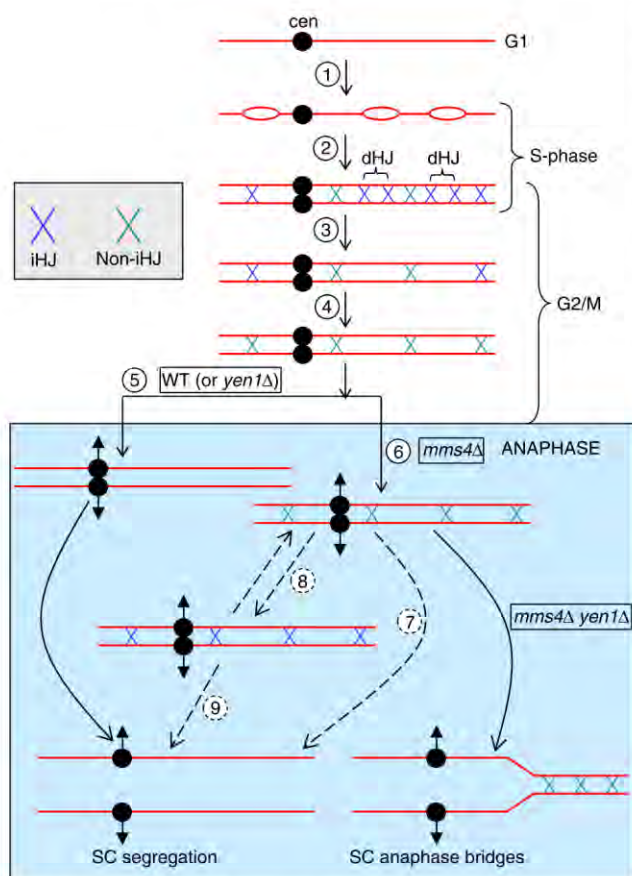


Figure 6 | Models of how Mus81-Mms4 and Yen1 might cooperate in anaphase to resolve anaphase bridges formed by nicked (and other discontinuous) Holliday junctions. Initially, stalled RFs in the previous S-phase are bypassed through the HR pathway, leaving behind JMs (steps 1 and 2). Some JMs can then be resolved by helicases through SDSA, whereas others end up as either iHJs or nHJs^{9–11}. The Sgs1-dependent dHJ dissolution pathway will then deal with much of the iHJs (step 3). Persistent nHJs, and probably other noncanonical HJs, would be processed by SSEs^{9–11}. Persistent iHJs are in theory possible as well (for example, single iHJs). However, they must be eventually converted into nHJs (step 4) (Fig. 5). Mus81-Mms4 is normally sufficient to resolve all nHJs in G2/M (step 5), and only under replicative stress would Mus81-Mms4 become saturated (Fig. 1a). Two main models are possible to unlink the sister chromatids by Yen1 in the absence of Mus81-Mms4 or when it becomes saturated. If Yen1 resolves nHJs *in vivo* it would directly compensate for the Mus81-Mms4 deficiency (dashed lines, step 7). If Yen1 is just an iHJ resolvase (step 9), nHJ and other non-iHJ species necessarily need to be converted into iHJs at some point, for example, by branch migration, nick ligation, gap filling and so on (step 8).

whether these bridges linked sister chromatids and whether they actually comprise JMs or, else, they might be formed by unreplicated DNA as it has been suggested in MUS81-EME1-related ultra-fine anaphase bridges⁵⁵.

A surprising finding in our study was the negligible genetic interactions that Slx4 showed with the other two SSEs. In higher eukaryotes, SLX4 has been proposed as a central scaffold protein where different branched DNA-processing activities can be assembled, including JM-resolving activities by MUS81-EME1 and SLX1 (refs 30–33). At first, we believed this might reflect a difference between higher eukaryotes and yeast in accordance with reports showing a lack of interactions between Slx4 and

Mus81-Mms4 (ref. 46). Nevertheless, another very recent report in this fast-moving field has pointed out that there is indeed an interaction bridged by Dpb11 (ref. 56). This raises new questions and suggests there may be two Mus81-Mms4 activities, being the Slx4-independent activity responsible for dealing with the JMs that led to SCBs in our hands. In contrast to Slx4, the clear genetic compensation between Mus81-Mms4 and Yen1 prompted us to deeply address the physical nature of the JMs that form the anaphase bridges. Strikingly, this study has uncovered some new and unexpected findings with important implication on the models of how HR bypasses SRFs. At present, there is a general consensus in that SRF-derived JMs are channelled towards dHJs that are then processed in pairs through the double HJ (dHJ) dissolution pathway, a job carried out by the Sgs1-Top3-Rmi1 (STR) helicase-topoisomerase complex¹². However, there is also evidence that not all JMs can be resolved by STR. Recently, it has been hypothesized that the prominent mitotic STR-refractory JM is the nHJ^{10,11}, which would be resolved by Mus81-Mms4 in G2/M^{24,57–59}. The actual role of Yen1 is still controversial, although it has been recently shown to act after Mus81-Mms4 on those HJs that persist until anaphase (for example, single iHJs)^{9–11,21,58,60,61}. Our *in vivo* results strongly support the nHJ hypothesis and the reported activity for Mus81-Mms4. Indeed, what we saw in telophase in the absence of both Mus81-Mms4 and Yen1 were noncanonical HJs carrying a discontinuity in one strand (either nHJs or HJs with small gaps, but clearly not iHJs). Surprisingly, these noncanonical HJ in an *mms4Δ* background were almost fully resolved after Yen1 expression in anaphase (Figs 4c and 5d). The simplest explanation of these results in the context of the nHJs hypothesis would be that Mus81-Mms4 and Yen1 are both nHJ-resolvases (Fig. 6). In agreement with this hypothesis, the *in vitro* specificity of Yen1 homologues in flies and humans is not restricted to iHJs^{62,63}. Also, a very recent report using full-length yeast Yen1 supports at last significant *in vitro* activities against branched DNA structures other than iHJs, including nHJs⁶⁰. An alternative possibility that would fit with Yen1 being just an iHJ-resolvase is that, in the absence of Mus81-Mms4, nHJs (and other discontinuous HJs) could be converted into iHJs and then process by Yen1 (Fig. 6). This step would take place by either branch migration out of the nick or the action of a ligase/polymerase, and could be either biologically induced or being part of a dynamic equilibrium where the discontinuous HJ forms would act as metastable states. In favour of this latter scenario is the fact that Yen1 gets activated in anaphase and that Mus81-Mms4 specificity may also change at this cell cycle stage to resolve iHJs as well as nHJs^{58,60,61}. Finally, we cannot completely rule out the possibility that these noncanonical HJs are formed *in vitro* during DNA extraction by branch migration towards a pre-existing nick, despite using controlled conditions known to minimize such migration⁶⁴. Nevertheless, and in support of these non-canonical HJs being present *in vivo*, it is also worth mentioning a very recent report where HJs comprising clear gaps of ssDNA close to the junction were visualized by electron microscopy on an artificial chromosome in yeast⁶⁵.

In conclusion, the structure-selective nucleases Mus81-Mms4 and Yen1, but not Slx1-Slx4, play an overlapping role in preventing and resolving a novel type of stable sister chromatid anaphase bridges formed by noncanonical and discontinuous forms of the Holliday junction molecule. In addition, we show that these unresolved recombination intermediates do not break apart when cells reach anaphase in the absence of both Mus81-Mms4 and Yen1. This sheds new light on the physical nature of anaphase bridges and the HJ molecule in eukaryotes as well as the physiological roles of the eukaryotic structure-selective nucleases.

Methods

Yeast strains and experimental conditions. All yeast strains used in this work are listed in Supplementary Table 1. Parental S288C strain carrying the *cdc15-2* allele, the *tetOs* array at cXIIr-Tel (*tetOs:1061*) and the TetR-YFP fusion has been described elsewhere³⁶. Gene deletions, marker swaps and allele/promoter replacements were engineered using PCR methods. All strains were grown overnight in air orbital incubators at 25 °C in YEPD media unless stated otherwise. G1-to-telophase experiments were performed as follows: asynchronous cultures were first adjusted to OD₆₀₀ = 0.5, then synchronized in G1 at 25 °C for 3 h by adding 50 ng ml⁻¹ of alpha-factor (all tested strains were *bar1Δ*), and finally released from the G1 arrest at 37 °C for 4 h. For the G1 release, cells were washed twice and resuspended in fresh media containing 0.1 mg ml⁻¹ of pronase E. When indicated, DNA damage was induced at the time of the G1 release by adding MMS. MMS was kept in the media until the telophase arrest and removed in such instances where cells were released from telophase to measure viability. In the dose-response experiments, cell cultures were split into ten flasks at the time of the G1 release and nine 1:3 serial dilutions of MMS were used. The MMS final concentrations ranged from 0.1 to 0.000015% (v/v). The tenth culture was left without MMS as a control. When galactose induction of the SSE genes was required, cells were grown in YP raffinose 2% (w/v). Raffinose was also used as the carbon source all through the G1-to-telophase synchronous cell cycle, and galactose was added at 2% (w/v) at the time of the *cdc15-2* telophase block while keeping the yeast culture at 37 °C.

Cell viability was measured by plotting number of colonies grown on YPD plates after 3 days at 25 °C relative to total cell number counted by a haemocytometer at the time of plating.

Error bars in all graphs represent the s.e.m. of independent technical replicates. The number of replicates (*N*) is indicated either in the figure legends or in the main text.

Single-cell analyses by flow cytometry and microscopy. Flow cytometry to follow up bulk DNA replication was carried out taking 300 μl of culture in 0.9 ml 100% ethanol. Cells were pelleted and resuspended in 1 × SSC buffer with 0.01 mg ml⁻¹ of RNaseA and incubated overnight at 37 °C. Fifty microlitres of 1 × SSC with 1.2 mg ml⁻¹ of proteinase K was added and incubated at 50 °C for 1 h. After that, 500 μl of 1 × SSC with propidium iodide 3 μg ml⁻¹ was added and incubated at room temperature for 1 h. Samples were analysed using a BD FACScalibur machine³⁶.

Cell cycle progression and cXIIr segregation were analysed by wide-field fluorescence microscopy³⁶. A stack of 20 z-focal plane images (0.3 μm depth) was collected on a Leica DMI6000, using a 63 × /1.30 immersion objective and an ultrasensitive DFC 350 digital camera, and processed with the AF6000 software (Leica). Gross DNA masses were stained for microscopy using DAPI at 1 μg ml⁻¹ final concentration in a 0.25% (v/v) Triton X-100 solution. The staining was performed right before visualization under the microscope in cell pellets previously frozen at -20 °C for 48 h.

Analyses of branched DNA structures and chromosome integrity. PFGE was used as the standard procedure to determine the presence of branched DNA structures at the chromosome level and also to quantify the changes among different strains, treatments and/or chromosomes^{21,48}. Two-dimensional neutral-neutral (NN-2D) and three-dimensional neutral-neutral-alkaline (NNA-3D) DNA electrophoresis were, respectively, used to study whether branched DNA corresponded to the HJ molecule and to distinguish between intact and discontinuous HJs⁵².

Yeast DNA for PFGE, NN-2D and NNA-3D was prepared in low-melting agarose plugs in conditions known to avert branch migration and preserve non-linear forms with no need of using psoralen to crosslink⁶⁴. In brief, 4 ml of OD₆₀₀ = 1 was pelleted and embedded into a 0.5% (w/v) agarose plug. Chromosome-sized DNA was obtained after subsequent overnight digestions of the plug with lyticase (2,500 units ml⁻¹), RNaseA (0.5 units ml⁻¹) and Proteinase K (1 mg ml⁻¹). All digestions were carried out at 37 °C (including the Proteinase K step) to minimize the heat-labile *in vitro* DNA shearing reported for MMS and any remaining migration of the branched DNA structures^{43,64}.

PFGE to see yeast chromosomes was performed using a CHEF DR-III system (Bio-Rad) in a 0.8% (w/v) agarose gel made with 0.5 × TBE buffer and run at 12 °C for 20 h at 6 V cm⁻¹ with an initial switching time of 80 s, a final of 150 s and an angle of 120°. PFGE to resolve better the chromosome XII (Fig. 3b) was performed at 3 V cm⁻¹ for 68 h with 300 and 900 s of initial and final switching time, respectively³⁶. Yeast chromosomes were visualized after staining with ethidium bromide and quantified with the QuantityOne software (Bio-Rad). To specifically visualize the chromosome XII, a Southern blot was carried out by a saline downwards transference onto positively charged membranes (Roche), followed by hybridization with a fluorescein-labelled probe (Roche) that covers both ITS regions within the rDNA unit. Detection was performed by chemiluminescence using an anti-fluorescein antibody coupled to alkaline phosphatase (Roche) and using CDP-star (Roche) as the substrate.

DNA NN-2D and NNA-3D electrophoresis to visualize JMs were carried out as following. First, the agarose plug was treated with the Proteinase K inhibitor Pefablock (Roche) at 1 mg ml⁻¹ followed by overnight digestion with

1,500 units ml⁻¹ of the restriction enzyme BglII (New England Biolabs). Then, one-half of the plug was loaded onto a 0.35% (w/v) agarose gel and the first dimension run at 0.8 V cm⁻¹ for 24 h. Next, the corresponding lane was sliced, re-oriented 90° anticlockwise and the second dimension was run in a 1% (w/v) agarose gel at 6 V cm⁻¹ for 9 h under the presence of 0.3 μg ml⁻¹ of ethidium bromide in both the gel and the running buffer. Importantly, the buffer was left recirculating through a cooling system to keep constant the running temperature at 16 °C. For NN-2D, the gel was then transferred to a positively charged membrane (Roche) for Southern blot analysis. In the case of NNA-3D⁵², the agarose gel obtained after the NN-2D procedure was first soaked in 0.04 N NaOH plus 2 mM EDTA five times for 1 h each for alkaline equilibration. Then, a third electrophoresis was run in the same orientation as the first one was. The running conditions for this 'third dimension' were 0.8 V cm⁻¹ for 38 h at 16 °C. Then, this 3D gel was used for Southern blot analysis. Before transference onto the membrane, a neutralization step was added before depurination just for this gel. The same procedure was followed when the X-shaped structure was cut out right after the NN-2D. In the case of treatment with RuvC (Abcam) we followed a procedure similar to a previous report⁶⁶. Thus, we first washed the agarose plug in RuvC buffer for 30 min at room temperature and then washed once for 30 min at 4 °C. Then the plugs were incubated in 150 μl of buffer with 3 μg RuvC for 4 h at 4 °C and then 1 h at 55 °C. In the case of treatment with T4 DNA ligase, we employed an adaptation of the RuvC protocol for this enzyme, taking also into account general protocols for the T4 ligase. Thus, we washed in T4 ligase buffer for 30 min at room temperature and then washed once in T4 ligase buffer for 30 min at 4 °C. Then the plugs were incubated in 150 μl of buffer with 3,500 cohesive end units of T4 DNA ligase either at 19 °C or 37 °C. The same procedures but without enzymes (mock) were followed with another plug as negative controls.

Southern blots of NN-2D and NNA-3D were carried out by a saline upwards transference followed by hybridization with the same fluorescein-labelled probe we used for PFGE. For quantifications of the X-shaped DNA molecules in the NN-2D, we took photos of the emitted light in a ChemiDoc MP apparatus (BioRad) and used the software ImageLab (BioRad). We picked a time exposure in all cases (360 s) where the signal of the X-shaped molecules was visible but not saturated. We then picked another time exposure for all linear 1N DNA signals where they were not saturated either (1 s). The 1N signals include the monomer spot and the smear that appeared during the first dimension (this smear is due to overloading and is frequently stronger from samples embedded in agarose plugs). In 28% of our NN-2Ds, the 1N signal also included a second smear trailing from the monomer spot in the second dimension, which has been previously defined as an artefact⁶⁷. Finally, we calculated the quotient [background - subtracted intensity of the Xs/ background - subtracted intensity of the 1N] and established the 100% signal as the one in the telophase-blocked *cdc15-2 mms4Δ yen1Δ* strain in raffinose. To calculate the relative amount of discontinuous HJs over the whole of X-shaped molecules, we directly quantified the ssDNAs resolved from the X-shaped structure after the NNA-3Ds according to the following formulae: [background - subtracted intensity of the full-length ssDNA line/background - subtracted intensity of the arc for smaller ssDNAs]. A ratio of 3:1 would be expected if all X-shaped structures were discontinuous HJs (Supplementary Fig. 7).

References

- Holm, C., Goto, T., Wang, J. C. & Botstein, D. DNA topoisomerase II is required at the time of mitosis in yeast. *Cell* **41**, 553–563 (1985).
- Strunnikov, A. V., Hogan, E. & Koshland, D. SMC2, a Saccharomyces cerevisiae gene essential for chromosome segregation and condensation, defines a subgroup within the SMC family. *Genes Dev.* **9**, 587–599 (1995).
- Uhlmann, F., Lottspeich, F. & Nasmyth, K. Sister-chromatid separation at anaphase onset is promoted by cleavage of the cohesin subunit Scc1. *Nature* **400**, 37–42 (1999).
- Torres-Rosell, J. *et al.* SMC5 and SMC6 genes are required for the segregation of repetitive chromosome regions. *Nat. Cell Biol.* **7**, 412–419 (2005).
- Machin, F., Torres-Rosell, J., Jarmuz, A. & Aragón, L. Spindle-independent condensation-mediated segregation of yeast ribosomal DNA in late anaphase. *J. Cell Biol.* **168**, 209–219 (2005).
- Gisselsson, D. *et al.* Chromosomal breakage-fusion-bridge events cause genetic intratumor heterogeneity. *Proc. Natl Acad. Sci. USA* **97**, 5357–5362 (2000).
- Fenech, M. *et al.* Molecular mechanisms of micronucleus, nucleoplasmic bridge and nuclear bud formation in mammalian and human cells. *Mutagenesis* **26**, 125–132 (2011).
- Chan, K. L. & Hickson, I. D. New insights into the formation and resolution of ultra-fine anaphase bridges. *Semin. Cell Dev. Biol.* **22**, 906–912 (2011).
- Rass, U. Resolving branched DNA intermediates with structure-specific nucleases during replication in eukaryotes. *Chromosoma* **122**, 499–515 (2013).
- Hickson, I. D. & Mankouri, H. W. Processing of homologous recombination repair intermediates by the Sgs1-Top3-Rmi1 and Mus81-Mms4 complexes. *Cell Cycle* **10**, 3078–3085 (2011).
- Schwartz, E. K. & Heyer, W.-D. Processing of joint molecule intermediates by structure-selective endonucleases during homologous recombination in eukaryotes. *Chromosoma* **120**, 109–127 (2011).

12. Wu, L. & Hickson, I. D. The Bloom's syndrome helicase suppresses crossing over during homologous recombination. *Nature* **426**, 870–874 (2003).
13. Paques, F. & Haber, J. E. Multiple pathways of recombination induced by double-strand breaks in *Saccharomyces cerevisiae*. *Microbiol. Mol. Biol. Rev.* **63**, 349–404 (1999).
14. Schwacha, A. & Kleckner, N. Identification of double Holliday junctions as intermediates in meiotic recombination. *Cell* **83**, 783–791 (1995).
15. Bzymek, M., Thayer, N. H., Oh, S. D., Kleckner, N. & Hunter, N. Double Holliday junctions are intermediates of DNA break repair. *Nature* **464**, 937–941 (2010).
16. Heyer, W.-D., Ehmsen, K. T. & Liu, J. Regulation of homologous recombination in eukaryotes. *Annu. Rev. Genet.* **44**, 113–139 (2010).
17. Mullen, J. R., Kaliraman, V., Ibrahim, S. S. & Brill, S. J. Requirement for three novel protein complexes in the absence of the Sgs1 DNA helicase in *Saccharomyces cerevisiae*. *Genetics* **157**, 103–118 (2001).
18. Kaliraman, V. & Brill, S. J. Role of SGS1 and SLX4 in maintaining rDNA structure in *Saccharomyces cerevisiae*. *Curr. Genet.* **41**, 389–400 (2002).
19. Gaillard, P.-H. L., Noguchi, E., Shanahan, P. & Russell, P. The endogenous Mus81-Eme1 complex resolves Holliday junctions by a nick and counternick mechanism. *Mol. Cell* **12**, 747–759 (2003).
20. Tay, Y. D. & Wu, L. Overlapping roles for Yen1 and Mus81 in cellular Holliday junction processing. *J. Biol. Chem.* **285**, 11427–11432 (2010).
21. Ho, C. K., Mazón, G., Lam, A. F. & Symington, L. S. Mus81 and Yen1 promote reciprocal exchange during mitotic recombination to maintain genome integrity in budding yeast. *Mol. Cell* **40**, 988–1000 (2010).
22. Ashton, T. M., Mankouri, H. W., Heidenblut, A., McHugh, P. J. & Hickson, I. D. Pathways for Holliday junction processing during homologous recombination in *Saccharomyces cerevisiae*. *Mol. Cell. Biol.* **31**, 1921–1933 (2011).
23. Mazón, G., Lam, A. F., Ho, C. K., Kupiec, M. & Symington, L. S. The Rad1-Rad10 nuclease promotes chromosome translocations between dispersed repeats. *Nat. Struct. Mol. Biol.* **19**, 964–971 (2012).
24. Szakal, B. & Branzei, D. Premature Cdk1/Cdc5/Mus81 pathway activation induces aberrant replication and deleterious crossover. *EMBO J.* **32**, 1155–1167 (2013).
25. Mazón, G. & Symington, L. S. Mph1 and Mus81-Mms4 Prevent Aberrant Processing of Mitotic Recombination Intermediates. *Mol. Cell* **52**, 63–74 (2013).
26. Ciccia, A., Constantinou, A. & West, S. C. Identification and characterization of the human mus81-eme1 endonuclease. *J. Biol. Chem.* **278**, 25172–25178 (2003).
27. Fricke, W. M., Bastin-Shanower, S. A. & Brill, S. J. Substrate specificity of the *Saccharomyces cerevisiae* Mus81-Mms4 endonuclease. *DNA Repair (Amst)* **4**, 243–251 (2005).
28. Ip, S. C. Y. *et al.* Identification of Holliday junction resolvases from humans and yeast. *Nature* **456**, 357–361 (2008).
29. Fricke, W. M. & Brill, S. J. Slx1-Slx4 is a second structure-specific endonuclease functionally redundant with Sgs1-Top3. *Genes Dev.* **17**, 1768–1778 (2003).
30. Wyatt, H. D. M., Sarbajna, S., Matos, J. & West, S. C. Coordinated actions of SLX1-SLX4 and MUS81-EME1 for Holliday Junction resolution in human cells. *Mol. Cell* **52**, 234–247 (2013).
31. Garner, E., Kim, Y., Lach, F. P., Kottmann, M. C. & Smogorzewska, A. Human GEN1 and the SLX4-associated nucleases MUS81 and SLX1 are essential for the resolution of replication-induced Holliday Junctions. *Cell Rep.* **5**, 207–215 (2013).
32. Castor, D. *et al.* Cooperative control of Holliday Junction resolution and DNA repair by the SLX1 and MUS81-EME1 nucleases. *Mol. Cell* **52**, 221–233 (2013).
33. Kim, Y. *et al.* Regulation of multiple DNA repair pathways by the Fanconi anemia protein SLX4. *Blood* **121**, 54–63 (2013).
34. Toh, G. W.-L. *et al.* Mec1/Tel1-dependent phosphorylation of Slx4 stimulates Rad1-Rad10-dependent cleavage of non-homologous DNA tails. *DNA Repair (Amst)* **9**, 718–726 (2010).
35. Machin, F. *et al.* Transcription of ribosomal genes can cause nondisjunction. *J. Cell Biol.* **173**, 893–903 (2006).
36. Quevedo, O., García-Luis, J., Matos-Perdomo, E., Aragón, L. & Machin, F. Nondisjunction of a single chromosome leads to breakage and activation of DNA damage checkpoint in *g2*. *PLoS Genet.* **8**, e1002509 (2012).
37. Torres-Rosell, J., Machin, F., Jarmuz, A. & Aragón, L. Nucleolar segregation lags behind the rest of the genome and requires Cdc14p activation by the FEAR network. *Cell Cycle* **3**, 496–502 (2004).
38. Clemente-Blanco, A. *et al.* Cdc14 inhibits transcription by RNA polymerase I during anaphase. *Nature* **458**, 219–222 (2009).
39. Fuchs, J. & Loidl, J. Behaviour of nucleolus organizing regions (NORs) and nucleoli during mitotic and meiotic divisions in budding yeast. *Chromosome Res.* **12**, 427–438 (2004).
40. D'Amours, D., Stegmeier, F. & Amon, A. Cdc14 and condensin control the dissolution of cohesin-independent chromosome linkages at repeated DNA. *Cell* **117**, 455–469 (2004).
41. Brewer, B. J. & Fangman, W. L. A replication fork barrier at the 3' end of yeast ribosomal RNA genes. *Cell* **55**, 637–643 (1988).
42. Keil, R. L. & Roeder, G. S. Cis-acting, recombination-stimulating activity in a fragment of the ribosomal DNA of *S. cerevisiae*. *Cell* **39**, 377–386 (1984).
43. Zou, H. & Rothstein, R. Holliday junctions accumulate in replication mutants via a RecA homolog-independent mechanism. *Cell* **90**, 87–96 (1997).
44. Lundin, C. *et al.* Methyl methanesulfonate (MMS) produces heat-labile DNA damage but no detectable in vivo DNA double-strand breaks. *Nucleic Acids Res.* **33**, 3799–3811 (2005).
45. Ohouo, P. Y., Bastos de Oliveira, F. M., Liu, Y., Ma, C. J. & Smolka, M. B. DNA-repair scaffolds dampen checkpoint signalling by counteracting the adaptor Rad9. *Nature* **493**, 120–124 (2013).
46. Schwartz, E. K. *et al.* Mus81-Mms4 functions as a single heterodimer to cleave nicked intermediates in recombinational DNA repair. *Mol. Cell Biol.* **32**, 3065–3080 (2012).
47. Blanco, M. G., Matos, J., Rass, U., Ip, S. C. Y. & West, S. C. Functional overlap between the structure-specific nucleases Yen1 and Mus81-Mms4 for DNA-damage repair in *S. cerevisiae*. *DNA Repair* **9**, 394–402 (2010).
48. Hennessy, K. M., Lee, A., Chen, E. & Botstein, D. A group of interacting yeast DNA replication genes. *Genes Dev.* **5**, 958–969 (1991).
49. Chan, K.-L., North, P. S. & Hickson, I. D. BLM is required for faithful chromosome segregation and its localization defines a class of ultrafine anaphase bridges. *EMBO J.* **26**, 3397–3409 (2007).
50. Osman, F., Dixon, J., Doe, C. L. & Whitty, M. C. Generating crossovers by resolution of nicked Holliday junctions: a role for Mus81-Eme1 in meiosis. *Mol. Cell* **12**, 761–774 (2003).
51. Ehmsen, K. T. & Heyer, W.-D. *Saccharomyces cerevisiae* Mus81-Mms4 is a catalytic, DNA structure-selective endonuclease. *Nucleic Acids Res.* **36**, 2182–2195 (2008).
52. Lucas, I. & Hyrien, O. Hemicatenanes form upon inhibition of DNA replication. *Nucleic Acids Res.* **28**, 2187–2193 (2000).
53. Liberi, G. *et al.* Methods to study replication fork collapse in budding yeast. *Methods Enzymol.* **409**, 442–462 (2006).
54. Fogg, J. M. & Lilley, D. M. Ensuring productive resolution by the junction-resolving enzyme RuvC: large enhancement of the second-strand cleavage rate. *Biochemistry* **39**, 16125–16134 (2000).
55. Ying, S. *et al.* MUS81 promotes common fragile site expression. *Nat. Cell Biol.* **15**, 1001–1007 (2013).
56. Gritenaite, D. *et al.* A cell cycle-regulated Slx4-Dpb11 complex promotes the resolution of DNA repair intermediates linked to stalled replication. *Genes Dev.* **28**, 1604–1619 (2014).
57. Gallo-Fernández, M., Saugar, I., Ortiz-Bazán, M. Á., Vázquez, M. V. & Tercero, J. A. Cell cycle-dependent regulation of the nuclease activity of Mus81-Eme1/Mms4. *Nucleic Acids Res.* **40**, 8325–8335 (2012).
58. Matos, J., Blanco, M. G., Maslen, S., Skehel, J. M. & West, S. C. Regulatory control of the resolution of DNA recombination intermediates during meiosis and mitosis. *Cell* **147**, 158–172 (2011).
59. Mukherjee, S., Wright, W. D., Ehmsen, K. T. & Heyer, W.-D. The Mus81-Mms4 structure-selective endonuclease requires nicked DNA junctions to undergo conformational changes and bend its DNA substrates for cleavage. *Nucleic Acids Res.* **42**, 6511–6522 (2014).
60. Blanco, M. G., Matos, J. & West, S. C. Dual control of Yen1 nuclease activity and cellular localization by Cdk and Cdc14 prevents genome instability. *Mol. Cell* **54**, 94–106 (2014).
61. García-Luis, J., Clemente-Blanco, A., Aragón, L. & Machin, F. Cdc14 targets the Holliday junction resolvase Yen1 to the nucleus in early anaphase. *Cell Cycle* **13**, 1392–1399 (2014).
62. Kanai, Y. *et al.* DmGEN shows a flap endonuclease activity, cleaving the blocked-flap structure and model replication fork. *FEBS J.* **274**, 3914–3927 (2007).
63. Rass, U. *et al.* Mechanism of Holliday junction resolution by the human GEN1 protein. *Genes Dev.* **24**, 1559–1569 (2010).
64. Cromie, G. A. *et al.* Single Holliday junctions are intermediates of meiotic recombination. *Cell* **127**, 1167–1178 (2006).
65. Giannattasio, M. *et al.* Visualization of recombination-mediated damage bypass by template switching. *Nat. Struct. Mol. Biol.* **21**, 884–892 (2014).
66. Wehrkamp-Richter, S., Hyppa, R. W., Prudden, J., Smith, G. R. & Boddy, M. N. Meiotic DNA joint molecule resolution depends on Nse5-Nse6 of the Smc5-Smc6 holocomplex. *Nucleic Acids Res.* **40**, 9633–9646 (2012).
67. Garvik, B., Carson, M. & Hartwell, L. Single-stranded DNA arising at telomeres in *cdc13* mutants may constitute a specific signal for the RAD9 checkpoint. *Mol. Cell Biol.* **15**, 6128–6138 (1995).

Acknowledgements

We specially thank Dr Luis Aragon for giving us the idea of overexpressing the *MMS4* and *YEN1* genes in telophase and also for allowing J.G.L. to learn the NN-2D technique in his lab under the supervision of Raul Torres. We also thank Dr Agustín Valenzuela for

kindly letting us use his ChemiDoc MP (Bio-Rad). We finally thank other members of the lab for fruitful discussions. This work was supported by Instituto de Salud Carlos III (PS09/00106 and PI12/00280 to F.M.), Fundación Canaria de Investigación y Salud (predoctoral fellowship 08/42 to J.G.-L.) and Spanish Ministry of Education (FPU predoctoral fellowship AP2009-2511 to J.G.-L.). All these programs were co-financed with the European Commission's ERDF structural funds.

Author contributions

J.G.-L. performed all the experimental work. F.M. and J.G.-L. planned and analysed the experiments. F.M. wrote the paper.

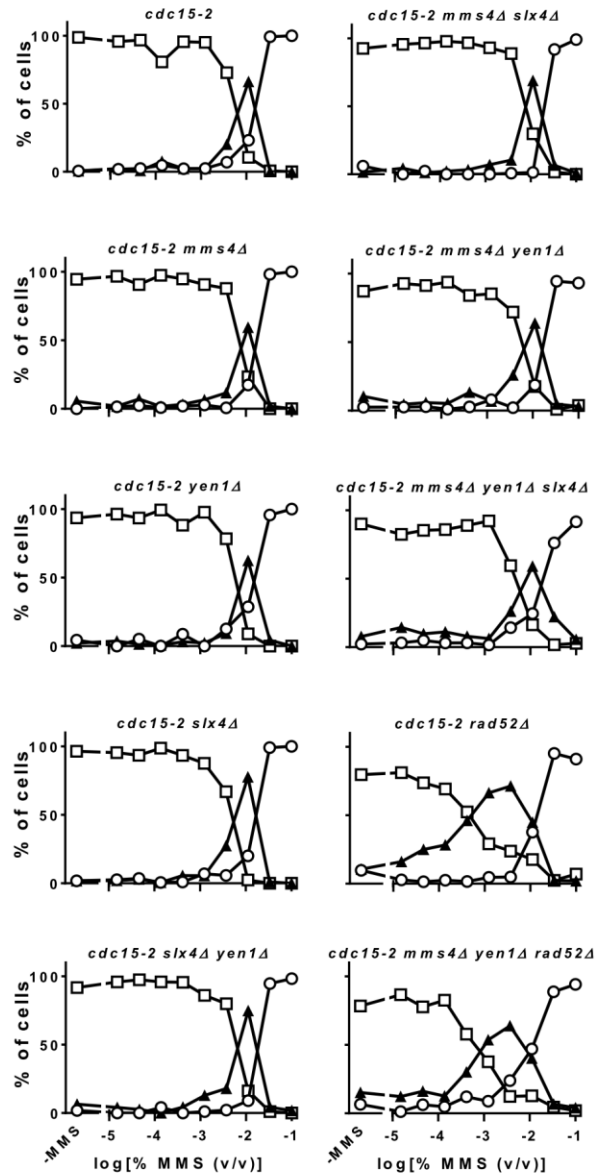
Additional information

Supplementary Information accompanies this paper at <http://www.nature.com/naturecommunications>

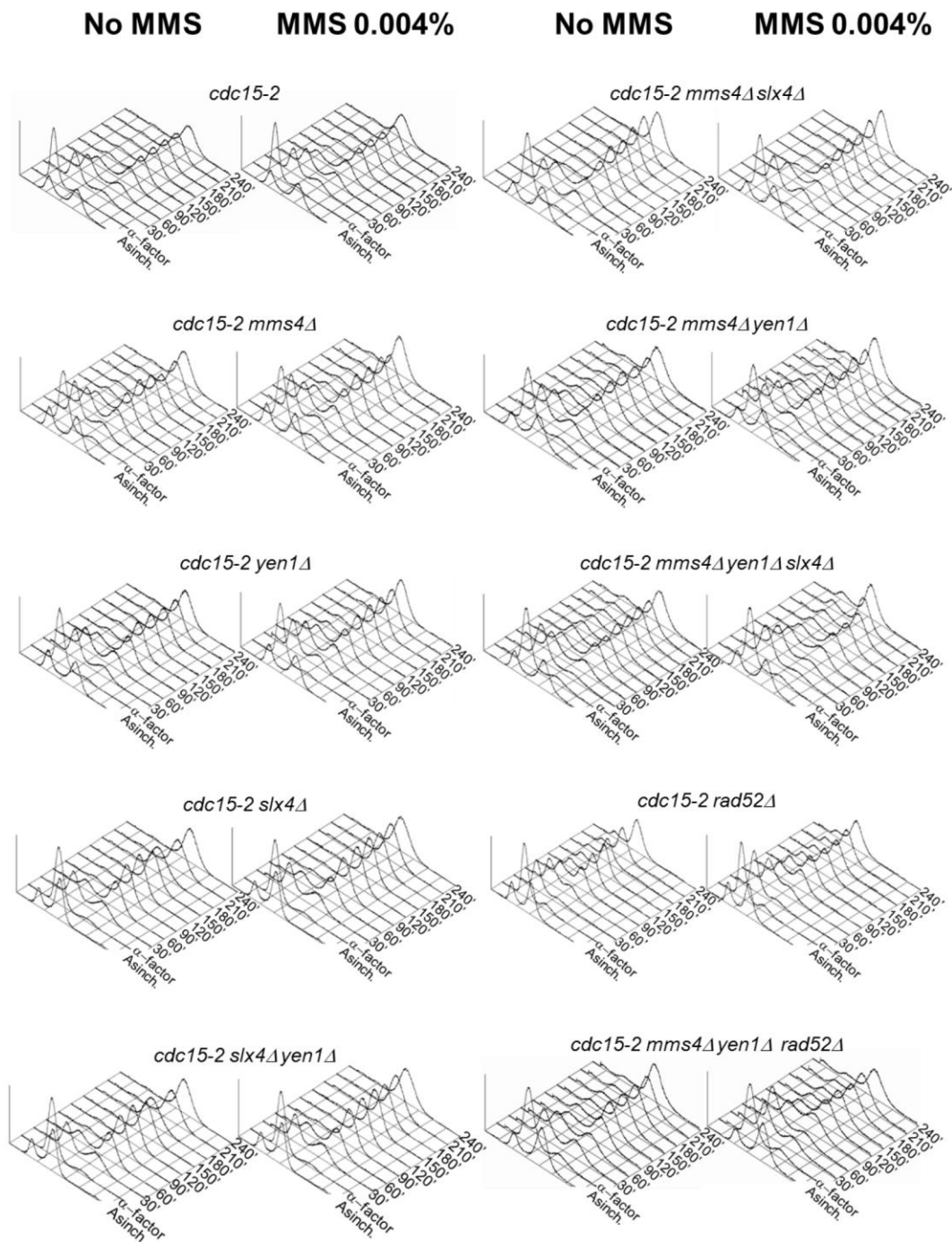
Competing financial interests: The authors declare no competing financial interests.

Reprints and permission information is available online at <http://npg.nature.com/reprintsandpermissions/>

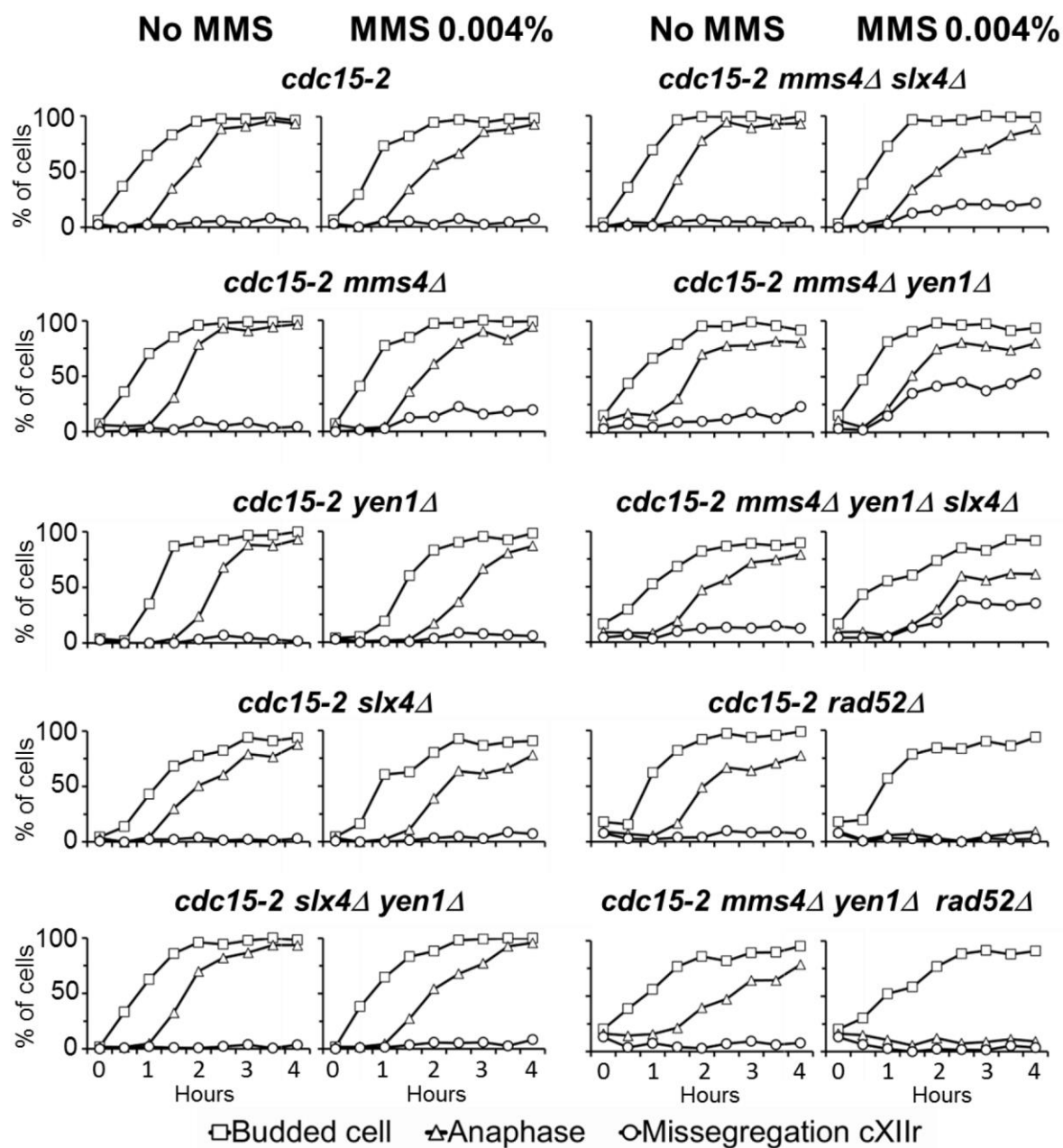
How to cite this article: Garcia-Luis, J. and Machin, F. Mus81-Mms4 and Yen1 resolve a novel anaphase bridge formed by noncanonical Holliday junctions. *Nat. Commun.* 5:5652 doi: 10.1038/ncomms6652 (2014).



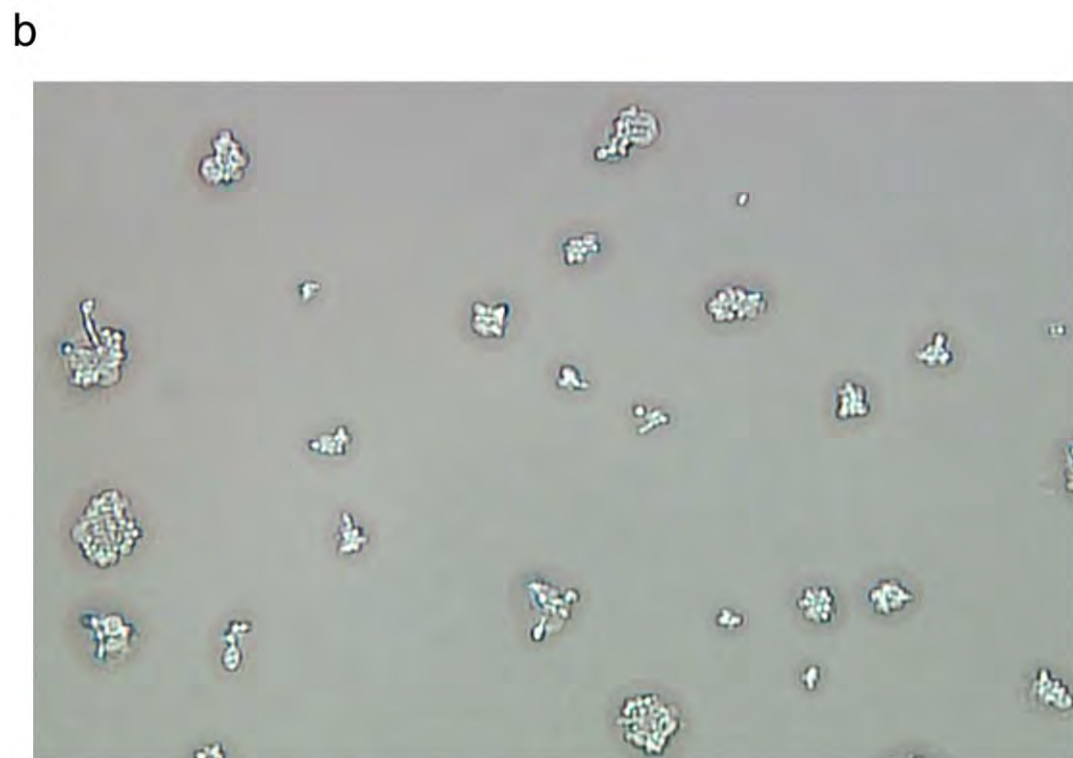
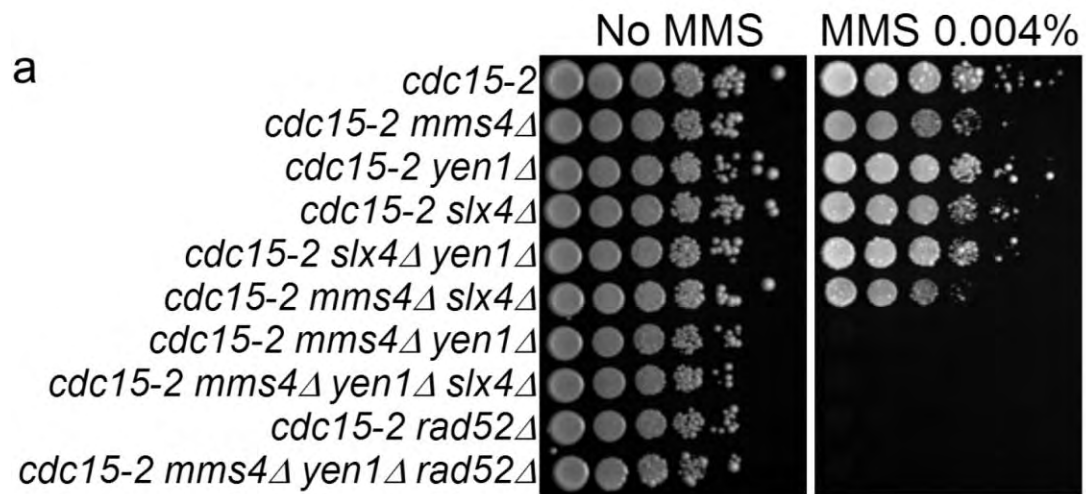
Supplementary Figure 1. Double deletion of the structure-selective endonucleases coding genes *MMS4* and *YEN1* does not change the G1 and G2/M checkpoint sensitivity to MMS. Overnight cultures of the strain FM588 (*cdc15-2 Tel-cXIIr::tetO tetR-YFP*), knocked out single mutant derivatives of FM588 for *RAD52*, *SLX4*, *MMS4* and *YEN1*, double mutants combinations for the endonucleases, and the triple mutants *slx4Δ mms4Δ yen1Δ* and *mms4Δ yen1Δ rad52Δ* were first arrested in G1 at 25 °C. They were then released into a synchronous cell cycle at 37 °C for 4 h either in the absence of MMS or in the presence of increasing concentrations of it. Then, cells were harvested and stained with DAPI for microscopy analysis of the cell cycle stage they were in. Unbudded cells were considered to be in G1 (open circle), budded mononucleated cells in S/G2/M (filled triangle), and budded binucleated to have reached anaphase (open square). In this latter category we also included cells with a long and stretched nuclear signal across the bud neck that connected two major segregated nuclear masses (>5 μm of distance all across), i.e. DAPI-stained anaphase bridges (see also Fig. 1).



Supplementary Figure 2. Double deletion of the structure-selective endonucleases coding genes *MMS4* and *YEN1* does not change the timing of the S-phase. Strains FM588 (*cdc15-2 Tel-cXII::tetO tetR-YFP*); knocked out single mutant derivatives of it for *RAD52*, *SLX4*, *MMS4* and *YEN1*, double mutants combinations for the endonucleases, and the triple mutants *slx4Δ mms4Δ yen1Δ* and *mms4Δ yen1Δ rad52Δ* were first arrested in G1 at 25 °C and then released into a synchronous cell cycle at 37 °C for 4 h. During the 4 h time course, samples were taken for DNA content analysis through flow cytometry. The asynchronous culture right before the G1 arrest was also taken as a reference for the 1N and 2N peaks.

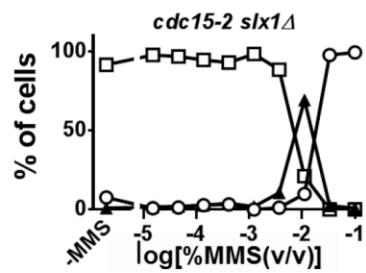


Supplementary Figure 3. Double deletion of the structure-selective endonucleases coding genes *MMS4* and *YEN1* does not change the timing of the anaphase onset. Strains FM588 (*cdc15-2 Tel-cXIIr::tetO tetR-YFP*); knocked out single mutant derivatives of it for *RAD52*, *SLX4*, *MMS4* and *YEN1*, double mutants combinations for the endonucleases, and the triple mutants *slx4Δ mms4Δ yen1Δ* and *mms4Δ yen1Δ rad52Δ* were first arrested in G1 at 25 °C and then released into a synchronous cell cycle at 37 °C for 4 h. During the 4 hours time course, samples were taken for fluorescence microscopy. Budded cells (open square), cells in anaphase as measured in Fig. 1 (open triangle) and cells with missegregated cXIIr (open circle) were plotted against time as percentage of total cell number.

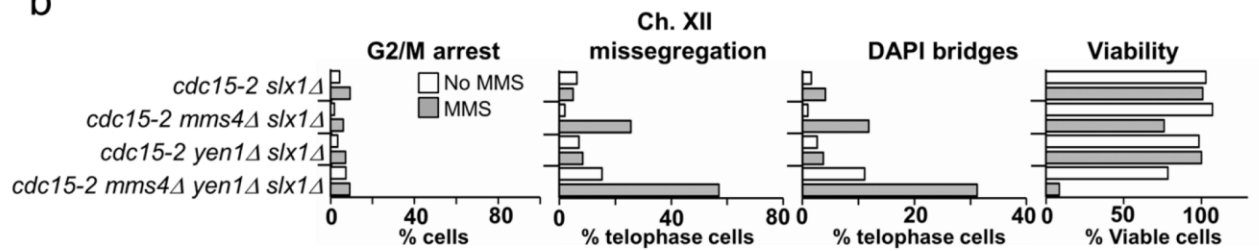


Supplementary Figure 4. The *mms4Δ yen1Δ* double mutant can grow in MMS for several generations before becoming unviable. (a) Overnight cultures of the strains used in Figure 1 were serially diluted and directly plated onto either YPD or YPD supplemented with MMS 0.004% (v/v). (b) Micrographs from the *mms4Δ yen1Δ* strain growing onto YPD + MMS plates after 3 days.

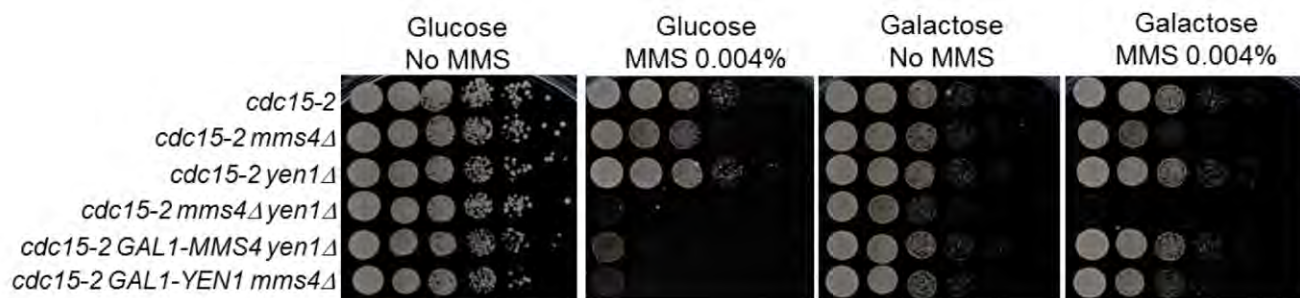
a



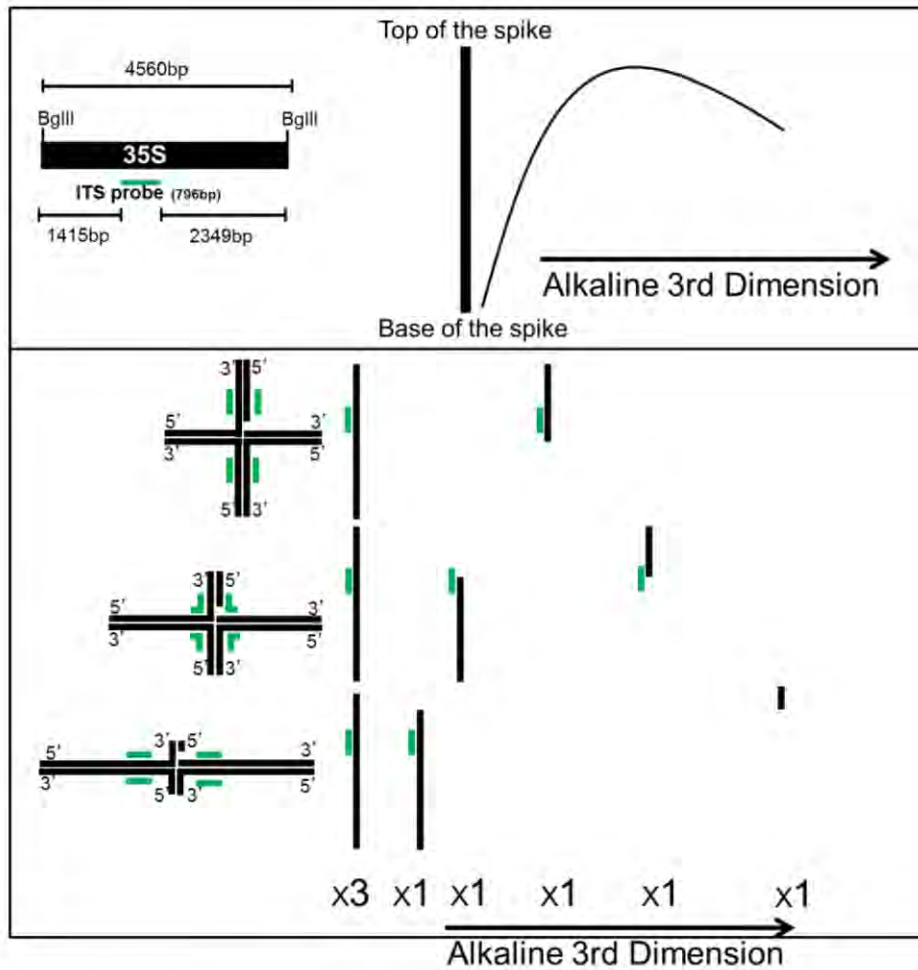
b



Supplementary Figure 5. Co-deletion of *SLX1* with other structure-selective nucleases leads to anaphase phenotypes similar to their *slx4Δ* counterparts. Overnight cultures of the strain FM961 (*cdc15-2 Tel-cXIIr::tetO tetR-YFP slx1Δ*), and its derivatives carrying also *mms4Δ*, *yen1Δ* and *mms4Δ yen1Δ* were subjected to the same MMS concentration profile of supplementary figure 1 (a), and the analysis to uncover anaphase abnormalities of figure 1a (b).



Supplementary Figure 6. Expression of either *MMS4* or *YEN1* under the galactose *GAL1* promoter rescue long-term sensitivity to MMS of the *mms4Δ yen1Δ* double mutant. Strains FM588 (*cdc15-2 Tel-cXIIr:tetO tetR-YFP*), knocked out single mutant derivatives for *MMS4* and *YEN1*, double mutant *mms4Δ yen1Δ* and mutants with controlled expression of each gene under galactose, *GAL1-MMS4 yen1Δ* and *mms4Δ GAL1-YEN1*, were grown overnight in YEPD, 1:10 serial diluted (from $OD_{600} = 0.8$ to 8×10^{-6}), and 5 μ l of each dilution spotted on YEPD or YEPG plates with and without 0.004% (v/v) MMS.



Supplementary Figure 7. Schematics of the expected migration pattern of nicked Holliday Junctions in a neutral, neutral, alkaline three-dimensional electrophoresis (NNA-3D). On the top-left corner, the BglII fragment that recognizes the ITS probe against the rDNA unit, including the length of the probe and the flanking sequences. On the right, the expected patterns of detectable fragments with the probe after an alkaline electrophoresis of an nHJ NN-2D spike providing there is a single nick at the junction. The thick line would correspond to the three full-length ssDNAs of the four-way Holliday junction, whereas the arc would correspond to the smaller ssDNAs coming from the nicked strand. At the bottom, a representation of ssDNAs from nHJs at different positions across the NN-2D spike, and the expected ssDNA stoichiometries. The first depicted nHJ would be at the head of the spike (i.e. symmetrical nHJ) and would render two almost identical small ssDNAs coming from the strand that carries the nick after the NNA-3D, although only one ssDNA would be detected by the ITS probe. The second nHJ would be around the middle of the NN-2D spike (i.e. asymmetrical nHJ) and would render two distinct ssDNAs. The probe can detect both smaller ssDNAs depending on their size. The third nHJ would be at the base of the spike (i.e. highly asymmetrical nHJ) and would also render two ssDNAs that largely differ in their size. One of them would be too small to be picked up by the probe whereas the other would be almost as big as the full-length ssDNAs and would hence migrate very close to the line. In all cases, the molecular stoichiometry would be three full-length ssDNAs versus one fragmented ssDNA. The ratio of overall probe intensity between the whole of the full-length ssDNAs line and the sum of the arc would be 3:1. Note that this NNA-3D pattern is also possible if there is a small gap at junction instead of just a nick.

Supplementary table 1. Strains used in this work.

Strain name	Relevant genotype	Origin
AS499	<i>MATa bar1Δ leu2-3,112 ura3-52 his3- Δ200 trp1- Δ63 ade2-1 lys2-801 pep4</i>	A. Strunnikov ^a
FM588	AS499; <i>TetR-YFP ADE2, TetO(5.6Kb):1061Kb ChrXII HIS3, cdc15-2:9myc:Hph</i>	F. Machín ^b
FM965	FM588; <i>slx4Δ::KanMX</i>	This work
FM992	FM588; <i>mms4Δ::KanMX</i>	This work
FM1010	FM588; <i>yen1Δ::KanMX</i>	This work
FM1185	FM588; <i>mms4Δ::KanMX, yen1Δ::BleMX</i>	This work
FM1192	FM588; <i>slx4Δ::KanMX, yen1Δ::BleMX</i>	This work
FM1212	FM588; <i>slx4Δ::KanMX, mms4Δ::NatMX</i>	This work
FM1458	FM588; <i>slx4Δ::KanMX, mms4Δ::NatMX, yen1Δ::BleMX4</i>	This work
FM889	FM588; <i>rad52Δ::KanMX</i>	This work
FM1354	FM588; <i>mms4Δ::KanMX, yen1Δ::BleMX4; rad52Δ::NatMX</i>	This work
FM1428	FM588; <i>yen1Δ::BleMX, KanMX:GAL1-MMS4</i>	This work
FM1432	FM588; <i>mms4Δ::BleMX, KanMX:GAL1-YEN1</i>	This work

FM1820	FM588; <i>slx1</i> Δ:: <i>KanMX</i> , <i>mms4</i> Δ:: <i>UraMX</i>	This work
FM1823	FM588; <i>slx1</i> Δ:: <i>KanMX</i> , <i>yen1</i> Δ:: <i>BleMX</i>	This work
FM1827	FM588; <i>slx1</i> Δ:: <i>KanMX</i> , <i>yen1</i> Δ:: <i>BleMX</i> , <i>mms4</i> Δ:: <i>UraMX</i>	This work

^a This is the parental strain of all the others. It is included in this table as a reference (it was not used in this work). It is a derivative of the S288C congenic strain YPH499. Details can be found at Freeman, L., Aragon-Alcaide, L. & Strunnikov, A. The condensin complex governs chromosome condensation and mitotic transmission of rDNA. *J. Cell Biol.* **149**, 811–24 (2000).

^b Quevedo, O., García-Luis, J., Matos-Perdomo, E., Aragón, L. & Machín, F. Nondisjunction of a single chromosome leads to breakage and activation of DNA damage checkpoint in *g2*. *PLoS Genet.* **8**, e1002509 (2012).

4.3 Article 3: Cdc14 targets the Holliday junction resolvase Yen1 to the nucleus in early anaphase

It was already known that Mus81-Mms4 is activated at the end of mitosis by a Cdc5 dependent phosphorylation. It was also known that Yen1 is activated soon afterwards to act as a back-up resolvase in the elimination of recombination intermediates. However little was known about how Yen1 is activated at the very end of mitosis. In this work we show that Cdc14, the mitotic master phosphatase, targets Yen1 to the nucleus in early anaphase through the FEAR network, giving access to its targets. The MEN-driven Cdc14 re-activation in late anaphase maintain Yen1 in the nucleus until the beginning of the next S phase. The activity of Yen1 imported into the nucleus through the first wave of Cdc14 activation is enough to remove any branched DNA structure and backup the SSE Mus81-Mms4.

Cdc14 targets the Holliday junction resolvase Yen1 to the nucleus in early anaphase

Jonay García-Luis¹, Andrés Clemente-Blanco^{2†}, Luis Aragón², and Félix Machín^{1,*}

¹Genomic Instability & Cancer Group; Unidad de Investigación; Hospital Universitario Nuestra Señora de Candelaria; Santa Cruz de Tenerife, Spain; ²Cell Cycle Group; MRC Clinical Sciences Centre; Imperial College London; London, UK

[†]Current affiliation: Instituto de Biología Funcional y Genómica; CSIC/Universidad de Salamanca; Salamanca, Spain

Keywords: Cdc14, Yen1, Mus81-Mms4, *Saccharomyces cerevisiae*, Holliday junction, anaphase, MMS

Abbreviations: HJ, Holliday junction; iHJ, intact HJ; nHJ, nicked HJ; dHJ, double HJ; SSE, structure-specific endonucleases; JM, joint molecules; HR, homologous recombination pathway; SRF, stalled replication forks; STR, Sgs1-Top3-Rmi1 complex; CDK, cyclin-dependent kinase; NLS, nuclear localization signal; FEAR, CDC fourteen early anaphase release; SPBs, spindle pole bodies; MEN, mitotic exit network; yeGFP, yeast enhanced green fluorescent protein; MMS, methyl methanesulfonate; Nz, nocodazole; α F, alpha-factor mating pheromone; PFGE, pulse field gel electrophoresis; SEM, standard error of the mean; BF, bright field

The only canonical Holliday junction (HJ) resolvase identified in eukaryotes thus far is Yen1/GEN1. Nevertheless, Yen1/GEN1 appears to have a minor role in HJ resolution, and, instead, other structure-specific endonucleases (SSE) that recognize branched DNA play the leading roles, Mus81-Mms4/EME1 being the most important in budding yeast. Interestingly, cells tightly regulate the activity of each HJ resolvase during the yeast cell cycle. Thus, Mus81-Mms4 is activated in G₂/M, while Yen1 gets activated shortly afterwards. Nevertheless, cytological studies have shown that Yen1 is sequestered out of the nucleus when cyclin-dependent kinase activity is high, i.e., all of the cell cycle but G₁. We here show that the mitotic master phosphatase Cdc14 targets Yen1 to the nucleus in early anaphase through the FEAR network. We will further show that this FEAR-mediated Cdc14-driven event is sufficient to back-up Mus81-Mms4 in removing branched DNA structures, which are especially found in the long chromosome arms upon replication stress. Finally, we found that MEN-driven Cdc14 re-activation in late anaphase is essential to keep Yen1 in the nucleus until the next G₁. Our results highlight the essential role that early-activated Cdc14, i.e., through the FEAR network, has in removing all kind of non-proteinaceous linkages that preclude faithful sister chromatid segregation in anaphase. In addition, our results support the general idea of Yen1 acting as a last resource endonuclease to deal with any remaining HJ that might compromise genetic stability during chromosome segregation.

Introduction

Joint molecules (JMs) comprise different branched DNA junctions that link chromatids and/or chromosomes. JMs are formed as intermediate products during the repair of DNA double-strand breaks (DSBs) through the homologous recombination pathway (HR).¹ HR-dependent JM are also formed during the bypass of stalled replication forks (SRF) and postreplicative gaps, which may arise due to DNA base damage, interstrand crosslink, etc.^{2,3} Several JMs can be distinguished according to the physical nature of the branched junction, being one of the most studied the so-called Holliday junction (HJ).^{1,4,5} This basic 4-way structure has, in turn, several variants with special features related to their processing: the intact (i.e., uninterrupted) HJ (iHJ), the nicked HJ (nHJ), and the double HJ (dHJ). Central to HJs processing, eukaryotic cells possess one helicase–topoisomerase complex

and 3 conserved structure-specific endonucleases (SSEs).^{3,6,7} The helicase–topoisomerase complex (hereafter refer to as STR) comprises the budding yeast helicase Sgs1 (Bloom syndrome BLM in humans), the type I topoisomerase Top3 (TOPOIII α), and the cofactor Rmi1 (RMI1-RMI2); whereas, the 3 SSEs are Slx1-Slx4 (SLX1-SLX4), Mus81-Mms4 (MUS81-EME1), and Yen1 (GEN1). In vitro, STR can eliminate model dHJ by branch migrating each iHJ toward each other in a process termed “dHJ dissolution”.⁸ By contrast, SSEs cut HJs, albeit with different specificities. Thus, Yen1 and Slx1-Slx4 are mostly active against iHJs, and Mus81-Mms4 prefers nHJs.^{9–14} In vivo, STR appears as the cell first and best choice in mitosis, because dHJ dissolution always results in no sequence exchange between chromatids (i.e., non-crossovers).^{8,15,16} As for the SSEs, cells may choose them when STR is presumed to fail (e.g., single iHJs and nHJs).^{7,17} Whereas many studies have shown that disruption of different

*Correspondence to: Félix Machín; Email: fmacconw@gmail.com

Submitted: 01/17/2014; Revised: 02/24/2014; Accepted: 02/26/2014; Published Online: 03/05/2014
http://dx.doi.org/10.4161/cc.28370

SSEs and the STR synergistically enhance the presence of JMs *in vivo*,¹⁸⁻²⁴ the question of why eukaryotes have 3 different SSE to process HJs remains open. This is more puzzling when just one SSE, the nHJ resolvase Mus81-Mms4, appears to be sufficient to accomplish all HJ resolution.⁷ Even more intriguing is the fact that the actual equivalent to the bacterial HJ resolvase RuvC, i.e., Yen1, has only a minor role in eukaryotes. In this context, several recent reports have defined the cell cycle regulation of STR, Mus81-Mms4, and Yen1 activities, and found that, while STR is active all throughout, Mus81-Mms4 becomes active once cells are in G₂/M, and Yen1 appears active shortly afterwards.^{13,24,25} Mus81-Mms4 activity depends on both high cyclin-dependent kinase (CDK) activity and the activation of the Polo-like kinase Cdc5, which, in turns, takes place at the G₂/M transition.^{13,24-26} Less is known about Yen1 activity. Aside from being active when purified from cells transiting in the M phase,¹³ Yen1 contains a nuclear localization signal (NLS) that is masked by phosphorylation through CDK.²⁷ Thus, Yen1 is nuclear when CDK activity is low, i.e., G₁, and cytoplasmic when CDK activity is high, i.e., S/G₂/M. This implies an intriguing paradox, since Yen1 appears active against HJ *in vitro*, when it is actually sequestered out of the nucleus *in vivo*.

CDK-mediated phosphorylation can be reverted in targeted proteins through 3 different, though not necessarily exclusive, manners. First, when all CDK activity drops at the very end of mitosis, *de novo* CDK-targeted proteins would remain unphosphorylated. This is particularly effective in those proteins with a rapid turnover. Second, the pool of different cyclins which substitute one another to maintain a high CDK activity from S to telophase can also change the substrate specificity of CDK.²⁸ Lastly, specific phosphatases can counteract CDK-dependent phosphorylation. When coupled to the lowering of CDK activity, these phosphatases accomplish that even stable proteins remain unphosphorylated. The master phosphatase that removes the phosphate from the CDK consensus site in *S. cerevisiae* is Cdc14.^{29,30} Sequestered through most of the cell cycle within the nucleolus, Cdc14 is released in 2 waves at the end of mitosis.^{31,32} The first wave takes place shortly after the anaphase onset and mediates dephosphorylation of selected CDK-targeted proteins. This wave is controlled by the so-called CDC fourteen early anaphase release network (FEAR). The FEAR coordinates precisely critical events that take place during anaphase, i.e., lengthening of the mitotic spindle, chromosome condensation, topological unlinkage of sister chromatids, control of the forces that pull apart sister chromatids, correct positioning of the spindle pole bodies (SPBs) in each daughter cell, etc.³³⁻³⁷ The second wave is triggered by the mitotic exit network (MEN), which is responsible for switching off CDK activity, thus promoting cytokinesis and the transition into a new G₁.³⁸⁻⁴¹

The nuclear location of Yen1 is a prerequisite for its HJ activity since budding yeast performed a close mitosis, i.e., the nuclear membrane is not dismantled in mitosis. Hence, in this work, we aimed to determine if Yen1 was ever targeted to the nucleus out of G₁, particularly in anaphase, and, if so, for how long and whether Cdc14 was important for this targeting *in vivo*. We indeed found that Yen1 shuttles from the cytoplasm to the nucleus in early anaphase, and that this is performed through the activation of

Cdc14. We further show that Cdc14 is epistatic to Yen1 in terms of JM resolution in the absence of Mus81-Mms4 activity.

Results and Discussion

We tried to address the issue of Yen1 subcellular localization by fluorescence microscopy through tagging the *YEN1* gene with the gene which encodes for the yeast-enhanced green fluorescent protein (yeGFP, or simply GFP hereafter). In order to follow the dynamics of Yen1-GFP localization, we performed time-course experiments during one synchronous G₁-to-telophase cell cycle. To block cells in telophase, before the CDK activity drops, we made use of a thermosensitive conditional allele for the critical MEN component Cdc15 (i.e., *cdc15-2*). To precisely follow up anaphase we further tagged the SPB component Spc42 with the RedStar fluorescent protein.

Yen1 seems to be present at low concentrations within the cell,⁴² and, indeed, we were unable to see the Yen1-GFP fusion when controlled by its own promoter. Because of this caveat, we chose to put the Yen1-GFP gene under the strong *GAL* promoter. The overexpressed C-terminal Yen1-GFP chimera happened to be non-toxic in galactose and fully functional in a growth assay with MMS (Fig. 1). Thus, in glucose, a *GAL-YEN1:GFP* strain that also carries the *mms4Δ* deletion was as hypersensitive to MMS as the double mutant *mms4Δ yen1Δ*. By contrast, growth in galactose abolished this high hypersensitivity, and the strain was able to grow as good as the *mms4Δ* single mutant (Fig. 1).

Next, we tried to visualize Yen1-GFP under the microscope. At least 1 h of continuous galactose induction was needed to see Yen1-GFP within the cell. As for the location pattern, galactose induction in the asynchronous culture yielded a strong nuclear signal in unbudded cells and a weaker and diffuse signal in budded cells (Fig. 2A). In order to better follow up the dynamics of Yen1-GFP we synchronized cells in G₁ before inducing *YEN1-GFP*, induced then the gene in galactose while keeping the cells in G₁, and finally released all cells into a synchronous cell cycle. In order to avoid interference with *de novo* synthesis of Yen1-GFP out of G₁, we switched the gene off at the time of the G₁ release. Finally, the temperature was also shifted to 37 °C in order to inactivate Cdc15-2 and thus cause a final block in telophase, i.e., a G₁-to-telophase synchronous cell cycle. Thus, we observed that Yen1-GFP was nuclear at the G₁ arrest but rapidly disappeared from the nucleus upon S-phase entry (Fig. 2A). Interestingly, there was a short window at about 100–120 min after the G₁ release, where we observed Yen1-GFP coming back to the nucleus when it was stretched between the mother and the bud (Fig. 2A). This new nuclear location peaked when the distance between the SPBs was between 3–6 μm, which roughly corresponds to early anaphase (Fig. 2B). When cells reached late anaphase/telophase; SPB distances > 8 μm, this nuclear Yen1-GFP signal faded away greatly. As mentioned above, Yen1 is a HJ resolvase, and steady-state levels of HJ can be increased by making cells use HR more often. Thus, we also follow a synchronous cell cycle upon continuous low levels of MMS (0.004% v/v). This low MMS concentration interfered little with the cell cycle progression in the *cdc15-2* and *cdc15-2 GAL-YEN1:GFP* strains

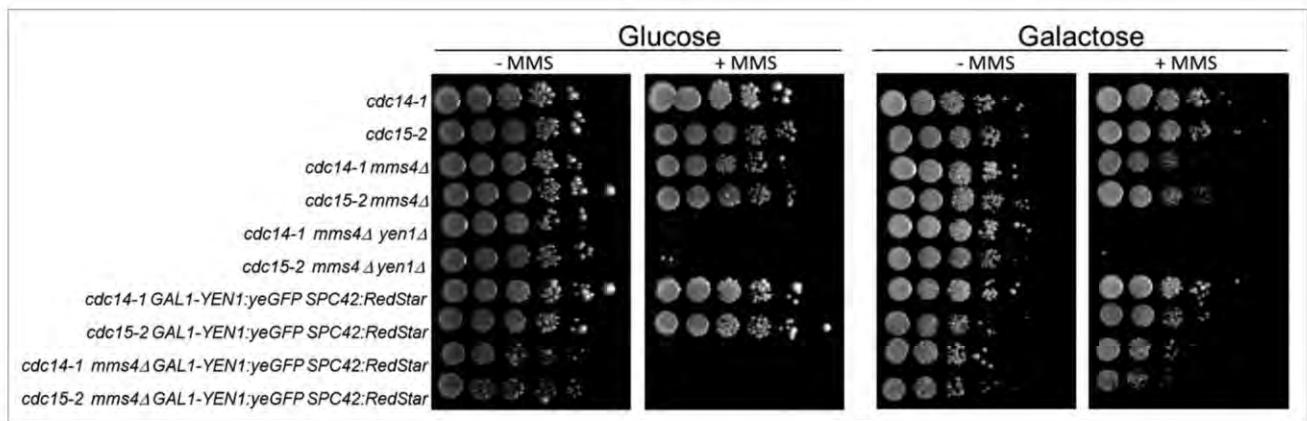


Figure 1. Overexpressed Yen1-GFP suppresses MMS hypersensitivity of the *mms4Δ yen1Δ* strain. Overnight cultures of the strains FM1292 (*cdc15-2*) and FM1272 (*cdc14-1*) plus their derivatives carrying *mms4Δ*, *mms4Δ yen1Δ*, *GAL:YEN1:GFP SPC42:RedStar*, and *mms4Δ GAL:YEN1:GFP SPC42:RedStar* were serially diluted and plated onto 4 different plates; YP glucose, YP galactose, and either media further supplemented with MMS 0.004% (v/v). Pictures to determine ability to grow were taken after 5 d of incubation at 25 °C.

(data not shown). Remarkably, the same relocalization pattern was observed upon MMS treatment, although the Yen1-GFP nuclear signal appeared more granulated and frequently formed distinct foci (Fig. 2A). These foci happened to be either on the nuclear DNA, as they clearly colocalized with DAPI, or between the 2 segregated nuclear masses (Fig. 2C).

The nuclear relocalization of Yen1 in early anaphase prompted us to check whether Cdc14 might be targeting Yen1 to the nucleus through the FEAR network. As described above, Yen1 bears a CDK consensus site within its NLS region. Phosphorylation of such a site masks the NLS and keeps Yen1 out of the nucleus.²⁷ Besides, Yen1 gets broadly dephosphorylated around G_2/M ,¹³ and Cdc14 is the master anti-CDK phosphatase that acts in that period of the cell cycle.³¹ In order to test the Cdc14-driven relocalization hypothesis, we performed the same cell cycle-dependent Yen1-GFP localization in a *cdc14-1* background at 37 °C. Upon Yen1-GFP overexpression in G_1 , its nuclear localization was equivalent to that of *cdc15-2*, and this location was lost in a similar way after entering S phase (Fig. 2A). However, no nuclear relocalization was seen throughout, not even when MMS was present (Fig. 2). This indicates that Cdc14 plays a key role in targeting Yen1 to the nucleus in early anaphase. Our results also point out that Cdc14-driven Yen1 relocalization occurs always in every cell cycle (i.e., this relocalization does not necessarily depend on induced DNA damage), although DNA damage causes Yen1-GFP to shift from a dispersed nucleoplasmic signal into distinct foci.

A striking result from the location pattern in the *cdc15-2* G_1 -to-telophase time course was the apparent transient nuclear location of Yen1-GFP. Thus, Yen1-GFP is nuclear in G_1 , cytoplasmic in S/ G_2 , nuclear in early anaphase, and again cytoplasmic in late anaphase (Fig. 2B). This is intriguing, since it points out toward 2 waves of nuclear relocalization for Yen1, one in early anaphase and another one in G_1 . Nevertheless, the result we obtained with the *cdc15-2* can be logic taking into account that FEAR elicits a first wave of Cdc14 activity, which is then turned off, unless MEN is immediately triggered afterwards.^{31,32} Since Cdc15 is a MEN

component, *cdc15-2* cannot sustain a prolonged Cdc14 activity at the restrictive condition. In addition, since MEN-driven full Cdc14 activation is the one that achieves the CDK activity drop, it is thus expected that Yen1 would become phosphorylated again and, hence, expelled from the nucleus, in late anaphase in a *cdc15-2* background. In order to confirm this hypothesis, we performed a release from the telophase arrest into a new G_1 (i.e., telophase-to- G_1 time course). In this case, we first synchronized the cell cycle in G_2 and then induced the *YEN1* gene to make sure that de novo Yen1-GFP was cytoplasmic and had never been in the nucleus before. Thus, induction of Yen1-GFP in nocodazole (Nz) yielded a clear cytoplasmic signal (Fig. 3A and B). A G_2 -to-telophase time course yielded a transient nuclear relocalization in the *cdc15-2* strain and no relocalization in *cdc14-1* (Fig. 3A and B). For instance, 30 min after Nz removal, 23% of anaphase cells had a nuclear signal in the *cdc15-2*, whereas this percentage dropped to 4% after an additional hour. In all cases, the whole Yen1-GFP protein levels remained constant (Fig. 3C), confirming that the loss of nuclear Yen1-GFP signal was due to re-localization rather than degradation. Upon release from telophase by shifting the temperature from 37 °C to 25 °C, Yen1 went to the nucleus in both strains, although the signal in the *cdc15-2* was much stronger than in the *cdc14-1* (likely reflecting the need of Cdc14-1 to get fully reconstituted by prolonging the incubation at the permissive temperature) (Fig. 3A).

All the results we have just shown above strongly point out that the 2 waves of Cdc14 activation, taking place in early and late anaphase, respectively, drive and sustain the relocalization of Yen1 to the nucleus. In order to further confirm that activation of Cdc14 was sufficient to relocalize Yen1-GFP to the nucleus, we overexpressed *CDC14* in a cell cycle stage other than anaphase; more precisely, in cells blocked in G_2 with Nz. This condition has been shown to activate Cdc14 without the need of FEAR or MEN execution.^{34,43} Thus, we found that galactose-driven co-overexpression of *GAL-CDC14* and *GAL-YEN1:GFP* causes Yen1-GFP to be nuclear in more than 80% of G_2 -blocked cells upon 90 min of induction (Fig. 3D).

In order to see whether the regulation of Cdc14 over Yen1 was important to prevent and/or resolve HJs, we looked at the presence of JMs in the *cdc14-1* background by pulse field gel electrophoresis (PFGE). Sister chromatids with DNA-mediated linkages (i.e., JMs or persistent SRFs) are known to not enter a PFGE.^{21,44} Thus, we observed that large chromosomes such as chromosome XII (cXII) and IV (cIV) were less visible in the *cdc15-2 mms4Δ yen1Δ* strain upon MMS treatment than in any other mutant combinations for *cdc15-2* (Fig. 4A and B). Like in the *cdc15-2* reference strain, most chromosomes were visible in a *cdc14-1* telophase block, even when DNA damage was induced with MMS

(Fig. 4A and B). Strikingly, cXII was barely visible in the *cdc14-1 mms4Δ* strain upon DNA damage, in a pattern very similar to *cdc15-2 mms4Δ yen1Δ* (Fig. 4A). However, *cdc14-1 yen1Δ* was not different to just *cdc14-1*, nor was *cdc14-1 mms4Δ yen1Δ* to *cdc14-1 mms4Δ*. Lastly, to make sure that this PFGE behavior was not due to stalled replication in the *cdc14-1 mms4Δ* mutant, we followed bulk DNA replication in all mutants and found no differences (Fig. 4C). In all cases, replication was completed by 90 min after the G₁ release (i.e., 2.5 h before we took the samples for PFGE analysis). Therefore, all these findings fit well with Cdc14 having a role in JM resolution through Yen1. Besides, this

Yen1 activity is complementary to that of Mus81-Mms4, which, in turn, is independent of Cdc14. Lastly, but not least, the Cdc14 pool activated by FEAR elicits enough endogenous Yen1 activity to resolve all remaining JMs.

The data we present herein showed that Yen1 is targeted to the nucleus in early anaphase, and this event depends on Cdc14. Taking into account that Mus81-Mms4 has been reported to mainly act in G₂/M,^{13,24-26} Yen1 may therefore serve as a last-resource backup JM-resolving pathway that operates from early anaphase until cytokinesis. Another interesting possibility is that, by restricting Yen1 to anaphase, the spindle pulling forces may give directionality to the resolution of HJs toward a less toxic or genetic-compromising outcome. The observed regulation of Cdc14 over Yen1 extends the key role of the former in preventing all types of non-proteinaceous sister chromatid linkages (i.e., catenations and DNA-mediated) that might form a bridge between segregating chromosomes in anaphase.^{36,43,45}

Materials and Methods

Yeast strains, growth, and experimental conditions

All yeast strains used in this work come from the S288C background and are listed in Table 1. N- and C-terminal

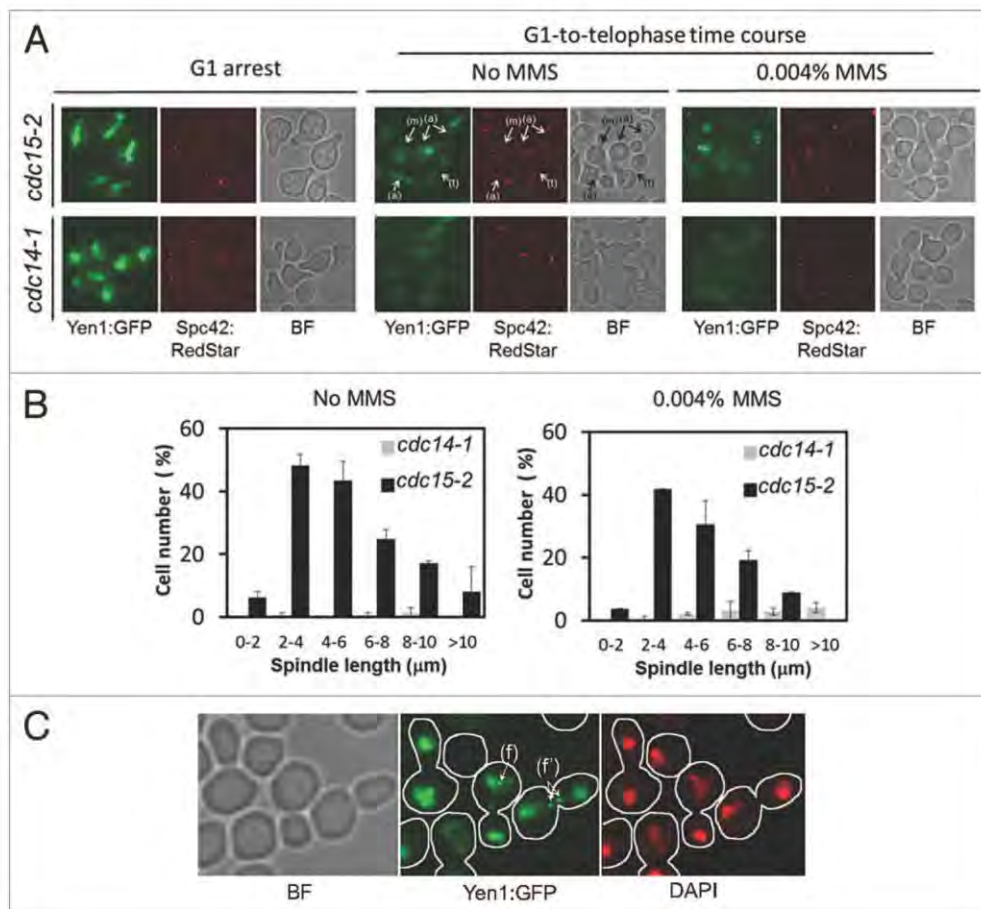


Figure 2. Yen1 re-localizes back to the nucleus in early anaphase in a Cdc14-dependent manner. Overnight YP raffinose cultures of the strains FM1799 (*cdc15-2 GAL:YEN1:GFP SPC42:RedStar*) and FM1804 (*cdc14-1 GAL:YEN1:GFP SPC42:RedStar*) were first arrested in G₁ with αF for 3 h in the growth media. Next, galactose 2% (w/v) was added and the culture was left blocked in G₁ for another 2 h. They then were split into 2 fresh YP glucose media, one of them containing MMS 0.004% (v/v), and finally released into a synchronous cell cycle at 37 °C for 4 h. (A) Representative micrographs of z-stack maximum projections from the G₁ blocks after 2 h of galactose addition (G₁ arrest), and about 100–120 min after the G₁ release at 37 °C with or without MMS. The label (m) points to an S/G₂ cell with an unaligned ~2 μm spindle (i.e., distance between SPBs) and no nuclear Yen1-GFP signal; the label (a) points to examples of cells in early anaphase according to spindle orientation and length, all with a visible nuclear Yen1; and the label (t) points to a cell already blocked in telophase with a much fainter nuclear Yen1 signal. (B) Percentage of cells with nuclear Yen1-GFP relative to the distance between SPBs (mean ± SEM, n = 3). Only budded cells with 2 SPBs were counted. (C) A sample from the FM1799 G₁-to-telophase time course in MMS was treated with DAPI to address if foci colocalized with nuclear DNA. The label (f) points to an example of a cell in anaphase with foci within the main nuclear DNA mass, whereas the label (f') points to a cell in anaphase with foci located between the 2 segregated nuclear masses. BF, bright field.

tagging with yeGFP or RedStar, gene deletions, marker swap, and allele/promoter replacements were engineered through PCR strategies.⁴⁶ All strains were grown overnight in air orbital incubators at 25 °C in YP raffinose media (yeast extract 1% w/v, peptone 2% w/v, and raffinose 2% w/v) supplemented with adenine 0.08 mg/ml unless stated otherwise. G₁ blocks were performed by incubating cultures at 0.3 OD₆₀₀ with 50 ng/ml of the α -factor mating pheromone (α F, all tested strains were *bar1* Δ) for 3 h. Yen1-GFP was then induced for 2 h by adding galactose 2% (w/v). The induction was monitored by fluorescence microscopy. The G₁-to-telophase synchronous cell cycle was performed as follows: G₁-blocked cells with induced Yen1-GFP were released from the block by first washing twice with YP glucose 2% w/v (stops Yen1-GFP production); resuspended in fresh YP supplemented with raffinose 2% w/v, glucose 2% w/v, adenine 0.08 mg/ml and pronase E 0.1 mg/ml; and incubated at 37 °C for 4 h. In the instances where DNA damage was exogenously induced, 0.004% (v/v) MMS was added at the time of the G₁ release. MMS was kept in the media until the telophase arrest. Throughout the G₁-to-telophase cell cycle, samples were taken at different time points for further analysis. G₂-to-telophase cell cycle was carried out in a similar manner. G₂ block was achieved by incubating the strains with 15 μ g/ml

of nocodazole for 3 h at 25 °C. *GAL-YEN1:GFP* galactose induction during the G₂ block lasted 1.5 h, and then the promoter was shut down by adding glucose. The same induction procedure was performed for the co-induction of *GAL-CDC14* and *GAL-YEN1:GFP*. G₂-to-telophase synchronous cell cycle was achieved

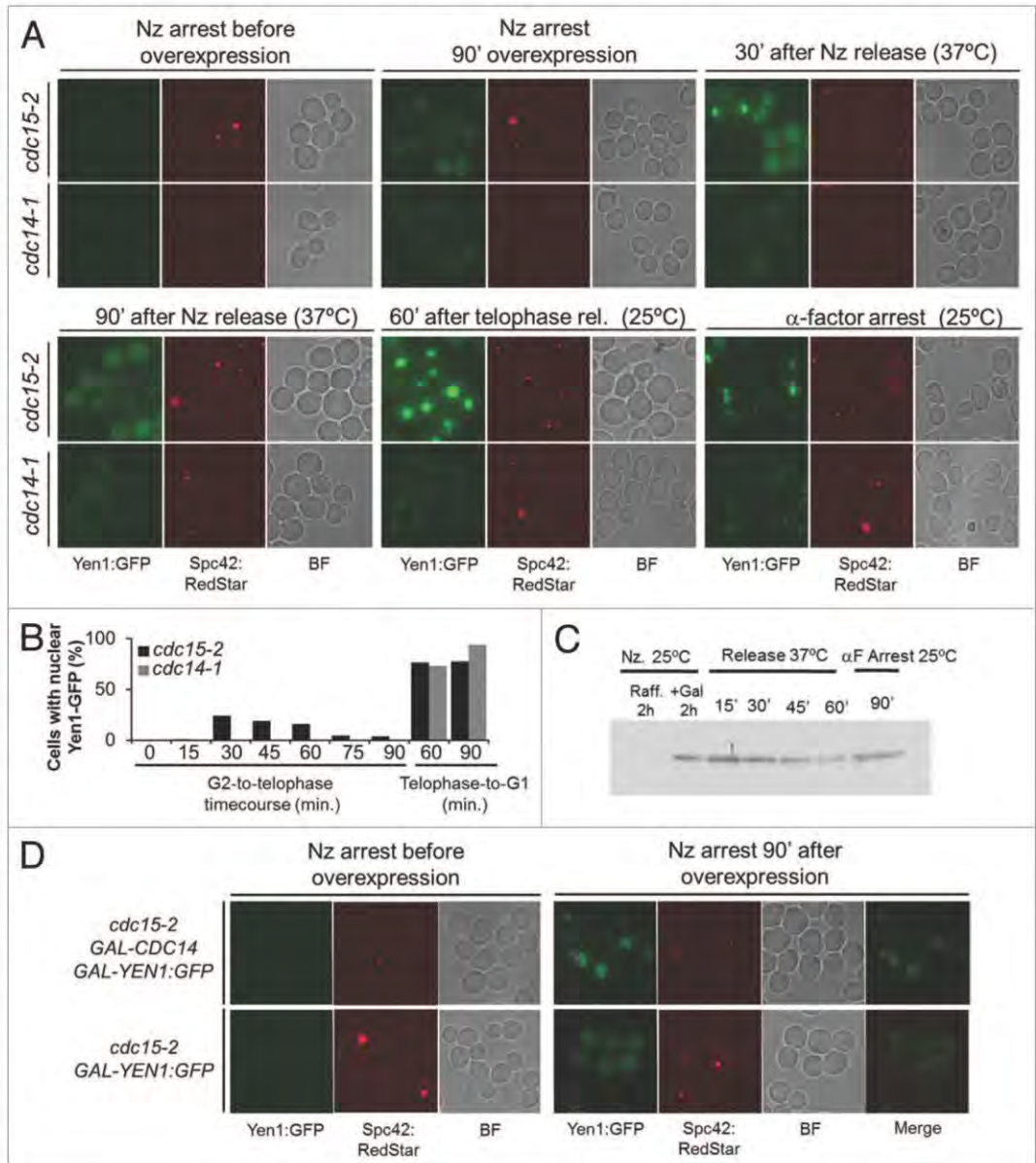


Figure 3. Yen1 nuclear relocalization in anaphase is dynamic and governed by the CDK/Cdc14 balance. Overnight YP raffinose cultures of the strains FM1799 (*cdc15-2 GAL:YEN1:GFP SPC42:RedStar*) and FM1804 (*cdc14-1 GAL:YEN1:GFP SPC42:RedStar*) were first arrested in G₂ with nocodazole (Nz) for 3 h. Next, galactose 2% (w/v) was added, and the culture was left blocked in G₂ for another 90 min. Next, Nz was removed from the media at the same time that glucose was added and the culture shifted to 37 °C. Cells were incubated in this condition for 90 min (G₂-to-telophase cell cycle) before shifting the temperature to 25 °C and adding α F (Telophase-to-G₁ cell cycle). (A) Representative micrographs of z-stack maximum projections from the different cell cycle blocks and/or time points of the corresponding releases. (B) Percentage of cells with nuclear Yen1-GFP at the different cell cycle blocks and/or time points of the corresponding releases. (C) Western blot against Yen1-GFP during the G₂-to-telophase and telophase-to-G₁ cell cycles. (D) Overnight YP raffinose cultures of the strains FM1799 (*cdc15-2 GAL:YEN1:GFP SPC42:RedStar*) and FM1850 (*cdc15-2 GAL-CDC14 GAL:YEN1:GFP SPC42:RedStar*) were first arrested in G₂ with nocodazole (Nz) for 3 h. Next, galactose 2% (w/v) was added while the cultures were left blocked in G₂ for another 90 min. BF, bright field.

by washing out Nz and shifting the temperature to 37 °C. For the telophase-to-G₁ cell cycle, cells were released from telophase by shifting the temperature from 37 °C back to 25 °C and adding 50 ng/ml of α F.

Error bars in graphs represent the standard error of the mean (SEM).

Fluorescence microscopy

Fluorescent proteins were analyzed by wide-field fluorescence microscopy as previously reported.⁴⁷ Synchrony was determined by cell morphology and segregation of the nucleus. In order to follow up segregation of the nucleus, an aliquot was frozen at -20 °C for 48 h before DNA was stained using DAPI

at 0.05 μ g/ml final concentration after short cell treatment with 0.01% v/v Triton X-100. This procedure was also used to determine if Yen1 foci colocalized with DNA. Yen1-GFP sub-cellular location and Spc42-RedStar were determined directly in cells freshly harvested. For the GFP we used 10 Z stacks, 0.6 μ m each, obtained through an YFP filter cube (Leica) using the following parameters: 1 s exposure, gain 7/10, and intensity 5/5. For the RedStar we also used ten Z stacks, 0.6 μ m each, obtained through a RFP filter cube (Leica) using the following parameters: 2 s exposure, gain 7/10, and intensity 4/5. Distances between Spc42-labeled SPBs was measured on 2D maximum projections.

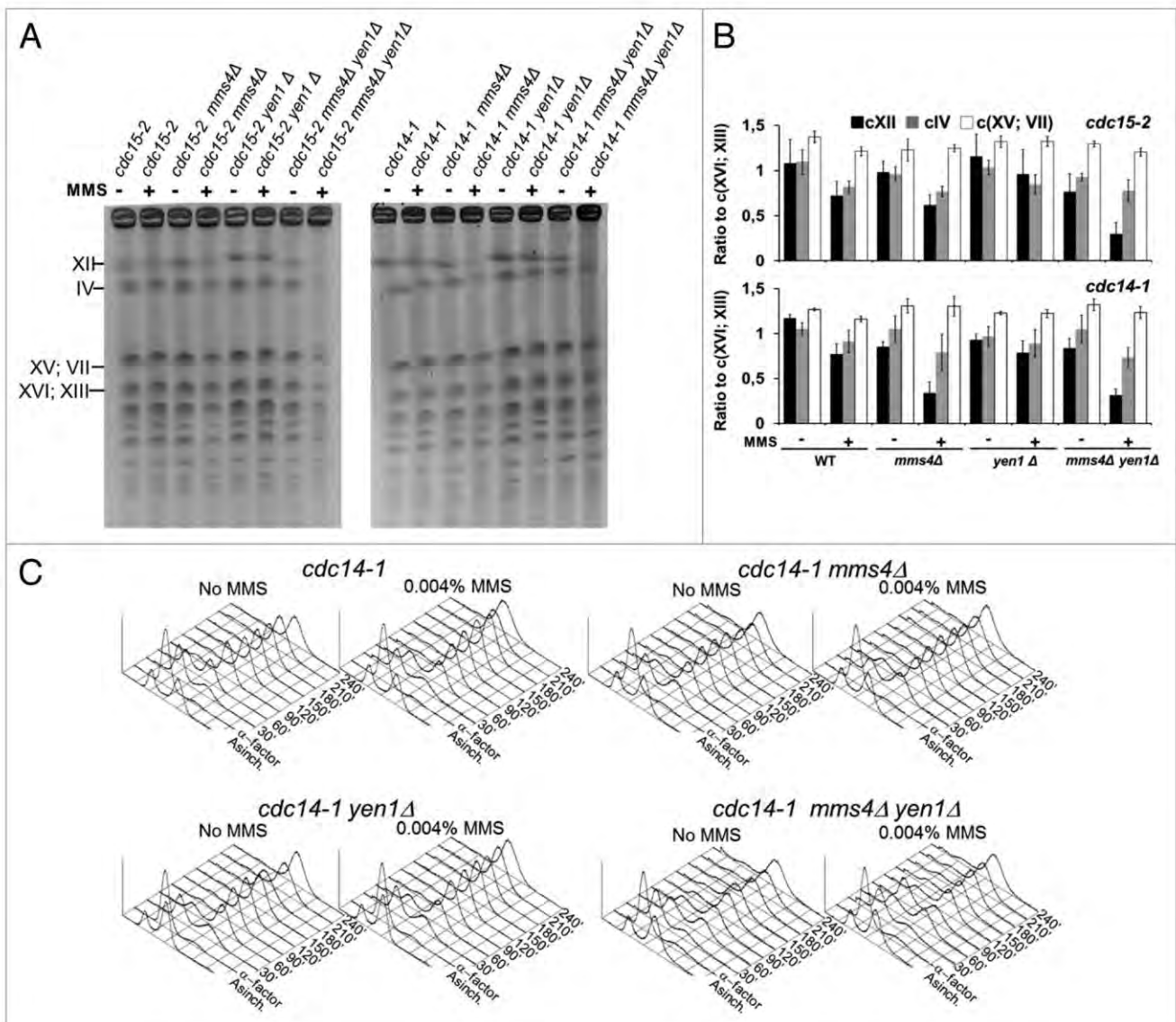


Figure 4. Yen1 and Cdc14 are epistatic in resolving Joint Molecules in the absence of Mus81-Mms4. Overnight YP glucose cultures of the strains FM1292 (*cdc15-2*) and FM1272 (*cdc14-1*), knocked out single mutant derivatives of them for *MMS4* and *YEN1*, and the double mutants *mms4* Δ *yen1* Δ were first arrested in G₁ at 25 °C. They were then split into 2 media, one of them containing MMS 0.004% v/v, and finally released into a synchronous cell cycle at 37 °C for 4 h. **(A)** PFGE of all yeast chromosomes at the telophase blocks. Minus sign, no MMS; plus sign, MMS 0.004% v/v. **(B)** Quantitation of the electrophoretic bands for the large chromosomes relative to the middle-sized chromosome pair XVI/XIII (mean \pm SEM, n = 3). **(C)** Flow cytometry analysis of the DNA content of the G₁-to-telophase time-course for the *cdc14-1* strains.

Table 1. Strains used in this work. Parental strain is also included

Strain name	Relevant genotype	Reference
A5499	<i>MATa bar1Δ leu2-3,112 ura3-52 his3-Δ200 trp1-Δ63 ade2-1 lys2-801 pep4</i>	A Strunnikov
FM1292	A5499; <i>cdc15-2:9myc:Hph</i>	This work
FM1362	FM1292; <i>mms4Δ::URA3MX</i>	This work
FM1185	FM1292; <i>mms4Δ::KanMX4; yen1Δ::BleMX4</i>	This work
FM1799	FM1292; <i>NatNT2::GAL1::YEN1:yeGFP:TRP1; SPC42::RedStar::KanMX</i>	This work
FM1806	FM1292; <i>mms4Δ::URA3MX; NatNT2::GAL1::YEN1:yeGFP:TRP1; SPC42::RedStar::KanMX</i>	This work
FM1272	A5499; <i>cdc14-1:9myc:TRP1</i>	This work
FM1358	FM1272; <i>mms4Δ::URA3MX</i>	This work
FM1453	FM1272; <i>mms4Δ::URA3MX; yen1Δ::BleMX4</i>	This work
FM1804	FM1272; <i>NatNT2::GAL1::YEN1:yeGFP:HphNT1; SPC42::RedStar::KanMX</i>	This work
FM1808	FM1272; <i>mms4Δ::URA3MX; NatNT2::GAL1::YEN1:yeGFP:HphNT1; SPC42::RedStar::KanMX</i>	This work
FM1850	FM1292; <i>NatNT2::GAL1::YEN1:yeGFP:TRP1; SPC42::RedStar::KanMX; ura3::GAL::CDC14::URA3</i>	This work

Pulse field gel electrophoresis (PFGE), flow cytometry, and western blots

PFGE to see all yeast chromosomes was performed using a CHEF DR-III system (Bio-Rad) in a 0.8% agarose gel in 0.5 × TBE buffer and run at 12 °C for 20 h at 6 V/cm with an initial switching time of 80 s, a final of 150 s, and an angle of 120°. Yeast chromosomes were photographed after staining with ethidium bromide.

Flow cytometry analysis was performed as previously described in order to follow up bulk DNA replication.⁴⁷

Western blots against Yen1-GFP were performed using a Mini-PROTEAN II gel apparatus (Biorad) in an 8% SDS-PAGE gel. Five OD₆₀₀ equivalents were harvested for each timepoint. Proteins were extracted with glass beads and SDS 2% for 2 min and then boiled in a water bath for 3 min. One hundred μl of 2× Laemmli buffer was added to each sample and boiled for an additional minute. Samples were briefly centrifuged, and 20 μl of the supernatant were loaded. After electrophoresis, proteins were transferred from the gel to an Immobilon-P PVDF membrane (Millipore). The membrane was blocked for 1 h in 5% (w/v) non-fat milk in TBST (100 mM Tris-Cl pH7.5, 0.9% NaCl, 0.1% Tween 20) at room temperature. After blocking, the membrane was incubated for 1 h with an anti-GFP antibody from rabbit at 1:8000 (Abcam) in 5% milk/TBST followed by an additional hour of incubation with a secondary

antibody anti-rabbit-AP (1:50000) (Promega). The membrane was washed and finally visualized with CDPStar (GE Healthcare) on X-ray films (GE Healthcare, Amersham Hyperfilm ECL).

Disclosure of Potential Conflicts of Interest

No potential conflicts of interest were disclosed.

Acknowledgments

We thank Stephen C West for sharing some unpublished data with us and Raimundo Freire for providing the anti-GFP antibody. We also thank other members of our labs for help and discussion. Authors contributed as follows: J.G.L. has performed most of the experimental work. J.G.L., A.C.B., L.A., and F.M. have planned the experiments. L.A. and F.M. have supervised this work. F.M. has written the paper. L.A. hosted J.G.L. in his lab for learning methods related to this work.

Funding

This work was supported by Instituto de Salud Carlos III (PS09/00106 and PS12/00280), Fundación Canaria de Investigación y Salud (08/42 to J.G.L.) and Spanish Ministry of Education (FPU fellowship AP2009-2511 to J.G.L.). All these programs were co-financed with the European Commission's ERDF structural funds

References

- Pâques F, Haber JE. Multiple pathways of recombination induced by double-strand breaks in *Saccharomyces cerevisiae*. *Microbiol Mol Biol Rev* 1999; 63:349-404; PMID:10357855
- Heyer W-D, Ehmsen KT, Liu J. Regulation of homologous recombination in eukaryotes. *Annu Rev Genet* 2010; 44:113-39; PMID:20690856; <http://dx.doi.org/10.1146/annurev-genet-051710-150955>
- Rass U. Resolving branched DNA intermediates with structure-specific nucleases during replication in eukaryotes. *Chromosoma* 2013; 122:499-515; PMID:24008669; <http://dx.doi.org/10.1007/s00412-013-0431-z>
- Schwacha A, Kleckner N. Identification of double Holliday junctions as intermediates in meiotic recombination. *Cell* 1995; 83:783-91; PMID:8521495; [http://dx.doi.org/10.1016/0092-8674\(95\)90191-4](http://dx.doi.org/10.1016/0092-8674(95)90191-4)
- Bzymek M, Thayer NH, Oh SD, Kleckner N, Hunter N. Double Holliday junctions are intermediates of DNA break repair. *Nature* 2010; 464:937-41; PMID:20348905; <http://dx.doi.org/10.1038/nature08868>
- Schwartz EK, Heyer W-D. Processing of joint molecule intermediates by structure-selective endonucleases during homologous recombination in eukaryotes. *Chromosoma* 2011; 120:109-27; PMID:21369956; <http://dx.doi.org/10.1007/s00412-010-0304-7>
- Hickson ID, Mankouri HW. Processing of homologous recombination repair intermediates by the Sgs1-Top3-Rmi1 and Mus81-Mms4 complexes. *Cell Cycle* 2011; 10:3078-85; PMID:21876385; <http://dx.doi.org/10.4161/cc.10.18.16919>
- Wu L, Hickson ID. The Bloom's syndrome helicase suppresses crossing over during homologous recombination. *Nature* 2003; 426:870-4; PMID:14685245; <http://dx.doi.org/10.1038/nature02253>
- Kaliraman V, Mullen JR, Fricke WM, Bastin-Shanower SA, Brill SJ. Functional overlap between Sgs1-Top3 and the Mms4-Mus81 endonuclease. *Genes Dev* 2001; 15:2730-40; PMID:11641278; <http://dx.doi.org/10.1101/gad.932201>
- Fricke WM, Brill SJ. Slx1-Slx4 is a second structure-specific endonuclease functionally redundant with Sgs1-Top3. *Genes Dev* 2003; 17:1768-78; PMID:12832395; <http://dx.doi.org/10.1101/gad.1105203>
- Fricke WM, Bastin-Shanower SA, Brill SJ. Substrate specificity of the *Saccharomyces cerevisiae* Mus81-Mms4 endonuclease. *DNA Repair (Amst)* 2005; 4:243-51; PMID:15590332; <http://dx.doi.org/10.1016/j.dnarep.2004.10.001>
- Ip SCY, Rass U, Blanco MG, Flynn HR, Shekel JM, West SC. Identification of Holliday junction resolvases from humans and yeast. *Nature* 2008; 456:357-61; PMID:19020614; <http://dx.doi.org/10.1038/nature07470>

13. Matos J, Blanco MG, Maslen S, Skehel JM, West SC. Regulatory control of the resolution of DNA recombination intermediates during meiosis and mitosis. *Cell* 2011; 147:158-72; PMID:21962513; <http://dx.doi.org/10.1016/j.cell.2011.08.032>
14. Schwartz EK, Wright WD, Ehmsen KT, Evans JE, Stahlberg H, Heyer W-D. Mus81-Mms4 functions as a single heterodimer to cleave nicked intermediates in recombinational DNA repair. *Mol Cell Biol* 2012; 32:3065-80; PMID:22645308; <http://dx.doi.org/10.1128/MCB.00547-12>
15. Ira G, Malkova A, Liberi G, Foiani M, Haber JE. Srs2 and Sgs1-Top3 suppress crossovers during double-strand break repair in yeast. *Cell* 2003; 115:401-11; PMID:14622595; [http://dx.doi.org/10.1016/S0092-8674\(03\)00886-9](http://dx.doi.org/10.1016/S0092-8674(03)00886-9)
16. Oh SD, Lao JP, Hwang PY-H, Taylor AF, Smith GR, Hunter N. BLM ortholog, Sgs1, prevents aberrant crossing-over by suppressing formation of multichromatid joint molecules. *Cell* 2007; 130:259-72; PMID:17662941; <http://dx.doi.org/10.1016/j.cell.2007.05.035>
17. Cromie GA, Hyppa RW, Taylor AF, Zakharyevich K, Hunter N, Smith GR. Single Holliday junctions are intermediates of meiotic recombination. *Cell* 2006; 127:1167-78; PMID:17174892; <http://dx.doi.org/10.1016/j.cell.2006.09.050>
18. Kaliraman V, Brill SJ. Role of SGS1 and SLX4 in maintaining rDNA structure in *Saccharomyces cerevisiae*. *Curr Genet* 2002; 41:389-400; PMID:12228808; <http://dx.doi.org/10.1007/s00294-002-0319-6>
19. Gaillard P-HL, Noguchi E, Shanahan P, Russell P. The endogenous Mus81-Eme1 complex resolves Holliday junctions by a nick and counternick mechanism. *Mol Cell* 2003; 12:747-59; PMID:14527419; [http://dx.doi.org/10.1016/S1097-2765\(03\)00342-3](http://dx.doi.org/10.1016/S1097-2765(03)00342-3)
20. Tay YD, Wu L. Overlapping roles for Yen1 and Mus81 in cellular Holliday junction processing. *J Biol Chem* 2010; 285:11427-32; PMID:20178992; <http://dx.doi.org/10.1074/jbc.M110.108399>
21. Ho CK, Mazón G, Lam AF, Symington LS. Mus81 and Yen1 promote reciprocal exchange during mitotic recombination to maintain genome integrity in budding yeast. *Mol Cell* 2010; 40:988-1000; PMID:21172663; <http://dx.doi.org/10.1016/j.molcel.2010.11.016>
22. Ashton TM, Mankouri HW, Heidenblut A, McHugh PJ, Hickson ID. Pathways for Holliday junction processing during homologous recombination in *Saccharomyces cerevisiae*. *Mol Cell Biol* 2011; 31:1921-33; PMID:21343337; <http://dx.doi.org/10.1128/MCB.01130-10>
23. Mazón G, Lam AF, Ho CK, Kupiec M, Symington LS. The Rad1-Rad10 nuclease promotes chromosome translocations between dispersed repeats. *Nat Struct Mol Biol* 2012; 19:964-71; PMID:22885325; <http://dx.doi.org/10.1038/nsmb.2359>
24. Szakal B, Branzei D. Premature Cdk1/Cdc5/Mus81 pathway activation induces aberrant replication and deleterious crossover. *EMBO J* 2013; 32:1155-67; PMID:23531881; <http://dx.doi.org/10.1038/emboj.2013.67>
25. Gallo-Fernández M, Saugar I, Ortiz-Bazán MÁ, Vázquez MV, Tercero JA. Cell cycle-dependent regulation of the nuclease activity of Mus81-Eme1/Mms4. *Nucleic Acids Res* 2012; 40:8325-35; PMID:22730299; <http://dx.doi.org/10.1093/nar/gks599>
26. Matos J, Blanco MG, West SC. Cell-Cycle Kinases Coordinate the Resolution of Recombination Intermediates with Chromosome Segregation. *Cell Rep* 2013;1-11.
27. Kosugi S, Hasebe M, Tomita M, Yanagawa H. Systematic identification of cell cycle-dependent yeast nucleocytoplasmic shuttling proteins by prediction of composite motifs. *Proc Natl Acad Sci U S A* 2009; 106:10171-6; PMID:19520826; <http://dx.doi.org/10.1073/pnas.0900604106>
28. Loog M, Morgan DO. Cyclin specificity in the phosphorylation of cyclin-dependent kinase substrates. *Nature* 2005; 434:104-8; PMID:15744308; <http://dx.doi.org/10.1038/nature03329>
29. Visintin R, Craig K, Hwang ES, Prinz S, Tyers M, Amon A. The phosphatase Cdc14 triggers mitotic exit by reversal of Cdk-dependent phosphorylation. *Mol Cell* 1998; 2:709-18; PMID:9885559; [http://dx.doi.org/10.1016/S1097-2765\(00\)80286-5](http://dx.doi.org/10.1016/S1097-2765(00)80286-5)
30. Jin F, Liu H, Liang F, Rizkallah R, Hurt MM, Wang Y. Temporal control of the dephosphorylation of Cdk substrates by mitotic exit pathways in budding yeast. *Proc Natl Acad Sci U S A* 2008; 105:16177-82; PMID:18845678; <http://dx.doi.org/10.1073/pnas.0808719105>
31. Stegmeier F, Amon A. Closing mitosis: the functions of the Cdc14 phosphatase and its regulation. *Annu Rev Genet* 2004; 38:203-32; PMID:15568976; <http://dx.doi.org/10.1146/annurev.genet.38.072902.093051>
32. Rock JM, Amon A. The FEAR network. *Curr Biol* 2009; 19:R1063-8; PMID:20064401; <http://dx.doi.org/10.1016/j.cub.2009.10.002>
33. Ross KE, Cohen-Fix O. A role for the FEAR pathway in nuclear positioning during anaphase. *Dev Cell* 2004; 6:729-35; PMID:15130497; [http://dx.doi.org/10.1016/S1534-5807\(04\)00128-5](http://dx.doi.org/10.1016/S1534-5807(04)00128-5)
34. Sullivan M, Higuchi T, Katis VL, Uhlmann F. Cdc14 phosphatase induces rDNA condensation and resolves cohesin-independent cohesion during budding yeast anaphase. *Cell* 2004; 117:471-82; PMID:15137940; [http://dx.doi.org/10.1016/S0092-8674\(04\)00415-5](http://dx.doi.org/10.1016/S0092-8674(04)00415-5)
35. Torres-Rosell J, Machín F, Jarmuz A, Aragón L. Nucleolar segregation lags behind the rest of the genome and requires Cdc14p activation by the FEAR network. *Cell Cycle* 2004; 3:496-502; PMID:15004526; <http://dx.doi.org/10.4161/cc.3.4.802>
36. Machín F, Torres-Rosell J, Jarmuz A, Aragón L. Spindle-independent condensation-mediated segregation of yeast ribosomal DNA in late anaphase. *J Cell Biol* 2005; 168:209-19; PMID:15657393; <http://dx.doi.org/10.1083/jcb.200408087>
37. Khmelinskii A, Lawrence C, Roostalu J, Schiebel E. Cdc14-regulated midzone assembly controls anaphase B. *J Cell Biol* 2007; 177:981-93; PMID:17562791; <http://dx.doi.org/10.1083/jcb.200702145>
38. Jaspersen SL, Charles JF, Tinker-Kulberg RL, Morgan DO. A late mitotic regulatory network controlling cyclin destruction in *Saccharomyces cerevisiae*. *Mol Biol Cell* 1998; 9:2803-17; PMID:9763445; <http://dx.doi.org/10.1091/mbc.9.10.2803>
39. Jaspersen SL, Morgan DO. Cdc14 activates cdc15 to promote mitotic exit in budding yeast. *Curr Biol* 2000; 10:615-8; PMID:10837230; [http://dx.doi.org/10.1016/S0960-9822\(00\)00491-7](http://dx.doi.org/10.1016/S0960-9822(00)00491-7)
40. Sanchez-Diaz A, Nkosi PJ, Murray S, Labib K. The Mitotic Exit Network and Cdc14 phosphatase initiate cytokinesis by counteracting CDK phosphorylations and blocking polarised growth. *EMBO J* 2012; 31:3620-34; PMID:22872148; <http://dx.doi.org/10.1038/emboj.2012.224>
41. Shou W, Seol JH, Shevchenko A, Baskerville C, Moazed D, Chen ZW, Jang J, Shevchenko A, Charbonneau H, Deshaies RJ. Exit from mitosis is triggered by Tem1-dependent release of the protein phosphatase Cdc14 from nucleolar RENT complex. *Cell* 1999; 97:233-44; PMID:10219244; [http://dx.doi.org/10.1016/S0092-8674\(00\)80733-3](http://dx.doi.org/10.1016/S0092-8674(00)80733-3)
42. Ghaemmaghami S, Huh W-K, Bower K, Howson RW, Belle A, Dephoure N, O'Shea EK, Weissman JS. Global analysis of protein expression in yeast. *Nature* 2003; 425:737-41; PMID:14562106; <http://dx.doi.org/10.1038/nature02046>
43. D'Amours D, Stegmeier F, Amon A. Cdc14 and condensin control the dissolution of cohesin-independent chromosome linkages at repeated DNA. *Cell* 2004; 117:455-69; PMID:15137939; [http://dx.doi.org/10.1016/S0092-8674\(04\)00413-1](http://dx.doi.org/10.1016/S0092-8674(04)00413-1)
44. Hennessy KM, Lee A, Chen E, Botstein D. A group of interacting yeast DNA replication genes. *Genes Dev* 1991; 5:958-69; PMID:2044962; <http://dx.doi.org/10.1101/gad.5.6.958>
45. Dulev S, de Renty C, Mehta R, Minkov I, Schwob E, Strunnikov A. Essential global role of CDC14 in DNA synthesis revealed by chromosome underreplication unrecognized by checkpoints in cdc14 mutants. *Proc Natl Acad Sci U S A* 2009; 106:14466-71; PMID:19666479; <http://dx.doi.org/10.1073/pnas.0900190106>
46. Janke C, Magiera MM, Rathfelder N, Taxis C, Reber S, Maekawa H, Moreno-Borchart A, Doenges G, Schwob E, Schiebel E, et al. A versatile toolbox for PCR-based tagging of yeast genes: new fluorescent proteins, more markers and promoter substitution cassettes. *Yeast* 2004; 21:947-62; PMID:15334558; <http://dx.doi.org/10.1002/yea.1142>
47. Quevedo O, García-Luis J, Matos-Perdomo E, Aragón L, Machín F. Nondisjunction of a single chromosome leads to breakage and activation of DNA damage checkpoint in G2. *PLoS Genet* 2012; 8:e1002509; PMID:22363215; <http://dx.doi.org/10.1371/journal.pgen.1002509>

5 Discussion

5.1 The *cdc15-2* block as a model to study missegregation and anaphase bridges formation

Faithful chromosome segregation during mitosis is of paramount importance to maintain genomic stability. The failure in eliminating the many physical linkages that maintain sister chromatids together can lead to the formation of anaphase bridges. Studies with the model organism *S. cerevisiae* have shown that unfinished replication, unresolved cohesion or catenated chromosomes can cause anaphase bridges formation (Holm et al. 1985; Uhlmann et al. 1999; Torres-Rosell et al. 2007). Previous studies have also shown that during unperturbed conditions higher eukaryotes as well as yeast cells form transient ultra-fine chromosome bridges during anaphase (Chan et al. 2007; Chan & Hickson 2009; Germann et al. 2014).

In this thesis we started creating a model that allowed us to study chromosome segregation. We took advantage of the temperature-sensitive allele *cdc15-2*. When grown at restrictive temperature the cells are blocked in telophase with two nuclei. We demonstrate that, in contrast to the *cdc14-1* mutants (another temperature-sensitive mutant used to block the cells in telophase), all the genome is correctly segregated in the *cdc15-2* block. We assessed the segregation not only by DAPI staining of the nuclei but also tagging different chromosomes with the tetR/*tetO* system including the cXII. cXII is the most challenging chromosome to be segregated due to its length, the presence of the hyper-recombinogenic rDNA array, and the rDNA high transcription rate that makes it prone to catenations. We concluded that our model with a temperature sensitive version *cdc15-2* tagged in the subtelomeric region of cXII is a powerful tool to study chromosome segregation due to the following reasons: 1) It correctly segregates the genome. 2) We can track the segregation of cXII, considered to be the segregation worst-case scenario. 3) Mother and daughter cells can be tracked since the *cdc15-2* mutants fail in performing cytokinesis. This is useful to identify missegregation of tagged chromosomes since we can correlate the presence of two resolved or unresolved chromosomes in one daughter cell with the absence of this chromosome tag in the other daughter cell. 4) The impairment in conducting cytokinesis also helps to maintain the structure of chromosome bridges that otherwise would be severed during cytokinesis (Holm et al. 1985; Uhlmann et al. 1999; Baxter & Diffley 2008b). 5) In addition, the use of *cdc15-2* allele allows to synchronize the cell in anaphase where chromosome segregation takes place. This makes it easier to correlate single-cell analysis with whole population analysis, in contrast to other models used to study chromosome segregation that are restricted to single-cell analysis due to the asynchrony of the culture.

5.2 The *mms4Δ yen1Δ* double mutant accumulates recombination intermediates that lead to chromatin anaphase bridges and ultrafine anaphase bridges

Recombination intermediates have been long discussed to be a physical linkage that can maintain sister chromatids together at the time of anaphase. In this thesis by using the aforementioned model we intended to check whether recombination intermediates form anaphase bridges. In order to boost recombination intermediates formation we made use of the alkylating agent MMS, known to increase replication fork stalling and replication fork restart associated to recombination, as well as mutants of SSEs implicated in the resolution of recombination intermediates.

We did observe that recombination intermediates accumulation at the time of anaphase can lead to chromosome missegregation. Our results show that concomitant deletion of two SSEs, *MMS4* and *YEN1*, led to increased cXII missegregation. Importantly, the missegregation phenotype was alleviated by deleting *RAD52*, a gene essential for all types of HR-mediated DNA repair in *S. cerevisiae*. This result supported the notion that HR intermediates are accumulated in this mutant. In addition, other studies have also shown that this double mutant has slow growth, higher accumulation of cells in G2/M in an asynchronous culture and increased sensitivity to DNA damaging agents. Accordingly, these works also showed that the high sensitivity to DNA damaging agents is alleviated by deleting *RAD52* (Ho et al. 2010; Blanco et al. 2010; Agmon et al. 2011). Our results are consistent with these data and point towards the structural basis behind these phenotypes. We hypothesize that accumulation of HR intermediates produce missegregation of chromosomes in anaphase. Missegregated chromosomes are then severed during cytokinesis. In the following cell cycle, cells will sense the damage triggering a G2/M arrest in order to repair the damage and as a result of this a slower progression in the cell cycle; i.e. slower doubling time.

We also observed that the inability of this double mutant to eliminate HR intermediates on time rendered the cells sensitive to the alkylating agent MMS. The increased sensitivity of the *mms4Δ mus81Δ* mutant to DNA damaging agents has also been reported in previous studies (Ho et al. 2010; Blanco et al. 2010; Agmon et al. 2011). In our case we further correlate the increased sensitivity to MMS to a massive failure in chromosome segregation and accumulation of HR intermediates. We show that this mutant accumulated HR intermediates by different evidences: 1) after MMS treatment large chromosomes are not able to enter in a PFGE. Importantly this condition is indicative of the existence of recombination intermediates and/or replication intermediates. We speculate that larger chromosomes are more likely to contain at least one HR intermediate that preclude the chromatids to enter into the gel. Additionally this

condition is worsened in cXII since it contains the rDNA array. 2) By NN-2D DNA electrophoresis probed against the rDNA we show that this mutant has a strong spike signal that corresponds to DNA molecules with double the size of a linear fragment and with a branched structure. This signal is conformed of HR intermediates (Friedman & Brewer 1995).

Intriguingly, the NN-2D DNA electrophoresis of the double mutant *mms4Δ mus81Δ* also had a faint signal of Y molecules (corresponding to replication forks) (Paper 2. Figure 4b). Replication intermediates have been reported to lead to anaphase bridges (Chan et al. 2007; Chan et al. 2009; Naim et al. 2013; Germann et al. 2014). We totally ruled out the possibility of these replication intermediates being responsible for the higher cXIIr missegregation for three reasons: 1) The faint signal of the Y-shaped molecules also appears with the same intensity with and without MMS in the single mutants and the reference strain. However *yen1Δ* or the WT do not have high levels of chromosome missegregation. 2) The overexpression of either Yen1 or Mms4 in a *mms4Δ yen1Δ* background rescue chromosome segregation and viability (Paper 2. Figure 3a). *In vitro* experiments have shown that Mms4-Mus81 as well as Yen1 are able to cut HR intermediates as well as replication-fork like structures (Gaillard et al. 2003; Ciccia et al. 2003). However it is highly unlikely that the improvement in chromosome segregation and viability upon overexpression are due to replication intermediates cleavage. In case of any of the two SSEs cutting a replication intermediate that maintain sister chromatids together a decrease in chromosome bridges would be expected but not an improvement in chromosome segregation (Fig 5.1). 3) As it was pointed out before, missegregation under unperturbed conditions in the *mms4Δ yen1Δ* mutant depends on homologous recombination since deletion of Rad52 improved chromosome segregation.

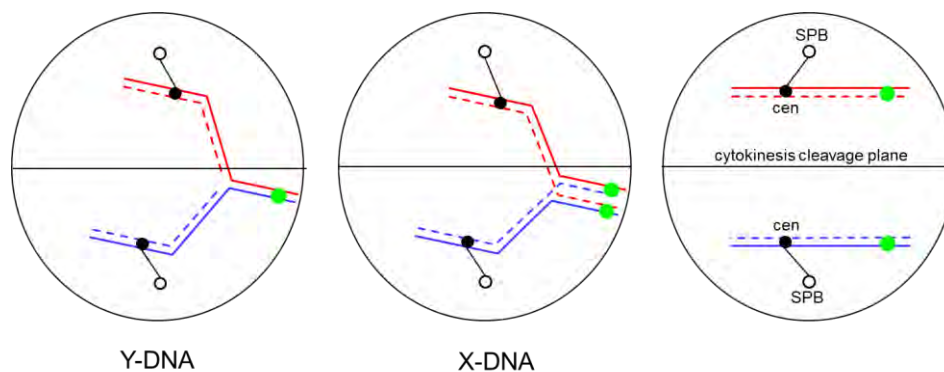


Figure 5.1: Schematic representing the potential substrates of Mms4 or Yen1 upon overexpression in telophase in a *mms4Δ yen1Δ* background. The only way to obtain correct chromosome segregation (the diagram on the right hand side) is if the structure maintaining sister chromatids together and precluding segregation is a HR intermediate (X-DNA) and not a replication intermediate (Y-DNA)

One explanation for the existence of the Y-signal can come from the small proportion of cells that are arrested in S/G2/M (<4%) even in unperturbed conditions i.e. without MMS. It is possible that some of these cells have not completed replication and are giving rise to the Y-signal. Alternatively it can also come from the cells with missegregated cXIIr (5-10%) that are visible even in unperturbed conditions in the reference strain. It is possible that these cells do not have complete replication at least within the rDNA that account for the observed missegregation. Interestingly the low levels of chromosome missegregation in the WT strain are not associated to DAPI visible bridges. This observation open the possibility of this missegregated chromatids to be connected by replication intermediates that lead to the formation of bridges not detectable by classical DNA dyes. Bridges formed by regions of non-replicated DNA that cannot be stained with classical DNA dyes have been reported before and called UFBs. (Ying et al. 2013; Naim et al. 2013). Coincidentally, the rDNA has the characteristics to be a slow replication zone due to the presence of the RFB and its highly repetitive nature (Lambert et al. 2005). Importantly, multiple studies have linked slow replication zones in the genome with formation of UFBs and chromosome instability resulting in neurological disorders and cancer (Lemoine et al. 2005; Lambert et al. 2005; Debacker & Kooy 2007; Ying et al. 2013; Naim et al. 2013). It would be of great interest to study more deeply the nature and the origin of the Y-signal in a WT strain in unperturbed conditions and its possible relation with the rDNA being a slow replication zone that can lead to UFBs.

In our model we used MMS to increase the usage of HR. The treatment of the double mutant *mms4Δ yen1Δ* with low doses of MMS (0.004% (v/v)) increased missegregation of cXIIr to levels of 70-80% and DAPI visible bridges to 20% (Paper 2. Figure 1a). Generally all those cells that had DAPI visible bridges also showed cXIIr missegregated. We tested if the missegregation status and DAPI chromosome bridges in the double mutant were reversible upon overexpression of Mms4 or Yen1. Interestingly we observed that the missegregation of cXIIr and DAPI bridges were enormously improved upon overexpression of Mms4 dropping to 10% and 1% respectively. Also overexpression of Yen1 made cXIIr missegregation and DAPI visible bridges drop to 20% and 10% respectively (Paper 2. Figure 3a). This result indicates three things: 1) Yen1 and Mms4 are active upon over expression in late mitosis, and are able to recognise the linkages that maintain the sister chromatids together and resolve them (discussed in the next section). 2) As stated before, the improvement in the segregation strongly indicates that the observed missegregation was due to recombination intermediates and not to broken DNA molecules or replication intermediates. The resolution of the linkages by these two SSEs and the pulling forces applied from the SPB are sufficient to improve segregation to levels similar to the reference strain. 3) More importantly, the enormous drop in chromosome missegregation (from 80% to 10% upon induction of Mms4) and the concomitant drop in DAPI visible bridges (from 40% to 1%) indicates that at least 30% of the missegregated cXIIr were forming a

bridge between the two daughter nuclei but were not visible by DAPI staining, a characteristic that allows to define them as an UFBs. UFBs have been detected before indirectly by tagging with fluorescent proteins or immunostaining of the helicase Sgs1 (the yeast homolog of the vertebrate BLM), Dpb11 (the yeast homolog of the vertebrate TopBP1) or the helicase PICH or more directly by incorporation of the nucleoside analogue 5-ethynyl-2'-deoxyuridine in the DNA during replication and subsequent immunostaining (Chan et al. 2007; Germann et al. 2014). With our model based in the use of tagged chromosomes with the system *tetO/tetR* in a *cdc15-2* background we describe a novel way to infer the presence of UFBs. Detection of UFBs with our model can be a good complement to indirect detection by immunofluorescence or tagging with fluorescent proteins since it allows to know the segregation output of the disappearing UFBs upon mitosis exit.

It has been shown that immunofluorescence or fluorescent tagging of Sgs1 (BLM), Dpb11 (TopBP1) or PICH can indirectly detect the presence of UFBs formed by catenations or replication intermediates but not HR intermediates (Chan et al. 2007; Baumann et al. 2007; Chan et al. 2009; Germann et al. 2014). However in our case we infer the presence of UFBs by different means. We test the improvement of cXIIr segregation in telophase cells to unveil the presence of UFBs not detected by DAPI staining. By using this approach we show that HR intermediates can also form UFBs. Importantly, these data point to the possibility of the existence of UFBs of a different nature that bind different proteins in order to be resolved. It would be of great interest to test the presence of the aforementioned proteins in the UFBs observed in our model to better characterize them. Also Mms4 and Yen1 are good candidates to test since they are able to resolve UFBs formed by HR intermediates, specially Yen1 considering that it forms foci preferentially in the space between two splitting nuclei in anaphase (Paper 3. Figure 2c).

5.3 Mms4 and Yen1 are able to resolve homologous recombination intermediates comprised by noncanonical Holliday junctions

The double mutant *mms4Δ yen1Δ* growing under unperturbed conditions accumulates HR intermediates that lead to the formation of chromosome bridges. This condition is worsened upon mild replication stress with MMS. Presumably and according to the conclusion from paper 1 and previous studies, the chromosome bridges will be severed during cytokinesis leading to the formation of DSBs (Ho et al. 2010; Cuylen et al. 2013). Accordingly the *mms4Δ yen1Δ* mutant shows a delay in G2/M due to the detection of the DNA damage, and a drop in viability to 60% compared to the reference strain (Paper 2. Figure 1a) (Ho et al. 2010; Blanco et al. 2010). Again, these phenotypes are worsened under low concentration of MMS leading to a drop in viability

to 1% compared to the reference strain. Surprisingly overexpression of either Yen1 or Mms4 in the *mms4Δ yen1Δ* mutant arrested in telophase reverts these phenotypes and improves chromosome segregation and viability at the same time that X-shaped DNA molecules detected by NN-2D DNA electrophoresis disappear (Paper 2. Figure 3 and 4c). This indicates that both SSEs are able to recognize and efficiently resolve the HJ-like structures that maintain the sister chromatids together.

Our data and many of the phenotypes that have been already described for *mms4Δ* mutants imply that Mus81-Mms4 is important for HJs resolution. However this appears to contradict the low activity of this complex on iHJs *in vitro*. To reconcile the apparent discrepancies between the *in vivo* and *in vitro* results two hypothesis have been proposed. The first one proposes that Mus81 may need to be activated to resolve iHJs. The activation would be a post-translational modification produced in some stage of the cell cycle or under DNA damage conditions. However at least Mus81-Mms4 purified from *S. cerevisiae* after DNA damage did not show apparent increase of iHJs cleavage *in vitro* (Ehmsen & Heyer 2008). Alternatively it has been suggested that an accessory protein could modulate substrate specificity, but no candidate has been identified yet genetically or biochemically (Schwartz & Heyer 2011). The second hypothesis proposes that the nHJs are the actual substrate of Mms4-Mus81. The nHJ would appear from the initial strand invasion event that precede the formation of a joint molecule or from the migration of an iHJ to a nick in the DNA molecule. Alternatively, the first nick might be introduced by another endonuclease, thus generating a substrate for Mms4-Mus81 (Wyatt & West 2014).

We characterized more in depth the physical nature of the X-shape molecules that appear in the NN-2D electrophoresis in the double mutant *mms4Δ yen1Δ* by NNA-3D DNA electrophoresis. With this technique we concluded that the HR intermediates accumulated in this mutant during anaphase are mostly nHJs or gapped HJs with a nick or a gap next to the junction. This result is consistent with the hypothesis of nHJs being the actual substrate of Mms4-Mus81 *in vivo*. However how nHJs are originated is not well known. Supporting the idea of another endonuclease introducing the first nick, in higher eukaryotes it has been found that the complex MUS81-EME1 and SLX1-SLX4 interact at the onset of mitosis thorough a CDK-dependent phosphorylation. *In vitro* this holoenzyme is able to cut iHJs more efficiently than any of the two components alone. The HJ resolution proceeds by a coordinated nick and counter-nick mechanism, the first nick is mediated by SLX1 and the second nick is introduced by MUS81 (Wyatt et al. 2013). A similar complex formed by Slx1-Slx4, Rtt107 and Dpb11 has been identified in budding yeast (Ohouo et al. 2010). The prediction is that if Slx1 is responsible of creating the first nick in a iHJ to then resolve the resulting nHJ by Mms4-Mus81, the double mutant *slx1Δ yen1Δ* could have a similar phenotype than the *mms4Δ yen1Δ* mutant. The *slx1Δ yen1Δ* mutant would accumulate iHJs that cannot be resolved by Mms4-Mus81. However we did not observe any decrease in viability or missegregation

in the *slx1Δ yen1Δ* mutant, indicating that in budding yeast Slx1 does not have a role in transforming iHJs to nHJs providing the right substrate to Mus81-Mms4 (Paper 2. Figure Supp.5b). Accordingly, another report has shown that in budding yeast the activity of Mus81-Mms4 forming part of the complex Slx4-Dpb11 towards iHJs does not change compared to the one that is not part of the complex (Gritenaite et al. 2014). More research is needed in order to elucidate the origin of nHJs in the DNA recombination intermediates metabolism. The power of the NNA-3D DNA electrophoresis to differentiate the physical nature of the different recombination intermediates in combination with different mutants for the DNA repair pathway can provide us enlightening information about the formation of the nHJs *in vivo*.

Similarly to Mms4, the overexpression of Yen1 in the *mms4Δ yen1Δ* mutant, is also able to improve chromosome segregation and viability with a concomitant drop of the signal of X-shaped DNA molecules. However, Yen1 has been shown to cut iHJs with high efficiency *in vitro* but its activity on nHJs or HJs with a gap had not been tested (Ip et al. 2008). From this data we speculated that either nHJs and/or gap HJs are an *in vivo* substrate of Yen1 or alternatively the cell can be able to change nHJs to iHJs upon overexpression of Yen1, in order to be resolved by Yen1. In agreement with the first hypothesis a recent report has shown that Yen1 is even more active on nHJs than on iHJs *in vitro* (Blanco et al. 2014).

Despite the overexpression of either Mms4 or Yen1 is able to improve viability and chromosome segregation, they do it with different efficiencies. Overexpression of Mms4 resolves chromosome bridges significantly faster than overexpression of Yen1, and after 3 hours of Yen1 overexpression the levels of missegregation are still higher compared to Mms4 counterpart. Furthermore, this differences in missegregation correlate with a lower viability after overexpressing Yen1 compared to Mms4 (Paper 2. Figure 3). We consider two possibilities to explain these differences: 1) Overexpression efficiency is different for both proteins. 2) Mus81-Mms4 has a higher affinity for nHJs or HJs with a gap than Yen1. This would explain why upon overexpression of Mms4 the bridges are resolved faster.

5.4 Cdc14 targets Yen1 to the nucleus in early anaphase

Yen1 location and activity is tightly regulated along the cell cycle. In contrast to Mus81-Mms4 it is inhibited by phosphorylation events that take place during G1/S transition and activated by dephosphorylation in anaphase. Phosphorylation of Yen1 introduces two layers of regulation, determining its localization and catalytic activity (García-Luis et al. 2014; Blanco et al. 2014; Eissler et al. 2014). During G1, when the CDK activity is low, Yen1 is dephosphorylated and is localized to the nucleus (Kosugi et al. 2009). In the G1/S transition Yen1 is phosphorylated by Cdc28-Clb5 in a highly

specific manner producing its exclusion from the nucleus and its biochemical inactivation (Ubersax et al. 2003; Loog & Morgan 2005; Eissler et al. 2014; Blanco et al. 2014). Yen1 has 9 CDK consensus sites. Phosphorylation of the residues localized to the C-terminal region avoid the import to the nucleus by masking its nuclear localization signal. On the other hand phosphorylation of the residues localized in the central region of the primary structure of the protein inhibits its biochemical activity, most likely by reducing its DNA binding affinity (Eissler et al. 2014; Blanco et al. 2014). In anaphase, at the time that chromosome segregation is started, the first wave of Cdc14 released from the nucleolus through the FEAR pathway, dephosphorylates Yen1, allowing its nuclear import and making it biochemically active (Stegmeier & Amon 2004; García-Luis et al. 2014; Blanco et al. 2014; Eissler et al. 2014). Intriguingly the activation of Yen1 by Cdc14 released through the FEAR network points out that this first wave of Cdc14 should not be exclusively nuclear as generally assumed. It necessarily has to reach the cytoplasm in order to dephosphorylate Yen1 and allow its import to the nucleus and catalytic activation.

Cdc14 has a really well characterized role in chromosome segregation during anaphase (Stegmeier & Amon 2004). It is tempting to speculate that the chromosome segregation problem observed in *cdc14-1* mutants at the restrictive temperature can be partially explained by the inability of these mutants to activate Yen1 and hence not eliminating any remaining recombination intermediate (Quevedo et al. 2012). However this possibility is very unlikely since in the PFGE gels of *cdc14-1* arrested cells the chromosomes are able to enter in the gel as in a wild type strain, indicating that the physical linkages between chromatids are not replication or recombination intermediates (Paper 3. Figure 4a). Besides this, *cdc14-1* has much more anaphase bridges than *cdc15-2 yen1Δ*.

5.5 Yen1 acts as a last resource backup of Mus81-Mms4 resolving joint molecules

Mus81-Mms4 and Yen1 act in consecutive and temporarily separable waves of HJs processing with Yen1 acting as a last resource endonuclease to deal with any remaining HJ that might compromise chromosome segregation. Scheduled activation of Yen1 in the cell cycle is crucial. A phosphorylation mutant of Yen1, constitutively active along the cell cycle has been studied. Strains carrying this mutant version of Yen1 appear to be more sensitive to DNA damaging agents such as MMS and show increased CO formation (Blanco et al. 2014). These data underscore the importance of restricting the activity of Yen1 to the last stages of mitosis but it still keeps open the question of why it is not active at the same time than Mus81-Mms4 in order to have more time to remove any recombination intermediate. It has been shown that Mms4-Mus81 contributes to replication fork restart by cleaving the fork (Hanada et al. 2007).

It is possible that the small window between the activation of Mus81-Mms4 and Yen1 is enough for the cell to repair and restart replication forks and finish recalcitrant replication in the presence of the Mus81-Mms4, potentially forming part of the complex Slx1-Slx4-Dpb11-Rtt107. In this small window of time the cell would avoid the activity of Yen1 over replication structures that can give rise to irreparable toxic products.

6 Conclusions

1. Cells arrested in a *cdc15-2* telophase block segregate correctly all their chromosomes. Including the cXII, the longest and most segregation-challenging chromosome arm in the yeast genome.
2. The combined deletion of *MMS4* and *YEN1* causes spontaneous anaphase chromatin bridges in 10% of the telophase arrested cells. Upon mild replication stress chromatin bridges increase to 20% of the telophase arrested cells.
3. The combined deletion of *MMS4* and *YEN1* causes spontaneous missegregation of cXII in 20% of the telophase arrested cells. Upon mild replication stress anaphase missegregation increase to 80% of the telophase arrested cells.
4. The combined deletion of *MMS4* and *YEN1* changes neither the timing of the S-phase nor the timing of anaphase onset.
5. The observed missegregation of cXII and formation of anaphase bridges are Rad52-dependent.
6. Mms4 and Yen1 compensate one another in resolving cXII and cIV sister chromatids DNA-DNA linkages in ongoing DNA damage. In a *mms4Δ yen1Δ* mutant arrested in a *cdc15-2* block, reactivation of either Mms4 or Yen1 reverts DAPI-stained anaphase bridges, missegregation of cXII, DNA-DNA linkages and restores viability of the progeny
7. The *mms4Δ yen1Δ* mutant accumulate DNA-DNA linkages comprised mainly by Holliday junctions with a discontinuity at the junction
8. Recombination intermediates can lead to the formation of UFBs. At least 30% of the *mms4Δ yen1Δ* mutant cells arrested in a *cdc15-2* block have cXII UFBs not detected by DAPI staining
9. Cdc14 released by the FEAR network targets Yen1 to the nucleus.

7 Literature cited

- Abraham J, Lemmers B, Hande MP, Moynahan ME, Chahwan C, Ciccio A, Essers J, Hanada K, Chahwan R, Khaw AK, McPherson P, Shehabeldin A, Laister R, Arrowsmith C, Kanaar R, West SC, Jasin M & Hakem R (2003) Eme1 is involved in DNA damage processing and maintenance of genomic stability in mammalian cells. *EMBO J.* 22, 6137–47.
- Abràmoff MD, Magalhães PJ & Ram SJ (2004) Image processing with ImageJ. *Biophotonics Int.* 11, 36–42.
- Agmon N, Yovel M, Harari Y, Liefshitz B & Kupiec M (2011) The role of Holliday junction resolvases in the repair of spontaneous and induced DNA damage. *Nucleic Acids Res.* 39, 7009–19.
- Aguilera A & Gómez-González B (2008) Genome instability: a mechanistic view of its causes and consequences. *Nat. Rev. Genet.* 9, 204–17.
- Ashton TM, Mankouri HW, Heidenblut A, McHugh PJ & Hickson ID (2011) Pathways for Holliday junction processing during homologous recombination in *Saccharomyces cerevisiae*. *Mol. Cell. Biol.* 31, 1921–33.
- Atkinson J & McGlynn P (2009) Replication fork reversal and the maintenance of genome stability. *Nucleic Acids Res.* 37, 3475–92.
- Azzam R, Chen SL, Shou W, Mah AS, Alexandru G, Nasmyth K, Annan RS, Carr SA & Deshaies RJ (2004) Phosphorylation by cyclin B-Cdk underlies release of mitotic exit activator Cdc14 from the nucleolus. *Science* 305, 516–9.
- Bakhoun SF & Compton DA (2012) Chromosomal instability and cancer: a complex relationship with therapeutic potential. *J. Clin. Invest.* 122, 1138–43.
- Baumann C, Körner R, Hofmann K & Nigg EA (2007) PICH, a centromere-associated SNF2 family ATPase, is regulated by Plk1 and required for the spindle checkpoint. *Cell* 128, 101–14.
- Baxter J (2015) “Breaking Up Is Hard to Do”: The Formation and Resolution of Sister Chromatid Intertwines. *J. Mol. Biol.* 427, 590–607.
- Baxter J & Aragón L (2010) Physical linkages between sister chromatids and their removal during yeast chromosome segregation. *Cold Spring Harb. Symp. Quant. Biol.* 75, 389–94.
- Baxter J & Diffley JFX (2008a) Topoisomerase II inactivation prevents the completion of DNA replication in budding yeast. *Mol. Cell* 30, 790–802.
- Baxter J & Diffley JFX (2008b) Topoisomerase II inactivation prevents the completion of DNA replication in budding yeast. *Mol. Cell* 30, 790–802.

- Bellaoui M, Chang M, Ou J, Xu H, Boone C & Brown GW (2003) Elg1 forms an alternative RFC complex important for DNA replication and genome integrity. *EMBO J.* 22, 4304–13.
- Berdichevsky A, Izhar L & Livneh Z (2002) Error-free recombinational repair predominates over mutagenic translesion replication in *E. coli*. *Mol. Cell* 10, 917–24.
- Bhalla N (2002) Mutation of YCS4, a Budding Yeast Condensin Subunit, Affects Mitotic and Nonmitotic Chromosome Behavior. *Mol. Biol. Cell* 13, 632–645.
- Bizard AH & Hickson ID (2014) The dissolution of double Holliday junctions. *Cold Spring Harb. Perspect. Biol.* 6.
- Blanco MG & Matos J (2015) Hold your horSSEs: controlling structure-selective endonucleases MUS81 and Yen1/GEN1. *Front. Genet.* 6, 253.
- Blanco MG, Matos J, Rass U, Ip SCY & West SC (2010) Functional overlap between the structure-specific nucleases Yen1 and Mus81-Mms4 for DNA-damage repair in *S. cerevisiae*. *DNA Repair (Amst)*. 9, 394–402.
- Blanco MG, Matos J & West SC (2014) Dual control of Yen1 nuclease activity and cellular localization by Cdk and Cdc14 prevents genome instability. *Mol. Cell* 54, 94–106.
- Boddy MN, Gaillard P-HL, McDonald WH, Shanahan P, Yates JR & Russell P (2001) Mus81-Eme1 Are Essential Components of a Holliday Junction Resolvase. *Cell* 107, 537–548.
- Boddy MN, Lopez-Girona A, Shanahan P, Interthal H, Heyer W-D & Russell P (2000) Damage Tolerance Protein Mus81 Associates with the FHA1 Domain of Checkpoint Kinase Cds1. *Mol. Cell. Biol.* 20, 8758–8766.
- Bosco G & Haber JE (1998) Chromosome break-induced DNA replication leads to nonreciprocal translocations and telomere capture. *Genetics* 150, 1037–47.
- Brewer BJ & Fangman WL (1988) A replication fork barrier at the 3' end of yeast ribosomal RNA genes. *Cell* 55, 637–43.
- Britt AB (2004) Repair of DNA Damage Induced by Solar UV. *Photosynth. Res.* 81, 105–112.
- Bugreev D V, Rossi MJ & Mazin A V (2011) Cooperation of RAD51 and RAD54 in regression of a model replication fork. *Nucleic Acids Res.* 39, 2153–64.
- Bzymek M, Thayer NH, Oh SD, Kleckner N & Hunter N (2010) Double Holliday junctions are intermediates of DNA break repair. *Nature* 464, 937–41.

- Champoux JJ & Been MD (1980) *Mechanistic Studies of DNA Replication and Genetic Recombination*,
- Chan KL & Hickson ID (2009) On the origins of ultra-fine anaphase bridges. *Cell Cycle* 8, 3065–6.
- Chan K-L, North PS & Hickson ID (2007) BLM is required for faithful chromosome segregation and its localization defines a class of ultrafine anaphase bridges. *EMBO J.* 26, 3397–409.
- Chan KL, Palmai-Pallag T, Ying S & Hickson ID (2009) Replication stress induces sister-chromatid bridging at fragile site loci in mitosis. *Nat. Cell Biol.* 11, 753–60.
- Chang JH, Kim JJ, Choi JM, Lee JH & Cho Y (2008) Crystal structure of the Mus81-Eme1 complex. *Genes Dev.* 22, 1093–106.
- Chen XB, Melchionna R, Denis CM, Gaillard PH, Blasina A, Van de Weyer I, Boddy MN, Russell P, Vialard J & McGowan CH (2001) Human Mus81-associated endonuclease cleaves Holliday junctions in vitro. *Mol. Cell* 8, 1117–27.
- Cherry JM, Hong EL, Amundsen C, Balakrishnan R, Binkley G, Chan ET, Christie KR, Costanzo MC, Dwight SS, Engel SR, Fisk DG, Hirschman JE, Hitz BC, Karra K, Krieger CJ, Miyasato SR, Nash RS, Park J, Skrzypek MS, Simison M, Weng S & Wong ED (2012) Saccharomyces Genome Database: the genomics resource of budding yeast. *Nucleic Acids Res.* 40, D700–5.
- Chu G, Vollrath D & Davis RW (1986) Separation of large DNA molecules by contour-clamped homogeneous electric fields. *Science* 234, 1582–5.
- Ciccia A, Constantinou A & West SC (2003) Identification and characterization of the human mus81-eme1 endonuclease. *J. Biol. Chem.* 278, 25172–8.
- Ciccia A, McDonald N & West SC (2008) Structural and functional relationships of the XPF/MUS81 family of proteins. *Annu. Rev. Biochem.* 77, 259–87.
- Clemente-Blanco A, Mayán-Santos M, Schneider D & F (2009) Cdc14 inhibits transcription by RNA polymerase I during anaphase. *Nature*.
- Clemente-Blanco A, Sen N, Mayan-Santos M, Sacristán MP, Graham B, Jarmuz A, Giess A, Webb E, Game L, Eick D, Bueno A, Merckenschlager M & Aragón L (2011) Cdc14 phosphatase promotes segregation of telomeres through repression of RNA polymerase II transcription. *Nat. Cell Biol.* 13, 1450–6.
- Cohen-Fix O, Peters J & Kirschner M (1996) Anaphase initiation in *Saccharomyces cerevisiae* is controlled by the APC-dependent degradation of the anaphase inhibitor Pds1p. *Genes &*, 3081–3093.

- Colnaghi R, Carpenter G, Volker M & O'Driscoll M (2011) The consequences of structural genomic alterations in humans: genomic disorders, genomic instability and cancer. *Semin. Cell Dev. Biol.* 22, 875–85.
- Constantinou A, Chen X, McGowan CH & West SC (2002) Holliday junction resolution in human cells : two junction endonucleases with distinct substrate speci ® cities. 21.
- Cuylen S, Metz J, Hruby A & Haering CH (2013) Entrapment of chromosomes by condensin rings prevents their breakage during cytokinesis. *Dev. Cell* 27, 469–78.
- Cybulski KE & Howlett NG (2011) FANCP/SLX4: a Swiss army knife of DNA interstrand crosslink repair. *Cell Cycle* 10, 1757–63.
- D'Amours D & Amon A (2004) At the interface between signaling and executing anaphase--Cdc14 and the FEAR network. *Genes Dev.* 18, 2581–95.
- D'Amours D, Stegmeier F & Amon A (2004) Cdc14 and condensin control the dissolution of cohesin-independent chromosome linkages at repeated DNA. *Cell* 117, 455–69.
- Davis AP & Symington LS (2004) RAD51-dependent break-induced replication in yeast. *Mol. Cell. Biol.* 24, 2344–51.
- Debacker K & Kooy RF (2007) Fragile sites and human disease. *Hum. Mol. Genet.* 16 Spec No, R150–8.
- Dehé P-M, Coulon S, Scaglione S, Shanahan P, Takedachi A, Wohlschlegel JA, Yates JR, Llorente B, Russell P & Gaillard P-HL (2013) Regulation of Mus81-Eme1 Holliday junction resolvase in response to DNA damage. *Nat. Struct. Mol. Biol.* 20, 598–603.
- Dendouga N, Gao H, Moechars D, Janicot M, Vialard J & McGowan CH (2005) Disruption of murine Mus81 increases genomic instability and DNA damage sensitivity but does not promote tumorigenesis. *Mol. Cell. Biol.* 25, 7569–79.
- Doe CL, Ahn JS, Dixon J & Whitby MC (2002) Mus81-Eme1 and Rqh1 involvement in processing stalled and collapsed replication forks. *J. Biol. Chem.* 277, 32753–9.
- Domínguez-Kelly R, Martín Y, Koundrioukoff S, Tanenbaum ME, Smits VAJ, Medema RH, Debatisse M & Freire R (2011) Wee1 controls genomic stability during replication by regulating the Mus81-Eme1 endonuclease. *J. Cell Biol.* 194, 567–79.
- Ehmsen KT & Heyer W-D (2008) *Saccharomyces cerevisiae* Mus81-Mms4 is a catalytic, DNA structure-selective endonuclease. *Nucleic Acids Res.* 36, 2182–95.

- Eissler CL, Mazón G, Powers BL, Savinov SN, Symington LS & Hall MC (2014) The Cdk/cDc14 module controls activation of the Yen1 holliday junction resolvase to promote genome stability. *Mol. Cell* 54, 80–93.
- Elborough KM & West SC (1990) Resolution of synthetic Holliday junctions in DNA by an endonuclease activity from calf thymus. *EMBO J.* 9, 2931–6.
- Fabre F, Chan A, Heyer W-D & Gangloff S (2002) Alternate pathways involving Sgs1/Top3, Mus81/ Mms4, and Srs2 prevent formation of toxic recombination intermediates from single-stranded gaps created by DNA replication. *Proc. Natl. Acad. Sci. U. S. A.* 99, 16887–92.
- Ferguson DO & Holloman WK (1996) Recombinational repair of gaps in DNA is asymmetric in *Ustilago maydis* and can be explained by a migrating D-loop model. *Proc. Natl. Acad. Sci. U. S. A.* 93, 5419–24.
- Frank-Vaillant M & Marcand S (2001) NHEJ regulation by mating type is exercised through a novel protein, Lif2p, essential to the ligase IV pathway. *Genes Dev.* 15, 3005–12.
- Freeman L, Aragon-Alcaide L & Strunnikov A (2000) The condensin complex governs chromosome condensation and mitotic transmission of rDNA. *J. Cell Biol.* 149, 811–24.
- Fricke WM & Brill SJ (2003) Slx1-Slx4 is a second structure-specific endonuclease functionally redundant with Sgs1-Top3. *Genes Dev.* 17, 1768–78.
- Friedman KL & Brewer BJ (1995) *DNA Replication*,
- Fu Y & Xiao W (2003) Functional domains required for the *Saccharomyces cerevisiae* Mus81-Mms4 endonuclease complex formation and nuclear localization. *DNA Repair (Amst)*. 2, 1435–47.
- Gaillard P-HL, Noguchi E, Shanahan P & Russell P (2003) The endogenous Mus81-Eme1 complex resolves Holliday junctions by a nick and counternick mechanism. *Mol. Cell* 12, 747–59.
- Gallo-Fernández M, Saugar I, Ortiz-Bazán MÁ, Vázquez MV & Tercero JA (2012) Cell cycle-dependent regulation of the nuclease activity of Mus81-Eme1/Mms4. *Nucleic Acids Res.*, 1–11.
- Gao H (2003) Mus81 Endonuclease Localizes to Nucleoli and to Regions of DNA Damage in Human S-phase Cells. *Mol. Biol. Cell* 14, 4826–4834.
- García-Luis J, Clemente-Blanco A, Aragón L & Machín F (2014) Cdc14 targets the Holliday junction resolvase Yen1 to the nucleus in early anaphase. *Cell Cycle* 13, 1392–9.

- García-Luis J & Machín F (2014) Mus81-Mms4 and Yen1 resolve a novel anaphase bridge formed by noncanonical Holliday junctions. *Nat. Commun.* 5, 5652.
- Gari K, Décaillet C, Stasiak AZ, Stasiak A & Constantinou A (2008) The Fanconi anemia protein FANCM can promote branch migration of Holliday junctions and replication forks. *Mol. Cell* 29, 141–8.
- Gaur V, Wyatt HDM, Komorowska W, Szczepanowski RH, de Sanctis D, Gorecka KM, West SC & Nowotny M (2015) Structural and Mechanistic Analysis of the Slx1-Slx4 Endonuclease. *Cell Rep.* 10, 1467–1476.
- Germann SM, Oestergaard VH, Haas C, Salis P, Motegi A & Lisby M (2011) Dpb11/TopBP1 plays distinct roles in DNA replication, checkpoint response and homologous recombination. *DNA Repair (Amst).* 10, 210–24.
- Germann SM, Schramke V, Pedersen RT, Gallina I, Eckert-Boulet N, Oestergaard VH & Lisby M (2014) TopBP1/Dpb11 binds DNA anaphase bridges to prevent genome instability. *J. Cell Biol.* 204, 45–59.
- Gerson SL (2004) MGMT: its role in cancer aetiology and cancer therapeutics. *Nat. Rev. Cancer* 4, 296–307.
- Gisselsson D (2003) Chromosome instability in cancer: how, when, and why? *Adv. Cancer Res.* 87, 1–29.
- Gottlieb S & Esposito RE (1989) A new role for a yeast transcriptional silencer gene, SIR2, in regulation of recombination in ribosomal DNA. *Cell* 56, 771–6.
- Gravel S, Chapman JR, Magill C & Jackson SP (2008) DNA helicases Sgs1 and BLM promote DNA double-strand break resection. *Genes Dev.* 22, 2767–72.
- Gritenaite D, Princz LN, Szakal B, Bantele SCS, Wendeler L, Schilbach S, Habermann BH, Matos J, Lisby M, Branzei D & Pfander B (2014) A cell cycle-regulated Slx4-Dpb11 complex promotes the resolution of DNA repair intermediates linked to stalled replication. *Genes Dev.* 28, 1604–19.
- Gruber S, Haering CH & Nasmyth K (2003) Chromosomal cohesin forms a ring. *Cell* 112, 765–77.
- Guacci V, Koshland D & Strunnikov A (1997) A direct link between sister chromatid cohesion and chromosome condensation revealed through the analysis of MCD1 in *S. cerevisiae*. *Cell* 91, 47–57.
- Haber JE, Ira G, Malkova A & Sugawara N (2004) Repairing a double-strand chromosome break by homologous recombination: revisiting Robin Holliday's model. *Philos. Trans. R. Soc. Lond. B. Biol. Sci.* 359, 79–86.

- Haering CH, Löwe J, Hochwagen A & Nasmyth K (2002) Molecular architecture of SMC proteins and the yeast cohesin complex. *Mol. Cell* 9, 773–88.
- Hakem R (2008) DNA-damage repair; the good, the bad, and the ugly. *EMBO J.* 27, 589–605.
- Hanada K, Budzowska M, Davies SL, van Drunen E, Onizawa H, Beverloo HB, Maas A, Essers J, Hickson ID & Kanaar R (2007) The structure-specific endonuclease Mus81 contributes to replication restart by generating double-strand DNA breaks. *Nat. Struct. Mol. Biol.* 14, 1096–104.
- Hartwell LH (1974) *Saccharomyces cerevisiae* cell cycle. *Bacteriol. Rev.* 38, 164–98.
- Hartwell LH & Weinert TA (1989) Checkpoints: controls that ensure the order of cell cycle events. *Science* 246, 629–34.
- Hegde ML, Hazra TK & Mitra S (2010) Functions of disordered regions in mammalian early base excision repair proteins. *Cell. Mol. Life Sci.* 67, 3573–87.
- Heller RC & Marians KJ (2006) Replication fork reactivation downstream of a blocked nascent leading strand. *Nature* 439, 557–62.
- Heng HH, Bremer SW, Stevens JB, Horne SD, Liu G, Abdallah BY, Ye KJ & Ye CJ (2013) Chromosomal instability (CIN): what it is and why it is crucial to cancer evolution. *Cancer Metastasis Rev.* 32, 325–40.
- Heyer W-D, Li X, Rolfmeier M & Zhang X-P (2006) Rad54: the Swiss Army knife of homologous recombination? *Nucleic Acids Res.* 34, 4115–25.
- Hicks WM, Kim M & Haber JE (2010) Increased mutagenesis and unique mutation signature associated with mitotic gene conversion. *Science* 329, 82–5.
- Hicks WM, Yamaguchi M & Haber JE (2011) Real-time analysis of double-strand DNA break repair by homologous recombination. *Proc. Natl. Acad. Sci. U. S. A.* 108, 3108–15.
- Higuchi T & Uhlmann F (2005) Stabilization of microtubule dynamics at anaphase onset promotes chromosome segregation. *Nature* 433, 171–6.
- Hirano T (2000) Chromosome cohesion, condensation, and separation. *Annu. Rev. Biochem.* 69, 115–144.
- Hirano T (2005) Condensins: organizing and segregating the genome. *Curr. Biol.* 15, R265–75.
- Ho CK, Mazón G, Lam AF & Symington LS (2010) Mus81 and Yen1 promote reciprocal exchange during mitotic recombination to maintain genome integrity in budding yeast. *Mol. Cell* 40, 988–1000.

- Hoffelder DR, Luo L, Burke NA, Watkins SC, Gollin SM & Saunders WS (2004) Resolution of anaphase bridges in cancer cells. *Chromosoma* 112, 389–97.
- Holliday R (1964) A mechanism for gene conversion in fungi. *Genet. Res* 5, 282–304.
- Holm C, Goto T, Wang JC & Botstein D (1985) DNA topoisomerase II is required at the time of mitosis in yeast. *Cell* 41, 553–563.
- Holt LJ, Krutchinsky AN & Morgan DO (2008) Positive feedback sharpens the anaphase switch. *Nature* 454, 353–7.
- Huang J & Moazed D (2003) Association of the RENT complex with nontranscribed and coding regions of rDNA and a regional requirement for the replication fork block protein Fob1 in rDNA silencing. *Genes Dev.* 17, 2162–76.
- Huertas P, Cortés-Ledesma F, Sartori AA, Aguilera A & Jackson SP (2008) CDK targets Sae2 to control DNA-end resection and homologous recombination. *Nature* 455, 689–692.
- Interthal H & Heyer WD (2000) MUS81 encodes a novel helix-hairpin-helix protein involved in the response to UV- and methylation-induced DNA damage in *Saccharomyces cerevisiae*. *Mol. Gen. Genet.* 263, 812–27.
- Ip SCY, Rass U, Blanco MG, Flynn HR, Skehel JM & West SC (2008) Identification of Holliday junction resolvases from humans and yeast. 456.
- Ira G, Pelliccioli A, Balijja A, Wang X, Fiorani S, Carotenuto W, Liberi G, Bressan D, Wan L, Hollingsworth NM, Haber JE & Foiani M (2004) DNA end resection, homologous recombination and DNA damage checkpoint activation require CDK1. *Nature* 431, 1011–7.
- Iraqi I, Chekkal Y, Jmari N, Pietrobon V, Fréon K, Costes A & Lambert SAE (2012) Recovery of arrested replication forks by homologous recombination is error-prone. *PLoS Genet.* 8, e1002976.
- Ivanov D & Nasmyth K (2005) A topological interaction between cohesin rings and a circular minichromosome. *Cell* 122, 849–60.
- Jackson S (2002) Sensing and repairing DNA double-strand breaks. *Carcinogenesis*.
- Jain S, Sugawara N, Lydeard J, Vaze M, Tanguy Le Gac N & Haber JE (2009) A recombination execution checkpoint regulates the choice of homologous recombination pathway during DNA double-strand break repair. *Genes Dev.* 23, 291–303.
- Janke C, Magiera MM, Rathfelder N, Taxis C, Reber S, Maekawa H, Moreno-Borchart A, Doenges G, Schwob E, Schiebel E & others (2004) A versatile toolbox for

- PCR-based tagging of yeast genes: new fluorescent proteins, more markers and promoter substitution cassettes. *Yeast* 21, 947–962.
- Kaliraman V & Brill S (2002) Role of SGS1 and SLX4 in maintaining rDNA structure in *Saccharomyces cerevisiae*. *Curr. Genet.* 41, 389–400.
- Kaliraman V, Mullen JR, Fricke WM, Bastin-Shanower SA & Brill SJ (2001) Functional overlap between Sgs1-Top3 and the Mms4-Mus81 endonuclease. *Genes Dev.* 15, 2730–40.
- Karow JK, Constantinou A, Li JL, West SC & Hickson ID (2000) The Bloom's syndrome gene product promotes branch migration of holliday junctions. *Proc. Natl. Acad. Sci. U. S. A.* 97, 6504–8.
- Knop M, Siegers K, Pereira G, Zachariae W, Winsor B, Nasmyth K & Schiebel E (1999) Epitope tagging of yeast genes using a PCR-based strategy: more tags and improved practical routines. *Yeast* 15, 963–72.
- Kobayashi T (2003) The Replication Fork Barrier Site Forms a Unique Structure with Fob1p and Inhibits the Replication Fork. *Mol. Cell. Biol.* 23, 9178–9188.
- Kolodner R (1996) Biochemistry and genetics of eukaryotic mismatch repair. *Genes Dev.* 10, 1433–1442.
- Van Komen S, Petukhova G, Sigurdsson S, Stratton S & Sung P (2000) Superhelicity-Driven Homologous DNA Pairing by Yeast Recombination Factors Rad51 and Rad54. *Mol. Cell* 6, 563–572.
- Kosugi S, Hasebe M, Tomita M & Yanagawa H (2009) Systematic identification of cell cycle-dependent yeast nucleocytoplasmic shuttling proteins.
- Krokan HE & Bjørås M (2013) Base excision repair. *Cold Spring Harb. Perspect. Biol.* 5, a012583.
- Kuilman T, Maiolica A, Godfrey M, Scheidel N, Aebersold R & Uhlmann F (2015) Identification of Cdk targets that control cytokinesis. *EMBO J.* 34, 81–96.
- Lambert S, Watson A, Sheedy DM, Martin B & Carr AM (2005) Gross chromosomal rearrangements and elevated recombination at an inducible site-specific replication fork barrier. *Cell* 121, 689–702.
- Lavoie BD, Hogan E & Koshland D (2004) In vivo requirements for rDNA chromosome condensation reveal two cell-cycle-regulated pathways for mitotic chromosome folding. *Genes Dev.* 18, 76–87.
- Lavoie BD, Tuffo KM, Oh S, Koshland D & Holm C (2000) Mitotic chromosome condensation requires Brn1p, the yeast homologue of Barren. *Mol. Biol. Cell* 11, 1293–304.

- Lee SE, Pâques F, Sylvan J & Haber JE (1999) Role of yeast SIR genes and mating type in directing DNA double-strand breaks to homologous and non-homologous repair paths. *Curr. Biol.* 9, 767–70.
- Lemoine FJ, Degtyareva NP, Lobachev K & Petes TD (2005) Chromosomal translocations in yeast induced by low levels of DNA polymerase a model for chromosome fragile sites. *Cell* 120, 587–98.
- León-Ortiz AM, Svendsen J & Boulton SJ (2014) Metabolism of DNA secondary structures at the eukaryotic replication fork. *DNA Repair (Amst)*. 19, 152–62.
- Li X, Stith CM, Burgers PM & Heyer W-D (2009) PCNA is required for initiation of recombination-associated DNA synthesis by DNA polymerase delta. *Mol. Cell* 36, 704–13.
- Lieber MR (1999) The biochemistry and biological significance of nonhomologous DNA end joining: an essential repair process in multicellular eukaryotes. *Genes Cells* 4, 77–85.
- Lieber MR (2008) The mechanism of human nonhomologous DNA end joining. *J. Biol. Chem.* 283, 1–5.
- Linskens MH & Huberman JA (1988) Organization of replication of ribosomal DNA in *Saccharomyces cerevisiae*. *Mol. Cell. Biol.* 8, 4927–35.
- Loog M & Morgan DO (2005) Cyclin specificity in the phosphorylation of cyclin-dependent kinase substrates. *Nature* 434.
- Lopes M, Foiani M & Sogo JM (2006) Multiple mechanisms control chromosome integrity after replication fork uncoupling and restart at irreparable UV lesions. *Mol. Cell* 21, 15–27.
- De los Santos T, Loidl J, Larkin B & Hollingsworth NM (2001) A Role for MMS4 in the Processing of Recombination Intermediates During Meiosis in *Saccharomyces cerevisiae*. *Genetics* 159, 1511–1525.
- Lucas I & Hyrien O (2000) Hemicatenanes form upon inhibition of DNA replication. *Nucleic Acids Res.* 28, 2187–93.
- Lydeard JR, Jain S, Yamaguchi M & Haber JE (2007) Break-induced replication and telomerase-independent telomere maintenance require Pol32. *Nature* 448, 820–3.
- Machín F, Torres-Rosell J, Jarmuz A & Aragón L (2005) Spindle-independent condensation-mediated segregation of yeast ribosomal DNA in late anaphase. *J. Cell Biol.* 168, 209–19.

- Machín F, Torres-Rosell J, De Piccoli G, Carballo JA, Cha RS, Jarmuz A & Aragón L (2006) Transcription of ribosomal genes can cause nondisjunction. *J. Cell Biol.* 173, 893–903.
- Malkova A, Naylor ML, Yamaguchi M, Ira G & Haber JE (2005) RAD51-dependent break-induced replication differs in kinetics and checkpoint responses from RAD51-mediated gene conversion. *Mol. Cell. Biol.* 25, 933–44.
- Mankouri HW, Ashton TM & Hickson ID (2011) Holliday junction-containing DNA structures persist in cells lacking Sgs1 or Top3 following exposure to DNA damage. *Proc. Natl. Acad. Sci. U. S. A.* 108, 4944–9.
- Matos J, Blanco MG, Maslen S, Skehel JM & West SC (2011) Regulatory control of the resolution of DNA recombination intermediates during meiosis and mitosis. *Cell* 147, 158–72.
- Matos J, Blanco MG & West SC (2013) Cell-cycle kinases coordinate the resolution of recombination intermediates with chromosome segregation. *Cell Rep.* 4, 76–86.
- Matos J & West SC (2014) Holliday junction resolution: Regulation in space and time. *DNA Repair (Amst).*
- Mayle R, Campbell IM, Beck CR, Yu Y, Wilson M, Shaw CA, Bjergbaek L, Lupski JR & Ira G (2015) DNA REPAIR. Mus81 and converging forks limit the mutagenicity of replication fork breakage. *Science* 349, 742–7.
- McClintock B (1932) A Correlation of Ring-Shaped Chromosomes with Variegation in Zea Mays. *Proc. Natl. Acad. Sci. U. S. A.* 18, 677–81.
- McClintock B (1941) The Stability of Broken Ends of Chromosomes in Zea Mays. *Genetics* 26, 234–82.
- McEachern MJ & Haber JE (2006) Break-induced replication and recombinational telomere elongation in yeast. *Annu. Rev. Biochem.* 75, 111–35.
- McGlynn P & Lloyd RG (2002) Recombinational repair and restart of damaged replication forks. *Nat. Rev. Mol. Cell Biol.* 3, 859–70.
- Mehta A & Haber JE (2014) Sources of DNA double-strand breaks and models of recombinational DNA repair. *Cold Spring Harb. Perspect. Biol.* 6, a016428.
- Michaelis C, Ciosk R & Nasmyth K (1997) Cohesins: chromosomal proteins that prevent premature separation of sister chromatids. *Cell* 91, 35–45.
- Michel B, Flores MJ, Viguera E, Grompone G, Seigneur M & Bidnenko V (2001) Rescue of arrested replication forks by homologous recombination. *Proc. Natl. Acad. Sci. U. S. A.* 98, 8181–8.

- Mimitou EP & Symington LS (2008) Sae2, Exo1 and Sgs1 collaborate in DNA double-strand break processing. *Nature* 455, 770–4.
- Mishina Y, Duguid EM & He C (2006) Direct reversal of DNA alkylation damage. *Chem. Rev.* 106, 215–32.
- Montgomery E, Wilentz RE, Argani P, Fisher C, Hruban RH, Kern SE & Lengauer C (2002) Analysis of anaphase figures in routine histologic sections distinguishes chromosomally unstable from chromosomally stable malignancies. *Cancer Biol. Ther.* 2, 248–52.
- Morgan DO (2007) *The Cell Cycle: Principles of Control*,
- Mullen JR, Kaliraman V, Ibrahim SS & Brill SJ (2001) Requirement for three novel protein complexes in the absence of the Sgs1 DNA helicase in *Saccharomyces cerevisiae*. *Genetics* 157, 103–18.
- Muñoz-galván S, Tous C, Blanco MG & Schwartz EK (2012) Distinct roles of Mus81, Yen1, Slx1-Slx4 and Rad1 nucleases in the repair of replication-born double strand breaks by sister chromatid exchange. *Cancer Res.*
- Naim V, Wilhelm T, Debatisse M & Rosselli F (2013) ERCC1 and MUS81-EME1 promote sister chromatid separation by processing late replication intermediates at common fragile sites during mitosis. *Nat. Cell Biol.* 15, 1008–15.
- Nasmyth KA (1982) Molecular genetics of yeast mating type. *Annu. Rev. Genet.* 16, 439–500.
- Nassif N, Penney J, Pal S, Engels WR & Gloor GB (1994) Efficient copying of nonhomologous sequences from ectopic sites via P-element-induced gap repair. *Mol. Cell. Biol.* 14, 1613–25.
- Neelsen KJ & Lopes M (2015) Replication fork reversal in eukaryotes: from dead end to dynamic response. *Nat. Rev. Mol. Cell Biol.* 16, 207–220.
- Nitiss JL (2009) DNA topoisomerase II and its growing repertoire of biological functions. *Nat. Rev.* 9, 327–37.
- Noguchi E, Noguchi C, McDonald WH, Yates JR & Russell P (2004) Swi1 and Swi3 are components of a replication fork protection complex in fission yeast. *Mol. Cell. Biol.* 24, 8342–55.
- O’Neil NJ, Martin JS, Youds JL, Ward JD, Petalcorin MIR, Rose AM & Boulton SJ (2013) Joint molecule resolution requires the redundant activities of MUS-81 and XPF-1 during *Caenorhabditis elegans* meiosis. *PLoS Genet.* 9, e1003582.

- Ohouo PY, Bastos de Oliveira FM, Almeida BS & Smolka MB (2010) DNA damage signaling recruits the Rtt107-Slx4 scaffolds via Dpb11 to mediate replication stress response. *Mol. Cell* 39, 300–6.
- Ortiz-Bazán MÁ, Gallo-Fernández M, Saugar I, Jiménez-Martín A, Vázquez MV & Tercero JA (2014) Rad5 plays a major role in the cellular response to DNA damage during chromosome replication. *Cell Rep.* 9, 460–8.
- Osman F, Dixon J, Doe CL & Whitby MC (2003) Generating crossovers by resolution of nicked Holliday junctions: a role for Mus81-Eme1 in meiosis. *Mol. Cell* 12, 761–74.
- Osman F & Whitby MC (2007) Exploring the roles of Mus81-Eme1/Mms4 at perturbed replication forks. *DNA Repair (Amst)*. 6, 1004–17.
- Ouspenski II, Cabello OA & Brinkley BR (2000) Chromosome condensation factor Brn1p is required for chromatid separation in mitosis. *Mol. Biol. Cell* 11, 1305–13.
- Pâques F & Haber JE (1999) Multiple pathways of recombination induced by double-strand breaks in *Saccharomyces cerevisiae*. *Microbiol. Mol. Biol. Rev.* 63, 349–404.
- Paulovich AG, Toczyski DP & Hartwell LH (1997) When Checkpoints Fail. *Cell* 88, 315–321.
- Payne CM, Crowley-Skillicorn C, Bernstein C, Holubec H & Bernstein H (2011) Molecular and cellular pathways associated with chromosome 1p deletions during colon carcinogenesis. *Clin. Exp. Gastroenterol.* 4, 75–119.
- Peter BJ, Ullsperger C, Hiasa H, Marians KJ & Cozzarelli NR (1998) The Structure of Supercoiled Intermediates in DNA Replication. *Cell* 94, 819–827.
- Petes TD (1979) Yeast ribosomal DNA genes are located on chromosome XII. *Proc. Natl. Acad. Sci.* 76, 410–414.
- Pines J (2011) Cubism and the cell cycle: the many faces of the APC/C. *Nat. Rev. Mol. Cell Biol.* 12, 427–38.
- Princz LN, Gritenaite D & Pfander B (2015) The Slx4-Dpb11 scaffold complex: coordinating the response to replication fork stalling in S-phase and the subsequent mitosis. *Cell Cycle* 14, 488–94.
- Qi Z, Redding S, Lee JY, Gibb B, Kwon Y, Niu H, Gaines WA, Sung P & Greene EC (2015) DNA Sequence Alignment by Microhomology Sampling during Homologous Recombination. *Cell* 160, 856–869.
- Queralt E, Lehane C, Novak B & Uhlmann F (2006) Downregulation of PP2A(Cdc55) phosphatase by separase initiates mitotic exit in budding yeast. *Cell* 125, 719–32.

- Quevedo O, García-Luis J, Matos-Perdomo E, Aragón L & Machín F (2012) Nondisjunction of a single chromosome leads to breakage and activation of DNA damage checkpoint in G2. *PLoS Genet.* 8, e1002509.
- Rahal R & Amon A (2008) The polo like kinase Cdc5 interacts with FEAR network components and Cdc14. 7, 3262–3272.
- Rass U (2013) Resolving branched DNA intermediates with structure-specific nucleases during replication in eukaryotes. *Chromosoma* 122, 499–515.
- Rass U, Compton SA, Matos J, Singleton MR, Ip SCY, Blanco MG, Griffith JD & West SC (2010) Mechanism of Holliday junction resolution by the human GEN1 protein. *Genes Dev.* 24, 1559–69.
- Reardon JT & Sancar A (2005) Nucleotide excision repair. *Prog. Nucleic Acid Res. Mol. Biol.* 79, 183–235.
- Resnick MA (1976) The repair of double-strand breaks in DNA: A model involving recombination. *J. Theor. Biol.* 59, 97–106.
- Rocuzzo M, Visintin C, Tili F & Visintin R (2015) FEAR-mediated activation of Cdc14 is the limiting step for spindle elongation and anaphase progression. *Nat. Cell Biol.* 17, 251–61.
- Rothkamm K, Krüger I, Thompson LH & Löbrich M (2003) Pathways of DNA double-strand break repair during the mammalian cell cycle. *Mol. Cell. Biol.* 23, 5706–15.
- Sarbajna S, Davies D & West SC (2014) Roles of SLX1-SLX4, MUS81-EME1, and GEN1 in avoiding genome instability and mitotic catastrophe. *Genes Dev.* 28, 1124–36.
- Saugar I, Vázquez MV, Gallo-Fernández M, Ortiz-Bazán MÁ, Segurado M, Calzada A & Tercero JA (2013) Temporal regulation of the Mus81-Mms4 endonuclease ensures cell survival under conditions of DNA damage. *Nucleic Acids Res.*, 1–16.
- Schwartz EK & Heyer W-D (2011) Processing of joint molecule intermediates by structure-selective endonucleases during homologous recombination in eukaryotes. *Chromosoma* 120, 109–27.
- Sebesta M, Burkovics P, Haracska L & Krejci L (2011) Reconstitution of DNA repair synthesis in vitro and the role of polymerase and helicase activities. *DNA Repair (Amst)*. 10, 567–76.
- Shim EY, Chung W-H, Nicolette ML, Zhang Y, Davis M, Zhu Z, Paull TT, Ira G & Lee SE (2010) *Saccharomyces cerevisiae* Mre11/Rad50/Xrs2 and Ku proteins regulate association of Exo1 and Dna2 with DNA breaks. *EMBO J.* 29, 3370–80.

- Shou W, Seol JH, Shevchenko A, Baskerville C, Moazed D, Chen ZW, Jang J, Charbonneau H & Deshaies RJ (1999) Exit from mitosis is triggered by Tem1-dependent release of the protein phosphatase Cdc14 from nucleolar RENT complex. *Cell* 97, 233–44.
- Smith CE, Llorente B & Symington LS (2007) Template switching during break-induced replication. *Nature* 447, 102–5.
- Smith S, Hwang J-Y, Banerjee S, Majeed A, Gupta A & Myung K (2004) Mutator genes for suppression of gross chromosomal rearrangements identified by a genome-wide screening in *Saccharomyces cerevisiae*. *Proc. Natl. Acad. Sci. U. S. A.* 101, 9039–44.
- Sonoda E, Hohegger H, Saberi A, Taniguchi Y & Takeda S (2006) Differential usage of non-homologous end-joining and homologous recombination in double strand break repair. *DNA Repair (Amst)*. 5, 1021–1029.
- Stegmeier F & Amon A (2004) Closing mitosis: the functions of the Cdc14 phosphatase and its regulation. *Annu. Rev. Genet.* 38, 203–32.
- Stegmeier F, Visintin R & Amon A (2002) Separase, Polo Kinase, the Kinetochores Protein Slk19, and Spo12 Function in a Network that Controls Cdc14 Localization during Early Anaphase. *Cell* 108, 207–220.
- Straight AF, Shou W, Dowd GJ, Turck CW, Deshaies RJ, Johnson AD & Moazed D (1999) Net1, a Sir2-associated nucleolar protein required for rDNA silencing and nucleolar integrity. *Cell* 97, 245–56.
- Strand M, Prolla TA, Liskay RM & Petes TD (1993) Destabilization of tracts of simple repetitive DNA in yeast by mutations affecting DNA mismatch repair. *Nature* 365, 274–6.
- Strunnikov A V, Hogan E & Koshland D (1995) SMC2, a *Saccharomyces cerevisiae* gene essential for chromosome segregation and condensation, defines a subgroup within the SMC family. *Genes Dev.* 9, 587–99.
- Sullivan M, Higuchi T, Katis VL & Uhlmann F (2004) Cdc14 Phosphatase Induces rDNA Condensation and Resolves Cohesin-Independent Cohesion during Budding Yeast Anaphase. *Cell* 117, 471–482.
- Sullivan M & Uhlmann F (2003) A non-proteolytic function of separase links the onset of anaphase to mitotic exit. *Nat. Cell Biol.* 5, 249–54.
- Sung P (1994) Catalysis of ATP-dependent homologous DNA pairing and strand exchange by yeast RAD51 protein. *Science* 265, 1241–3.

- Svendsen JM, Smogorzewska A, Sowa ME, O'Connell BC, Gygi SP, Elledge SJ & Harper JW (2009) Mammalian BTBD12/SLX4 assembles a Holliday junction resolvase and is required for DNA repair. *Cell* 138, 63–77.
- Symington LS, Rothstein R & Lisby M (2014) Mechanisms and regulation of mitotic recombination in *Saccharomyces cerevisiae*. *Genetics* 198, 795–835.
- Szakai B & Branzei D (2013) Premature Cdk1/Cdc5/Mus81 pathway activation induces aberrant replication and deleterious crossover. *EMBO J.*, 1–13.
- Szostak JW, Orr-Weaver TL, Rothstein RJ & Stahl FW (1983) The double-strand-break repair model for recombination. *Cell* 33, 25–35.
- Takeuchi Y, Horiuchi T & Kobayashi T (2003) Transcription-dependent recombination and the role of fork collision in yeast rDNA. *Genes Dev.* 17, 1497–506.
- Tan TLR, Kanaar R & Wyman C (2003) Rad54, a Jack of all trades in homologous recombination. *DNA Repair (Amst)*. 2, 787–94.
- Tay YD & Wu L (2010) Overlapping roles for Yen1 and Mus81 in cellular holliday junction processing. *J. Biol. Chem.* 285, 11427–11432.
- Teng SC, Chang J, McCowan B & Zakian VA (2000) Telomerase-independent lengthening of yeast telomeres occurs by an abrupt Rad50p-dependent, Rif-inhibited recombinational process. *Mol. Cell* 6, 947–52.
- Thangavel S, Berti M, Levikova M, Pinto C, Gomathinayagam S, Vujanovic M, Zellweger R, Moore H, Lee EH, Hendrickson EA, Cejka P, Stewart S, Lopes M & Vindigni A (2015) DNA2 drives processing and restart of reversed replication forks in human cells. *J. Cell Biol.* 208, 545–62.
- Toh GW-L, Sugawara N, Dong J, Toth R, Lee SE, Haber JE & Rouse J (2010) Mec1/Tell1-dependent phosphorylation of Slx4 stimulates Rad1-Rad10-dependent cleavage of non-homologous DNA tails. *DNA Repair (Amst)*. 9, 718–26.
- Torres-Rosell J, Machín F, Farmer S, Jarmuz A, Eydmann T, Dalgaard JZ & Aragón L (2005) SMC5 and SMC6 genes are required for the segregation of repetitive chromosome regions. *Nat. Cell Biol.* 7, 412–9.
- Torres-Rosell J, Machín F, Jarmuz A & Aragón L (2004) Nucleolar segregation lags behind the rest of the genome and requires Cdc14p activation by the FEAR network. *CELL CYCLE* 3, 496–502.
- Torres-Rosell J, De Piccoli G, Cordon-Preciado V, Farmer S, Jarmuz A, Machín F, Pasero P, Lisby M, Haber JE & Aragón L (2007) Anaphase onset before complete DNA replication with intact checkpoint responses. *Science* 315, 1411–5.

- Traverso EE, Baskerville C, Liu Y, Shou W, James P, Deshaies RJ & Charbonneau H (2001) Characterization of the Net1 cell cycle-dependent regulator of the Cdc14 phosphatase from budding yeast. *J. Biol. Chem.* 276, 21924–31.
- Ubersax JA, Woodbury EL, Quang PN, Paraz M, Blethrow JD, Shah K, Shokat KM & Morgan DO (2003) Targets of the cyclin-dependent kinase Cdk1. *Nature* 425, 859–64.
- Uhlmann F, Lottspeich F & Nasmyth K (1999) Sister-chromatid separation at anaphase onset is promoted by cleavage of the cohesin subunit Scc1. *Nature* 400, 37–42.
- Vilenchik MM & Knudson AG (2003) Endogenous DNA double-strand breaks: production, fidelity of repair, and induction of cancer. *Proc. Natl. Acad. Sci. U. S. A.* 100, 12871–6.
- Visintin R, Craig K, Hwang ES, Prinz S, Tyers M & Amon A (1998) The phosphatase Cdc14 triggers mitotic exit by reversal of Cdk-dependent phosphorylation. *Mol. Cell* 2, 709–18.
- Visintin R, Hwang ES & Amon A (1999) Cfi1 prevents premature exit from mitosis by anchoring Cdc14 phosphatase in the nucleolus. *Nature* 398, 818–23.
- Wang JC, Caron PR & Kim RA (1990) The role of DNA topoisomerases in recombination and genome stability: A double-edged sword? *Cell* 62, 403–406.
- Wang X, Ira G, Tercero JA, Holmes AM, Diffley JFX & Haber JE (2004) Role of DNA replication proteins in double-strand break-induced recombination in *Saccharomyces cerevisiae*. *Mol. Cell. Biol.* 24, 6891–9.
- Warner JR (1999) The economics of ribosome biosynthesis in yeast. *Trends Biochem. Sci.* 24, 437–40.
- Wechsler T, Newman S & West SC (2011) Aberrant chromosome morphology in human cells defective for Holliday junction resolution. *Nature* 471, 642–6.
- Wehrkamp-Richter S, Hyppa RW, Prudden J, Smith GR & Boddy MN (2012) Meiotic DNA joint molecule resolution depends on Nse5-Nse6 of the Smc5-Smc6 holocomplex. *Nucleic Acids Res.* 40, 9633–46.
- West SC, Blanco MG, Chan YW, Matos J, Sarbajna S & Wyatt HDM (2015) Resolution of Recombination Intermediates: Mechanisms and Regulation. *Cold Spring Harb. Symp. Quant. Biol.*
- Winzeler EA, Shoemaker DD, Astromoff A, Liang H, Anderson K, Andre B, Bangham R, Benito R, Boeke JD, Bussey H, Chu AM, Connelly C, Davis K, Dietrich F, Dow SW, El Bakkoury M, Foury F, Friend SH, Gentalen E, Giaever G, Hegemann JH, Jones T, Laub M, Liao H, Liebundguth N, Lockhart DJ, Lucau-Danila A, Lussier M, M'Rabet N, Menard P, Mittmann M, Pai C, Rebischung C, Revuelta

- JL, Riles L, Roberts CJ, Ross-MacDonald P, Scherens B, Snyder M, Sookhai-Mahadeo S, Storms RK, Véronneau S, Voet M, Volckaert G, Ward TR, Wysocki R, Yen GS, Yu K, Zimmermann K, Philippsen P, Johnston M & Davis RW (1999) Functional characterization of the *S. cerevisiae* genome by gene deletion and parallel analysis. *Science* 285, 901–6.
- Wu L & Hickson ID (2003) The Bloom's syndrome helicase suppresses crossing over during homologous recombination. *Nature* 426, 870–4.
- Wyatt HDM, Sarbajna S, Matos J & West SC (2013) Coordinated actions of SLX1-SLX4 and MUS81-EME1 for Holliday junction resolution in human cells. *Mol. Cell* 52, 234–47.
- Wyatt HDM & West SC (2014) Holliday junction resolvases. *Cold Spring Harb. Perspect. Biol.* 6, a023192.
- Yamamoto A, Guacci V & Koshland D (1996) Pds1p, an inhibitor of anaphase in budding yeast, plays a critical role in the APC and checkpoint pathway(s). *J. Cell Biol.* 133, 99–110.
- Ying S, Minocherhomji S, Chan KL, Palmai-Pallag T, Chu WK, Wass T, Mankouri HW, Liu Y & Hickson ID (2013) MUS81 promotes common fragile site expression. *Nat. Cell Biol.* 15, 1001–7.
- Zhang C, Roberts TM, Yang J, Desai R & Brown GW (2006) Suppression of genomic instability by SLX5 and SLX8 in *Saccharomyces cerevisiae*. *DNA Repair (Amst)*. 5, 336–46.
- Zheng X-F, Prakash R, Saro D, Longrich S, Niu H & Sung P (2011) Processing of DNA structures via DNA unwinding and branch migration by the *S. cerevisiae* Mph1 protein. *DNA Repair (Amst)*. 10, 1034–43.
- Zhu Z, Chung W-H, Shim EY, Lee SE & Ira G (2008) Sgs1 helicase and two nucleases Dna2 and Exo1 resect DNA double-strand break ends. *Cell* 134, 981–94.

8 Appendix: Media, Solutions & Suppliers

I. Media for *Saccharomyces cerevisiae* culture.

- liquid YPD medium
 - 1% yeast extract
 - 2% peptone
 - 2% glucose

- solid YPD medium:
 - 1% yeast extract
 - 2% peptone
 - 2% glucose
 - 2% agar

- liquid YPr Raff:
 - 1% yeast extract
 - 2% peptone
 - 2% raffinose

- solid YPr Raff:
 - 1% yeast extract
 - 2% peptone
 - 2% galactose
 - 2% agar

- liquid YPgal:
 - 1% yeast extract
 - 2% peptone
 - 2% galactose

- solid YPgal:
 - 1% yeast extract
 - 2% peptone
 - 2% galactose
 - 2% agar

II. Solutions

II.1. Preparation of competent cells of and transformation of *Saccharomyces cerevisiae*.

- SORB solution:
 - 100 mM lithium acetate
 - 10 mM Tris/HCl pH 8
 - 1 mM EDTA
 - 1 M sorbitol

- PEG solution:
 - 100 mM lithium acetate
 - 10 mM Tris/HCl pH 8
 - 1 mM EDTA
 - 40 % polyethylenglycol 3350

II.2. Preparation of high-molecular weight DNA samples.

- SCE:
 - 1 M sorbitol
 - 0.1 M trisodium citrate dehydrate salt
 - 0.06 M EDTA

- SB1:
 - SCE
 - 5 µl/ml β-mercaptoethanol
 - 100 U/ml zymolyase 100T or 2500 U/ml Lyticase

- LMPA solution:
 - 1% low melting point agarose
 - 0.125 M EDTA

- SB2:
 - 0.45 M EDTA
 - 0.01 M Tris/HCl pH 7.5
 - 7.5% β-mercaptoethanol
 - 10 µg/ml RNase

- SB3:
 - 0.25 M EDTA
 - 0.01 M Tris/HCl pH 7.5
 - 1% L-laurylsarcosine
 - 1 mg/ml proteinase K

- Storage solution:

- 70% glycerol
- 0.05 M EDTA

II.3. Genomic DNA preparation

- Breaking buffer solution:
 - 10 mM Tris/HCl pH 8
 - 1 mM EDTA
 - 1% (w/v) SDS
 - 100mM NaCl
 - 2 % Triton X-100

- TE 1X pH 8
 - 10 mM Tris-Cl pH 8
 - 1mM EDTA pH 8

II.4. Agarose gel electrophoresis

- 1X TAE:
 - 40 mM Tris base
 - 20 mM acetic acid
 - 1 mM EDTA
 -
- 1X TBE:
 - 89 mM Tris base
 - 89 mM boric acid
 - 2 mM EDTA

- 0.5X TBE:
 - 44.5 mM Tris base
 - 44.5 mM boric acid
 - 1 mM EDTA

- Alkaline Buffer
 - 40 mM NaOH
 - 2 mM EDTA

II.5. Southern-Blot

- Denaturing solution:
 - 0.4 M NaOH
 - 1 M NaCl
- Neutralisation solution:
 - 1.5 M NaCl
 - 0.5 M Tris-HCl
 - Adjust pH to 7.5 with HCl

- Depurinating solution
 - 0.125 M HCl

- 20X SSC, pH 7
 - 3 M NaCl
 - 0.34 M trisodium citrate dehydrate salt

- Blocking membrane solution
 - 5X SSC
 - 0.1 % SDS
 - 5 % Dextran sulphate
 - 5 % Rapid-hyb Buffer (GE Healthcare)

- Primary washing solution
 - 1X SSC
 - 0.1 % SDS

- Secondary washing solution
 - 0.5X SSC
 - 0.1 % SDS

- AB buffer
 - 100 mM Tris-HCl
 - 0.15 M NaCl

II.6. Western-Blot

- Laemmli buffer (2X):
 - 120 mM Tris/HCl pH 6.8
 - 20 % glycerol
 - 4% SDS
 - 4% β -mercaptoethanol
 - 0.02 % bromophenol blue

- Running buffer:
 - 3 g/l Tris base
 - 14,4 g/l glycine
 - 0.6 g/l SDS

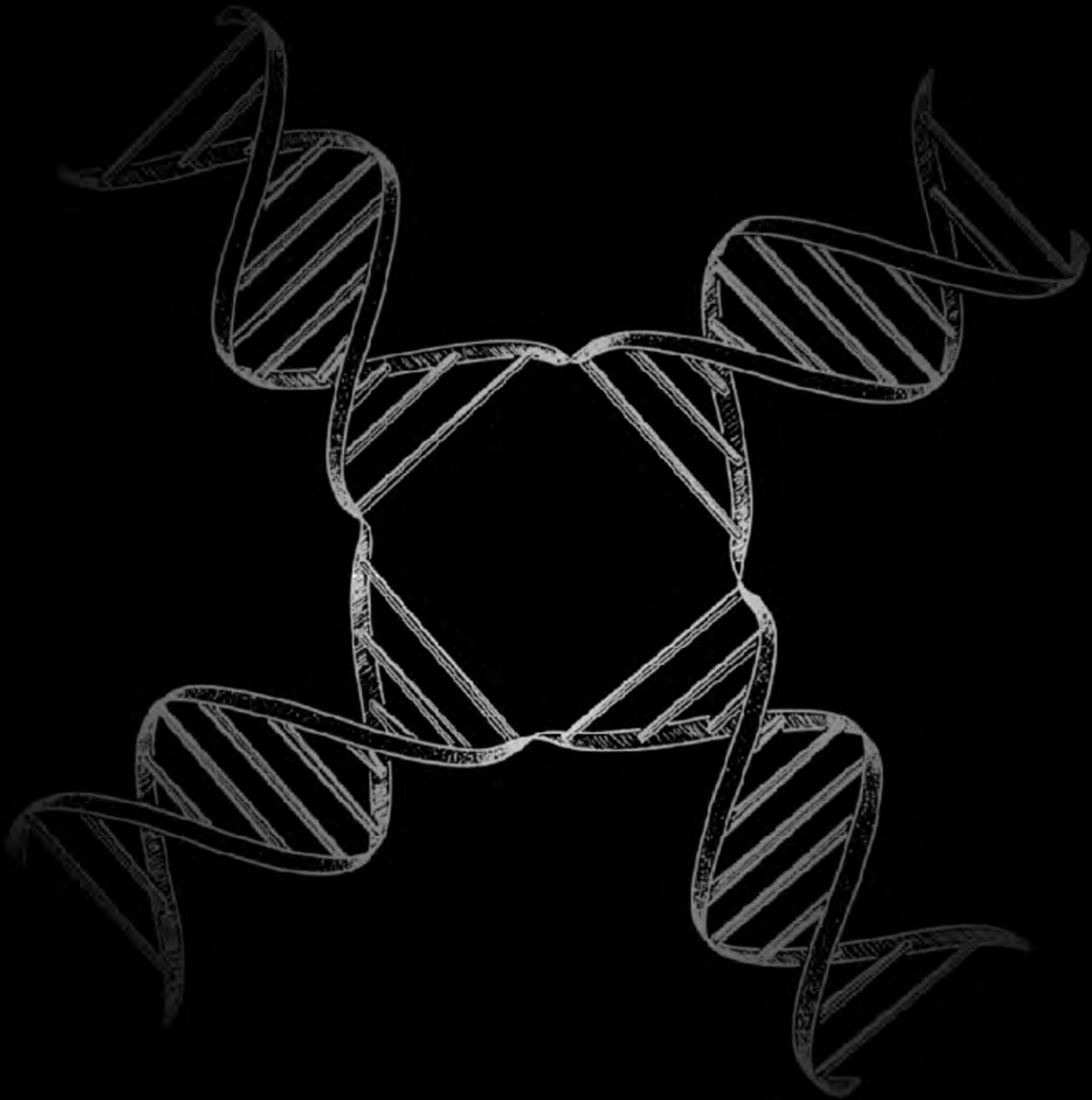
- Transfer buffer:
 - 25 mM Tris/HCl pH 8.3
 - 192 mM glycine
 - 20% methanol
 - 0.1% SDS

- TBST:
 - 100 mM Tris/HCl pH 7.5
 - 150 mM NaCl
 - 0.1% Tween 20

II.7. List of suppliers

Table 4: List of suppliers

React./Enz.	Supplier	React./Enz.	Supplier
Acetic acid	Sigma-Aldrich	Lyticase	Sigma-Aldrich
Acrylamide	Promega	Methanol	Panreac
Adenine	Panreac	MgCl ₂	Sigma-Aldrich
Agar	Pronadisa	MgSO ₄	Sigma-Aldrich
Agarose	Panreac	MMS	Sigma-Aldrich
Bacto™ tryptone	BD-Difco	Nylon Membrane, positively charged	Roche Applied Sci.
BglII	NEB	NaCl	Promega
Bisacrylamide	Promega	NaOH	Panreac
Boric acid	Panreac	Nocodazole	Sigma-Aldrich
Bromophenol blue	Sigma-Aldrich	Peptone	Pronadisa
clonNAT	Werner BioAgents	Pefablock SC	Roche Applied Sci.
CDP-Star	GE Healthcare	Phenol: chloroform: isoamyl alcohol (25:24:1)	Sigma-Aldrich
DAPI	Fluka	Phleomycin	Sigma-Aldrich
dATP	Promega	Polyethylenglycol	Sigma-Aldrich
dCTP	Promega	Pronase E	VWR
dGTP	Promega	Propidium iodide	Fluka
Dropout ADE/HIS/LEU/TRP-	BD Biosciences	Proteinase K	Roche Applied Sci.
dTTP	Promega	PVDF membranes	Millipore
EDTA	Promega	Raffinose	Panreac Life Science
Ethanol	Panreac	RNaseA	Roche Applied Sci.
G-418 solution	Roche Applied Sci.	RuvC	Abcam
Galactose	Merck	Salmon sperm DNA	Sigma-Aldrich
Glucose	Merck	SDS	Sigma-Aldrich
Glycerol	Promega	Sorbitol	Sigma-Aldrich
Glycine	Promega	T4 DNA ligase	Roche
HCl	Sigma-Aldrich	Tris base	Promega
Herring Sperm DNA	Promega	Trisodium citrate dehydrate salt	Sigma-Aldrich
Histidine	Panreac	Triton X-100	Promega
Hydroxyurea	Sigma-Aldrich	Tryptophan	Panreac
Hygromycin B	Sigma-Aldrich	Tween 20	Promega
KCl	Sigma-Aldrich	Yeast extract	Pronadisa
L-laurylsarcosine	Sigma-Aldrich	Yeast nitrogen base	Pronadisa
Leucine	Panreac	Zymolyase 100T	Zymoresearch
Lithium acetate	Promega	α-factor	Sigma-Aldrich
Low melting point agarose	Promega	β-mercaptoethanol	Sigma-Aldrich



A study of chromosome segregation where persistent DNA junctions are present between sister chromatids carried out in *Saccharomyces cerevisiae*.